

PhD Thesis

**AUTOPHAGY DEPENDENT CELL DEATH,
SENESCENCE AND DIFFERENTIATION BY ABRUS
AGGLUTININ IN CANCER THERAPEUTICS**

Prashanta Kumar Panda



Department of Life Science

National Institute of Technology, Rourkela

**Autophagy dependent cell death, senescence and
differentiation by *Abrus agglutinin* in cancer therapeutics**

*Dissertation submitted in partial fulfillment
of the requirements of the degree of
Doctor of Philosophy*

in

Department of Life Science

by

Prashanta Kumar Panda

(511LS607)

*based on research carried
out under the supervision*

of

Dr. Sujit Kumar Bhutia



April 19th, 2017

**Department of Life Science
National Institute of Technology Rourkela**



**Department of Life Science
National Institute of Technology Rourkela**

April 19th, 2017

Certificate of Examination

Roll Number: 511LS607

Name: Prashanta Kumar Panda

Title of Dissertation: “**Autophagy dependent cell death, senescence and differentiation by *Abrus agglutinin* in cancer therapeutics**”

We the below signed, after checking the dissertation mentioned above and the official record book (s) of the student, hereby state our approval of the dissertation submitted in partial fulfillment of the requirements of the degree of Doctor of Philosophy in Life Science at National Institute of Technology Rourkela. We are satisfied with the volume, quality, correctness and originality of the work.

Sujit Kumar Bhutia (Principal Supervisor)

Surajit Das (Member, DSC)

Debasish Sarkar (Member, DSC)

Suman Jha (Member, DSC)

(External examiner)

Samir Kumar Patra (Chairperson, DSC)

Sujit Kumar Bhutia (Head of the Department)



Department of Life Science
National Institute of Technology Rourkela

April 19th, 2017

Dr. Sujit Kumar Bhutia
(Assistant Professor)

Supervisor's certificate

This is to certify that the work presented in the dissertation entitled, “**Autophagy dependent cell death, senescence and differentiation by *Abrus* agglutinin in cancer therapeutics**” submitted by **Prashanta Kumar Panda, Roll Number 511LS607**, is a record of original research carried out by him under my supervision and guidance in partial fulfillment of the requirements of the degree of Doctor of Philosophy in Life Science. Neither this dissertation nor any part of it has been submitted earlier for any degree or diploma to any institute or university in India or abroad.

Sujit K. Bhutia
Assistant Professor

*Dedicated to my beloved father
Late Nishakar Panda*

Prashanta Kumar Panda

Declaration of originality

I, **Prashanta Kumar Panda, Roll Number 511L607** hereby declare that this dissertation entitled “**Autophagy dependent cell death, senescence and differentiation by *Abrus agglutinin* in cancer therapeutics**” presents my original work carried out as a doctoral student of NIT Rourkela and to the best of my knowledge, contains no material previously published or written by another person, nor any material presented by me for the award of any degree or diploma of NIT Rourkela or any other institution. Any contribution made to this research by others, with whom I have worked at NIT Rourkela or elsewhere, is explicitly acknowledged in the dissertation. Works of other authors cited in this dissertation have been duly acknowledged under the sections “Reference”. I have also submitted my original research records to the scrutiny committee for evaluation of my dissertation. I am fully aware that in case of any noncompliance detected in future, the Senate of NIT Rourkela may withdraw the degree awarded to me on the basis of the present dissertation.

April 19th, 2017
National Institute of Technology Rourkela

Prashanta Kumar Panda

Acknowledgment

First and foremost, I would like to acknowledge my supervisor, **Dr. Sujit Kumar Bhutia** (Assistant Professor and Head, Department of Life Science, NIT Rourkela) for giving me the opportunity to work with him. He has helped me during challenging times of research and is the main proponent to completion of my thesis. He raised me up to more than I can be and spurring me on to develop myself as an independent researcher. I will always be grateful for the experience I have gained from him and have enjoyed being a member of his lab.

I wish to thank members of my Doctoral Scrutiny Committee; **Dr. Samir Kumar Patra, Dr. Surajit Das, Dr. Suman Jha,** and **Dr. Debashis Sarkar** for their guidance, which has been beneficial in all aspects of my PhD work. I am extremely indebted to all faculty members of Department of Life Science for their advice and cooperation during the course of this study.

I also like to place on record my sense of gratitude and indebtedness to my thesis evaluator **Dr. Rama Shanker Verma** (Professor, Department of Biotechnology, Indian Institute of Technology Madras, India) for critically reviewing and giving constructive suggestions for a better thesis. In addition, a big thank you to **Dr. Edward A. Ratovitski** (Professor, School of Medicine, Johns Hopkins University, USA) giving his valuable time for reviewing my thesis from his busy schedule.

Initially, I would like to thank Department of Biotechnology (DBT) and Ministry of Human Resource Development (MHRD), Government of India for funding my five years of research.

I would like to acknowledge **Dr. Tapas Kumar Maiti** (Professor, Department of Biotechnology, Indian Institute of Technology Kharagpur, India) for enjoying his lab facilities during initial period of my thesis. I would also like to acknowledge **Dr. Rajesh Agarwal** (Professor, University of Colorado, Skaggs School of Pharmacy and Pharmaceutical Sciences, Aurora, USA) for providing electron microscope facility. I extend my gratitude to **Dr. Gautam Sethi** (Associate Professor, Department of Pharmacology, National University of Singapore, Singapore) for *in vivo* study and constructive advice during preparation of this thesis. My special thanks to **Dr. Biswa Ranjan Meher** (Assistant professor, Central University of Jharkhand, India) for helping *in silico* simulation studies. I would also like to appreciate high performance computing facilities (ARJUN cluster) at Molecular Biophysics Unit, Indian Institute of Science, Bangalore, India.

Finally special gratitude to my beloved mother **Mrs. Basanti lata Panda**, brother **Sushanta and Basanta**, my sister **Sukanti and Madhusmita** who have supported me during the difficult times of my life in this period of research. It will be unfair if I will not mention my adorable **Bapa** (nephew, **Tridibesh**) as talking with him makes me fresh during period of thesis preparation.

I would specially like to express my gratitude to my research colleagues **Manu, Prajna, Sumanta, Bikash, Subhadip, Niharika, Prakash, Chandra, Debasna, Payal, Pradipta, Hirak and Moonmoon** for their constant support and help on and off the work bench.

Last but not the least I express my deepest gratitude to Almighty for giving me strength for successfully completion of this thesis.

April 19th, 2017
National Institute of Technology Rourkela

Prashanta Kumar Panda

Abstract

Abrus agglutinin (AGG), a type II ribosome inactivating protein has been found to induce mitochondrial apoptosis. Initially, we documented that AGG mediated Akt dephosphorylation led to ER stress resulting in the induction of autophagy dependent cell death through the canonical pathway in cervical cancer cells. At the molecular level, AGG induced ER stress in PERK dependent pathway and inhibition of ER stress by salubrinal, eIF2 α phosphatase inhibitor as well as siPERK reduced autophagic death in the presence of AGG. Further, our *in silico* and colocalization study showed that AGG interacted with pleckstrin homology (PH) domain of Akt to suppress its phosphorylation and consequent downstream mTOR dephosphorylation in HeLa cells. Besides autophagy, we investigated mitophagy inducing potential of PUMA triggered by AGG in U87MG cells and established AGG induced ceramide as a chief mediator of mitophagy dependent cell death through activation of mitochondrial ROS and ER stress. Mechanistically, we identified a LC3 interacting region (LIR) at C-terminal end of PUMA which interacts with LC3 to induce mitophagy. Furthermore, we identified senescence inducing potential governed by AGG induced autophagy in prostate cancer cell line. Our study showed that accelerated expression of SIRT1 facilitated LAMP1 deacetylation in response to AGG insult and modulated autophagy. Likely, AGG induced colon CSC differentiation by increasing expression of BMP2. As per retrospective tumor specimen analysis, BMP2 expression was down regulated with colon cancer progression indicating its tumor suppressor function. Significant interaction of AGG induced BMP2 with hVps34 may be a breakthrough in autophagy machinery. The present study provided deep insight into the mechanism of AGG mediated tumor inhibition through activation of autophagy for the development of cancer therapeutics.

Key words: Autophagy, Mitophagy, Lipophagy, Senescence, Differentiation, SIRT1, hVPS34

Contents

Certificate of Examination		ii
Supervisors' certificate		iii
Dedication		iv
Declaration of originality		v
Acknowledgement		vi
Abstract		viii
List of symbols		xiii
List of figures		xv
List of table		xvii
Chapter 1	Introduction	1-5
	1. Introduction	2
	1.1. Autophagy	2
	1.2. Mitophagy	2
	1.3. Autophagy and Cancer stem cells	3
	1.4. Autophagy and Senescence	3
	1.5. Ribosome Inactivating Protein Type II and <i>Abrus</i> Agglutinin	3
Chapter 2	Review of literature and objectives	6-18
	2. Introduction	7
	2.1. Autophagy and its Regulation	7
	2.2. Autophagy and Cancer	10
	2.2.1 Autophagy and Tumor Suppression	10
	2.2.2 Autophagy and Senescence	11
	2.2.3 Autophagy and Oxidative Stress	12
	2.2.4 Autophagy and Genome Damage	12
	2.2.5 Autophagy and Metastasis	13
	2.2.6 Autophagy and Cancer Metabolism	14
	2.3 Autophagy and Apoptosis Connection in Cancer Therapy	14
	2.3.1 Inducing both Apoptosis and Autophagic Cell Death –“Simultaneous” Approach	14
	2.3.2 Inducing Apoptosis and Autophagy – “Survival” Approach	15
	2.3.3 Autophagy Switches to Apoptosis – “Successive” Approach	15
	2.3.4 Inducing Autophagic Cell Death in Apoptosis Deficient/Resistant Cells – “Substitutive” Approach	16
	2.3.5. Inducing Apoptosis and Inhibition of Autophagy – “Suppressive” Approach	16
	2.4. Autophagy as Cancer Preventive	17
	2.5. <i>Abrus</i> Agglutinin: The Golden Bullet	17
	2.6. Objectives of the PhD work	18
Chapter 3	<i>Abrus</i> agglutinin inhibits Akt/PH domain to induce endoplasmic reticulum stress mediated autophagy dependent cell death	19-44
	Abstract	20
	3.1. Introduction	20
	3.2. Materials and Methods	22
	3.2.1 Reagents	22
	3.2.2 Antibodies	22

3.2.3 Purification of AGG	23
3.2.4 Cell Culture	23
3.2.5 MTT Assay	23
3.2.6 Plasmids, Small Interfering RNA and Transfection	23
3.2.7 Acridine Orange Staining	24
3.2.8 Transmission Electron Microscopy	24
3.2.9 Measurement of Autophagy by GFP-LC3 Transfection	24
3.2.10 Western Blot Analysis	24
3.2.11 Immunofluorescence Analysis	24
3.2.12 Reactive Oxygen Species (ROS) Measurement	25
3.2.13 Colocalization Study by ER-Tracker, LysoTracker and MitoTracker	25
3.2.14 Caspase-Glo 3/7 Assay	25
3.2.15 RITC Labeling of AGG for Colocalization Study with Akt-PH Domain	25
3.2.16 Modeling PH-AGG Complex Through Docking and Molecular Dynamics Simulation	25
3.2.17 Statistical Analysis	26
3.3 Results	26
3.3.1. AGG Induced Autophagic Cell Death in Cervical Carcinoma	26
3.3.2. AGG Induced Autophagic Cell Death is Mediated through Canonical Pathway	29
3.3.3. Crosstalk Between AGG Induced Apoptosis and Autophagic Cell Death	30
3.3.4. AGG Induced Autophagic Cell Death in Apoptosis Deficient and Resistant Cervical Cancer Cells	33
3.3.5. AGG Induced Autophagic Cell Death Mediated through PERK Mediated ER Stress	34
3.3.6. AGG Mediated Inhibition of Akt/PH Domain Promoted ER Stress Induced Autophagic Cell Death	38
3.4. Discussion	42
Chapter 4 PUMA dependent mitophagy by <i>Abrus</i> agglutinin contributes to apoptosis through ceramide generation	45-76
Abstract	46
4.1. Introduction	46
4.2. Materials and Methods	49
4.2.1 Reagents and Chemicals	49
4.2.2 Antibodies	49
4.2.3 Plasmid and siRNA	49
4.2.4 Cell Culture	50
4.2.5 Acridine Orange Staining	50
4.2.6 Measurement of Autophagy by GFP-LC3 Transfection	50
4.2.7 Western Blot and Immunoprecipitation Analysis	50
4.2.8 Electron Microscopy	51
4.2.9 Immunofluorescence Staining for Confocal Imaging	51
4.2.10 Colocalization Study by Confocal Imaging	51
4.2.11 Caspase Activity Assays	51
4.2.12 Measurement of Mitochondrial Respiration Rate and Glycolysis Study	51

	4.2.13 Measurement of Cellular ATP Level	52
	4.2.14 Comet Assay	52
	4.2.15 Modeling PUMA-LC3 Complex through Docking and Molecular Dynamics Simulation	52
	4.2.16 Statistical Analysis	52
	4.3. Results	53
	4.3.1 AGG Induces DNA Damage Mediated Apoptosis	53
	4.3.2 AGG Induces Autophagy through AMPK/mTOR Dependent Pathway	54
	4.3.3 AGG Induces Mitochondrial Autophagy	55
	4.3.4 AGG Induced Ceramide Regulates Autophagy and Apoptosis	60
	4.3.5 AGG Activates Class III PI3K around Depolarized Mitochondria	63
	4.3.6 AGG Induced Mitophagy through Abrogation of Mitochondrial Bioenergetics	64
	4.3.7 PUMA: The Master Regulator of AGG Induces Mitophagy	65
	4.3.8 PUMA Interacts with LC3 for Mitophagy Induction	68
	4.3.9 Effect of PUMA Ubiquitination on AGG Induced Mitophagy Induction	70
	4.3.10 PUMA Interacts with Adaptor Protein p62/SQSTM1 for Mitophagy Induction.	71
	4.3.11 AGG Induced Mitophagy Switches to Apoptosis	72
	4.4 Discussion	73
Chapter 5	SIRT1/LAMP1 Signaling Activation By <i>Abrus</i> Agglutinin Regulates Autophagy-Mediated Senescence	77-93
	Abstract	78
	5.1. Introduction	78
	5.2. Materials and Methods	80
	5.2.1 Reagents	80
	5.2.2 Antibodies	80
	5.2.3 Cell Culture	80
	5.2.4 β -Galactosidase Assay	80
	5.2.5 Acridine Orange Staining	81
	5.2.6 Western Blot and Immunoprecipitation Analysis	81
	5.2.7 Flow Cytometry Analysis of Cell Cycle Distribution	81
	5.2.8 Immunofluorescence	81
	5.2.9 Total Lipid and Free Fatty Acid Analysis	82
	5.2.10 Statistical Analysis	82
	5. 3. Results	82
	5. 3.1 AGG Induces Senescence and Growth Arrest	82
	5.3.2 AGG Induced Autophagy Regulates Senescence	84
	5.3.3 AGG Induced Lipophagy Modulates Senescence	86
	5.3.4 SIRT1 Regulates AGG Induced Autophagy	88
	5.4. Discussion	90
Chapter 6	<i>Abrus</i> Agglutinin Induces Cancer Stem Cell Differentiation Through BMP2 Mediated Autophagy	94-112
	Abstract	95
	6.1. Introduction	95
	6.2. Materials and Methods	97
	6.2.1 Reagents	97

6.2.2 Antibodies	98
6.2.3 Cell and Sphere Culture	98
6.2.4 Immunofluorescence Staining of Colonospheres Confocal Imaging	98
6.2.5 RNA Extraction and Semiquantitative RT-PCR	98
6.2.6 Western Blot Analysis	99
6.2.7 Alkaline Phosphatase Assay	99
6.2.8 Colocalization Study by Immunofluorescence Analysis	99
6.2.9 <i>In Vivo</i> Mice Experiment	100
6.2.10 Immunohistochemical Staining and Scoring	100
6.2.11 Statistical Analysis	100
6.3. Results	100
6.3.1 Expression of BMP2 and β -Catenin in Colorectal Cancer and Non-Cancer Tissue Samples	100
6.3.2 AGG Inhibits HT-29 Colonospheres Formation	101
6.3.3 AGG Inhibits Stemness and Induces Differentiation in Colonospheres	104
6.3.4 AGG Induces Autophagy in HT-29 Colonospheres	105
6.3.5 AGG Promotes BMP2 Expression in Colonospheres	106
6.3.6 Role of Autophagy in AGG Induced Differentiation In Colonospheres	107
6.3.7 AGG Induced Differentiation Potential in Mouse Xenograft Model	108
6.4 Discussion	109
Chapter 7 Summary and Conclusions	113-116
7.1. Summary	114
7.2. Scope of the Present Investigations	115
References	118-132
Curriculum Vitae	133-138

Appendix A: List of symbols

AGG	<i>Abrus</i> agglutinin
ATP	Adenosine triphosphate
BSA	Bovine serum albumin
CSC	Cancer stem cell
CO ₂	Carbon dioxide
DAPI	4', 6-Diamidino-2-phenylindole dihydrochloride
DMEM	Dulbecco's Modified Eagle Medium
DMSO	Dimethyl sulphoxide
DNA	Deoxyribonucleic acid
DHE	Dihydroethidium
DHR123	Dihydrorhodamine 123
DTT	Dithiothreitol
ECL	Enhanced chemiluminescence
EDTA	Ethylene diamine tetra acetate
ER	Endoplasmic reticulum
FACS	Fluorescence cell sorter
FBS	Fetal bovine serum
FITC	Fluorescein isothiocyanate
FFA	Free fatty acid
g	Gram
h (s)	Hour (s)
H ₂ O ₂	Hydrogen peroxide
HBSS	Hank's balanced salt solution
kDa	Kilo Dalton
kg	Kilogram
L	Litre
MEM	Minimal essential medium
mg	Milligram
min	Minute
ml	millilitre
mM	Millimolar
MMP	Mitochondrial membrane potential
MTT	3-[4,5-dimethylthiazol-2-yl]-2,5-diphenyltetrazolium
NaCl	Sodium chloride
NAC	N-acetylcysteine
ng	Nanogram
nm	Nanometer
°C	Degree Centigrade
OCR	Oxygen consumption rate
OD	Optical density
<i>P</i>	Probability level
PAGE	Polyacrylamide gel electrophoresis
PARP	Poly (ADP-ribose) polymerase
PBS	Phosphate buffer saline
PBST	Phosphate buffered saline with Tween-20
PI	Propidium iodide
PUMA	P53 upregulated modulator of apoptosis
Rh 123	Rhodamine123

RIP	Ribosome inhibiting protein
ROS	Reactive oxygen species
Rpm	Rotation per minute
s.c.	Subcutaneous
SD	Standard deviation
SDS	Sodium dodecyl sulfate
shRNA	Short hairpin RNA
TE	Tris-EDTA
Tris	Tris (hydroxymethyl) amino methane
v/v	Volume/volume
w/v	Weight/volume
µg	Microgram
µl	Microlitre
µM	Micromolar

Appendix B: List of figure

Figure No.	Figure legend	Page No.
Fig. 1.1.	Mechanism of action of type II ribosome inactivating proteins in mammalian cells	5
Fig. 2.1.	The process of autophagy	9
Fig. 2.2.	Pro- and anti-tumor roles of autophagy in different stages of cancer	11
Fig. 2.3.	Apoptosis autophagy interaction during cancer therapy	15
Fig. 3.1.	AGG induced autophagic cell death in cervical cell carcinoma	27
Fig. 3.2.	Analysis of AGG induced autophagy by electron microscopy and Western blot	28
Fig. 3.3.	AGG induced autophagic cell death was mediated through the canonical pathway	30
Fig. 3.4.	The relationship between AGG induced apoptosis and autophagic cell death	31
Fig. 3.5.	Effect of AGG induced apoptosis in autophagy deficient cells	31
Fig. 3.6.	The role of reactive oxygen species in AGG induced autophagic death	32
Fig. 3.7.	The role of Bax in AGG induced autophagic death.	33
Fig. 3.8.	AGG induced autophagic cell death in apoptosis resistant cervical cancer cells	34
Fig. 3.9.	Colocalization of ER and lysosome in AGG treated HeLa cells	35
Fig. 3.10.	Colocalization of mitochondria and lysosome in AGG treated HeLa cells	35
Fig. 3.11.	AGG induced ER stress in HeLa cells	37
Fig. 3.12.	The role of ER stress in AGG induced autophagic cell death.	38
Fig. 3.13.	Interaction of Akt-PH domain and AGG	39
Fig. 3.14.	Colocalization of AGG and Akt-PH domain	40
Fig. 3.15.	Akt plays a master signal for inducing autophagy by increasing ER stress	41
Fig. 3.16.	Schematic representation of AGG induced ER stress mediated autophagy dependent cell death in HeLa cells	42
Fig. 4.1.	AGG facilitates DNA damage in U87MG cells	53
Fig. 4.2.	AGG induces apoptosis in U87MG cells	54
Fig. 4.3.	AGG induces autophagy in U87MG cells	55
Fig. 4.4.	TEM analysis in AGG treated U87MG cells	57
Fig. 4.5.	Colocalization of GFP-LC3 and TOM20 in AGG treated U87MG cells	58
Fig. 4.6.	Effect of AGG on mitophagy associated proteins in U87MG cells	59
Fig. 4.7.	Effect of autophagy inhibition on AGG induced mitophagy U87MG cells	60
Fig. 4.8.	AGG induces ceramide in U87MG cells	61
Fig. 4.9.	Effect of AGG on Ceramide synthase1 in U87MG cells	62
Fig. 4.10.	AGG induced ceramide regulates autophagy and apoptosis	63
Fig. 4.11.	AGG induced fragmented mitochondria and activates class III PI3K around depolarized mitochondria	64
Fig. 4.12.	AGG induced mitophagy through abrogation of mitochondrial bioenergetics	65
Fig. 4.13.	AGG induces PUMA and is associates with TOM20 in U87MG cells.	66
Fig. 4.14.	Gain and loss of function of PUMA regulate AGG induced mitophagy.	66
Fig. 4.15.	Gain and loss of function of PUMA regulate AGG induced	67

	mitochondrial dysfunction.	
Fig. 4.16.	PUMA contains LIR to interact with LC3.	69
Fig. 4.17.	PUMA interacts with LC3 for mitophagy induction	70
Fig. 4.18.	Effect of PUMA ubiquitination AGG induced mitophagy induction	71
Fig. 4.19.	PUMA interacts with adaptor protein p62 for mitophagy induction	72
Fig. 4.20.	AGG induced mitophagy switches to apoptosis	73
Fig. 4.21.	Schematic representation of PUMA and LC3 interaction.	76
Fig. 4.22.	Schematic representation of PUMA induced mitophagy ends with apoptosis	76
Fig. 5.1.	AGG induces SA- β -Gal staining in dose and time dependent way in PC3 cells	83
Fig. 5.2.	Effect of AGG on cell cycle	84
Fig. 5.3.	AGG induces autophagy in PC3 cells	85
Fig. 5.4.	AGG induced autophagy regulates senescence in PC3.	85
Fig. 5.5.	AGG abrogates lipid store and escalates free fatty acid content in PC3 cells	86
Fig. 5.6.	Effect of lalistat on AGG induced lipophagy in PC3 cells	87
Fig. 5.7.	AGG induces lipophagy to prompt senescence	87
Fig. 5.8.	Effect of AGG on expression of SIRT1 in PC3 cells	88
Fig. 5.9.	SIRT1 interacts and deacetylates LAMP in PC3 cells	89
Fig. 5.10.	Effect of SIRT1 inhibition of AGG induced lipophagy in PC3 cells.	89
Fig. 5.11.	Schematic representation of AGG induced lipophagy mediated senescence	93
Fig. 6.1.	Expression of BMP2 and β -catenin in human colorectal cancer and non-cancer tissue samples	101
Fig. 6.2.	AGG inhibited formation of HT-29 colonospheres	102
Fig. 6.3.	AGG inhibits the stemness and preferentially targets self-renewal potential in colonospheres	104
Fig. 6.4.	AGG induces differentiation in colonosphere	105
Fig. 6.5.	Effect of AGG on expression of stemness and differentiation gene and alkaline phosphate activity in colonospheres	105
Fig. 6.6.	AGG induces autophagy in HT-29 colonospheres	106
Fig. 6.7.	AGG promotes BMP2 expression in colonosphere.	106
Fig. 6.8.	Interaction of BMP2 and hVps34.	107
Fig. 6.9.	Effect of AGG induced autophagy colonosphere differentiation.	108
Fig. 6.10.	AGG elicits the expression of BMP2 and LC3 in HT-29 xenograft tissue	109
Fig. 6.11.	Schematic representation of BMP2 mediated autophagy induces differentiation	112
Fig. 7.1.	Schematic presentation of the present PhD thesis	116

Appendix C: List of figure

Table No.	Table legend	Page No.
6.1.	Clinicopathological representation of cohort	103

Chapter 1

Introduction

1. Introduction

1.1. Autophagy

Autophagy is an evolutionarily conserved catabolic process where a cell self digests its cytoplasmic contents (the expression derives from Greek; “auto” – self and “phagia” – eating), and it is a critical adaptive response that recycles energy and nutrients during starvation or stress. Autophagy is regulated by a limited number of highly conserved genes called ATGs (for AuTophagy genes). Forty ATGs have been identified that are required for the autophagy process to occur. Autophagy maintains cellular homeostasis by engulfing damaged organelles, protein aggregates and cytoplasmic materials for degradation and in turn nurturing the cellular nutrient pool to cope with different types of stress. In addition to its constitutive role in housekeeping functions, autophagy is induced by various stimuli, such as cytokines, stress, pathogens, misfolded or aggregated proteins, damaged organelles, and even inhibition of protein synthesis (Panda et al., 2014; Bhutia et al., 2013; Mizushima et al., 2010).

Autophagy plays a very prominent role in physiological and pathological conditions, such as cancer. It is vital for the removal of damaged or long-lived proteins and organelles, for which defects are associated with susceptibility to genome damage, metabolic stress, and tumorigenesis. Although autophagy acts as a tumor suppressor, it can lead to stress tolerance, which allows tumor cells to survive under adverse conditions. Thus, the pro-survival role of autophagy is a major obstacle for successful cancer therapy (Bhutia et al., 2013).

1.2. Mitophagy

Other than general autophagy, organelles specific selective autophagy has been explored for easy selection of cargo by autophagosome –lysosomal process. Several specific autophagy like autophagy in ribosomes (ribophagy), endoplasmic reticulum (endoplasmic reticulum–phagy/reticulophagy), peroxisomes (pexophagy), and mitochondria (mitophagy) have been recently reported (Kraft et al., 2008; Lipatova et al., 2013; Schuck et al., 2014; Nazarko et al., 2014; Saito et al., 2015). The study shows that both general autophagy and mitophagy share similar machinery for the formation of autophagosome as well as mitophagosome (Itakura et al., 2012). Mitochondria are the most dynamic organelles which move within the cell and mitochondrion needs to be separated from the mitochondrial network to be entrapped by the autophagosome. Autophagic adapters and mitochondrial receptors take part for selective removal of mitochondria. However, during severe stress excessive mitophagy

prevents the mitochondrial biogenesis and depletion of bioenergetics pool in other mitochondria lead to subsequent cell death (Kubli et al., 2012).

1.3. Autophagy and Cancer stem cells

Accumulating evidence shows that cancer stem cells (CSCs) refer to a subset of tumor cells that has the ability of exclusive self-renewal capacity, aggressive invasive potential, hierarchical differentiation as well as sustained tumorigenicity encourage for tumor initiation and chemoresistance (Wicha et al., 2014, Naik et al., 2016). Several rationalizations have been formulated for the origin of the CSC, like dynamic transitions of non-CSCs to CSCs. Similarly, oncogenic genetic mutations in the progenitor or partly differentiated cells and matured cells may lead to the dedifferentiation cells into stem-like cells. However, accumulating observation indicates that during cancer therapy some of the non-killed residual tumor cells acquire stemness property. Cancer stem cells provide a protective effect against current cancer therapeutics through autophagy, and therefore inhibition of autophagy results in better therapeutic responses.

1.4. Autophagy and Senescence

Cellular senescence is defined as a biological state of irreversible cell cycle arrest in which cells limit the ability to proliferate without alteration of metabolic activity (Panda et al., 2015, Evan et al., 2009). Generally, three types of senescence have been investigated like replicative senescence, oncogene-induced senescence, and premature (accelerated or stress-induced) senescence. Replicative senescence occurs due to shortening of telomere while oncogene induced senescence corresponds to the delay in the expression of the oncogene like RAS while premature, accelerated, or stress-induced senescence occurs due to exposure of the exogenous cytotoxic assault normally associated with DNA damage (Rachel et al., 2012). Stress induced senescence (SIS) is involved in the clearance of the tumour through help of the immune system as well as it is a sharp indication of lack of self-renewal potential in the tumour population besides that SIS gets delayed by inhibition of the autophagy (Xue et al., 2007; Gewirtz et al., 2008). Although interconnection between autophagy and apoptosis is clearly investigated but crosstalk between senescence and autophagy is poorly understood. The first direct connection between autophagy and senescence reported by Young et al., 2009 where genetical and pharmacological inhibition of autophagy abrogated the senescence phenotype (Young et al., 2009, Gewirtz et al., 2013).

1.5. Ribosome inactivating protein type II and Abrus agglutinin

Lectins are ubiquitous proteins, or glycoproteins, that are non-immunoglobulin in nature and contain at least one non-catalytic domain that binds reversibly to specific carbohydrates without altering their structure (Panda et al., 2014). Out of three major lectin families like i)

the legume lectin, ii) the type II ribosome inactivating proteins (RIPsII) and GNA related lectins, the type II ribosome inactivating protein has been extensively studied due its antitumour and immune modulatory activities.

Ribosome-inactivating proteins (RIPs) are proteins which inhibit protein synthesis irreversibly. RIPs exert their cytotoxicity effect by binding to the larger 60S ribosomal subunit on which they act as N-glycosidase by cleaving the A-4324 in the 28S ribosomal rRNA subunit. Although, RIPs ubiquitously present in nature but they are predominantly found in the plants, fungi as well as in bacteria. Generally RIPs have been categorized into three types (i) type-I (consists of single polypeptide chain having molecular weight approximately 30 kDa (ii) type-II (consists of toxic A chain and carbohydrate binding B chain) (iii) type-III RIPs which acts as a inactive precursor (ProRIPs) to form RIPs (Wesche et al., 1999). As type II RIPs contained carbohydrate binding B chain, therefore, it was considered as a lectin and also categorized as one the major family of lectins (Dang et al., 2015).

Generally, type II RIPs uses an efficient strategy for entering to the mammalian cells and for that cause they are generally potent toxins even at picomolar range. For example, *Abrus* agglutinin binds to glycoconjugate receptors on the cell surface with their carbohydrate binding B chain which facilitates the entry of the protein into the cell following endocytic pathway. Subsequent transport from the endosome to the Golgi, RIPs reach the ER lumen by retrograde transport mechanism, where the catalytic A chain reductively separated from the carbohydrate binding B chain domain and enters the cytosol and escape degradation due to its low lysine content, therefore blocking the interaction between the Elongation factor 2 (EF-2) and ribosome resulting arrest of protein synthesis ultimately inducing apoptotic or autophagic cell death. Very often type-II RIPs are more efficient for animal ribosomes (Fig.1.1).

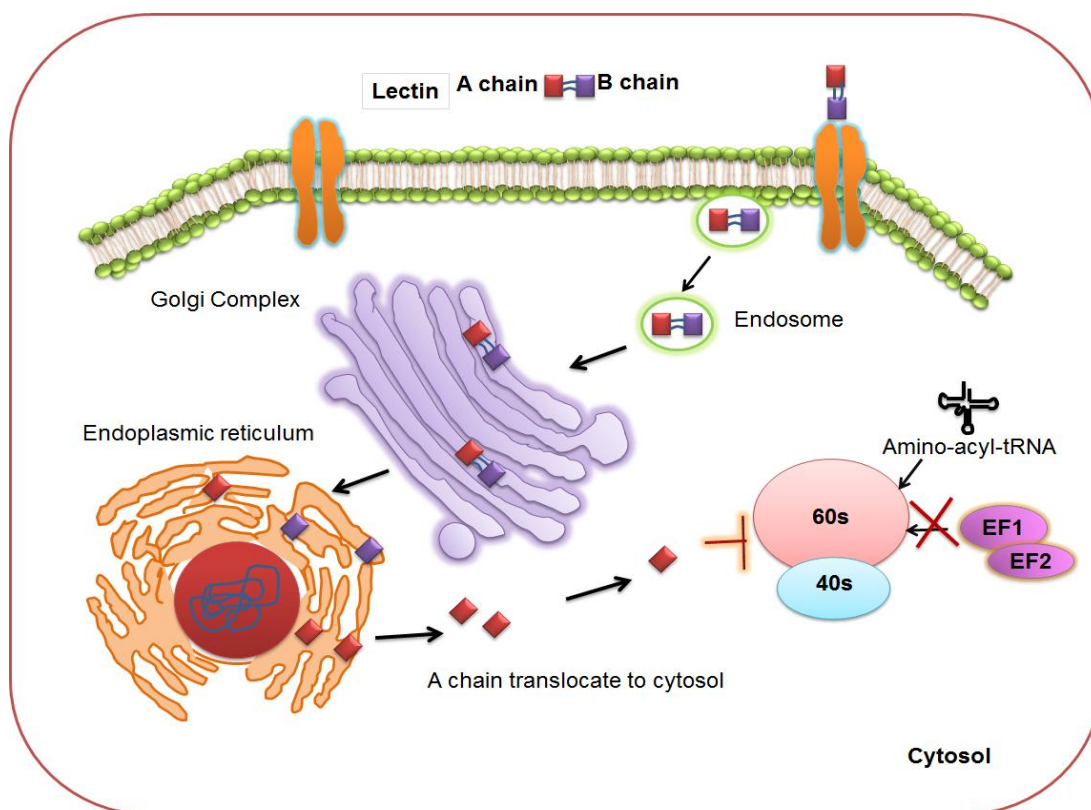


Fig.1.1. Mechanism of action of type II ribosome inactivating proteins in mammalian cells.

AGG is a type II ribosome inactivating proteins isolated from the seeds of *Abrus precatorius*, a hetero-tetrameric glycoprotein of 134-kDa molecular weight, composed of two A and two B chains linked through disulfide bridges. AGG has specificity towards [gal (β 1 \rightarrow 3) gal NAC] with a protein synthesis inhibitory concentration (IC_{50}) of 0.469 μ g/ml and a lethal dose (LD_{50}) 5 mg/kg body weight in mice (Hegde et al., 1991; Bhutia et al., 2008). AGG contains cytotoxic A chain having ribosomal RNA N-glycosidase activity which cleaves glycosidic bond at position A-4324 within the universally conserved α -sarcin loop of the 28S ribosomal RNA of eukaryotes while the B chain binds to carbohydrate moieties on the cell surface and facilitates the internalization of the entire toxin into the cell (Bagaria et al., 2006).

Chapter 2

Review of literature and objectives

2. Introduction

Autophagy in cancer is an intensely debated concept in the field of translational research. The dual nature of autophagy implies that it can potentially modulate the pro-survival and pro-death mechanisms in tumor initiation and progression. There is a prospective molecular relationship between defective autophagy and tumorigenesis that involves in the accumulation of damaged mitochondria and protein aggregates, which leads to the production of reactive oxygen species (ROS) and ultimately causes DNA damage that, can lead to genomic instability. Moreover, autophagy regulates necrosis and is followed by inflammation, which limits tumor metastasis. On the other hand, autophagy provides a survival advantage to detached, dormant metastatic cells through nutrient fuelling by tumour-associated stromal cells. Manipulating autophagy for induction of cell death, inhibition of protective autophagy at tissue and context dependent for apoptosis modulation has therapeutic implications.

Cancer is known to comprise a deadly array of many diseases in which tissues grow and spread throughout the body, ultimately leading to death, and it is manifested by various hallmarks such as high proliferative signal, resistance to cell death, avoidance of growth suppressors, a high replication potential and sustained angiogenesis along with activation of tissue invasion and metastasis, as well as the avoidance of immune attacks (Hanahan et al., 2011).

2.1. Autophagy and its Regulation

Autophagy initiation occurs with the formation of a phagophore, or isolation membrane (Fig.2.1). In mammals, Unc-51-like kinases 1/2 (Ulk1/2) exist in a complex with Atg13 along with the scaffold protein FIP200 (ortholog of yeast Atg17) and the mammalian target of rapamycin (mTOR). The activity in this complex is controlled by nutrient sensing. Between mTORC1 and mTORC2, mTORC1 is the predominant form that is associated with autophagy. Under nutrient starvation, a decrease in mTORC1 activity leads to dephosphorylation of Ulk1/2 and activates Ulk1/2 to phosphorylate mAtg13 and FIP200. A new mAtg13 interacting protein, Atg101, which interacts with Ulk1 in an mAtg13 dependent manner, is essential for autophagy. The Ulk complex accumulates during the initiating time of isolation membrane formation. The phagophore formation is controlled by the activation of the class III phosphatidylinositol 3-kinase (PI3K) (Vps34), which exists in a complex with BECN1 and p150 (homolog of Vps15) and can convert phosphatidylinositol (PtdIns) to PtdIns(3)P. Two Vps34 positive mediators, ultraviolet irradiation resistance-associated gene (UVRAG) and bax interacting factor-1 (Bif-1) can enhance the activity by interacting with

BECN1. In contrast, Bcl-2, Bcl-xL, and run domain BECN1 interacting cysteine-rich containing protein (Rubicon) inhibit this interaction. The Vps34 interacts with Atg14, which directs the complex to the nascent autophagosomal membrane and then the PtdIns(3)P recruits PI3P effector proteins to the phagophore sites for guiding the growth of the autophagic membrane (Simonsen et al., 2009; Funderburk et al., 2010).

Elongation of the isolation membrane and conversion to a nascent closed autophagosome is mediated by the two ubiquitin like protein conjugated systems. The ubiquitin-like Atg12 is activated by the E1-like enzyme Atg7 and binds to the E2-like enzyme Atg10 before being transferred to Atg5. The Atg12–Atg5 conjugate noncovalently interacts with the small coiled coil protein, Atg16L (ortholog of yeast Atg16), finally oligomerizing to form a large multimeric Atg12–Atg5–Atg16L complex. Atg16L directs this complex to the outer autophagosomal membrane, which is, partially responsible for the membrane's concave nature, and it dissociates from the membrane upon completion of the autophagosome (Geng et al., 2008). The second ubiquitin like pathway involves LC3 (mammalian ortholog of Atg8) lipidation, which plays an essential role in membrane dynamics during autophagy. LC3 is synthesized as a precursor protein, proLC3, and it is then cleaved at its C-terminus by the protease Atg4B, resulting in the cytosolic isoform LC3-I. LC3-I is conjugated to phosphatidylethanolamine (PE) in a reaction involving Atg7 (E1-like) and Atg3 (E2-like) to form membrane-bound LC3-II. LC3-II is recruited to both the outer and inner surfaces of the autophagosomal membrane. It specifically targets the elongating autophagosome membrane and remains the completed autophagosomes until fusion with lysosomes. After fusion, LC3-II on the cytoplasmic face of autolysosomes can be delipidated by Atg4 and recycled, whereas proteins found on the internal surface of autophagosomes are degraded in autolysosomes (Kabeya et al., 2000).

The maturation process first involves fusion of the autophagosome with endosomes or endosome-derived vesicles to form an amphisome, and then with lysosomes to form an autolysosome. Lysosomal-associated membrane protein 2 (LAMP2) and Ras-related protein Rab-7a is essential for the docking and fusion of autophagosomes with lysosomes to form autolysosomes. UVRAG is also involved in the maturation step by recruiting tethering proteins to the autophagosomal membrane, thus activating Rab7 by promoting fusion with lysosomes. After fusion, autophagosomal cargo is digested by acidic hydrolases, resulting in nutrient and energy reflux (Bhutia et al., 2013; Kimura et al., 2008).

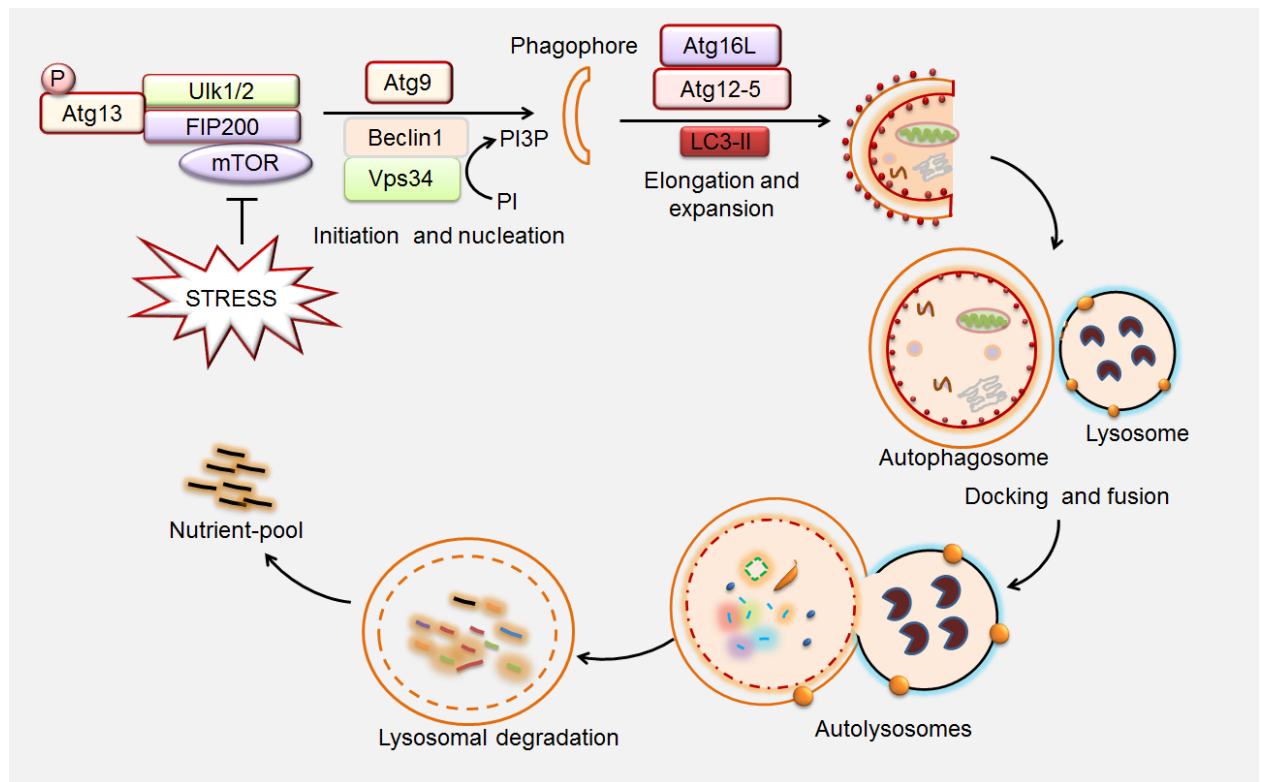


Fig. 2.1. The process of autophagy. Autophagy is initiated with the formation of a phagophore, which is regulated by the Uik1/2–Atg13–FIP200 complex. Phagophore formation is promoted by activation of the class III phosphatidylinositol 3-kinase, (Vps34) which exists in a complex with BECN1, and p150 (homolog of Vps15). The phagophore elongation is mediated by two ubiquitin-like protein conjugated systems, Atg12–Atg5 and PE-conjugated Atg8 (LC3-II), and is converted to an autophagosome. The autophagosome fuses with endosomes or endosome-derived vesicles to form an amphisome and then with lysosomes to form the end-stage vesicle of autophagy: the autolysosome.

Although autophagy is considered to be a random degradation process engulfing the cargo indiscriminately, recently, showed that phagophore membrane can interact with specific protein aggregates and organelles for selective autophagy. The best example in this process is the targeting polyubiquitinated protein aggregates through multi-adaptor molecule p62 which interacts with Atg8/LC3 on the phagophore for degradation (Panda et al., 2015). Similarly, damaged lysosomes are selectively engulfed by autophagosome through ubiquitin dependent autophagy to control lysosome biogenesis (Maejima et al., 2013). Moreover, Atg32 present on the surface of mitochondria during oxidative stress has been identified in yeast enables mitophagy, selective uptake of mitochondria (Okamoto et al., 2009). For pexophagy in yeast, Atg36 interacts with peroxisomal membrane protein Pex3 at the peroxisomal membrane which recruits Atg8 and the adaptor Atg11 for peroxisomes degradation (Motley et al., 2012). In addition, Ypt/Rab GTPase, regulators of vesicular transport in association with autophagic protein Atg11 regulates ER-phagy to clear excess and/or misfolded proteins on aberrant ER structures for maintenance cellular homeostasis (Lipatova et al., 2013).

2.2. Autophagy and Cancer

Autophagy is connected to cancer through its pro-survival and pro-death functions (Fig.2.2). Its pro-survival function helps cancer cells to survive in nutrient-limited conditions and resist ionizing radiation and chemotherapies. Alternatively, the pro-death function helps to kill cancer cells, either spontaneously or when they are exposed to radiation and chemotherapy.

2.2.1 Autophagy and Tumor Suppression

A substantial amount of circumstantial evidence exists to support a role for autophagy inhibition in tumorigenesis, indicating that autophagy may be a bonafide tumor suppressor mechanism. Among autophagy genes, BECN1 was initially identified as a tumor suppressor (Liang et al., 1999 and Qu et al., 2008); the BECN1 locus is located at 17p21, and this region is deleted in up to 75% of ovarian cancers and 50–70% of breast cancers. Heterozygous BECN1 increases the frequency of spontaneous malignancies and accelerates the development of hepatitis B virus induced premalignant lesions. Atg4C knockdown mice showed increased susceptibility to developing fibrosarcoma induced by chemical carcinogens (Marino et al., 2007). A recent report showed that frameshift mutations in Atg2B, Atg5, Atg9B, and Atg12 are associated with gastric and colorectal cancers (Kang et al., 2009). Loss of Bif-1 suppresses programmed cell death and promotes colon adenocarcinomas. Although Bif-1 null mice develop normally, with the exception of an enlarged spleen, they have an increased incidence of spontaneous tumor formation; 82.8% of Bif-1 null mice developed lymphoma compared with 14.3% of their wild type counterparts (Coppola Qu et al., 2008). Similarly, a mutation in another autophagy gene, exon 8 of UVRAG, resulted in decreased autophagy activity and increased the occurrence of colorectal and gastric carcinoma (Kim et al., 2008). Interestingly, loss of UVRAG is correlated with increased tumorigenesis, and the UVRAG^{-/-} tumorigenic phenotype, whereas the administration of exogenous UVRAG shows the reverse effect (Liang et al., 2006). Likewise, MAP1LC3 is localized to 16q24.1, a locus frequently deleted in the liver, breast, prostate, and ovarian cancers (Jin et al., 2006). The liver of Atg7 conditional knockout mice developed hepatomegaly, which may lead to malignant transformation, and their hepatocytes accumulate abnormal mitochondria as well as polyubiquitinated protein aggregates (Komatsu et al., 2005). Overall, there is strong evidence that ATG proteins display tumor suppression characteristics, and the associated reduction in autophagy might lead to tumorigenesis.

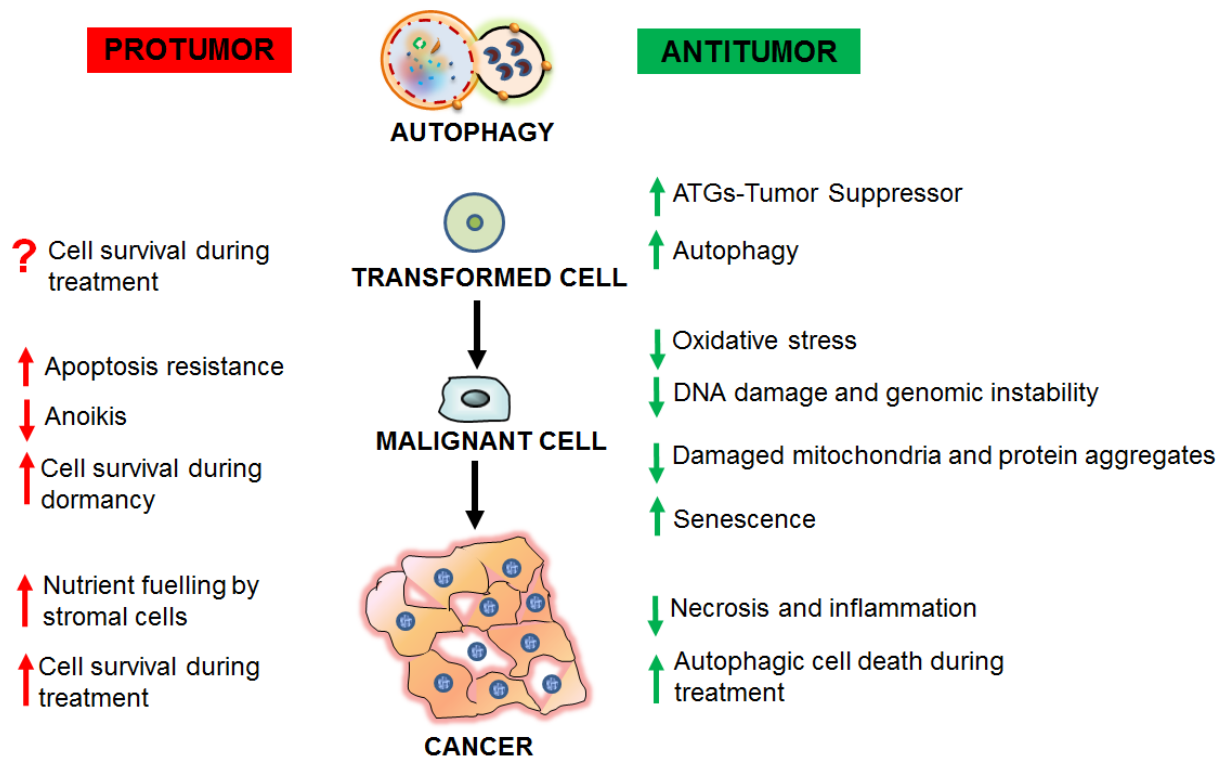


Fig.2.2. Pro- and anti-tumor roles of autophagy in different stages of cancer. The antitumor potential of autophagy manifests in several ways, such as the tumor suppressive role of Atg proteins, oncogene induced senescence, mitigating oxidative stress, removing damaged mitochondria and protein aggregates, inhibiting necrosis and inflammation, and preventing DNA damage and genome instability. The pro-tumor activity of autophagy is characterized by increasing resistance to apoptosis, avoiding anoikis, metastasis and survival during therapy. However, the pro-tumor role of autophagy during the initial period of tumor progression is not clear when therapy is introduced.

2.2.2 Autophagy and Senescence

Cellular senescence is a state of irreversible cell cycle arrest that limits the proliferation of damaged cells. It is considered as a tumor suppressor mechanism. Autophagy limits tumorigenesis by inducing tumor senescence via regulation of oncogenes (Young et al., 2009). Accordingly, autophagy is activated during oncogene- and DNA damage-induced senescence. For example, autophagy was shown to mediate Ras oncogene induced senescence. RNAi mediated depletion of Atg5 or Atg7 facilitates the ability of cells to bypass oncogene induced senescence and delays senescence-associated cytokine production, indicating that autophagy may contribute to senescence arrest. Similarly, a subset of Atgs (Ulk1/3) is upregulated during senescence; overexpression of Ulk3 was shown to induce autophagy and senescence simultaneously. These results indicate that basal autophagy plays an important role in restricting cell growth and proliferation during oncogenic stress as well as precluding further genomic insults. Additionally, senescence induced by hyperactivation of Akt was mediated through mTORC1, although details regarding the involvement of autophagy in this mechanism need to be elucidated (Astle et al., 2012). Moreover, it was

observed that combining autophagy inhibitors with radiation treatment could trigger premature senescence in both cancer cells and xenograft models, which is an approach to restoring radiosensitivity (Nam et al., 2013).

2.2.3 Autophagy and Oxidative Stress

Oxidative stress plays a vital role in the induction of autophagy, and particularly mitophagy, to prevent tumor growth and progression. Autophagy suppresses tumors by regulating intracellular ROS levels through the removal of damaged mitochondria and protein aggregates. The excessive accumulation of damaged mitochondria and unfolded protein masses in autophagy defective cells leads to increased ROS levels, which causes DNA damage as well as p62 accumulation (Karantza-Wadsworth et al., 2007 and Komatsu et al., 2010). During this process, damaged mitochondria lose membrane potential by activating PTEN induced putative kinase 1 (PINK1) following activation of the E3 ligase parkin (PARK2) to ubiquitylate mitochondrial outer membrane proteins, thus providing the autophagic degradation signal. PARK2 is a tumor suppressor gene and its deletion causes hepatocellular carcinoma in mice (Fujiwara et al., 2008). In addition to hepatocellular carcinoma, PARK2 was frequently mutated in colorectal cancer in mouse and human glioblastomas (Veeriah et al., 2010). Moreover, p62 accumulation in response to metabolic stress leads to ROS generation, thereby producing a positive feedback loop. In this system, constitutive p62 accumulation activates NF- κ B and other antioxidant defenses to protect autophagy deficient damaged cells from oxidative stress, thus favoring tumorigenesis (White et al., 2012).

2.2.4 Autophagy and Genome Damage

In autophagy deficient cells, there is an accumulation of DNA damage and chromosomal instability, including double stranded DNA breaks, centrosome abnormalities, and increased DNA content before the onset of tumorigenesis (Mathew et al., 2007). When autophagy is defective, misfolded proteins, dysfunctional mitochondria, generation of ROS and oxidative stress, and failure of energy homeostasis potentially induce genome damage when autophagy is defective. Autophagy defects activate the DNA damage response *in vitro* and in mammary tumors *in vivo*, promoting gene amplification and it also synergizes with defective apoptosis to promote mammary tumorigenesis (Luo et al., 2013). It is speculated that autophagy inhibition induces genome damage by promoting toxic ROS or by directly regulating DNA repair mechanisms. Studies have shown that compromised autophagy can activate the DNA damage response and encourage genome damage, potentially challenging DNA repair mechanisms; additionally, ROS generation promotes a cascade of events, including increased oxidative stress, DNA damage, and chromosomal instability, which ultimately

lead to inhibition of the NF- κ B pathway and development of hepatocarcinoma (Bhutia et al., 2013; Karantza-Wadsworth et al., 2007).

2.2.5 Autophagy and Metastasis

Another important autophagy mediated tumor suppression mechanism is the inhibition of necrotic cell death of apoptosis resistant cells during metabolic stress (Bhutia et al., 2013). In the tumor microenvironment, necrosis that occurs in response to hypoxia and metabolic stress induces inflammation and leads to the invasion of inflammatory cells to tumor sites (DeNardo et al., 2009). Although certain inflammatory cells, including cytotoxic T cell and natural killer cells, are antimetastatic, tumor inflammation associated with severe hypoxia and metabolic stress largely supports pro-tumor immunity. Importantly, infiltration of pro-tumor, inflammatory macrophages correlates with poor clinical prognosis (DeNardo et al 2009). The tumor suppressive activity of autophagy functions by restricting necrosis in apoptosis resistant cells and preventing macrophage-associated tumor inflammation (Degenhardt et al., 2016). Apoptosis deficient, autophagy incompetent cells are more prone to becoming necrotic in response to metabolic stress, thus promoting cancer progression. Moreover, this study showed that growth factors promote tumor growth and progression enhanced necrotic cell death, which are achieved through suppression of autophagy by activating the PI3K–Akt–mTOR pathway.

Anoikis is a form of apoptosis that serves as a protective mechanism against cancer progression when cells are detached from the extracellular matrix. Matrix detachment promotes cell survival by inducing autophagy in nontumorigenic epithelial lines and primary epithelial cells. Although autophagy-mediated cell death was initially recognized to be associated with anoikis, a more recent study provided evidence to support the protective nature of autophagy in anoikis (Funget al., 2008; Kenific et al., 2010). The AMP activated protein kinase (AMPK) stress response pathway is involved in mediating anoikis resistance by inhibiting mTOR and suppression of protein synthesis. The Ras/mitogen activated protein kinase (MAPK) and PI3K/Akt pathways are common mechanisms utilized by cancer cells to evade anoikis (Ng et al., 2012). During dormancy, autophagy may allow residual or metastasizing tumor cells to tolerate metabolic deprivation and recover when favorable growth conditions occur. This is a daunting clinical problem, and the frequent reemergence of tumors occurs even after treatment because of prolonged dormancy (Aguirre-Ghiso et al., 2006). In ovarian cancer cells, autophagy is upregulated by the tumor suppressor aplasia Ras homolog member I (ARHI), which promotes *in vivo* survival of dormant cells in tumor microenvironments (Bhutia et al., 2013; Lu et al., 2008). In fact, dormant cells are not

proliferative and are thus resistant to conventional chemotherapy that typically targets rapidly growing cells.

2.2.6 Autophagy and Cancer Metabolism

During tumorigenesis, cancer cells trigger oxidative stress in bystander cells, including adjacent tumor-associated fibroblasts (TAFs) and possibly other stromal cells, to feed cancer cells. This is known as the reverse Warburg effect (Martinez-Outschoorn et al., 2010). ROS driven oxidative stress induces autophagy and mitophagy as well as loss of mitochondrial function. It increases aerobic glycolysis, which releases nutrients, such as lactate and ketones, into stromal cells in the tumor microenvironment; this leads to stromal overproduction of recycled nutrients, including energy rich metabolites (Lisanti et al., 2010). The recycled nutrients or chemical building blocks then help drive mitochondrial biogenesis in cancer cells, which in turn “fuel” mitochondrial generation and oxidative phosphorylation in cancer cells, thereby promoting the anabolic growth of cancer cells. These results showed that ketones and lactate stimulate tumor growth and metastasis and could serve as chemo-attractants for cancer cells (Pavrides et al., 2010). Autophagy in TAFs and mitochondrial metabolism in cancer cells produce an aggressive tumor phenotype. Recently, damage regulated autophagy modulator (DRAM) and liver kinase B1 (LKB1) overexpressing autophagic fibroblasts showed mitochondrial dysfunction and increased production of mitochondrial fuel. Alternatively, GOLPH3 overexpressing autophagy resistant breast cancer cells had signs of increased mitochondrial biogenesis and function, which resulted in increased tumor growth (Salem et al., 2012).

2.3. Autophagy and Apoptosis Connection in Cancer Therapy

In response to cancer therapy, tumor cells undergo apoptosis and/or autophagic cell death. The connection between autophagy and apoptosis is complex and is currently being investigated. The interactions between apoptosis and autophagy manifest in various ways, such that the induction of autophagy/apoptosis can be simultaneous, sequential, independent, synergistic, or antagonistic of one another (Fig.2.3).

2.3.1 Inducing both Apoptosis and Autophagic Cell Death –“Simultaneous” Approach

Apoptosis and autophagic cell death may occur simultaneously and inhibition of autophagic activity in cells may switch responses to death signals from autophagic cell death to apoptotic cell death and vice versa. Molecules that induce both autophagic death and apoptosis would have better therapeutic potential for cancer treatment. Several studies have shown that certain anticancer drugs, including both natural and synthesized molecules are able to simultaneously elicit both the type I and II forms of programmed cell death. For example, butyrate and suberanilohydroxamic acid (SAHA), which are HDAC inhibitors,

induce both mitochondria mediated apoptosis and caspase independent cell death, which has therapeutic implications for treating different types of cancers. Similarly, the multiple tyrosine kinase inhibitor sorafenib induces both autophagic and apoptotic cell death in prostate cancer cells (Ullén et al., 2010). Additionally, cannabidiol is an inherently potent, natural compound that inhibits the AKT/mTOR/4EBP1 signaling pathway and induces both apoptosis and autophagic cell death in breast cancer cells (Shrivastava et al., 2011).

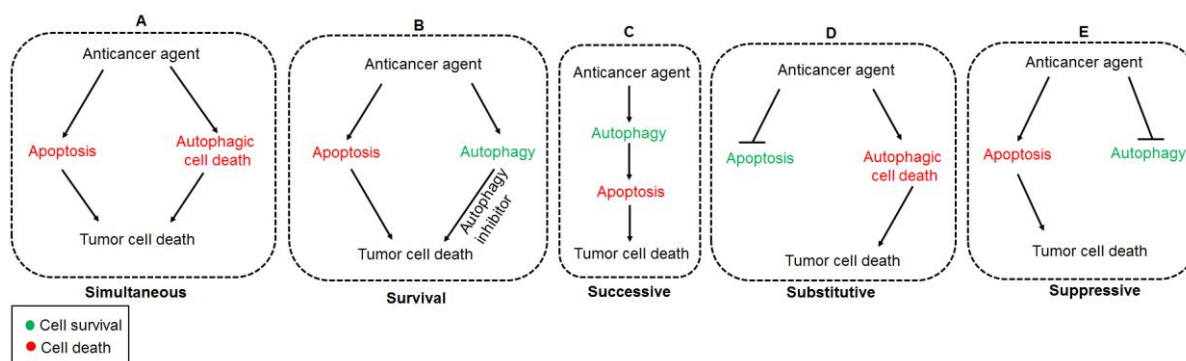


Fig.2.3. Apoptosis–autophagy interaction during cancer therapy. In response to cancer therapy, tumor cells undergo apoptosis and/or autophagic cell death. (A) Apoptosis and autophagy may occur in a simultaneous manner, and inhibition of autophagic cell death switches to apoptosis or vice versa (Simultaneous approach). (B) Apoptosis and autophagy occur at the same time; inhibition of protective autophagy shifts to apoptosis (Survival approach). (C) Apoptosis is preceded by or depends on autophagy; inhibition of autophagy delays apoptosis but the reverse does not occur (Successive approach). (D) Autophagic cell death is an alternative to apoptosis-resistant/deficient cancer cells (Substitutive approach). (E) Apoptosis is promoted, and protective autophagy is inhibited (Suppressive approach).

2.3.2 Inducing Apoptosis and Autophagy – “Survival” Approach

In this case, anticancer drugs induce apoptosis and protective autophagy, and both processes are manifested simultaneously. Inhibition of protective autophagy increases apoptotic cell death and inhibition of apoptosis, by broad-range caspase inhibitors, fails to affect or enhance protective autophagy. These types of responses are widely observed to have clinical implications for several currently used chemotherapeutic agents. Anticancer drugs in combination with autophagy inhibitors, including CQ/HCQ, inhibit protective autophagy and may provide better therapeutic outcomes in cancer patients.

2.3.3 Autophagy Switches to Apoptosis – “Successive” Approach

In some situations, a manifestation of apoptosis is preceded by and even depends on the occurrence of autophagy. In these situations, inhibition of autophagy delays apoptosis, whereas broad range caspase inhibitors fail to inhibit autophagy. Our previous report showed that ATGs are involved in autophagy to apoptosis switching in different cellular settings (Panda et al., 2014). Activation of caspases and calpains cleave autophagic proteins that inhibit autophagy and was followed by apoptosis. For example, we showed that protective autophagy mediated by mda-7/IL24 switches to apoptosis through cleavage of ATG5 in

prostate cancer cells (Bhutia et al., 2010). Moreover, different anticancer molecules have this approach to induce cancer cell death. Interestingly, selenite, a common dietary chemotherapeutic agent, inhibited heat shock protein 90 mediated activation of NF- κ B, which switches autophagy to apoptosis through BECN1 transcriptional inhibition in NB4 cells (Jiang et al., 2011). Moreover, MS-275, a synthetic benzamide derivative of HDAC, induced autophagy switching to apoptosis through p38 modulation in human colon cancer cells (Ullén et al., 2010; Zhan et al., 2012). Similarly, inhibition of Akt reverses the acquired resistance to sorafenib by switching protective autophagy to apoptosis in hepatocarcinoma (Zhai et al., 2014). These findings demonstrate that excessive autophagy regulates the apoptotic pathway, and the potential for autophagy and apoptosis crosstalk as a possible mechanism of action for effective antitumor responses can be exploited as a unique strategy for treating cancer.

2.3.4 Inducing Autophagic Cell Death in Apoptosis Deficient/Resistant Cells – “Substitutive” Approach

Autophagic death or type II programmed cell death, as an alternative mechanism in apoptosis-deficient/resistant cells could enhance the effect of cancer therapy as well as address the emerging problem of drug resistance. The clinical utility of taxanes in advanced cases of breast and ovarian cancers is limited because of their chemoresistance. With respect to this interaction, Ajabnoor et al. induced paclitaxel resistance in MCF-7 cells at clinically relevant drug doses with profound downregulation of apoptotic molecules and showed a progressive mechanistic shift to autophagic death as the principal mechanism of drug induced cytotoxicity (Ajabnoor et al., 2012). Similarly, naturally occurring alkaloid molecules, including isoliensinine, dauricine, and cepharanthine induce autophagic death in apoptosis defective cells. In most invasive carcinoma cases, particular molecules like PI3K, Akt, mTOR, NF- κ B, and MEK/ERK were aberrantly expressed, resulting in apoptotic resistance to various therapeutic approaches (Shackelford et al., 2009, Santarpia et al., 2012). Interestingly, Akt inhibition stimulated autophagy and sensitized PTEN null tumors to lysosomotropic agents (Degtyarev et al., 2008).

2.3.5 Inducing Apoptosis and Inhibition of Autophagy – “Suppressive” Approach

In this case, anticancer molecules activate apoptosis and simultaneously inhibit protective autophagy, which acts as a survival mechanism of cancer cells. In this context, protective autophagy inhibition is induced by the same anticancer molecules that induce apoptosis. For example, progesterone, in combination with epirubicin, was shown to increase apoptosis and decrease protective autophagy in human hepatoma HA22T/VGH cells (Chang et al., 2014). Similarly, dihydro-selenoquinazoline, a seleno-compound, induced apoptosis and inhibited

autophagy through downregulation of S6 ribosomal protein signaling in MCF-7 cells, revealing a valuable approach for preventing and overcoming resistance in cancer cells (Moreno et al., 2014).

2.4. Autophagy as Cancer Preventive

Diet associated autophagy may be an effective approach to cancer prevention. Autophagy induction by carotenoids, lycopene, lutein, polyphenols, resveratrol, curcumin and epigallocatechin-3-gallate has been implicated in the ability of these dietary compounds to inhibit reactive oxygen/nitrogen species accumulation. For example, curcumin treatment stimulated G2-M arrest along with nonapoptotic cell death in malignant glioma cells following the inhibition of the Akt/mTOR/p70S6 kinase pathway and activation of the ERK1/2 pathway (Shinojima et al., 2007). On the other hand, treatment with soyasaponins in human colon cancer cells was shown to suppress proliferation and induce autophagy by the pronounced accumulation of autophagosomes. Besides apoptosis, the food polyphenol quercetin can specifically stimulate autophagic vacuolization in Ha-Ras transformed human Caco2 colon cancer cells (Ellington et al., 2005). Acting as a vital tool in cancer prevention, vitamin D induced autophagy was shown to abrogate the risk of developing blood, prostate, colon, and breast cancers (Wang et al., 2008 and Bristol et al., 2012). Studies report that calorie restriction extended life span by stimulating autophagy, reducing insulin and glucose levels, and decreasing growth hormone insulin like growth factor-I axis signaling (Yang et al., 2014). Some epidemiological factors can increase autophagy that is associated with decreased cancer risk. For example, physical exercise stimulates Bcl-2 regulated autophagy, which maintains muscle glucose homeostasis (Grumati et al., 2011). Exercise induces autophagy in muscle, liver, pancreatic cells, and adipose tissue and mice that exhibit increased autophagy in these tissues are protected against glucose intolerance, leptin resistance, as well as increased serum cholesterol and triglyceride levels induced by a high fat diet (He et al., 2012). It remains a paramount concern whether autophagy-based preventive approaches can be developed into suitable therapeutic strategies.

2.5. Abrus Agglutinin: The Golden Bullet

Use of plant products in cancer research are extensively studied for their cost effective and ease available. Moreover, AGG, the plant lectin showed early tumoricidal activity in both rat and mice (Bhutia et al 2016). Besides, our group reported several antitumors and immunomodulatory activity in AGG in both *in vitro* and *in vivo*. Both native and heat denatured AGG found to proliferate splenocytes derived T cells and B cells acting as a potential immune regulator (Ghosh et al., 2009, Ghosh et al., 2007, Tripathi et al., 2005; Tripathi et al., 2003). Importantly, *Abrus* agglutinin derived peptide from 10 kDa molecular

weight cut-off membrane showed significant antitumor and immunostimulatory induction potential in tumor loaded mice (Bhutia et al., 2008; Bhutia et al., 2008a; Bhutia et al., 2009). Likely, AGG induces caspase dependent cell death by inhibiting the expression of HSP90 and phosphorylation of Akt in liver cancer HepG2 cells. It also suppresses the growth of liver cancer xenograft and decreases the staining of both CD-31 and Ki-67 in AGG treated mice (Mukhopadhyay et al., 2014). Recently our group documented AGG induces both intrinsic and extrinsic apoptosis through ROS dependent manner and inhibits IGFBP-2 expression and consequently angiogenesis. AGG also reduces the size of the of the tumor xenograft in nude mice (Bhutia et al., 2016).

2.6. Objectives of the PhD Work

With this background support of significant antitumor potential of *Abrus* agglutinin both *in vitro* and *in vivo*, we have tried to decipher the autophagy inducing potential of *Abrus* agglutinin as an alternative tumor suppressor mechanism. The objective of the present piece of work as follows:

- *Abrus* agglutinin inhibits Akt/PH domain to induce endoplasmic reticulum stress mediated autophagy dependent cell death
- PUMA dependent mitophagy by *Abrus* agglutinin contributes to apoptosis through ceramide generation
- SIRT1/LAMP1 signaling activation by *Abrus* agglutinin regulates autophagy mediated senescence
- *Abrus* agglutinin induces cancer stem cell differentiation through BMP2 mediated autophagy

Chapter 3

***Abrus* agglutinin inhibits Akt/PH domain to induce endoplasmic reticulum stress mediated autophagy dependent cell death**

Abstract

Abrus agglutinin (AGG), a type II ribosome-inactivating protein has been found to induce mitochondrial apoptosis. In the present study, we documented that AGG mediated Akt dephosphorylation led to ER stress resulting in the induction of autophagy dependent cell death through the canonical pathway in cervical cancer cells. Inhibition of autophagic death with 3-Methyladenine (3-MA) and siRNA to BECN1 and ATG5 increased AGG induced apoptosis. Further, inhibiting apoptosis by Z-DEVD-FMK and N-acetyl cysteine (NAC) increased autophagic cell death after AGG treatment, suggesting that AGG simultaneously induced autophagic and apoptotic death in HeLa cells. Additionally, it observed that AGG induced autophagic cell death in Bax knock down (Bax-KD) and 5-FU resistant HeLa cells, confirming as an alternate cell killing pathway to apoptosis. At the molecular level, AGG induced ER stress in PERK dependent pathway and inhibition of ER stress by salubrinal, eIF2 α phosphatase inhibitor as well as siPERK reduced autophagic death in the presence of AGG. Further, our *in silico* and colocalization study showed that AGG interacted with pleckstrin homology (PH) domain of Akt to suppress its phosphorylation and consequent downstream mTOR dephosphorylation in HeLa cells. We showed that Akt overexpression could not augment GRP78 expression and reduced autophagic cell death by AGG as compared to pcDNA control, indicating Akt modulation was the upstream signal during AGG's ER stress mediated autophagic cell death. In conclusion, we established that AGG stimulated cell death by autophagy might be used as an alternative tumor suppressor mechanism in human cervical cancer.

Key words: *Abrus* agglutinin; autophagic cell death; apoptosis; ER stress; Akt; PH domain

3.1. Introduction

Autophagy is an evolutionary conserved catabolic process in which stressed cells form cytoplasmic, double layered, crescent shaped membranes known as phagophores, which mature into complete autophagosomes. The autophagosome engulfs damaged cytoplasmic organelles and long lived proteins to provide cellular energy and building blocks for cellular biosynthesis (Panda et al., 2015 and Bhutia et al., 2013). The autophagosome fuse with lysosome to form autolysosome and cargo are digested by lysosomal hydrolases to metabolites and released back to the cytosol for recycling. The autophagic process is regulated by the ATG genes (autophagy-related genes) and the proteins encoded by the autophagy related genes (ATG) are required for the regulation of autophagic vesicles. Initially, the autophagic pathway functions as an adaptive response to stress. However, in the

face of extreme or protracted stress, cells are committed to autophagic cell death; type II programmed cell death (PCD) (Panda et al., 2015; Panda et al., 2014).

Cervical cancer is the fourth leading cause of cancer cell death and third most commonly diagnosed cancer occur in developing countries including India, and other parts of Asia due to inadequate access to screening services and lack of human papillomavirus (HPV) vaccination (Jemal et al., 2011; Suneja et al., 2015). In the era of cancer therapy, apoptosis induction in tumor cells is increasingly seen as prime candidates for the development of anticancer therapeutics for cervical cancer. However, development of resistance phenomena to apoptosis and ineffectiveness of single treatment modality allow cancer cells to survive, consequently escape current cancer therapy. Therefore, novel therapeutic strategies are needed to enhance the effect of cancer therapy as well as address the emerging problem of drug resistance. Induction of autophagic death, a type II programmed cell death, could be a potentially useful therapeutic approach in apoptosis resistant cancer cells. (Panda et al., 2015; Dalby et al., 2010). Moreover, because cancer cells often display defective apoptotic propensity, autophagy is considered as a tumor suppressor mechanism. As an alternative therapy for cancer, recently more efforts are made for the development of novel molecules that specifically targets the autophagic cell death mechanism (Liu et al., 2013; Fu et al., 2011; Moustapha et al., 2015).

Abrus agglutinin (AGG) is one such prime candidate whose autophagic attributes are being documented in this work. AGG isolated from the seeds of *A. precatorius* is a heterotetrameric glycoprotein of 134-kDa molecular weight, composed of two A and two B chains linked through disulfide bridges. AGG has specificity towards [gal (β 1 \rightarrow 3) gal NAc] and belongs to type II ribosome inactivating protein family (RIP II) with a protein synthesis inhibitory concentration (IC₅₀) of 0.469 μ g/ml and a lethal dose (LD₅₀) 5 mg/kg body weight in mice (Hegde et al., 1991; Bhutia et al., 2008). AGG contains cytotoxic A chain having ribosomal RNA N-glycosidase activity which cleaves glycosidic bond at position A-4324 within the universally conserved α -sarcin loop of the 28S ribosomal RNA of eukaryotes while the B chain binds to carbohydrate moieties on the cell surface and facilitates the internalization of the entire toxin into the cell (Bagaria et al., 2006). Our groups have previously elucidated the anticancer effects of AGG in several tumor models at sublethal doses by direct killing of tumor cells through extrinsic and intrinsic apoptosis (Ghosh et al., 2007; Mukhopadhaya et al., 2014; Bhutia et al., 2016). Along with direct antitumor potential, AGG generates potent humoral and cellular immune responses in normal as well as tumor-bearing animals (Ghosh et al., 2009; Tripathi et al., 2003; Tripathi et al., 2005). The adjuvant property of AGG is reported in oil emulsion and an aqueous solution for

potentiating the systemic immune response (Tripathi et al., 2003). AGG activates splenocytes and induces production of a Th1 type of immune response. Further, AGG stimulates the innate effector arms like macrophage and natural killer cells. Furthermore, heat denatured and tryptic digested AGG show potent antitumor as well as immunomodulatory activity in normal as well as tumor bearing mice (Bhutia et al., 2008; Tripathi et al., 2003; Bhutia et al., 2008; Bhutia et al., 2009).

Although the apoptotic potential of AGG has been extensively investigated and well characterized, its ability to induce autophagy dependent cell death in mammalian cells has not been documented. In this report, the study was designed to decipher the role of AGG in autophagic death and discuss the possible role of autophagic death in relation with apoptosis in HeLa cells. Further, we examined that AGG inhibited Akt/PH domain to induce endoplasmic reticulum stress mediated autophagy dependent cell death.

3.2. Materials and Methods

3.2.1 Reagents

4,6-Diamidino-2-phenylindole dihydrochloride (DAPI), Dihydrorhodamine 123, Propidium iodide (PI), 3-[4,5-Dimethylthiazol-2-yl]-2,5-diphenyltetrazolium (MTT), Dimethylsulfoxide (DMSO), Caspase inhibitor Z-DEVD-FMK, 3-Methyl adenine (3 MA), N-acetyl-L-cysteine (NAC), 5-fluorouracil (5-FU), and Agarose were purchased from Sigma–Aldrich (St. Louis, MO). Minimal essential medium (MEM), Fetal bovine serum (FBS) (sterile-filtered, South American origin), Dulbecco’s minimal essential medium (DMEM), antibiotic- antimycotic (100X) solution, LysoTracker red, ER-Tracker Green, and Lipofectamine® 2000 were purchased from Invitrogen (Waltham, MA). Salubrinal obtained from Millipore (Billerica, MA).

3.2.2 Antibodies

LC3 (NB100-2220) from Novus Biological (Littleton, CO); Phospho mTOR (Ser2448) (2971), mTOR (2983), BECN1 (3738S), ATG5 (2630S), PARP (9542S), Akt (pan) (4691S), Phospho Akt (Ser473) (4060S), Bax (2772BC), Phospho eIF2 α (Ser 51) (9721S), GRP94 (2104BC), CHOP (5554BC) and PERK (3192) from Cell Signaling Technologies (Danvers, MA); GRP78 (610978), p62/SQSTM1 (610832) from BD Biosciences (Franklin Lakes, NJ); Phospho-PERK(Thr 981) (sc-32577), siPERK (sc-36213), and ATF6 (sc-22799) were procured from SantaCruz (Dallas, TX); actin (A5316) was purchased from Sigma (St. Louis, MO).

3.2.3 Purification of AGG

Purification of AGG was carried out according to the previously reported method. The crude extract of *Abrus precatorius* seed kernels was extracted with 30–90 % ammonium sulfate precipitation followed by affinity chromatography using lactamyl Sephadex G-100 affinity column. Purified AGG from *Abrus* abrin was obtained performing Sephadex G-100 gel permeation chromatography using FPLC. Lectin activity of AGG was analyzed by haemagglutination assay and purity of AGG was checked by SDS and Native PAGE analysis (Hegde et al., 1991).

3.2.4 Cell Culture

Human cervical cancer cell lines HeLa, SiHa, and CaSki were obtained from the National Centre for Cell Science, Pune, India. HeLa, SiHa were cultured in modified eagle medium (MEM) and supplemented with antibiotic-antimitotic and 10 % fetal bovine serum. CaSki cells were grown in RPMI 1640 medium supplemented with antibiotic-antimitotic and 10% fetal bovine serum. HaCaT (human keratinocyte cell line) were maintained in Dulbecco's modified Eagle medium (DMEM) containing similar supplements. After that, all cells were incubated at 37°C in a humidified 95 % air, 5 % CO₂ incubator. The 5-FU resistant HeLa cell line was achieved by continuous stepwise exposure to 5-FU with an initial concentration of 10 µM to final 100 µM (Liu et al., 2013).

3.2.5 MTT Assay

Cells from the logarithmic phase were maintained in culture after that they were counted in a hemocytometer using trypan blue solution. About 5×10^4 HeLa cells/ml was incubated with various concentrations of AGG in a 96 well plate. The efficacy of AGG on the viability of various cancer cell lines was determined using MTT dye reduction assay by determining the optical density at 595 nm using a micro-plate reader spectrophotometer (Perkin-Elmer, Waltham, MA) (Bhutia et al., 2008).

3.2.6 Plasmids, Small Interfering RNA and Transfection

HeLa cells were cultured in 60mm Petri plate and transfected with an 80% confluency using Lipofectamine® 2000 reagent (Invitrogen) following manufacturer's protocol. Transfections were done in the presence of human specific, GFP-LC3 (Addgene plasmid No-11546), Akt (Addgene plasmid No- 9008), pGFP-Akt-PH (Addgene plasmid No-18836), BAX knock down (KD), vector (Addgene plasmid No- 16575) as well as with an empty backbone pcDNA (Addgene plasmid No-10792) used for mock transfection. siRNA for BECN1 (sc-29797), ATG5 (sc-41445), and PERK (sc-36213) were purchased from Santa Cruz Biotechnology. HeLa cells were transfected with specific siRNA by using Lipofectamine®

2000, following the manufacturer's instructions. After 48 h of transfection cells were treated with AGG and autophagy and apoptosis were studied.

3.2.7 Acridine Orange Staining

Quantification of acidic organelles was done by acridine orange staining. After treatment with various doses of AGG for 24 h cells were stained with 0.5 µg/ml of acridine orange at 37°C in the dark for 15 min and washed twice with PBS. Images of acridine orange staining were taken immediately using a fluorescence microscope (Olympus IX71, Tokyo, Japan) (Panda et al., 2014).

3.2.8 Transmission Electron Microscopy

For transmission electron microscopy (TEM), HeLa cell populations were rinsed with 0.1 Sorensen's buffer (pH 7.5), fixed in 2.5 % glutaraldehyde for 1.5 h, and subsequently dehydrated and embedded in Spurr's resin. The block was then sectioned into 60-100 nm ultrathin sections and picked up on copper grids. For routine analysis, ultrathin sections were stained with 2 % uranyl acetate and lead citrate. Electron micrographs were obtained using a transmission electron microscope (Salzar et al., 2009).

3.2.9 Measurement of Autophagy by GFP-LC3 Transfection

HeLa cells were transfected with pEGFP-LC3 (Addgene plasmid 11546) using Lipofectamine® 2000 reagent (Gibco) according to the manufacturer's instructions. The GFP-LC3 HeLa stable clone was generated using G418 screening. HeLa cells were treated with different doses of AGG for 24 h and analyzed by a confocal laser scanning microscope. The level of autophagy was quantified by counting the mean number of puncta displaying intense staining and a minimum of 100 GFP-LC3 transfected cells were counted.

3.2.10 Western Blot Analysis

HeLa cells were treated with AGG followed by extraction of proteins. Cell extracts in cell lysis buffer were prepared, and equal amount of proteins were resolved by SDS/PAGE, transferred to PVDF membrane, and evaluated for LC3, BECN1, ATG5, p62, GRP78, GRP94, p-eIF2α, Akt, p-Akt, PARP, PERK, p-PERK, ATF6, Bax, actin protein level as described by Ref. (Bhutia et al., 2008).

3.2.11 Immunofluorescence Analysis

HeLa cells were treated with various doses of AGG for 24 h followed by fixation with 10 % formaldehyde. Cell permeabilization was done in 0.1 % Triton X 100 which followed to blocking in 5 % BSA. Following this, cells were incubated with primary antibodies p-eIF2α and CHOP . Following washing in PBST cells were incubated with secondary antibodies conjugated with the Alexa Flour. Imaging was done using a high end fluorescence inverted microscope (Olympus- IX71) using Cell Sens Standard software.

3.2.12 Reactive Oxygen Species (ROS) Measurement

To detect reactive oxygen species (ROS), HeLa cells were treated with AGG for 24 h and incubated with 2.5 µg/ml Dihydrorhodamine123 (Dhr123) in PBS for 30 min in a CO₂ incubator. Dhr123 is rapidly taken up by cells and is converted to rhodamine 123 in the presence of ROS. HeLa cells were harvested and suspended in PBS, and ROS generation was measured by the fluorescence intensity (FL-1, 530 nm) of 5×10⁴ cells (Bhutia et al., 2008).

3.2.13 Colocalization Study by ER-Tracker, LysoTracker and MitoTracker

Cells were treated with AGG for the different time interval and stained with pre warmed ER-Tracker™ Green (BODIPY®FLglibenclamide) (500 nM) staining solution and were incubated for 20-30 minutes at 37°C. Glibenclamide attaches to the sulphonylurea receptors of ATP sensitive K⁺ channels which are generally prominently present on ER. At the same time, cells were stained with LysoTracker Red DND-99 (100 nM) for 30 minutes at 37°C. LysoTracker probes are specific for acidic organelles. The dye ER-Tracker colocalized with LysoTracker, representing the occurrence of autophagy ER or ER-phagy. Colocalization was measured applying JACoP plugin in single Z-stack sections of deconvoluted images.

3.2.14 Caspase-Glo 3/7 Assay

Caspase 3/7 activity in HeLa cells was measured using Caspase-Glo 3/7 Assay kits (Promega, USA) according to the manufacturer's instructions. Caspase activities were measured and expressed as relative luciferase units.

3.2.15 15 RITC Labeling of AGG for Colocalization Study with Akt-PH Domain

For colocalization study, AGG were labeled with Rhodamine B isothiocyanate (RITC) dissolved in water (1 mg in 100 µl water) and 1 mg of AGG dissolved in 1 ml of 100 mM NaHCO₃ buffer). After that, the mixture was incubated for 4 h in dark at room temperature followed by treatment with 1M Ethanolamine to inactivate the residual RITC. The solution was left in the dark for 2 h and dialyzed against PBS for 48 h and lyophilized. After 30 min of AGG (10 µg/ml) treatment in GFP-Akt-PH domain transfected HeLa cells, cells were washed and colocalization study was performed on a confocal microscope (Leica TCS SP8) and colocalization was measured by using the JACoP plugin in single Z-stack sections of deconvoluted images (Bhutia et al., 2008).

3.2.16 Modeling PH-AGG Complex Through Docking and Molecular Dynamics Simulation

The crystal structures of the pleckstrin homology (PH) domain and AGG were obtained from the PDB with PDB ids: 2Q3N (Bagaria et al., 2006) for the AGG and 1UNQ (Milburn et al., 2003) for the PH domain. The docking algorithm was carried out by the ClusPro 2.0

protein–protein docking server. Finally, a structure with the highest score was considered for the MD simulation with the ff12SB force field and TIP3P waters in the AMBER12 package (Meher et al., 2012; Meher et al., 2012; Meher et al., 2015). The system was then minimized in four phases and equilibrated in a total of 400 ps. The PHAGG complex trajectory was run for 15 ns and was used for the analysis. The binding free energies were calculated using the MM-PB/GBSA method implemented in AMBER 12. The MMPBSA.py method in Amber12 was applied to calculate the binding free energy of the PH domain to the AGG.

3.2.17 Statistical Analysis

All the results were represented as the mean±SD. Experimental data were analyzed by Student's t-test. The level of significance was regarded as $P<0.05$ for values obtained for treatment compared to control. The IC₅₀ values of various cell lines after AGG treatment were calculated by using the program GraphPad Prism 5 (GraphPad Software, San Diego, CA) to fit a variable slope-sigmoidal-dose-response curve.

3.3. Results

3.3.1 AGG Induced Autophagic Cell Death in Cervical Carcinoma

To investigate the role of AGG on growth and proliferation of cervical cancer cells, we performed cell viability assay. AGG was treated in various concentrations in several cervical cancer cell lines and the effective concentration at which cell growth inhibited by 50 % (IC₅₀) for HeLa, SiHa, and CaSki are 7.2 ± 1.2 , 9 ± 3 , and 10.2 ± 2.2 µg/ml respectively. However, we did not observe any significant growth inhibitory activity of AGG in normal keratinocyte cell line (HaCaT) in comparison to cervical cancerous cell lines. This depicted the selective antitumor activity of AGG towards cervical cancer cells (Fig.3.1.a).

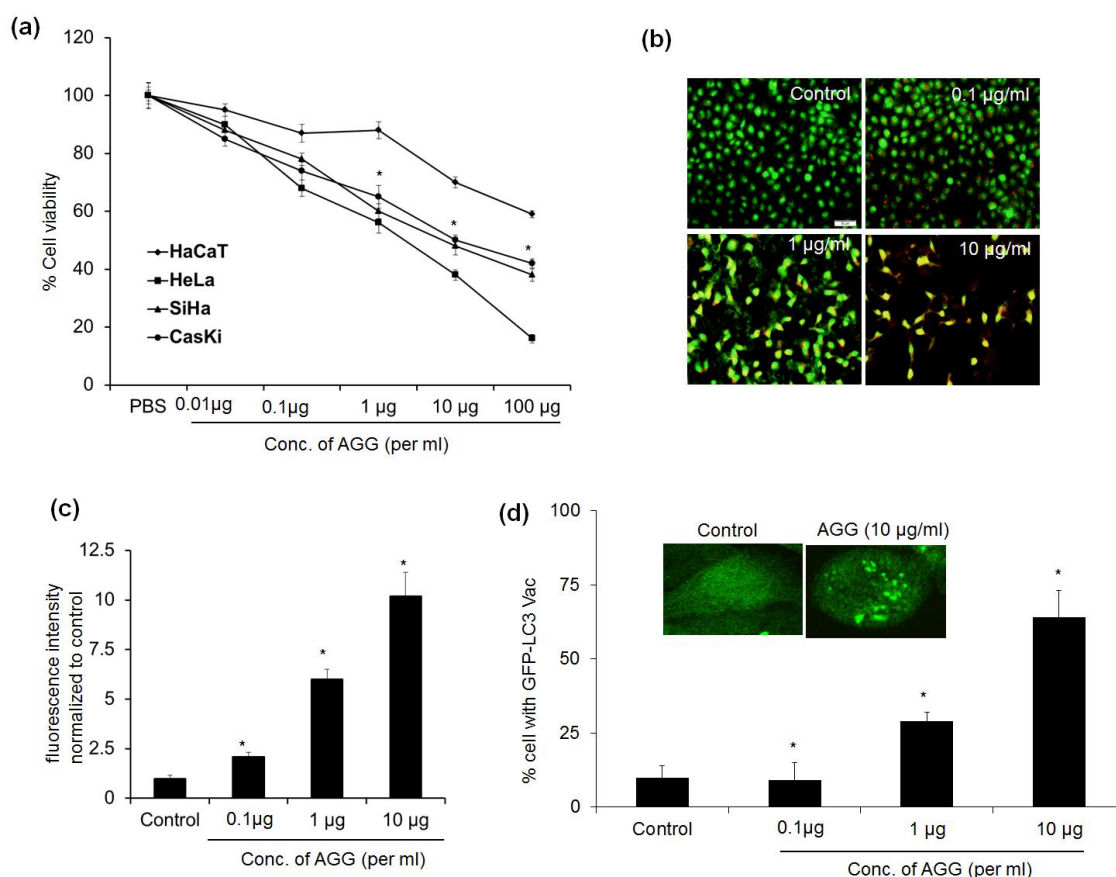


Fig.3.1 AGG induced autophagic cell death in cervical cell carcinoma. The normal HaCaT cell and different cervical cell carcinoma (HeLa, SiHa, CaSki) were treated with different concentration of AGG for 72 h and cell viability was performed by MTT assay (a). HeLa cells were treated with different doses of AGG (0.1, 1, and 10 μ g/ml) for 24 h, and acridine orange staining was performed for late autophagic vesicles, which were visualized with an inverted fluorescence microscope (Olympus IX71, 200X) (b). All images were quantified by using Image J (c). HeLa cells were transfected with GFP-LC3 and stable GFP-LC3 HeLa was generated and treated with different concentration of AGG for 24 h, localization of LC3 in transfected cells was examined by confocal microscopy (magnification 1000X), and autophagosome formation was quantified and data presented as percentage of GFP-LC3 transfected cells with puncta fluorescence to autophagosome formation. A minimum of 200 GFP-LC3 transfected cells were counted (d). The values are the means \pm SD of three independent experiments. *corresponds statistically significant change in comparison to control (* P < 0.05).

In our initial experiment for detecting of the acidic vesicles, we used the lysosomotropic agent acridine orange, a weak base that moves freely across biological membranes when uncharged. The cytoplasm and the nucleus show dominant green fluorescence. Its protonated form accumulates in acidic compartments, where it forms fluorescence bright red color aggregates. The HeLa cells were incubated with different concentration of AGG for 24 h and acridine orange staining was performed to observe in a fluorescence microscope. The data showed that the acidic content as the red signal was increased in a dose dependent way (Fig.3.1.b,c). Similarly, the intracellular localization of LC3 in autophagic vacuoles induced by AGG was determined by transient transfection of HeLa cells with a plasmid expressing green fluorescent protein fused with LC3 (GFP-LC3) followed by AGG treatment. In control, GFP-LC3 was found predominantly as diffuse green

fluorescence in the cytoplasm. However, in AGG treated cells, characteristic puncta fluorescent patterns were observed, indicating the recruitment of GFP-LC3 during autophagosome formation (Fig.3.1.d, Upper panel). Moreover, the numbers of cells with GFP-LC3 puncta increased significantly in a dose dependent manner after 24 h of AGG (Fig.3.1.d, lower panel).

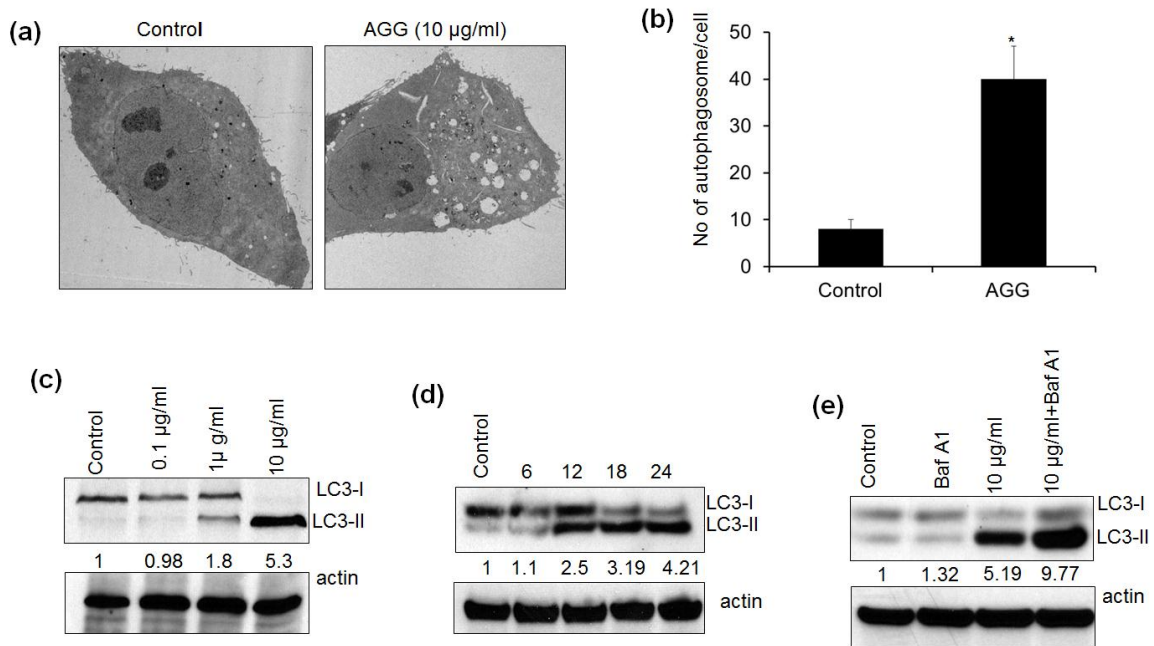


Fig.3.2. Analysis of AGG induced autophagy by electron microscope and Western blot. HeLa cells were treated with different doses of AGG and cells were fixed and processed for electron microscopy (a). The numbers of autophagosomes in HeLa cells 24 h after AGG treatment was quantified (b). After 24 h of AGG treatment, LC3-II expression was analyzed by Western blot both dose (c) and time (d) dependent manner. For the occurrence of autophagic flux, LC3-II expression was analyzed in the presence of bafilomycin A1 (100 nM) in 24 h AGG treated HeLa cells (e). The values are the means \pm SD of three independent experiments. *corresponds statistically significant change in comparison to control ($*P < 0.05$). Densitometry was performed on the original blots, considering the ratio of LC3-II to actin in control cells was 1.

We further verified AGG induced autophagy in HeLa cells by electron microscopy. Electron micrographs of control showed the normal morphology of all organelles, with mitochondria scattered homogenously throughout the cell (Fig.3.2.a). Images captured 24 h with AGG indicated a marked accumulation of membrane-bound electron dense structures sequestering cellular components, a distinctive feature of autophagosomes. Furthermore, the number of autophagosomes as well as autolysosomes was increased in AGG treated cells as compared to control (Fig.3.2.b). Next, we monitored changes in expression of endogenous LC3 in HeLa cells. Treatment of AGG led to a rapid accumulation of the LC3-II form in a dose- and time-dependent manner when compared to control cells (Fig.3.2.c,d). The increase in LC3-II accumulation can be associated with either an enhanced formation of

autophagosomes or impaired autophagosome degradation. To differentiate between these two possibilities, LC3-II accumulation was assessed in the presence of bafilomycin A1, an inhibitor of V-ATPase that interferes with the fusion of autophagosomes and lysosomes and hence blocks the autophagosome as well as LC3-II degradation. Interestingly, AGG showed further accumulation of LC3-II in the presence of bafilomycin A1 in HeLa cells. These observations suggest that the increased LC3-II association with vesicles mediated by AGG was a consequence of increased autophagosome formation (Fig.3.2.e).

3.3.2 AGG Induced Autophagic Cell Death is Mediated through Canonical Pathway

Autophagy can be induced by the canonical pathway in which BECN1 induces the autophagosome generation by forming a multiprotein complex with class III phosphatidylinositol-3-kinase or hVps34 or by the non-canonical pathway that is independent of BECN1 and hVps34. Initially, the expression of different types of autophagy proteins was analyzed by Western blot and showed that AGG increased the expression of BECN1 and ATG5 in a dose dependent manner. At the same time, p62 was degraded in the presence of AGG (Fig.3.3.a). Further, we used an siRNA approach to knock down essential autophagy (ATG) genes, such as BECN1, ATG5 and quantified LC3-II accumulation and GFP-LC3 puncta formation. The specific siRNAs significantly were downregulated the corresponding proteins (Fig.3.3.b). Inhibition of BECN1 and ATG5 decreased the LC3-II levels and percentage of GFP-LC3 positive cells (Fig.3.3.c,d) upon AGG treatment indicating that AGG triggered autophagic cell death via the canonical pathway.

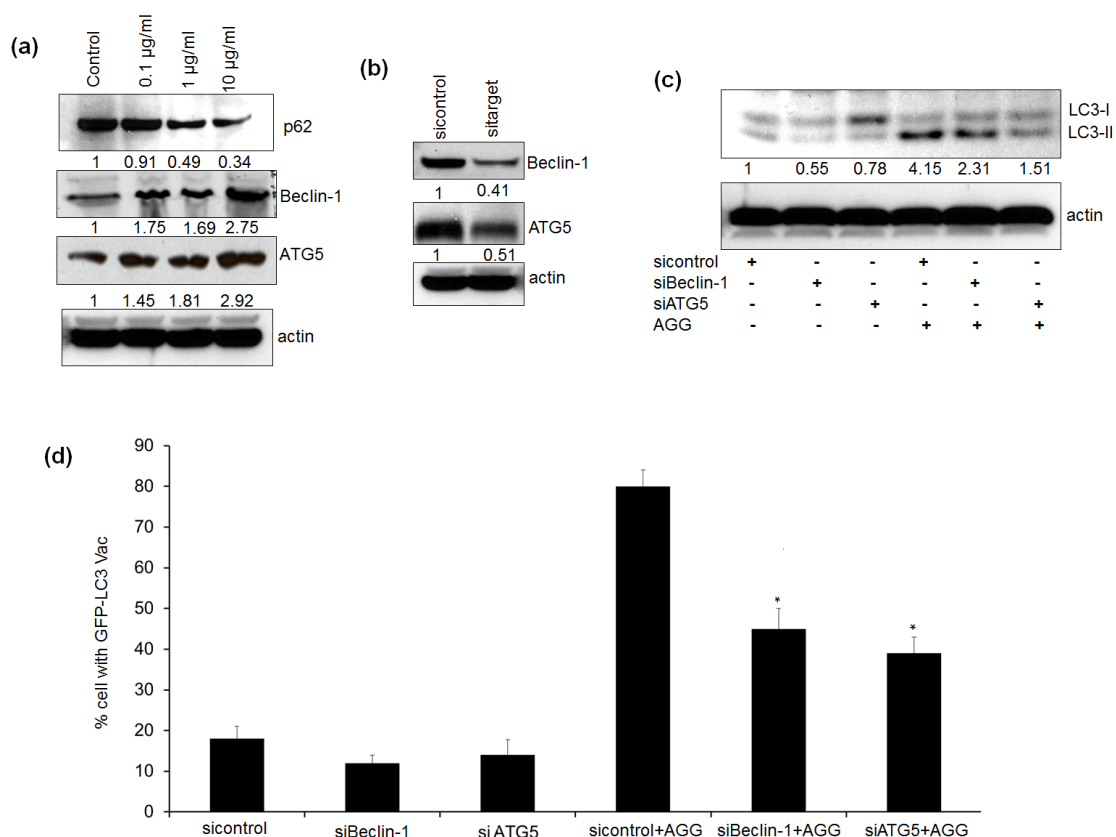


Fig.3.3. AGG induced autophagic cell death was mediated through the canonical pathway. HeLa cells were treated with AGG for 24 h and expression of p62, BECN1, and ATG5 were analyzed by Western blot (a). After 48 h transfection with siRNAs (b), HeLa cells were treated with AGG for 24 h and LC3-II expression was determined Western blot (c). GFP-LC3 stable HeLa cells were transfected with the indicated siRNAs followed by AGG treatment and cytoplasmic aggregation of GFP-LC3 was determined (d). A minimum of 200 GFP-LC3-transfected cells were counted. * $P < 0.05$ compared with sicontrol AGG. Densitometry was performed on original blots, considering the ratio of protein to actin in control cells was 1.

3.3.3 Crosstalk Between AGG Induced Apoptosis and Autophagic Cell Death

To investigate the role of AGG in apoptotic and autophagic death, HeLa cell were cultured in presence of PI3K-III inhibitor, 3-Methyladenine (3-MA) and caspase inhibitor (Z-DEVD-FMK) and monitored the alteration in cell viability, and autophagic or the apoptotic progression. HeLa cells were pretreated with inhibitors and followed to AGG treatment for 24 h. The microscopic image showed that AGG induced cell death and neither of the inhibitors could revert back the cell death (Fig.3.4.a). Inhibiting apoptosis by Z-DEVD-FMK found to increase LC3-II accumulation along with a decrease in caspase 3 activity in AGG treatment (Fig.3.4.b,c). Similarly, inhibition of autophagic cell death with 3-MA augmented AGG induced apoptosis in HeLa cells (Fig.3.4.b,c). In addition, AGG increased caspase activity in BECN1 and ATG5 deficient HeLa cells indicating that inhibition of autophagy increased the AGG induced apoptosis and vice versa (Fig.3.5.a,b). This study concluded that AGG simultaneously induced apoptotic and autophagic cell death.

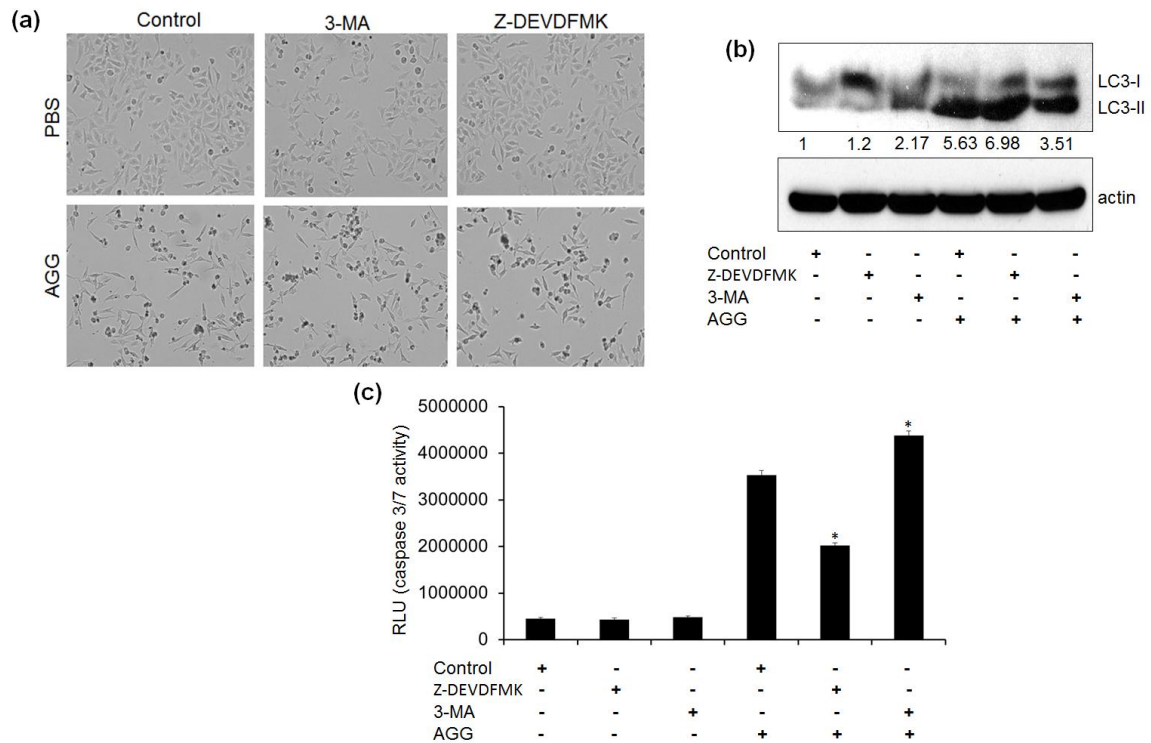


Fig.3.4. The relationship between AGG induced apoptosis and autophagic cell death. HeLa cells were pretreated with PI3K-III inhibitor 3-Methyladenine (3-MA) (5 μ M) and caspase inhibitor (Z-DEVD-FMK) (10 μ M) for 2 h followed by 24 h AGG treatment and photographed (a), expression LC3-II was analyzed by Western blot (b) and caspase activity was measured by caspase Glo assay (c). The values were the means \pm SD of three independent experiments. *represents statistically significant change vs. AGG treated group (* P < 0.05). Densitometry was performed on the original blots, considering the ratio of protein to actin in control cells was 1.

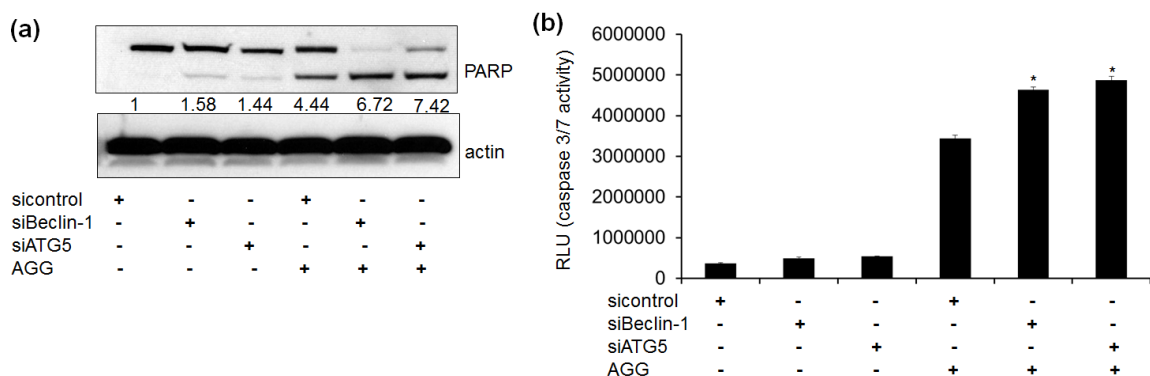


Fig.3.5. Effect of AGG induced apoptosis in autophagy deficient cells. HeLa cells were transfected with the indicated siRNAs followed by AGG treatment and PARP expression was analyzed by Western blot (a) and caspase activity was measured by caspase Glo assay (b). The values were the means \pm SD of three independent experiments. *represents statistically significant change vs. AGG treated group (* P < 0.05). Densitometry was performed on the original blots, considering the ratio of protein to actin in control cells was 1.

It is well reported that AGG ROS and is associated with apoptosis induction. In the present investigation, we deciphered the role of ROS in AGG induced autophagic cell death in HeLa cells. HeLa cells were pretreated with N-acetyl-L-cysteine (NAC; a thiol-containing antioxidant that is a precursor of reduced glutathione, 10 μ M) ROS scavenger, for 2 h followed by AGG treatment for 24 h and HeLa cells were analyzed by flow cytometry and

western blot. The data showed that AGG increased the ROS generation and AGG induced ROS generation was inhibited in the presence of NAC (Fig.3.6.a). The western blot analysis showed that AGG in presence of NAC decreased PARP cleavage and increased LC3-II accumulation as well as GFP-LC3 puncta formation as compared to only AGG treated group in HeLa cells (Fig.3.6.b,c). This study concluded that AGG induced ROS generation induced apoptosis and inhibition of AGG induced ROS found to switch from apoptosis to autophagic cell death in HeLa cells.

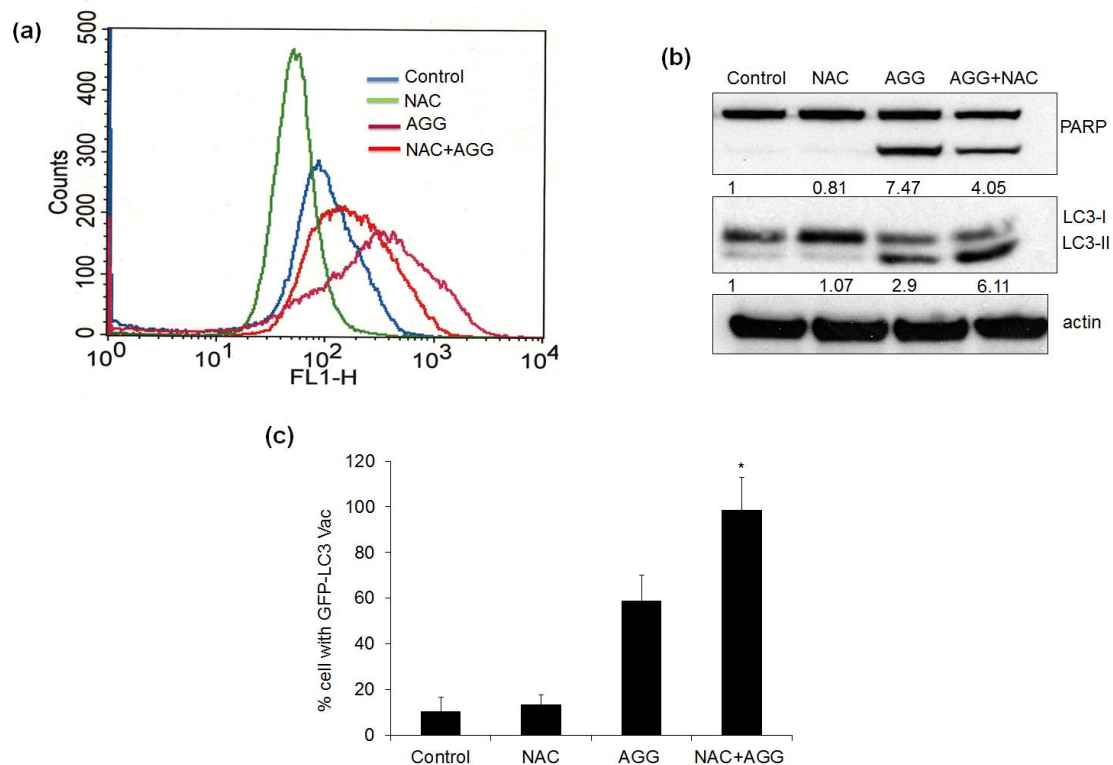


Fig.3.6. The role of reactive oxygen species in AGG induced autophagic death. HeLa cells were pretreated with NAC (10 mM, 2 h) followed by AGG (10 µg/ml) for 24 h, and ROS generation was then analyzed using flow cytometry (a). HeLa cells were treated with AGG in the presence of NAC, LC3-II accumulation by Western blot (b) and GFP-LC3 puncta (c) were quantified (* $P < 0.05$, compared with only AGG treated group).

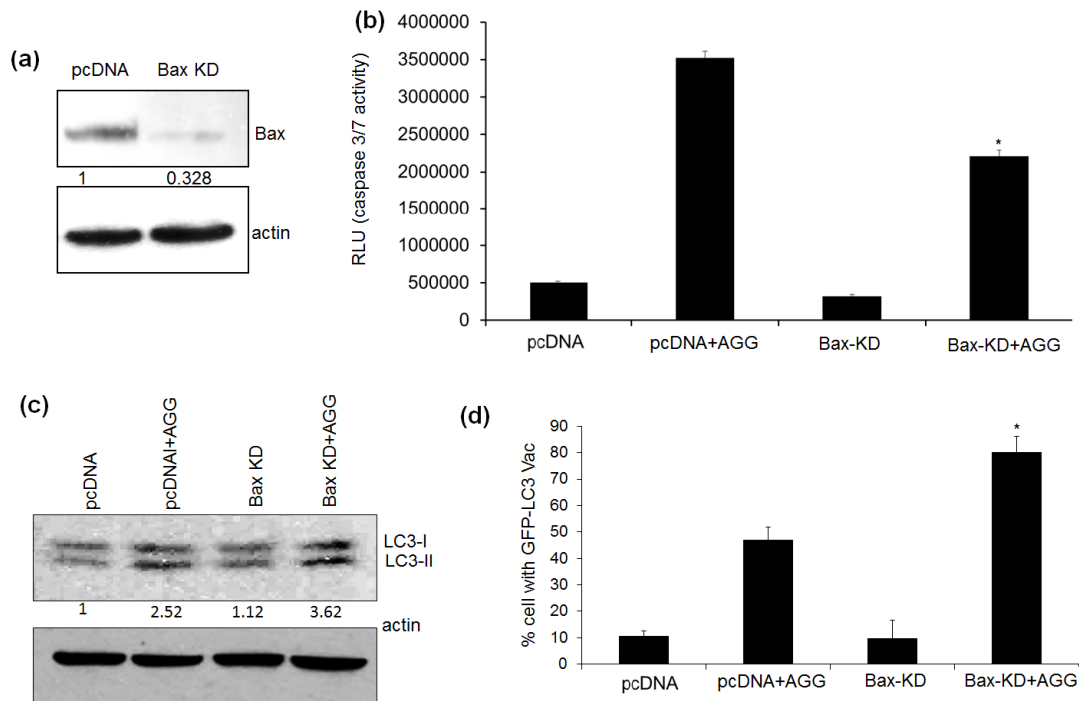


Fig.3.7. The role of Bax in AGG induced autophagic death. HeLa cells were transfected with shBax for 48 h (a). After 24 h of AGG treatment, caspase 3/7 activity by caspase Glo assay (b) and LC3-II expression by western blot (c) was analyzed in shBax transfected HeLa cells. Stably transfected GFP-LC3 clones were transfected with shBax and percentage of GFP-LC3 puncta cells was examined by confocal microscopy (magnification 1000X) (d). *corresponds statistically significant change in pcDNA-AGG (* $P < 0.05$). Densitometry was performed on the original blots, considering the ratio of protein to actin in control cells was 1.

3.3.4 AGG Induced Autophagic Cell Death in Apoptosis Deficient and Resistant Cervical Cancer Cells

To examine the role of AGG mediated autophagic death in apoptosis deficient and resistant cells, autophagic death was investigated in BAX-KD and 5-FU resistant HeLa cells. The shBax HeLa cells were characterized showing that knockdown of proapoptotic protein Bax blocks apoptosis induction by AGG (Fig.3.7.a). However, AGG treated shBax HeLa cells continued to exhibit higher autophagic phenotypes compared with pcDNA as evidenced by LC3-II accumulation and GFP-LC3 puncta vacuole formation (Fig.3.7.b,c). In addition, to demonstrate the effect of AGG in resistant HeLa cells we developed 5-FU resistant cells through continuous exposure of 5-FU to HeLa cells. Initially, we checked the cell viability against 5-FU and AGG in parent and resistance HeLa cells. It was found that there was a significant increase in cell viability in 5-FU-R HeLa cells as compared to parent HeLa cells against 5-FU (Fig.3.8.a). But we could not find any significant difference between AGG treated both parental and resistant HeLa cells (Fig.3.8.b). Further, we examined the apoptotic and autophagic cell death in AGG treated 5-FU resistant HeLa cells and observed there was significantly decrease of apoptosis level in 5-FU-R HeLa cells compare with parent HeLa as quantified by caspase 3/7 Glo activity (Fig.3.8.c).

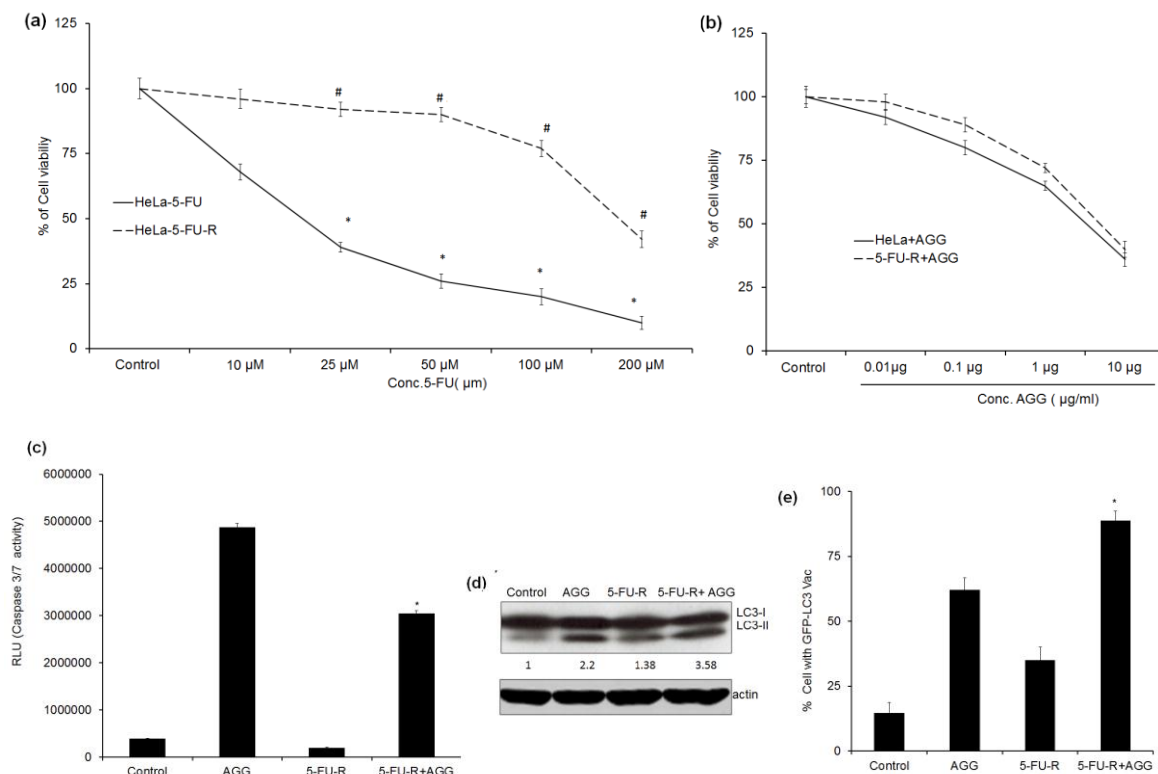


Fig.3.8. AGG induced autophagic cell death in apoptosis resistant cervical cancer cells. HeLa (parent and 5-FU resistant) cells were treated with different concentration of 5-FU and AGG for 72 h and cell viability was performed by MTT assay (a, b). *corresponds statistically significant change in comparison to control ($*P < 0.05$). After 24 h of AGG treatment, caspase 3/7 activity by caspase Glo assay (c) and LC3-II expression by Western blot (d) was analyzed in parent and 5-FU resistant HeLa cells. Transfected GFP-LC3 HeLa cells (parent and 5-FU resistant cells) were treated AGG for 24 h and percentage of GFP-LC3 puncta cells was examined by confocal microscopy (magnification 1000X) (e). *corresponds statistically significant change in AGG treated group ($*P < 0.05$). Densitometry was performed on the original blots, considering the ratio of protein to actin in control cells was 1.

On the contrary, the autophagic cell death was significantly enhanced in 5-FU-R HeLa cells as to parent groups as demonstrated by LC3-II accumulation and GFP-LC3 puncta vacuole formation, indicating the cell death mechanism by AGG was switched to autophagic cell death in apoptosis resistant cells (Fig.3.8.d, e). The above findings strongly support our hypothesis that AGG could be potential alternative tumor preventive molecule to apoptotic resistant cells.

3.3.5 AGG Induced Autophagic Cell Death Mediated through PERK Mediated ER Stress

As ROS was not the regulating factor for AGG induced autophagic death, we investigated whether endoplasmic reticulum (ER) stress might contribute to autophagic cell death through induction of ER-phagy, selective autophagy of the ER (Salzar et al., 2009). To test this hypothesis, HeLa cells were treated with AGG for different time periods and analyzed for colocalization of ER and lysosome by staining with ER-Tracker Green and LysoTracker

Red as well as mitochondria and lysosome by MitoTracker Green and LysoTracker Red through a confocal microscope. The control group did not demonstrate the interaction of ER and lysosome. The treatment group showed strong colocalization of the two organelles as intense yellow color and this interaction was significantly increased in time dependent manner. These studies indicated that ER interacted with the lysosome and induced ER-phagy (Fig.3.9). Additionally, we did not find any interaction of mitochondria and lysosome as demonstrated by confocal microscopy (Fig.3.10) which nullified role of mitophagy in AGG induced autophagic cell death.

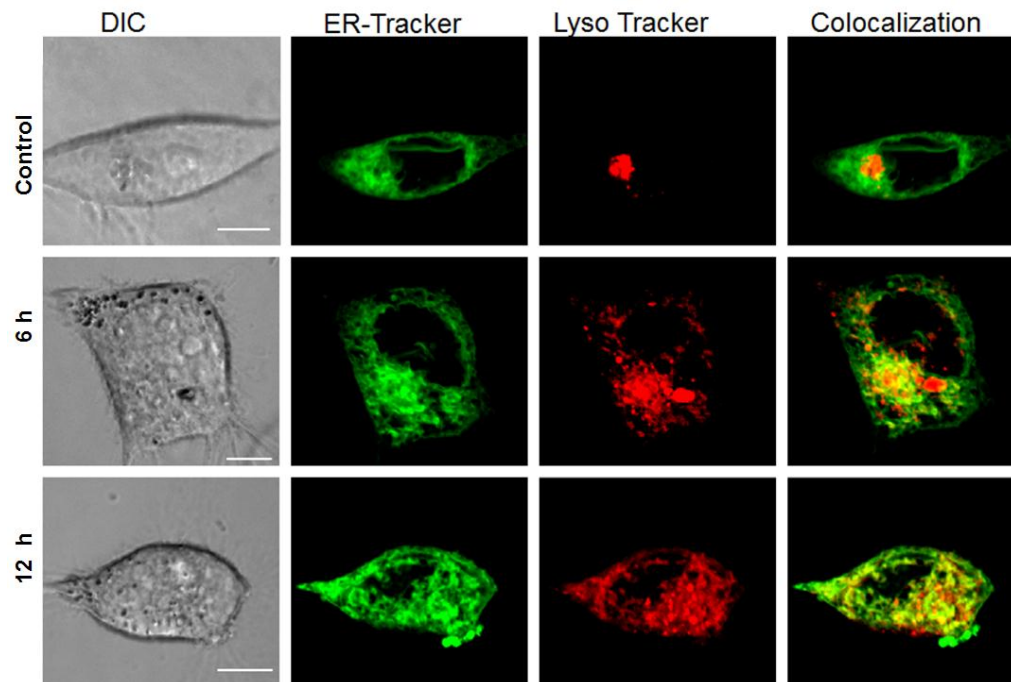


Fig.3.9. Colocalization of ER and lysosome in AGG-treated HeLa cells. HeLa cells were treated with AGG for indicated time periods and colocalization of ER and lysosome was analyzed with ER-Tracker green (500 nM) and LysoTracker red (100 nM) through confocal microscopy.

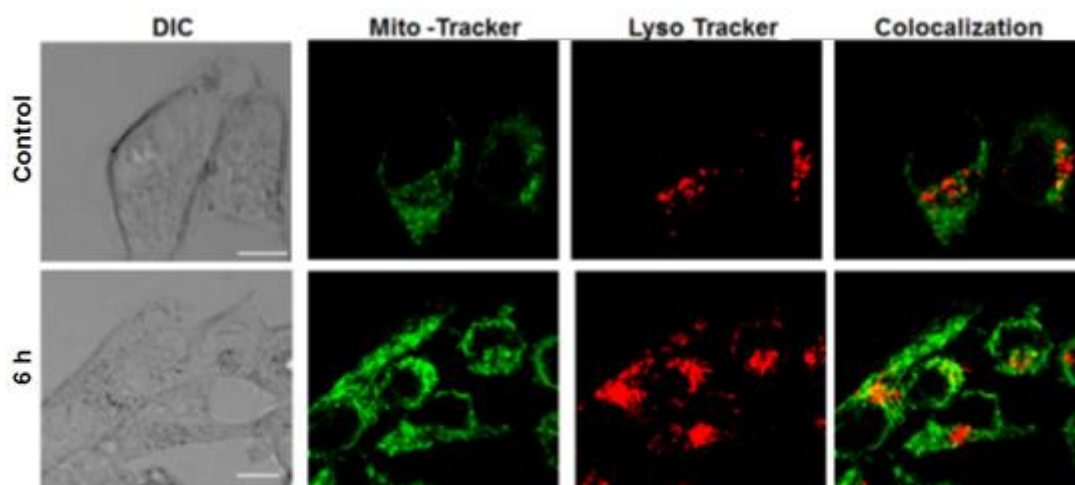


Fig.3.10. Colocalization of mitochondria and lysosome in AGG-treated HeLa cells. HeLa cells were treated with AGG for indicated time periods and colocalization of mitochondria and lysosome was analyzed with MitoTracker green (300 nM) and LysoTracker red (100 nM) through confocal microscopy.

Further, we monitored the change in ER stress regulated proteins in the presence of AGG in HeLa cells. C/EBP homologous protein (CHOP), which is commonly known as growth arrest and DNA damage inducible gene 153 (GADD153) and expression of CHOP is the most sensitive ER stress marker, was increased expression in dose dependent manner (Fig.3.11.a-d). Besides that, an increase in phosphorylation of eukaryotic translation initiation factor ($eIF2\alpha$) in different time point after AGG treatment was observed in HeLa cells (Figure 6d and e). After 24 h AGG treatment, AGG found to increase the expression of GRP78/BiP and GRP94, the major chaperones and central regulators of unfolded protein response in dose dependent manner in HeLa cells. Besides that ATF6 one of the important ER stress sensor which induces CHOP expression was also increased in dose dependent way as shown by western blot (Fig.3.11.e). Moreover, AGG increased the phosphorylation of PERK, one of the major transducers of ER stress indicating AGG induced ER stress followed PERK mediated pathway (Fig.3.11.f). We next determined whether AGG mediated ER stress contribute to AGG stimulated autophagy using a cell permeable form $eIF2\alpha$ dephosphorylation inhibitor salubrinal, which inhibits $eIF2\alpha$ activity. Pretreatment of salubrinal reduced the expression of GRP78 and ER stress in AGG treated cells as compared to only AGG treated cells (Fig.3.12.a). Intriguingly, LC3-II accumulation and percentage GFP-LC3 puncta cells were reduced after addition of salubrinal in AGG treated the group as to only AGG treated HeLa cells (Fig.3.12.a,b). Further, the role of PERK mediated ER stress by AGG was demonstrated through siRNA approach. We found that knock down of PERK significantly inhibited autophagy induction by AGG as shown by LC3-II accumulation and GFP-LC3 puncta vacuole formation (Fig.3.13.c,d). Collectively, our data demonstrate that AGG influenced ER stress contributed to autophagy induction.

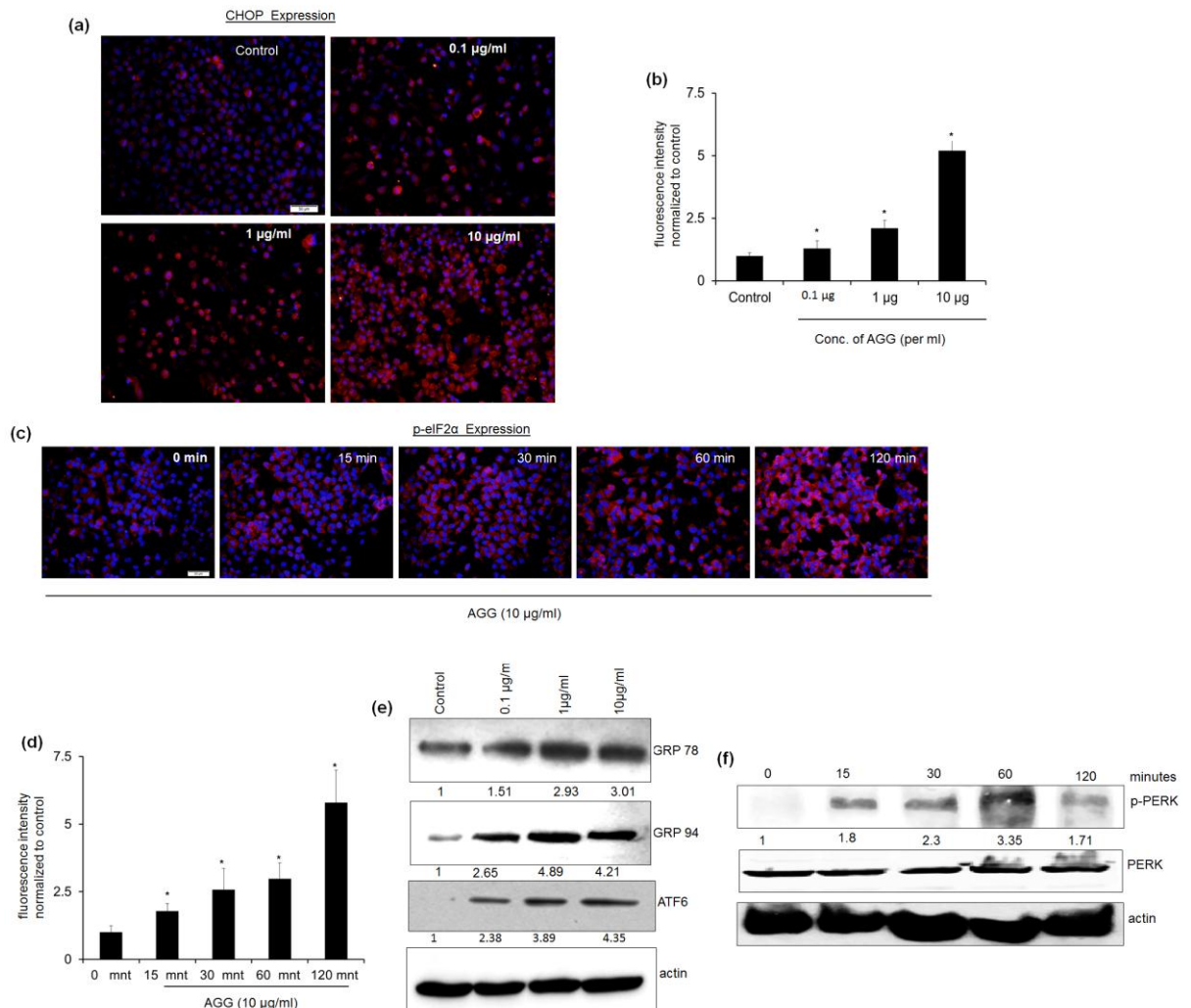


Fig.3.11. AGG induced ER stress in HeLa cells. HeLa cells were treated with AGG for indicated time periods and expression of CHOP (a, b) and p-eIF2α (c, d) analyzed by immunofluorescence microscopy (Olympus IX71, 200X, All images were quantified by using Image J) and GRP78, GRP94, and p-PERK, analyzed by Western blot (e, f). *corresponds statistically significant change in comparison to control (* $P < 0.05$). Densitometry was performed on the original blots, considering the ratio of protein to actin in control cells was 1.

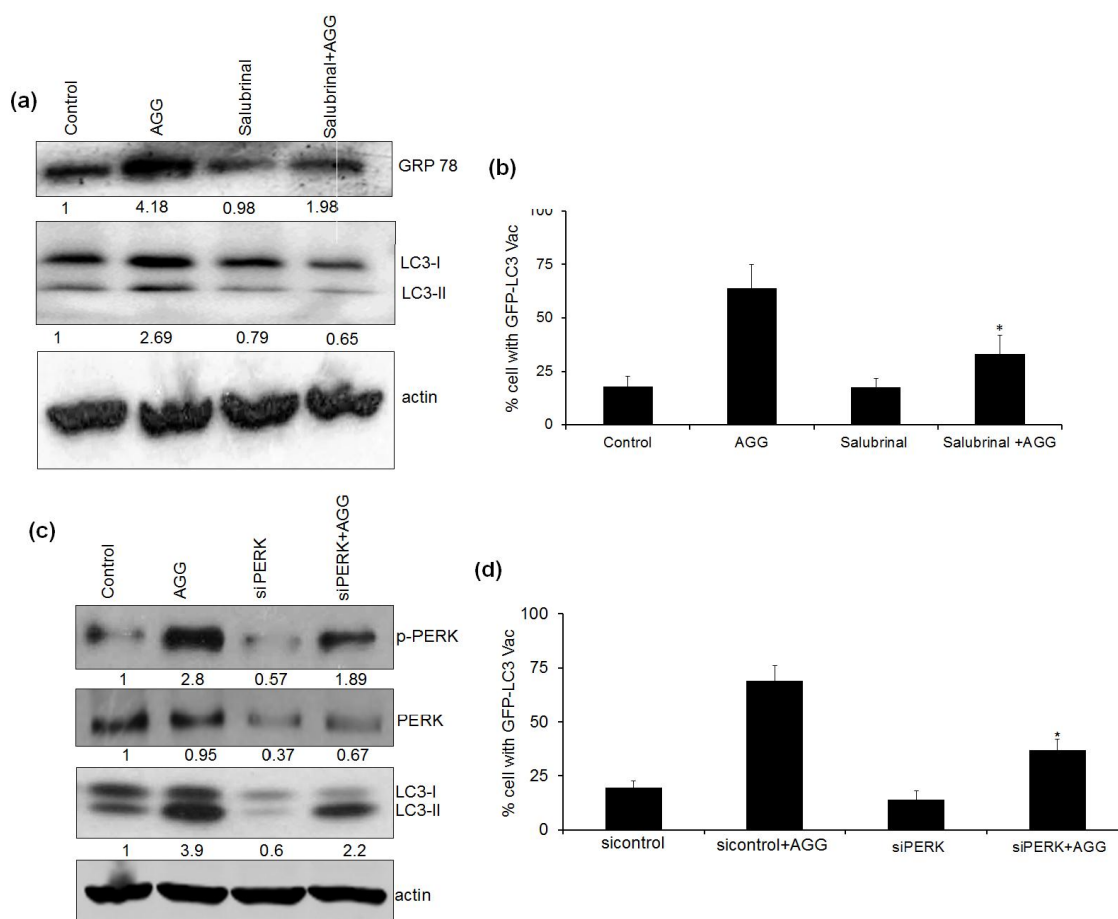


Fig.3.12. The role of ER stress in AGG induced autophagic cell death. HeLa cells were pretreated with salubrinal (5 μ M) for 2 h followed by AGG treatment (10 μ g/ml) for 24 h and LC3-II expression was analyzed by Western blot (a). Stably transfected GFP-LC3 clones were treated with salubrinal (5 μ M) prior to AGG treatment and autophagosome formation was quantified and data presented as a percentage of GFP-LC3 puncta cells by confocal microscopy (b). After 48 h transfection with siPERK, HeLa cells were treated with AGG for 24 h and LC3-II expression was determined Western blot (c). GFP-LC3 stable HeLa cells were transfected with the siPERK followed by AGG treatment and cytoplasmic aggregation of GFP-LC3 was determined (d). The values are expressed as the mean \pm SD of three independent experiments (* P < 0.05, compared with only AGG treated group). Densitometry was performed on the original blots, considering the ratio of protein to actin in control cells was 1.

3.3.6 AGG Mediated Inhibition of Akt/PH Domain Promoted ER Stress Induced Autophagic Cell Death

Akt, the active component of the phosphoinositide 3-kinase (PI3K) is well-known to contribute to the mTOR activation, which is a vital regulator of autophagy, either directly or indirectly through phosphorylation and suppression of TSC2. Akt can be activated after binding to phosphatidylinositol (3,4,5)-trisphosphate (PIP3) via its pleckstrin homology (PH) domain which controls membrane translocation, as well as phosphorylation of Thr308 in the activation loop and Ser473 in the hydrophobic domain (Panda et al., 2015; Mahadevan et al., 2008). In order to study, the interactions between the PH domain and AGG, we performed a 15 ns long molecular dynamics (MD) simulation of the docked PH-

AGG complex. At the end of the simulation, the complex looked to be quite stable with root mean square deviations (RMSD) value of 2 to 2.5 Å for the Ca backbone atoms (Fig.3.13).

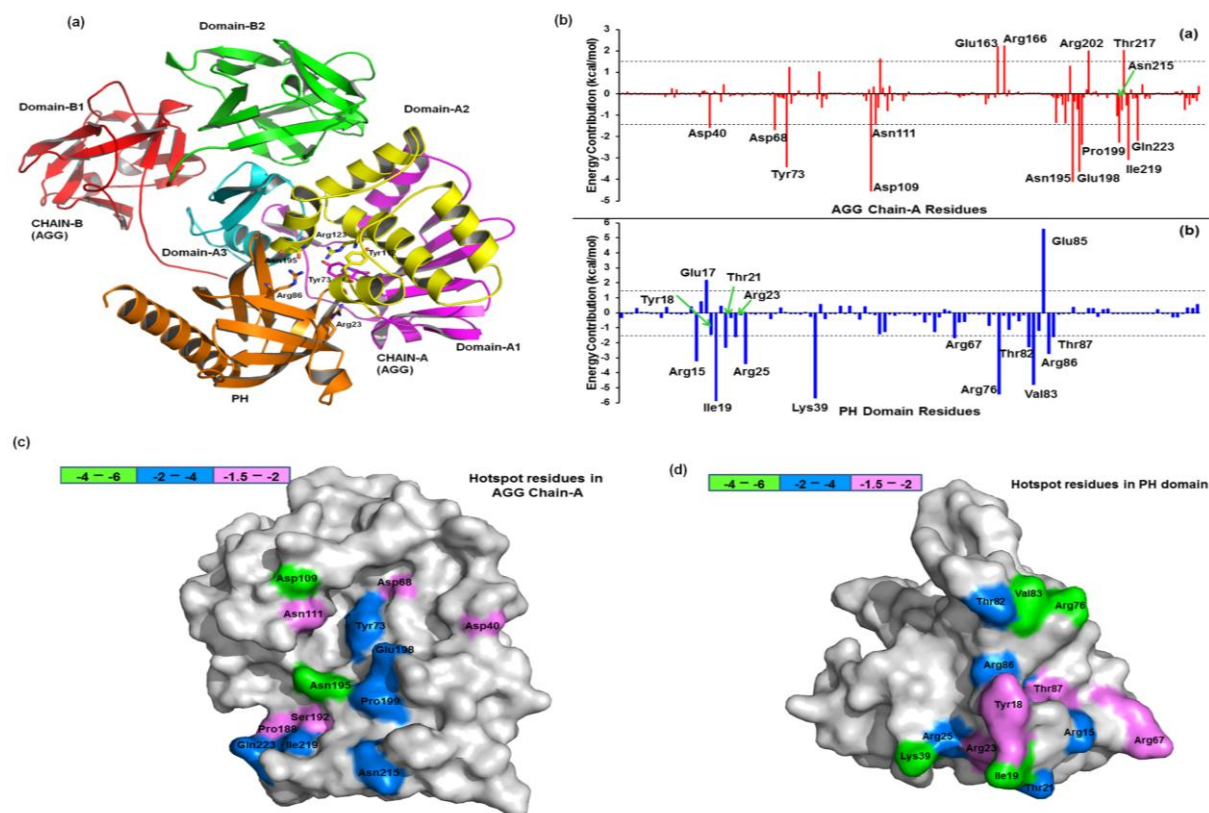


Figure 3.13. Interaction of Akt-PH domain and AGG. A schematic ribbon representation of the PH domain-AGG complex structure shown in different colors. The PH domain was shown in orange color while the three domains (A1, A2 and A3) in chain A of AGG are shown in purple, yellow and cyan colors, respectively. The two domains (B1 and B2) in chain B of AGG are also shown in red and green colors respectively (a). Decomposition of ΔG on a per-residue basis or the pair interaction energy between PH domain and AGG chain A the contribution of each residue in AGG to PH domain binding; the contribution of each residue in PH domain to AGG binding (b). Distributions of the identified hot spot residues on the PH domain surface and AGG chain A surface. Coloured bars show the range of contributions by residues in the unit kcal/mol. Chain B for AGG protein was not shown, as it didn't interact with the PH domain (c,d).

It was observed that several residues from both the PH domain (Arg15, Arg23, Arg25, Arg76, Val83, Arg86, and Thr87) and AGG (Asp109, Asp113, Asn195, Glu198 and Asn215) interface forms the H-bonds making the stable complex (Fig.3.13.a,b). To ensure the interactions from energetics point of view, MM-PB/GBSA based binding free energies were calculated. It was found that the MM-PBSA based binding free energies are larger: $-88.91 \text{ kcal mol}^{-1}$ than $-56.54 \text{ kcal mol}^{-1}$ the MM-GBSA based. The favorable contribution from the direct electrostatic interactions between PH domain and AGG was recompensed by the electrostatic desolvation free energy upon binding, which progressed to an unfavorable contribution as a whole, consistent with other MM-PB/GBSA studies. In contrast, nonpolar interactions, $\Delta G_{\text{nonpolar}}$ (including van der Waals interactions and nonpolar solvation) contributed favorably to the binding process. Therefore, the binding of PH domain and AGG was largely compelled by intermolecular electrostatic interactions and nonpolar interactions,

including the van der Waals and nonpolar solvation. Through decomposing the binding free energy into the contribution from each residue, it was likely to recognize the binding hot spots for PH domain and AGG. For PH domain, the residues Arg15, Ile19, Thr21, Arg25, Lys39, Arg76, Thr82, Val83, and Arg86 provide significant contributions (>2 kcal/mol) were basically from three anti-parallel beta sheets present and the loops connecting them. For AGG Tyr73, Asp109, Asn195, Glu198, Pro199, Asn215, Ile219 and Gln223 were recognized as hotspots basically from the active site region and adjacent areas of A chain in AGG (Fig.3.13.c,d). To validate the in silico finding, HeLa cells were transfected with GFP-Akt-PH domain for 48 h followed to RITC labeled AGG ($10 \mu\text{g/ml}$) for 30 min and analyzed for interaction of AGG and PH domain by confocal microscopy. Overlapping of two proteins (RITC-AGG and GFP-Akt-PH) were visible showing intense yellow color with Pearson's coefficient (R_r -0.903) as well as total overlap coefficient (R -0.931) (Fig.3.14).

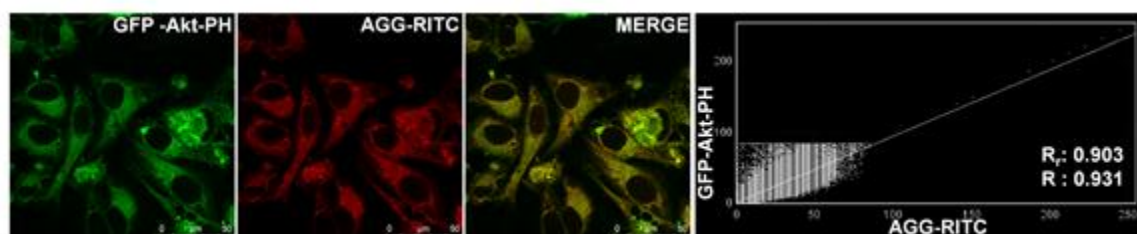


Fig.3.14. Colocalization of AGG and Akt-PH domain. Colocalization of RITC-AGG treated and GFP-Akt-PH transfected cells was performed in confocal microscopy (magnification 630X) (Leica TCS SP8) and colocalization was measured using JACoP plugin in single Z-stack sections of de-convoluted images.

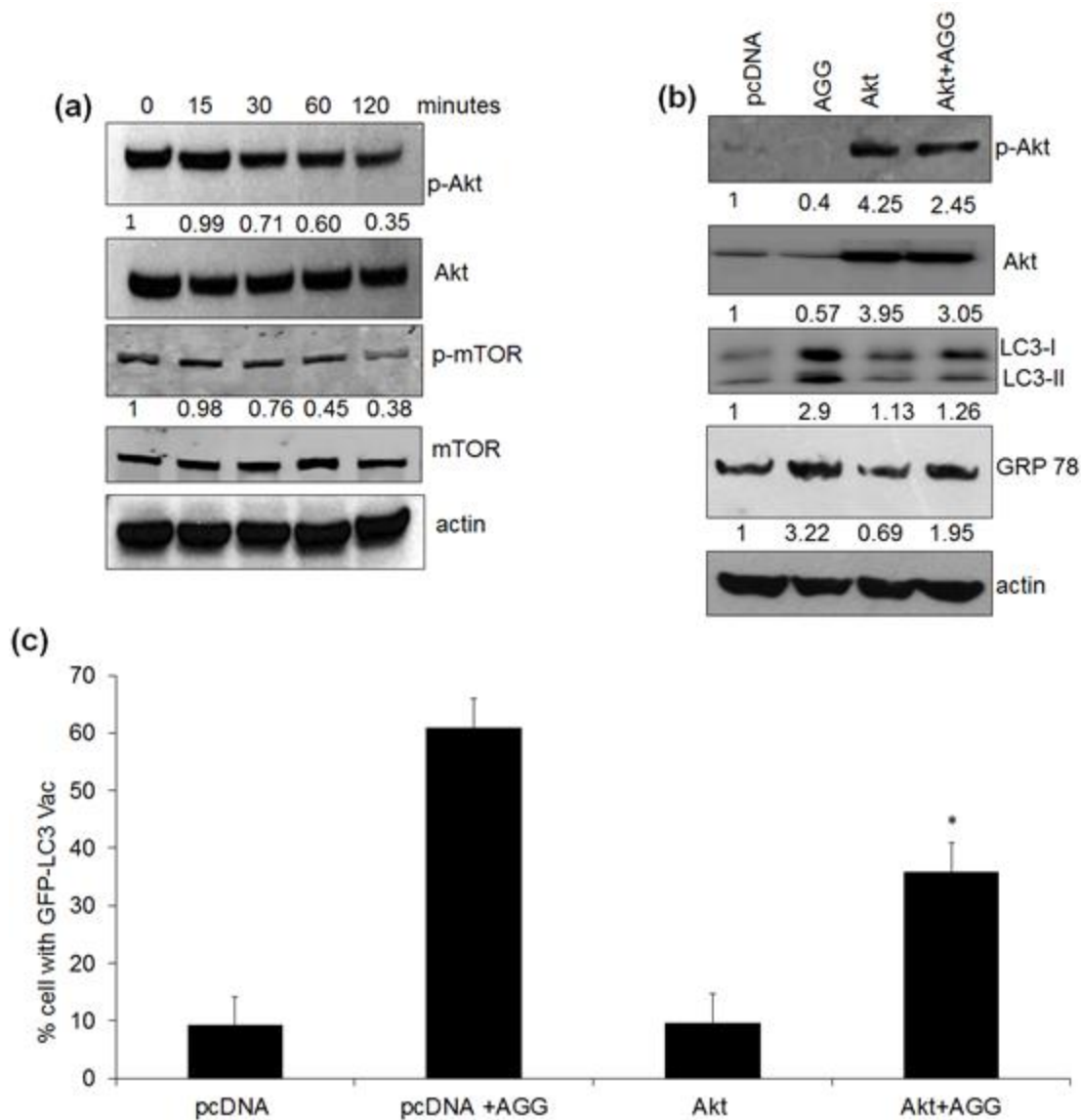


Fig.3.15. Akt plays a master signal for inducing autophagy by increasing ER stress. HeLa cells were treated with AGG (10 μ g/ml) for different times followed by analysis of Akt and mTOR expression by Western blot (a). The expression of LC3 II and GRP78 levels were analyzed in Akt overexpressed HeLa cells (b). Stably transfected GFP-LC3 clones were overexpressed with Akt and after AGG treatment autophagosome formation was quantified and data presented as a percentage of GFP-LC3 puncta cells by confocal microscopy (magnification 1000X) (c). Data represented as the mean \pm S.D. of three independent experiments. *represents statistically significant change vs. corresponding AGG treated group (* $P < 0.05$). Densitometry was performed on the original blots, considering the ratio of protein to actin in control cells was 1.

To examine the role of AGG in Akt phosphorylation, HeLa cells were treated with AGG for different time periods and the expression of Akt was analyzed. Treatment of AGG caused a significant time dependent reduction in the phosphorylation of Akt (Ser473). On the contrary, the total Akt expression remained unaltered at said time kinetics in the presence of AGG (Fig.3.15a). Further, AGG treatment resulted in diminished levels of the phosphorylated form of mTOR (Ser2448) without altering total mTOR (Fig.3.15a), revealing a potent inhibitory effect of AGG treatment on Akt/mTOR signaling. The critical role of Akt was further supported by the rescue experiment by transfecting constitutive

active Akt in HeLa cells. As expected overexpression of Akt interfere the AGG mediated ER stress, which was corroborated by reduced LC3-II accumulation and GFP-LC3 puncta, ultimately overcome the cell death by AGG (Fig.3.15.b,c). Therefore it could be firmly concluded that AGG induced ER stress associated with autophagic cell death by inhibition of Akt through PH domain in HeLa cells (Fig..16).

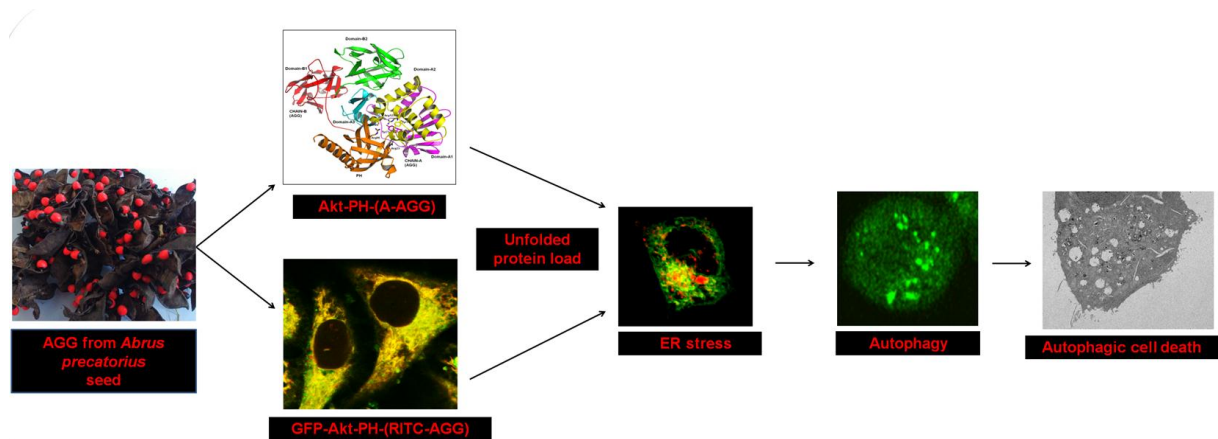


Fig.3.16. Schematic representation of AGG induced ER stress mediated autophagy dependent cell death in HeLa cells.

3.4. Discussion

Autophagy, an alternative tumor-suppressing mechanism have evolved as a potential novel approach for cancer therapies for induction of cell death, either in addition to or instead of, apoptosis induced treatment. A number of studies have reported that autophagic cell death is activated in cancer cells in response to various anticancer molecules including Tamoxifen, Temozolomide (TMZ), γ -irradiation, sodium butyrate, and suberoylanilide hydroxamic acid (SAHA), arsenic trioxide (As₂O₃) (Panda et al., 2015; Panda et al., 2014). Moreover, several clinical and preclinical studies established plant lectins including Phytohemagglutinin, Wheat germ agglutinin, Concanavalin A, *Momordica charantia* lectin, Mistletoe lectins, Soybean lectin, and Peanut agglutinin-induced autophagic cell death in different types of cancer (Liu et al., 2013; Fu et al., 2011; Panda et al., 2014; Chang et al., 2007; Roy et al., 2014; Zhang et al., 2015; Choi et al., 2012; Mukhopadhya et al., 2014). For instance, a lectin from *Polygonatum cyrtonema* induced apoptosis and autophagy in human melanoma A375 cells through a mitochondria-mediated ROS-p38-p53 pathway (Liu et al., 2009). Another lectin Concanavalin A from Jack bean seeds inhibited hepatoma cells through BNIP3 mediated mitochondria autophagy (Chang et al., 2007). Similarly, Korean mistletoe lectins, another type II ribosome inactivating protein (RIP II) regulated self renewal of placenta derived mesenchymal stem cells inducing autophagy at its low concentrations. Accordingly, in the present study, we documented that AGG induced

BECN1 dependent autophagic cell death through ER stress in human cervical cancer cells along with apoptosis inducing potential. In addition, AGG induced downregulation of Akt phosphorylation modulated autophagic cell death through strengthening ER stress.

In response to cancer therapy, cell death in tumor cells is induced in many ways including induction of autophagic cell death or apoptosis simultaneously, sequentially, or in a mutually exclusive manner (Panda et al., 2015; Li et al., 2011). Accordingly, we observed that AGG simultaneously induced apoptosis and autophagic cell death in cervical cells. Inhibition of autophagic death by 3-MA and knock down by siBECN1 and siATG5 significantly switched the cell death to apoptosis induced by AGG. In support, a previous study showed that several anticancer drugs SAHA and plant lectins induced both autophagic death and apoptosis (Panda et al., 2015; Liu et al., 2010; Li et al., 2014). Further, AGG induced significantly enhanced autophagic cell death in shBax transfected cells and 5-FU resistant cells indicating AGG could be very effective against apoptosis deficient and resistant cells. Accumulating data indicate that ER stress promotes autophagy as an adaptive mechanism and upon persistent stress, it can switch into cell death mechanisms, the autophagic cell death (Salzar et al., 2019 ; Li et al., 2008). Our study showed that AGG found to stimulate ER stress markers including GRP78, GRP94, CHOP, and eIF2 α phosphorylation through PERK dependent pathway. In this connection, GRP78, a major chaperone is considered to be the central regulator of UPR which acts as a novel obligatory component of autophagy in mammalian cells. For instance, knockdown of GRP78 inhibited autophagosome formation, which was induced by ER stress or by nutrient starvation in HeLa cells (Li et al., 2008). Similarly, stress dependent CHOP is important in the transcriptional activation of genes involved in the formation, elongation, and function of the autophagosome. Intriguingly, we demonstrated that inhibition of ER stress with salubrinal and si PERK reduced AGG induced autophagic cell death, suggesting a potential role of ER stress in AGG induced autophagy. In support, it was demonstrated that *Abrus* abrin-induced ER stress through stress kinases p38 MAPK to regulate apoptosis in Jurkat cells (Mishra et al., 2014). Akt can mediate cell survival and growth and its activity is regulated by phosphorylation on two regulatory residues, Thr308 in the activation loop of the catalytic domain and Ser473 in the regulatory domain. Akt inhibits autophagy through mTORC1 activation in response to growth factor stimulation (Panda et al., 2015; Bhutia et al., 2013; Panda et al., 2014). The mutational Akt hyperactivation diminishes autophagy during metabolic stress, whereas Akt inhibition by different types of antitumor molecules induces autophagic cell death. Our result showed that treatment of AGG caused significant time dependent reduction in the phosphorylation of Akt (Ser473) in HeLa cells and

overexpression of Akt found to suppress AGG induced autophagic death. A previous study showed that naturally occurring agents including Concanavalin A and Plumbagin-induce autophagy by inhibiting the Akt/mTOR in cancer cells (Roy et al., 2014; Kuo et al., 2006). For the first time, AGG demonstrated to bind with PH domain of Akt through the active site region and adjacent areas, located in the cleft made by three domains of A chain preserved among the type II RIPs (Bagaria et al., 2006). Apart from N-glycosidase enzymatic activity, our study documented an unknown function of A chain of AGG and AGG could be considered as nonlipid based PH domain inhibitor which needs to be deciphered in detail. Further, how does A chain of AGG inhibit PH domain and influence Akt phosphorylation and translocation are not known. In our study, induction of ER stress through inhibition of Akt was the master signal for AGG induced autophagic cell death. Numerous studies were available where Akt-mTOR pathway was associated with the ER stress induced induction of apoptosis as well as autophagy (Jiang et al., 2013; Jung et al., 2013; Yu et al., 2015). Recently it was reported that resveratrol a natural polyphenol triggers ER stress which leads to autophagic cell death in prostate cancer cells via down regulation of Akt-mTOR pathway (Selvaraj et al., 2015). In conclusion, the present results establish that AGG stimulated cell death by autophagy through ER stress and Akt dephosphorylation by binding with PH domain might be explored as an alternative tumor suppressor mechanism in cervical carcinoma.

Chapter 4

PUMA dependent mitophagy by *Abrus* agglutinin contributes to apoptosis through ceramide generation

Abstract

PUMA, a BH3-only pro-apoptotic Bcl-2 family protein translocates from the cytosol to mitochondria to induce apoptosis. Interestingly, the induction of PUMA by p53 also plays a critical role in DNA damage induced apoptosis. In this study, we identified mitophagy inducing potential of PUMA triggered by *Abrus* agglutinin (AGG), a lectin from Indian medicinal plant in U87MG cells and established AGG induced ceramide as a chief mediator of mitophagy dependent cell death through activation of mitochondrial ROS and ER stress. Importantly, AGG upregulated PUMA expression in U87MG cells with the generation of dysfunctional mitochondria along with gain and loss of function of PUMA altered mitophagy induction. At the molecular level, we identified an LC3 interacting region (LIR) at the C-terminal end of PUMA and found to interact with LC3 to induce mitophagy. In addition, AGG was also shown to trigger ubiquitination in PUMA which interacted with p62 to induce mitophagy suggesting AGG mediated mitophagy through PUMA contributed both in p62 dependent and independent manner in U87MG cells. Further pre treatment of Mdivi-1, an inhibitor of Drp1, resulted in an increase in outer mitochondrial membrane protein TOM20 expression and decrease in caspase activity in response to AGG in U87MG cells, indicating AGG induced mitophagy switched to apoptosis.

Keywords: *Abrus* agglutinin, Apoptosis, LC3 interacting region, Mitophagy, PUMA, p62, Ubiquitin

4.1. Introduction

Autophagy is an evolutionarily conserved self degradative process where a cell digests its own cytoplasmic contents to recycle nutrient pool and energy at critical times in development and in response to various stress stimuli. Basically, autophagy plays a pro survival role; however, extensive or prolonged stress may lead to the autophagic point of no return and ultimately cell death (Bhutia et al., 2013; Panda et al., 2015). Moreover, recent advancement in the field of autophagy has elucidated that in contrast to bulk degradation, there exists an independent process of selective degradation of cytoplasmic contents and organelles called as selective autophagy (Fimia et al., 2013; Van Der Vaart et al., 2008; Zaffagnini & Sascha., 2016). In this context, the selective clearance of damaged and superfluous mitochondria referred as “Mitophagy” are highly investigated in many pathophysiological conditions owing to the fact that mitochondria are the central regulator of energy balance and mitochondrial quality control is of utmost importance in maintaining cellular homeostasis. In fact, mitophagy plays an indispensable role in paternal

mitochondrial degradation, terminal differentiation of RBCs, ischemia, neurodegenerative diseases, cancer and or drug-induced tissue injury (Lemasters, 2005; Kim et al., 2007; Youle & Narendra, 2011; Ashrafi & Swartz, 2013).

After the inception of the concept of selective clearance, the first question arose was to decipher how the mitochondria are primed and recruited to the autophagosome for its specific degradation. In this perspective, several autophagy adaptors like p62 and NBR1 have been identified and characterized to act as cargo receptors for degradation of ubiquitinated substrates which provides a mechanistic insight into the process of mitophagy. Moreover, several reports have documented the direct interaction between these autophagic adaptors and the autophagosomal marker protein LC3 via a specific LIR (LC3-interacting region) motif (Johansen & Lamark, 2011). Depolarized ubiquitylated mitochondria were recruited to ubiquitin-binding adaptor protein p62 in the perinuclear region forming mitoaggregates before ending with lysosomal degradation (Narendra et al., 2008; Sandoval et al., 2008; Narendra et al., 2010). Further, for mitophagy to happen, dysfunctional mitochondria must be selectively recognized through the mitophagy receptor, which is expressed on the outer mitochondrial membrane, to be removed (Kim et al., 2007; Yamaguchi et al., 2016). The involvement of specific molecules in sensing damaged mitochondria for selective engulfment by autophagosomes in mammalian cells remains elusive. A recently identified pathway that has emerged as a paradigm for mammalian mitophagy is mediated by the PINK1 and the E3 ubiquitin ligase Parkin. During stress, PINK1 is stabilized on damaged mitochondria resulting in the recruitment of Parkin for ubiquitinating several outer mitochondrial proteins followed by recruitment to the adaptor proteins like p62 which then interact with LC3 to induce mitophagy (Ashrafi et al., 2013, Bjorkoy et al., 2009 ; Chang et al., 2016). Several proteins that have the propensity to interact with autophagosomal marker protein LC3, are now identified to act as mitophagy receptor in directing mitochondria to autophagosomes including cardiolipin, FUNDC1, BNIP3, NIX, VDAC1, PINK1 and BCL2L13 (Yamaguchi et al., 2016). Ubiquitination of the mitochondrion, and/or the interaction of a receptor with the LC3 appear to be important in the targeting of the autophagosome, but in each case, the details of this recruitment remain unclear. Previously, C18-pyridinium ceramide treatment or endogenous C18-ceramide production by ceramide synthase 1 (CerS1) expression was reported to trigger autophagic cell death in cancer. C18 ceramide promoted LC3IB lipidation to LC3BII and provoked selective targeting of mitochondria by LC3B-II containing autophagolysosomes via direct interaction between ceramide and LC3B-II (Sentelle et al., 2012). Moreover, the

involvement of several BH3 only protein like Bcl-2/E1B 19 kDa-interacting protein 3-like protein (BNIP3) and Nix (BNIP3L) are reported to be associated with the removal of damaged mitochondria (Zhang & Ney., 2009, Novak et al., 2010). Recently, another BH3 only protein Bcl-2-like protein 13 (Bcl2L13) was shown to induce Parkin independent mitophagy via its direct interaction with LC3 through the WXXI motif indicating the existence of alternate pathways for mitophagy (Murakawa et al., 2015). In response to therapies, cancer cells may undergo either apoptosis and/or autophagic cell death which are in a quite complicated relationship. Apoptosis or autophagy may occur simultaneously, or autophagy may follow to apoptosis, or they may occur autonomously of each other (Panda et al., 2015). In this context, mounting evidence indicate an intricate crosstalk between autophagy and apoptotic molecule to govern cell fate (Mukhopadhyaya et al., 2014). Several BH3only proteins BNIP3, Bad, and BH3 mimetics were shown to trigger autophagy by competitively inhibiting the interaction between BECN1 and Bcl-2 or Bcl-xL. Likewise, BH3- only proapoptotic PUMA and Bax were reported to stimulate autophagy which followed to apoptosis (Yee et al., 2009).

Tumors of glial origin referred as gliomas are the most common primary brain tumors. The High grade gliomas (HGGs) including glioblastoma (GBM) and anaplastic astrocytoma (AA) are the most frequent intrinsic adult brain tumors (Phillips et al., 2006; Holla et al., 2016). Glioblastoma multiforme (grade IV) is reported to be one of the most aggressive cancers, with a median survival of less than 1 year. Despite recent advances in field of oncology, this median survival has not altered significantly over the past few years (Peterson et al., 2016). In the present study, we have investigated glioma inhibitory activity of *Abrus* agglutinin (AGG), a natural compound through induction of mitophagy mediated cell death as an alternative tumor suppressor mechanism. AGG, a galactose specific lectin isolated from the seeds of Indian medicinal plant, *Abrus precatorius*. It belongs to the class II ribosome inactivating protein family with protein synthesis inhibitory activity. It is a hetero-tetrameric glycoprotein of 134-kDa MW, composed of two A and two B chains linked through disulfide bridges. It induces both extrinsic and intrinsic apoptosis and showed antitumor effect in several tumor models at sub-lethal doses (Bagaria et al., 2006). Furthermore, it leads to the activation of macrophages and NK cells to boost immune response (Tripathi et al., 2005 ; Mukhopadhyay et al, 2014). AGG inhibited expression of the pro-angiogenic factor IGFBP-2 in an AKT-dependent manner, reducing angiogenic phenotypes both *in vitro* and *in vivo* (Bhutia et al., 2016). AGG derived peptides induce ROS dependent mitochondrial apoptosis through JNK and Akt/P38/P53 pathways in HeLa cells (Behera et al., 2014). In the previous chapter, AGG mediated Akt dephosphorylation led to

ER stress resulting induction of autophagy dependent cell death through the canonical pathway in cervical cancer cells (Panda et al., 2017). In this study, we identified mitophagy inducing potential of PUMA triggered by AGG in U87MG cells and established AGG induced ceramide as a chief mediator of mitophagy dependent cell death through activation of mitochondrial ROS and ER stress to better cancer therapeutics.

4.2 Materials and Methods

4.2.1 Reagents and Chemicals

3-(4,5-dimethylthiazol-2-yl)-2,5-diphenyltetrazolium (MTT), 4',6-diamidino-2-phenylindole dihydrochloride (DAPI), Dimethylsulfoxide (DMSO), Propidium iodide (PI), N-acetyl-L-cysteine (NAC), Ceramide (C8104-50TST), 3-Methyl adenine (3-MA), Salubrinal (324895), Chloroquine, Myriocin (M1177-5mg), Methyl pyruvate (371173), Mdivi-1 (M0199) and Dihydroethidium (DHE) were purchased from Sigma-Aldrich (St Louis, MO, USA). Fetal bovine serum (FBS) (sterile-filtered, South American origin), Minimal essential medium (MEM), opti-MEM, Lipofectamine® 2000, MitoTracker Green (M7514), CMXRos (M7512) were purchased from Invitrogen. Caspase Glo- 3/7 assay kit (T8090), Caspase Glo- 8 assay kit (G8200), Caspase Glo- 9 assay kit (G8210) were purchased from Promega (Madison, Wisconsin, USA).

Abrus agglutinin was purified as described in chapter 3 of this thesis.

4.2.2 Antibodies

Antibodies are used: Ceramide (C8104-50TST) was obtained from Sigma-Aldrich; Anti-PUMA (4976S), BECN1 (3738S), ATG5-ATG12 (2630S), Bax (2772S), Bcl-2 (2870S), COXIV (4850), pDRP1 (3455), PARP (9542S), p53 (2527BC) were purchased from Cell Signaling Technology (Danvers, MA, USA); LC3 (NB100-2220) was obtained from Novus Biological (Littleton, CO); mouse secondary Alexaflour green (A11001), mouse secondary Alexaflour red (A11004), rabbit secondary Alexaflour green (A11008) were purchased from Invitrogen; p62 (610832), TOM20 (612278) and GRP78 (610978) were purchased from BD Bioscience, γ H2AX (05363) was purchased from Millipore, β -actin (11-13012) was purchased from Abgenex (BBSR, India).

4.2.3 Plasmid and siRNA

U87MG cells were transiently transfected with pEX-HcRed-hLC3WT (Addgene plasmid # 24991) and pEX- HcRed -hLC3 Δ G (Addgene plasmid#24992) which were a gift from Isei Tanida (Addgene plasmid # 24991). Besides, glioblastoma cells were transfected with pBABEpuro-HA-p62-LIR and this plasmid was a gift from Jayanta Debnath (Addgene plasmid # 71306). P(40)PX-EGFP plasmid was transfected in glioma cells for

autophagosome clustering study which was a gift from Michael Yaffe (Addgene plasmid # 19010). Overexpression of PUMA was performed by transfecting BI-EGFP-PUMA which was a gift from Bert Vogelstein (Addgene plasmid # 16590). siRNA for BECN1 (sc29797) from Santa Cruz Biotechnology. A corresponding empty backbone vector was transfected for every plasmid of interest.

4.2.4 Cell Culture

Human glioblastoma cell line (U87MG) was obtained from National Centre for Cell Sciences (NCCS), Pune, India and cultured in Minimal Essential Medium (MEM) containing 10% fetal bovine serum (FBS) with 1X antibiotic-antimitotic and incubated at 37°C temperature in a humidified 95% air, 5% CO₂ incubator.

4.2.5 Acridine Orange Staining

U87MG cells were treated with various doses of AGG for 24 h and cells were stained with acridine orange at 37°C in the dark for 15 min and washed twice with PBS. Acridine orange fluorescence intensity was analyzed by fluorescence microscope (Olympus IX71, Tokyo, Japan) (Panda et al., 2014).

4.2.6 Measurement of Autophagy by GFP-LC3 Transfection

U87MG cells were transiently transfected with pEGFP-LC3 (Addgene plasmid #11546) using Lipofectamine® 2000 reagent (Gibco) according to the manufacturer's instructions. The GFP-LC3- U87MG stable clone was made using G418 screening. U87MG cells were treated with different doses of AGG for 24 h and analyzed by a confocal laser scanning microscope. Quantification was done by counting the mean number of puncta displaying intense staining and a minimum of 100 GFP-LC3 transfected cells were counted (Panda et al., 2017).

4.2.6 Western Blot and Immunoprecipitation Analysis

U87MG cells were treated with AGG followed by extraction of proteins. Cell were lysed with a lysis buffer and about 50 µg protein was subjected to SDS-PAGE electrophoresis, followed by transfer onto a nitrocellulose membrane, which was blocked with 5 % BSA (in PBST) at room temperature for 1 h. After that blots were incubated with primary antibody anti-BECN1, ATG5, LC3, actin, p-AMPK, p-S6K, p-mTOR, TOM20, COX-IV, DRP1, p-DRP1, PRAP, Bax, Bcl-2, GRP78 for 14-16 hour followed by secondary antibody labeled with horseradish peroxidase-conjugate secondary antibody and the expression were documented in chemiluminescence Image Quant LAS500 (GE Healthcare, USA). For immunoprecipitation, the cell lysates were incubated overnight at 4°C with the mentioned antibodies followed by coupling with protein A-Sepharose (Invitrogen Corporation, CA,

USA) followed by after that western blot was performed with suitable antibody (Mukhopadhyay et al., 2015).

4.2.7 Electron Microscopy

After the 24 h of treatment, the cells were fixed with 2.5% glutaraldehyde buffered with 0.1M sodium phosphate at pH 7.4. Then the samples were fixed with osmium tetroxide followed by staining with uranyl acetate, dehydrated in ethanol and embedded in uranyl acetate. After sectioning, samples were collected on uncoated nickel grids and documented and damaged mitochondria were photographed using a transmission electron microscope.

4.2.8 Immunofluorescence Staining for Confocal Imaging

Cells were grown on chamber slides and treated with AGG in a dose dependent and time dependent manner along with different inhibitors like ISP, salubrinal, NAC prior to 2 h of treatment according to the experiment setup. Cells were pretreated with Pyr-41 for observing effect of ubiquitination on TOM20 expression. Post-treatment with AGG, cells were fixed in 10 % formaldehyde, washed with PBS, permeabilized with 0.2 % Triton X-100 for 20 min at RT and incubated overnight with primary antibody for ceramide and TOM20. Then the cells were washed with PBS and incubated with secondary antibody for 6 h followed by DAPI counterstaining. The expression pattern of concerned marker proteins was analyzed by confocal laser microscope (Leica TCS SP8) (Panda et al., 2017).

4.2.9 Colocalization Study by Confocal Imaging

The transfected cells were seeded on chambered slide and treated with AGG for 24 h hour at 37°C. The cells were processed as described before and incubated with primary antibody TOM20 for overnight at 4°C followed by secondary antibody conjugated with the Alexa Flour. And then co-localization expression was studied by confocal laser microscope (Leica TCS SP8) (Panda et al., 2017).

4.2.10 Caspase Activity Assays

U87MG cells were grown on 6 well plates and treated with AGG for 24 h along with prior 2 h of ISP treatment according to the experimental setup. After treatment, caspase 3/7, caspase 8 and caspase 9 activities in U87MG cells were measured using Caspase-Glo 3/7, Caspase-Glo 8 and Caspase-Glo 9 Assay kits (Promega Corp., Madison, WI, USA) according to the manufacturer's protocol. Caspase activities were analysed and quantified as relative luciferase units (Panda et al., 2014).

4.2.11 Measurement of Mitochondrial Respiration Rate and Glycolysis Study

For determination of oxygen consumption rate (OCR), 1×10^5 U87MG cells per well were seeded in a 96 well plate. OCR measurement was done using XF-24 Extracellular Flux Analyzer (Seahorse Bioscience, MA, USA) according to (Mukhopadhyay et al., 2015). The

rate of aerobic glycolysis in terms of enzymatic lactate production was determined in U87MG cells after AGG treatment at different time interval (Mukhopadhyay et al., 2015).

4.2.12 Measurement of Cellular ATP Level

Cellular ATP quantification was analyzed in U87MG cell lysates post 24 h of AGG treatment by following the protocol described on the ENLITEN[®] ATP Assay System Bioluminescence kit from Promega (Madison, WI, USA) (Mukhopadhyay et al., 2015).

4.2.13 Comet Assay

AGG treated U87MG cells embedded in agarose were layered on the frosted slides that were pre-coated with 1 % agarose for both controls and treated cell suspensions. The procedure was followed as described before (Panda et al., 2014). The intensity of the comet tail relative to the head reflects the degree of DNA breaks. Imaging was done at each concentration and by fluorescence microscopy (Olympus IX71).

4.2.14 Modeling PUMA-LC3 Complex through Docking and Molecular Dynamics Simulation

Due to the unavailability of a crystal structure for the protein hPUMA, the 3D structure of the same was predicted from the FASTA sequence (Yu et al., 2001) by the *ab initio* modeling in PHYRE-2 software (Kelley et al., 2015). The sequence information for hPUMA describes amino acids from 128 to 165 (AA128-AA165) as an alpha-helix by Chou-Fasman method, that has been exactly predicted in the structure. The crystal structure of microtubule associated protein light chain 3 (LC3), a mammalian homologue of *Saccharomyces cerevisiae* Atg8 was obtained from the Protein Data Bank (PDB). The PDB entry was: 1UGM (Sugawara et al., 2004). X-ray structure of the LC3 domain has some missing residues both in the C- and N-terminal region, which were eventually predicted by the PHYRE-2 software. LC3 domain contains 119 residues after the modelling through PHYRE-2. The docking algorithm was then used to locate the optimal configuration of the LC3 protein near to the active site of hPUMA. Initially, the LC3 domain was positioned near the active site, and the docking algorithm was carried out by the ClusPro 2.0 protein-protein docking server (Comeau et al., 2004). Using protein-protein docking algorithms, the optimal orientation of two proteins could be found by scoring the energy based on the van der Waal's (VDW) contacts and corresponding electrostatics. Therefore, the grid based score was generated by calculating the nonbonded terms of the molecular mechanics force field, and the structure with the highest score was then considered for the MD simulation.

4.2.15 Statistical Analysis

All the results were represented as the mean Experimental data were analyzed by Student's t-test. The level of significance was regarded as $P < 0.05$ for values obtained for treatment

compared to control. The IC₅₀ values of various cell lines after AGG treatment were calculated by using the program GraphPad Prism 5 (GraphPad Software, San Diego, CA) to fit a variable slope-sigmoidal-dose-response curve.

4.3. Results

4.3.1 AGG Induces DNA Damage Mediated Apoptosis

AGG has been shown to induce apoptosis in different cellular settings and associate with tumor suppressor mechanism. We have described AGG induced DNA damage as upstream signal for induction of autophagy and in this study we were interested to examine involvement of DNA damage pathway in autophagy induction. Primarily, AGG induced DNA damage was analyzed in U87MG cells by performing γ H2AX foci formation (Fig.4.1.a, b) and comet tail assay (Fig.4.1.c, d). We further confirmed the apoptosis inducing potential of AGG through Annexin V (Fig.4.2.a) and DAPI staining (Fig.4.2.b) in U87MG cells and data showed that chromatin condensation, nuclear blebbing was increased in presence of AGG in comparison to control cells. Interestingly, AGG triggered apoptotic cell death was evidenced by decrease of anti-apoptotic Bcl-2 protein expression and increase of Bax, PARP and p53 activation (Fig.4.2.c). Similarly, AGG increased the activation of caspase (3/7), caspase 8 and caspase 9 (Fig.4.2.d) in treated cells conforming AGG induces both extrinsic and intrinsic apoptosis in U87MG cells.

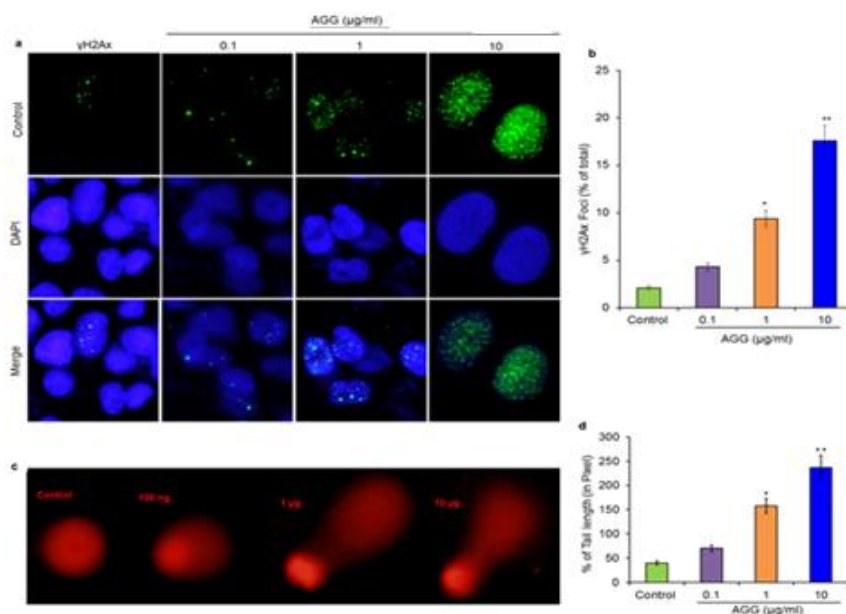


Fig.4.1. AGG facilitates DNA damage in U87MG cells. U87MG cells were treated with AGG for 6 h and γ H2AX staining was performed to measure foci formation by fluorescence microscopy (Olympus IX71; 400X). Number of foci formation per nucleus was calculated and percentage was taken to plot the histogram. U87MG cells were treated for 6 h with different doses of AGG (0.1, 1, 10 μ g/ml) followed by comet assay. After propidium iodide staining, photographs were taken in fluorescence microscope (Olympus IX71, 400X) (c, d). Data reported as the mean \pm S.D. of three independent experiments and compared to PBS control. * P value < 0.05; ** P value < 0.01 were considered significant.

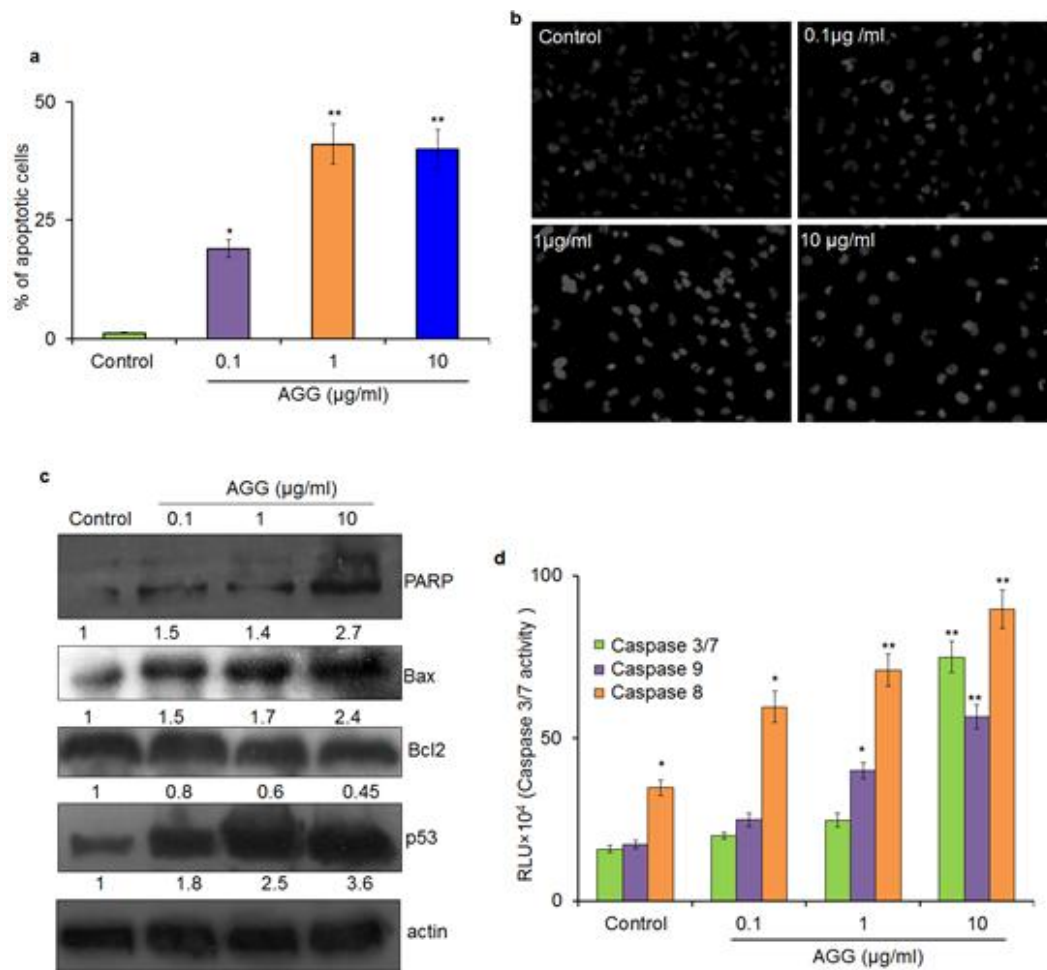


Fig.4.2. AGG induces apoptosis in U87MG cells. U87MG cells were treated with AGG 24 h and apoptosis was quantified by Annexin V/PI staining through flow cytometry (a), DAPI staining (b), expression of apoptotic proteins by Western blot (c) and caspase activity by Caspase Glo assay (d). Data reported as the mean \pm S.D. of three independent experiments and compared to PBS control. *P value < 0.05; **P value < 0.01 were considered significant. Densitometry was performed on the original blots, considering the ratio of protein to actin in control cells was 1.

4.3.2 AGG Induces Autophagy through AMPK/mTOR Dependent Pathway

Our previous study showed that AGG induces autophagy dependent cell death in cervical carcinoma. We were interested in what way autophagy is induced and its molecular mechanism with AGG in glioblastoma model. To discover the autophagy inducing potential of AGG in glioblastoma cell line U87MG, the cells were treated with different concentration of AGG (0.1, 1 and 10 $\mu\text{g/ml}$) for 24 h and different assay for autophagy was performed. Our data showed that red intensity in acridine orange stained cells was increased in dose dependent manner showing the occurrence of autophagy in U87MG cells (Fig.4.3.a, b). Next, GFP-LC3 transfection was performed for quantification of punctate structure in both control and AGG treated U87MG cells. Diffuse GFP-LC3 green fluorescence was found in the cytoplasm of control group while punctate fluorescence structure was found in the

treated cells confirming the recruitment of GFP-LC3 during induction of autophagy. Further, the percentage of GFP-LC3 punctate structure was significantly increased in case of AGG treated cells than control (Fig.4.3.c, d). Likely, we monitored the endogenous expression of LC3 in U87MG cells in presence of AGG and our data showed that AGG induced increase in LC3-II accumulation in dose dependent manner in comparison to control. Interestingly, the expression of autophagic proteins including BECN1 and ATG5 were noticed in AGG treated U87MG cells, confirming AGG induces autophagy in glioblastoma model (Fig.4.3.e). To examine whether AGG follows general AMPK/mTOR signaling axis, we treated U87MG cells with AGG (10 μ g/ml) for different time intervals and analyzed the expression autophagy regulatory protein in this pathway. Importantly, we noticed the diminished expression of the mTOR and its downstream molecule p-S6K expression in time dependent manner while increased in activation of AMPK (Fig.4.3.f). The mTOR is considered as a central cell-growth regulator while AMPK is a key energy sensor which maintains homeostasis is associated in AGG induced autophagy (Kim et al., 2011).

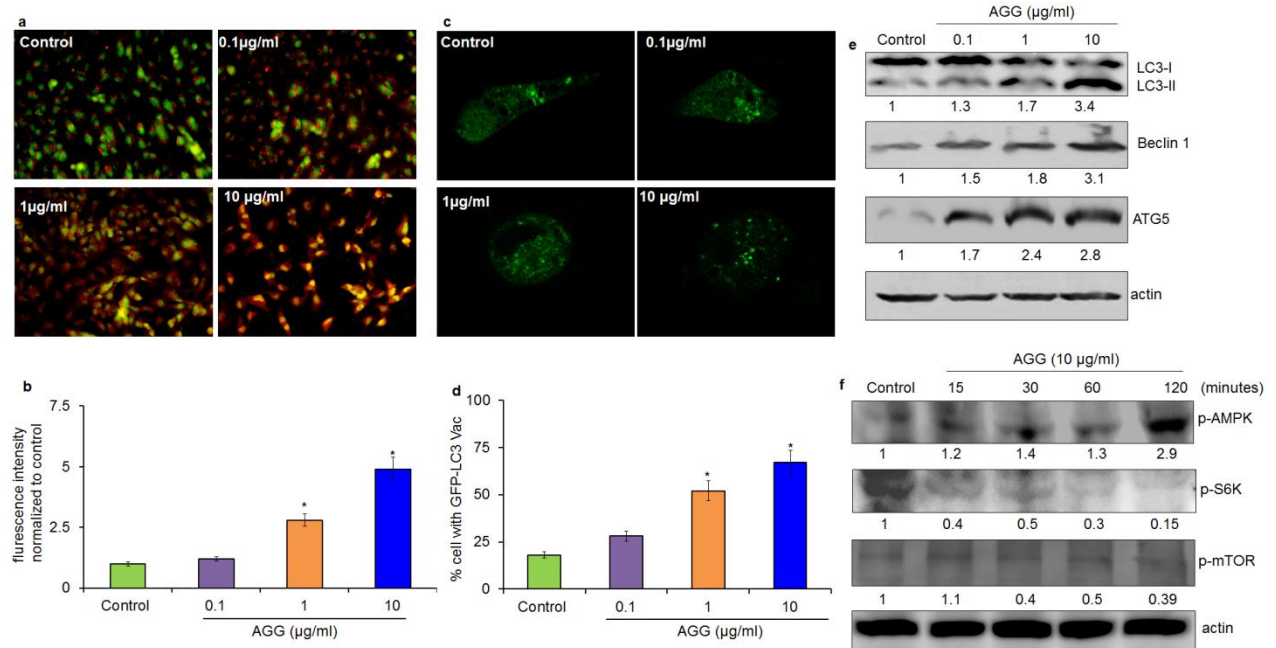


Fig.4.3. AGG induces autophagy in U87MG cells. U87MG cells were treated AGG for 24 h and acridine orange staining was performed (a,b) and GFP-LC3 puncta analysis were performed (c,d), autophagic proteins (e) and autophagic regulator (f) by western blot was quantified. Data reported as the mean \pm S.D. of three independent experiments and compared to PBS control. * P value < 0.05; ** P value < 0.01 were considered significant. Densitometry was performed on the original blots, considering the ratio of protein to actin in control cells was 1.

4.3.3 AGG Induces Mitochondrial Autophagy

Next, we were intended in determining to what extent AGG induced autophagy contributes to mitochondrial degradation in U87MG cells. After 24 h of AGG treatment, we analyzed U87MG cells for mitophagy induction through transmission electron microscopy. The

electron micrograph showed that mitochondria were specifically affected in AGG treated U87MG cells as compared to control (Fig.4.4.a, b). The number of healthy mitochondria could be recognized by identifying intact cristae and was (60 ± 5.9 %) and (4 ± 0.43 %) in control and treated respectively. The percentage of fragmented mitochondria was demonstrated by observing dramatically disrupted cristae after AGG treatment and found $28 \pm 2.7/50 \pm 5.1$ % in control/AGG treated U87MG cells. Importantly, we identified double membrane autophagosome engulfed damaged mitochondria in AGG treated cells. Moreover, some of the depolarized fragmented swollen mitochondria more appropriately mitochondrial remnants were engulfed by the autophagosome and their percentage in control and in AGG treated was (2 ± 0.21) and (6 ± 0.61) respectively. In addition, there was significantly increasing in the number of autophagic structures in AGG treated cells (40 ± 4.1 %) in comparison to control (10 ± 0.7 %) (Fig.4.4.b). Next, we transfected the cells with GFP-LC3 for autophagosome marker and stained with TOM20 found in the outer mitochondrial membrane. In control, we could not find any remarkable increase in GFP-LC3 and TOM20 positive cells, however in AGG treated U87MG cells there was a significant increase of GFP-LC3 and TOM20 positive cells (Fig.4.5.a, b) which indicate AGG induced depolarized mitochondria undergoes mitochondrial clearance. TOM20 down regulation is generally associated with clearance of mitochondria resulting from mitophagy and both western blot and immunofluorescence analysis revealed TOM20 expression was decreased dose and time dependent manner after exposure with AGG for 24 h in U87MG cells. Interestingly, we quantified the reduction of integral inner mitochondrial membrane protein cytochrome c oxidase subunit IV (COX IV) after AGG treatment (Fig.4.6.a). Dynamin related protein 1 (Drp1) is generally known as the master regulator of mitochondrial fission process was decreased at the phosphorylation Ser637 in AGG treatment resulting depolarized mitochondria generation and mitophagy (Fig.4.6).

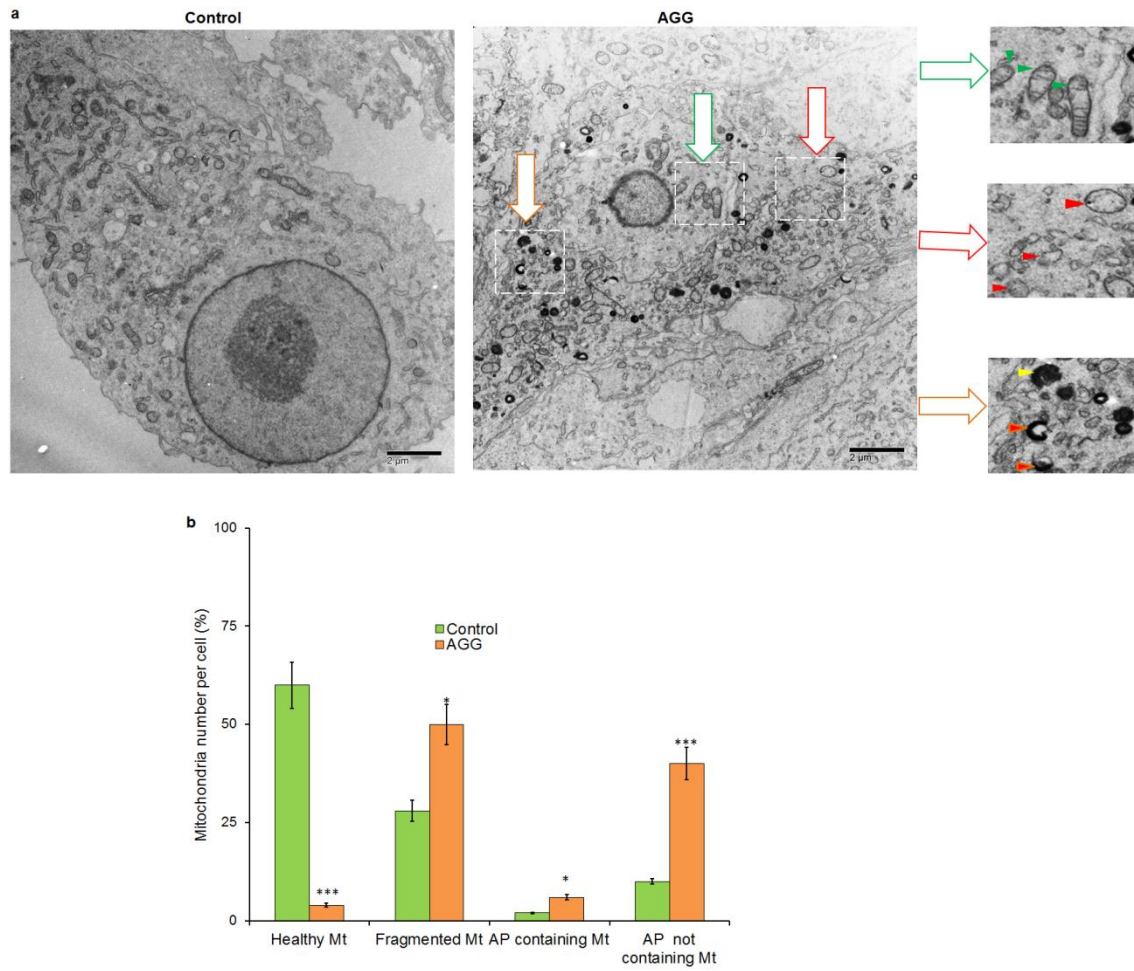


Fig.4.4. TEM analysis in AGG treated U87MG cells. U87MG cells were treated with AGG for 24 h and cells were fixed and processed for electron microscopy (a). The numbers of healthy and damaged mitochondria with autophagosome was quantified (b). Data reported as the mean \pm S.D. of three independent experiments and compared to PBS control. * P value < 0.05 ; ** P value < 0.01 were considered significant.

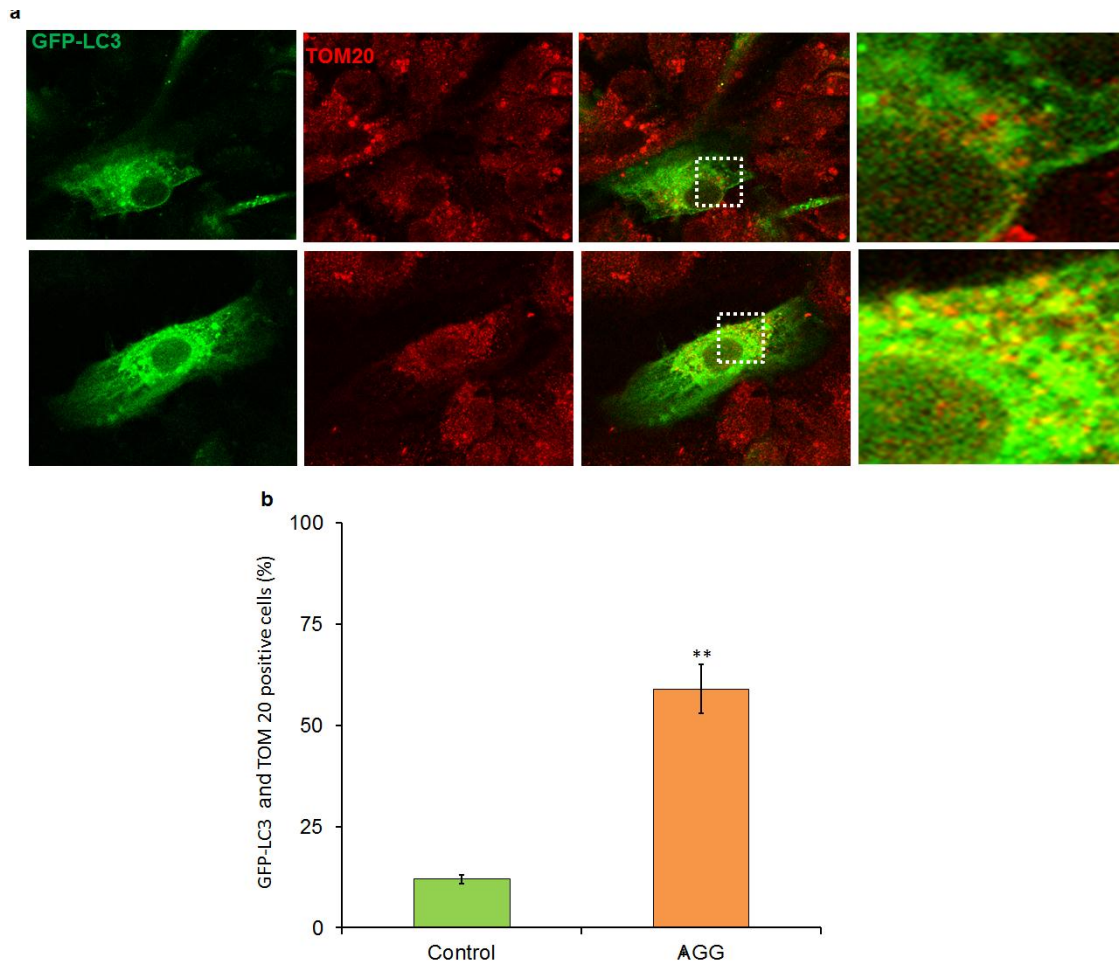


Fig.4.5. Colocalization of GFP-LC3 and TOM20 in AGG treated U87MG cells. U87MG cells were transfected with GFP-LC3 and stained with TOM20 after 24 h AGG treatment and interaction of GFP-LC3 and TOM20 was analyzed through confocal microscopy (a, b). Data reported as the mean \pm S.D. of three independent experiments and compared to PBS control. * P value $<$ 0.05; ** P value $<$ 0.01 were considered significant.

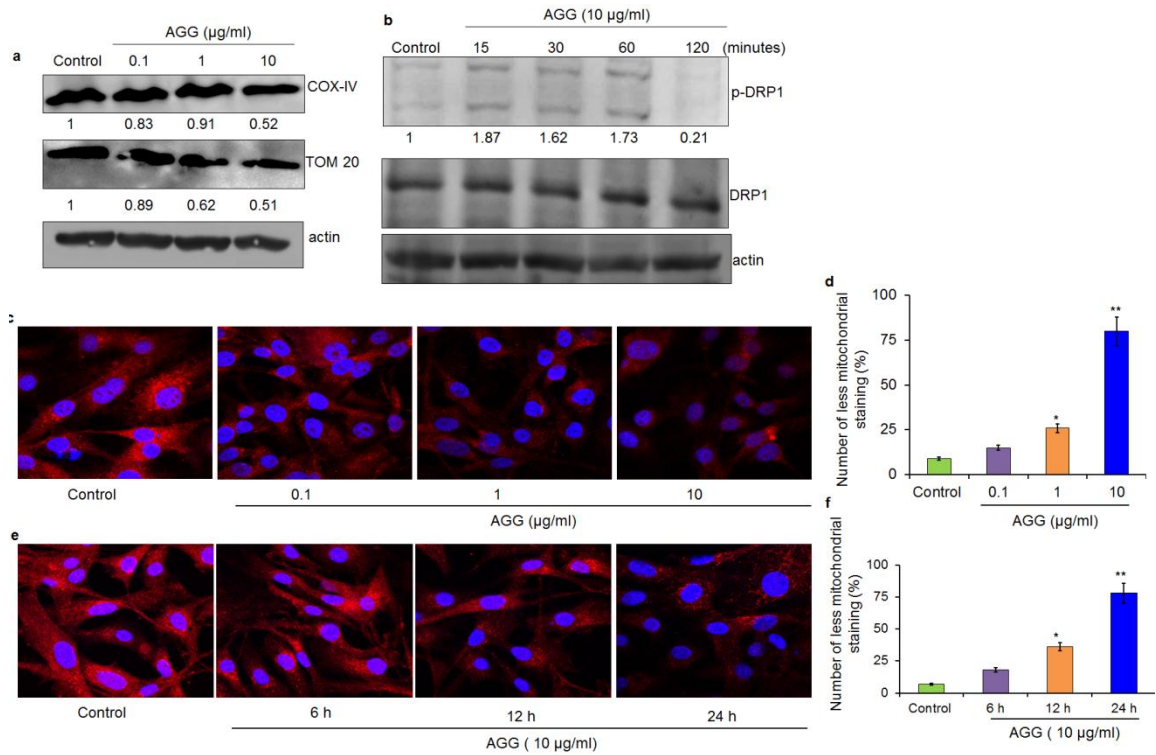


Fig.4.6. Effect of AGG on mitophagy associated proteins in U87MG cells. U87MG cells were treated with AGG and expression of COX IV, TOM20, p-DRP1, Total DRP1 by western blot (a,b) and expression of TOM20 through confocal microscopy (c). Data reported as the mean \pm S.D. of three independent experiments and compared to PBS control. * P value < 0.05 ; ** P value < 0.01 were considered significant. Densitometry was performed on the original blots, considering the ratio of protein to actin in control cells was 1.

Further, we quantified AGG induced mitophagy in BECN1 knockdown cells and in presence of autophagy inhibitors. Our data showed that AGG significantly restores the decrease in expression of TOM20 in BECN1 deficient cells as compared to sicontrol (Fig.4.7.a, b). Similarly, the expression of COX IV was dramatically reinstated in the siBECN1 knock down cells as to sicontrol in presence of AGG in U87MG cells (Fig.4.7.c). The pretreatment of pharmacological inhibitors including 3-MA and chloroquine inhibited AGG induced mitophagy in U87MG cells (Fig.d-g) confirming AGG induced mitochondrial damage leads to mitophagy for mitochondrial clearance.

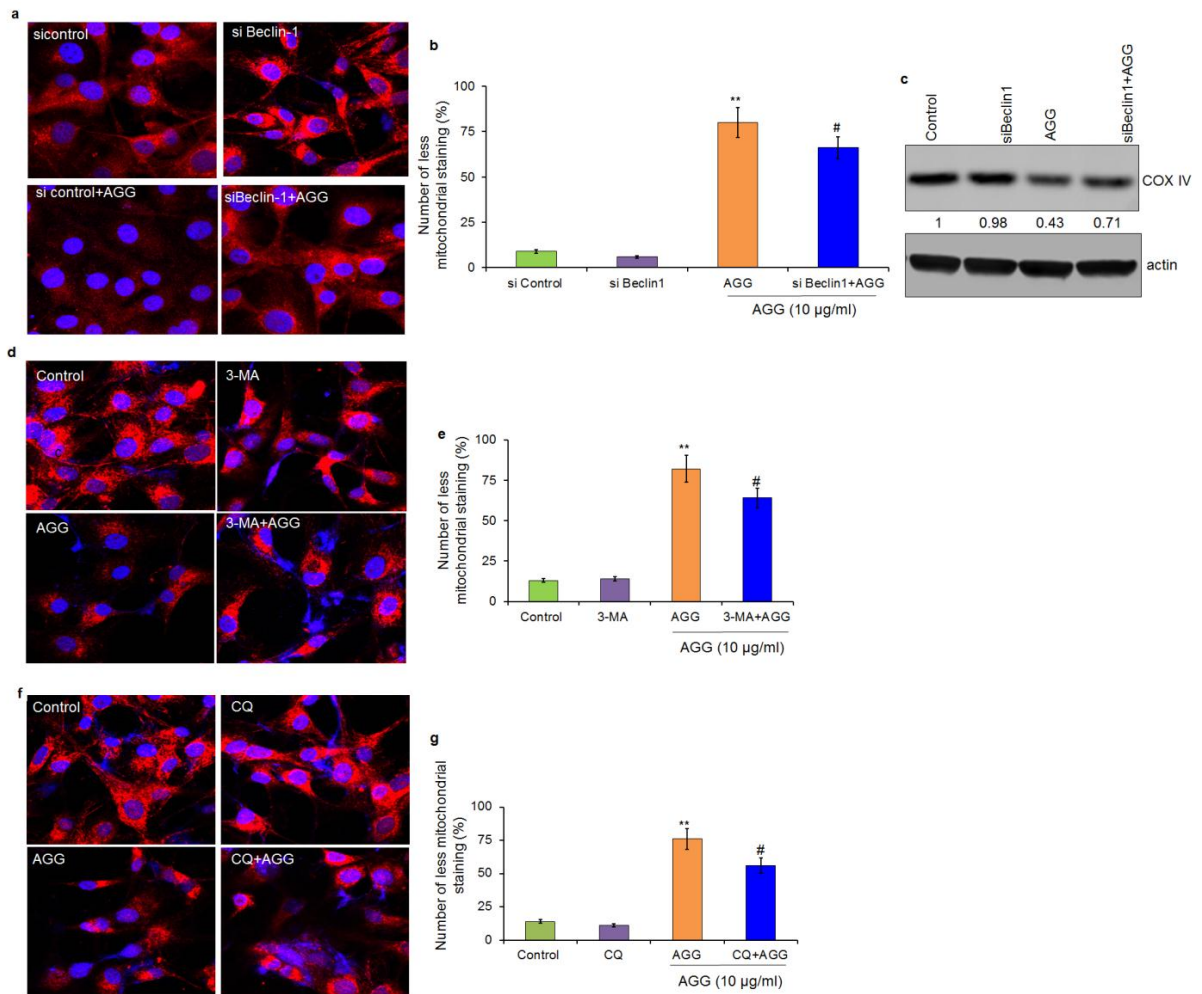


Fig.4.7. Effect of autophagy inhibition on AGG induced mitophagy U87MG cells. U87MG cells were transfected with siBECN1 and expression of TOM20 and COXIV was analyzed by confocal microscopy and Western blot respectively (a-c). U87MG cells were treated with AGG in presence of 3-MA (5 µM, 2 h) and CQ (20 µM, 2 h) and TOM20 expression were quantified by confocal microscopy (d-g). Data reported as the mean \pm S.D. of three independent experiments and compared to PBS control. **P* value < 0.05; ***P* value < 0.01 were considered significant. #*P* value < 0.05 was considered significant as compared AGG treated group. Densitometry was performed on the original blots, considering the ratio of protein to actin in control cells was 1.

4.3.4 AGG Induced Ceramide Regulates Autophagy and Apoptosis

Ceramide is one of the bioactive sphingolipids that plays a key role for autophagy and apoptosis in different cancers (Salazar et al., 2009; Sentelle et al., 2012). Ceramide synthase 1 (CerS1) expression is associated with the C18-ceramide generation which takes part in mitophagy. Here, we investigated whether AGG could able to generate ceramide in U87MG cells. The increase of ceramide both dose and time dependent manner was observed in AGG treated U87MG cells (Fig.4.8.a-d) and ceramide synthesis was again confirmed observing a decrease of ceramide signaling in presence of myriocin-1 (ISP-1), an inhibitor of serine palmitoyltransferase (SPT) (Fig.4.8.e,f).

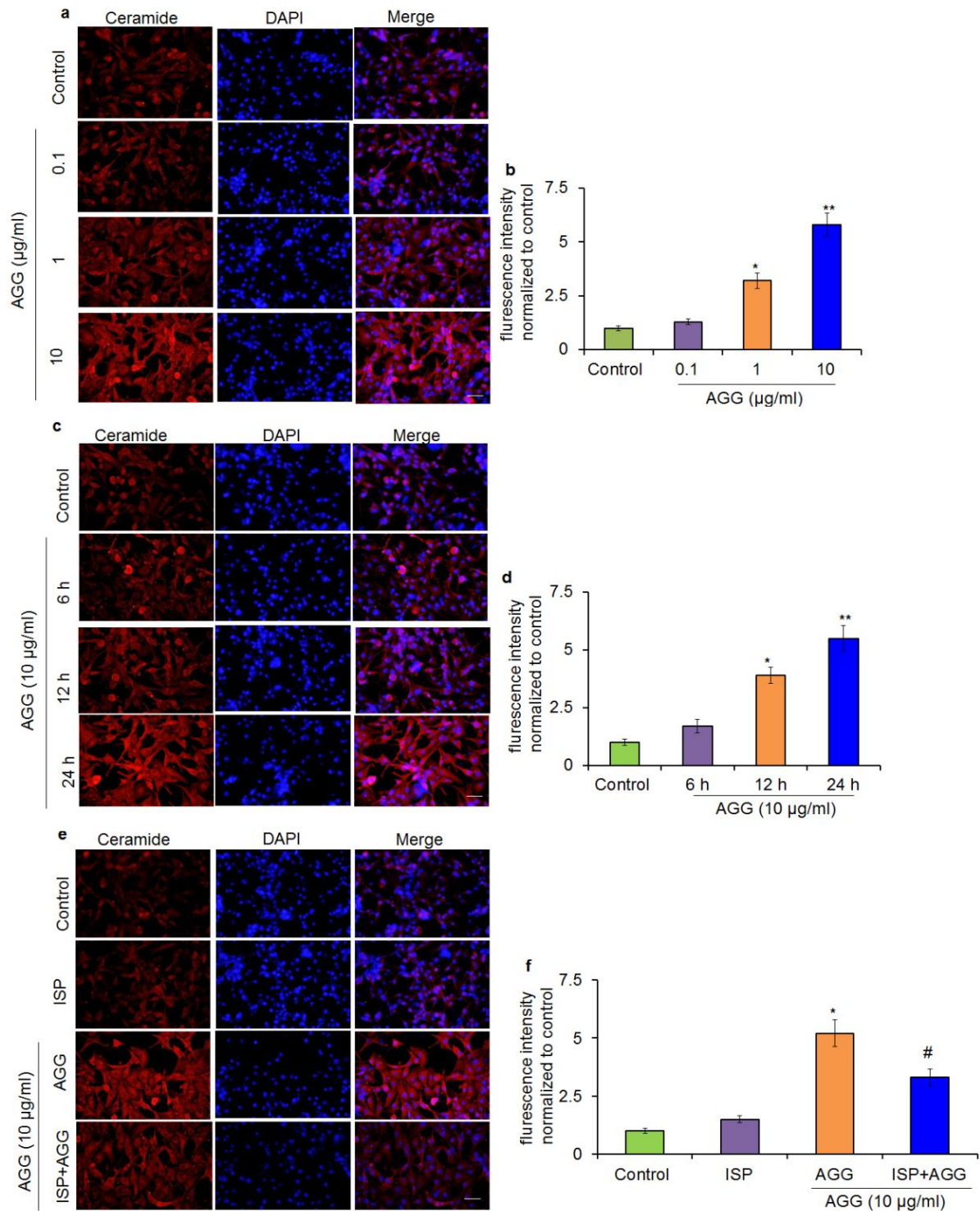


Fig.4.8. AGG induces ceramide in U87MG cells. U87MG cells were treated with AGG as indicated and expression of ceramide was quantified using anti-ceramide antibody through fluorescence microscopy (a-d). U87MG cells were treated with AGG in presence of ISP-1 (1 µM, 2 h) and expression of ceramide was quantified using anti-ceramide antibody through fluorescence microscopy (e-f). Data represented as the mean \pm S.D. of three independent experiments and compared to PBS control. * P value < 0.05 ; ** P value < 0.01 were considered significant. # P value < 0.05 was considered significant as compared to AGG treated group.

Further, U87MG cells were treated with RITC labeled AGG and stained with CerS1 and analyzed in confocal microscopy. Our data showed that AGG had strong colocalization with CerS1 evidenced from intense yellow color in U87MG cells (Fig.4.9.a). Interestingly,

AGG was found to increase the expression of CerS1 in dose dependent manner in U87MG cells (Fig.4.9.b, c) indicating AGG activated CerS1 associates with C-18 ceramide generation for mitophagy induction.

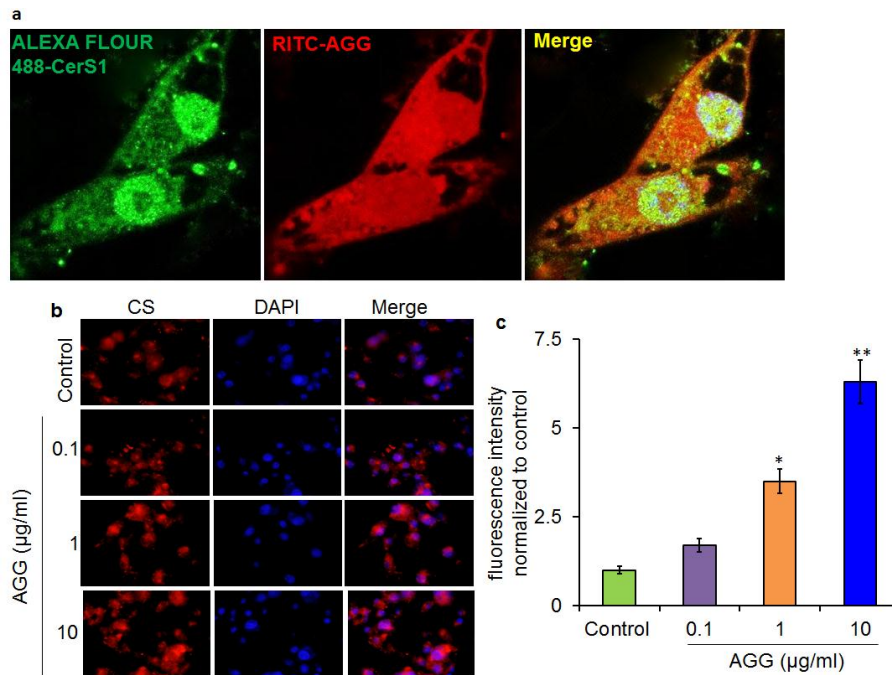


Fig.4.9. Effect of AGG on Ceramide synthase1 in U87MG cells. U87MG cells were treated with RITC-AGG for 6 h and stained with CerS1 and colocalization was studied in confocal microscopy (a). U87MG cells were treated with AGG for 24 h and expression of CerS1 was examined through fluorescence microscopy (b). Data reported as the mean \pm S.D. of three independent experiments and compared to PBS control. * P value < 0.05 ; ** P value < 0.01 were considered significant. # P value < 0.05 was considered significant as compared AGG treated group.

ER stress and ROS have been shown to be associated with regulation of AGG induced autophagy and apoptosis respectively. In this study, we investigated whether AGG induced mitophagy was modulated by ROS and ER stress and their relationship with ceramide generation. Initially, we examined mitophagy induction in presence of ISP-1, ceramide inhibitor and our data showed that AGG induced decrease in TOM20 expression was upregulated in presence of ISP-1 as compared to only AGG treated group (Fig.4.10.a, b). Further, pretreatment of salubrinal and NAC in AGG insulted U87MG cells, restored the decrease in TOM20 expression. (Fig.4.10.c-f). Moreover, AGG triggered apoptosis and autophagy were suppressed in presence of ISP-1 as demonstrated with a decrease in caspase 3/7 activity, cleaved PARP and LC3 accumulation respectively in U87MG cells. Likely, AGG activated ER stress and GRP78 expression in U87MG cell was suppressed in presence of ISP-1 (Fig.10. g, h). In addition, pretreatment of ISP-1 prevented AGG induced ROS generation (Fig.4.10.i) establishing ceramide generation is upstream of AGG associated ER stress and ROS accumulation to promote mitophagy.

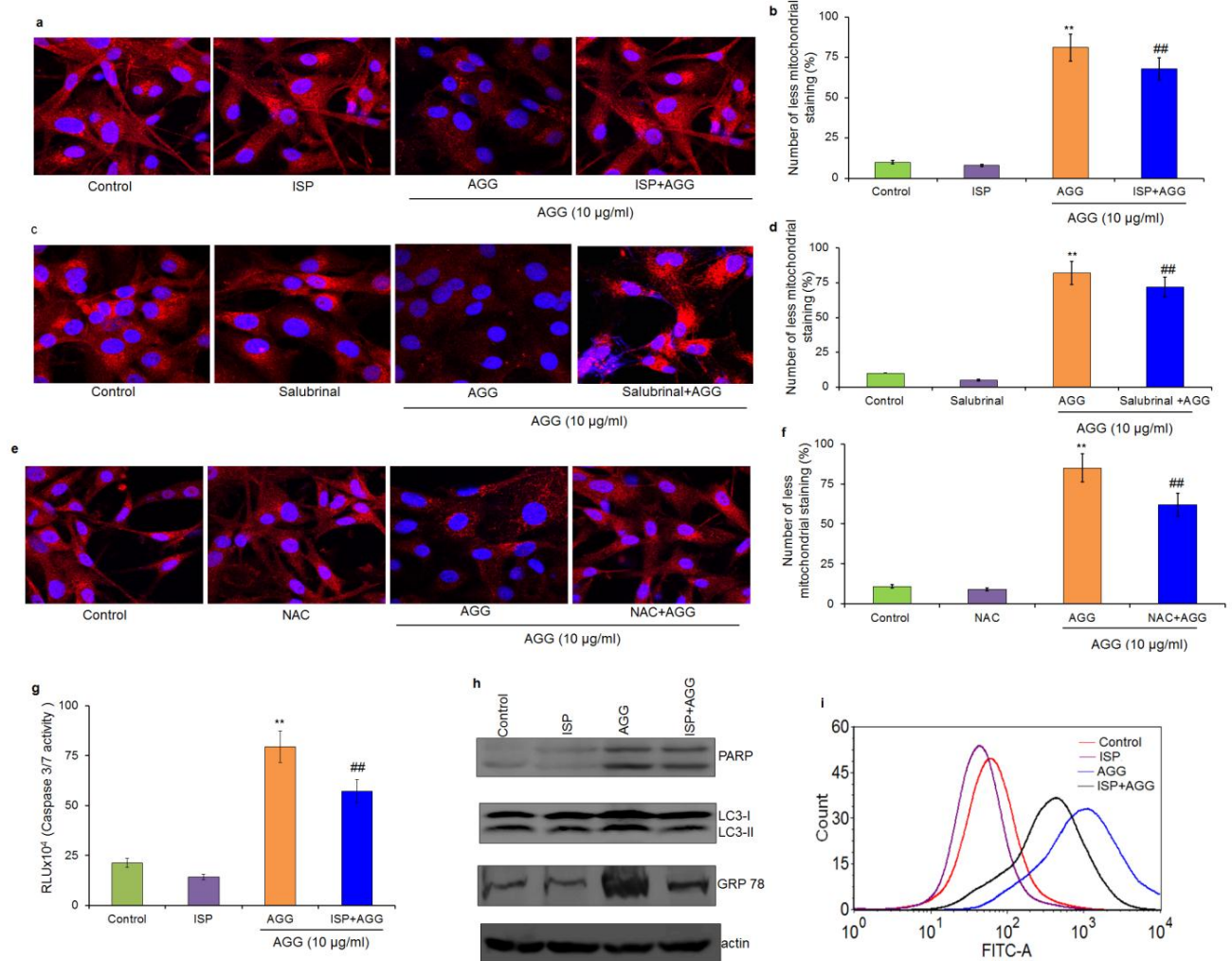


Fig.4.10. AGG induced ceramide regulates autophagy and apoptosis. U87MG cells were treated AGG in presence of ISP (1 µM, 2 h), Salubrinal (5 µM, 2 h), NAC (10 µM, 2 h) and expression of TOM20 was analyzed by confocal microscopy. U87MG cells were treated with AGG in presence of ISP-1 and caspase 3/7 activity by caspase Glo assay and expression of indicated proteins by Western blot were and ROS through flow cytometry were analyzed. Data reported as the mean ± S.D. of three independent experiments and compared to PBS control. ***P* value < 0.01 was considered significant. ##*P* value < 0.01 was considered significant as compared AGG treated group. Densitometry was performed on the original blots, considering the ratio of protein to actin in control cells was 1.

4.3.5 AGG Activates Class III PI3K around Depolarized Mitochondria

We investigated whether AGG induced dysfunctional mitochondria ready for mitophagy induction. After AGG treatment in U87MG cells, healthy and dysfunctional mitochondria were analyzed using MitoTracker Green FM and MitoTracker Red CMXRos through flow cytometry. Our data showed that AGG upregulated percentage of damaged mitochondria in U87MG cells (Fig.4.11.a). Next, we analyzed activation of class III PI3K around depolarized mitochondria in AGG treated U87MG cells. To evaluate this hypothesis, we transfected the plasmid expressing p40(phox)PX-EGFP fusion protein. As PX domain of

p40(phox) specifically interacts with the product of class III PI3K-phosphatidylinositol 3-phosphate (PtdIns-3-P), the p40(phox)PX-EGFP have been taken as a probe for evaluating the subcellular levels and distribution of PtdIns-3-P (Van Humbeeck et al., 2011). The transfected cells were stained with TOM20 after exposing to AGG and analyzed through confocal microscopy. Our data showed that mitochondrial staining had diminished in AGG treated U87MG cells and remaining mitochondria were concentrated in juxtannuclear clusters and apposed with p40(phox)PX-EGFP hotspots (Fig.4.11.b,c), confirming the hypothesis.

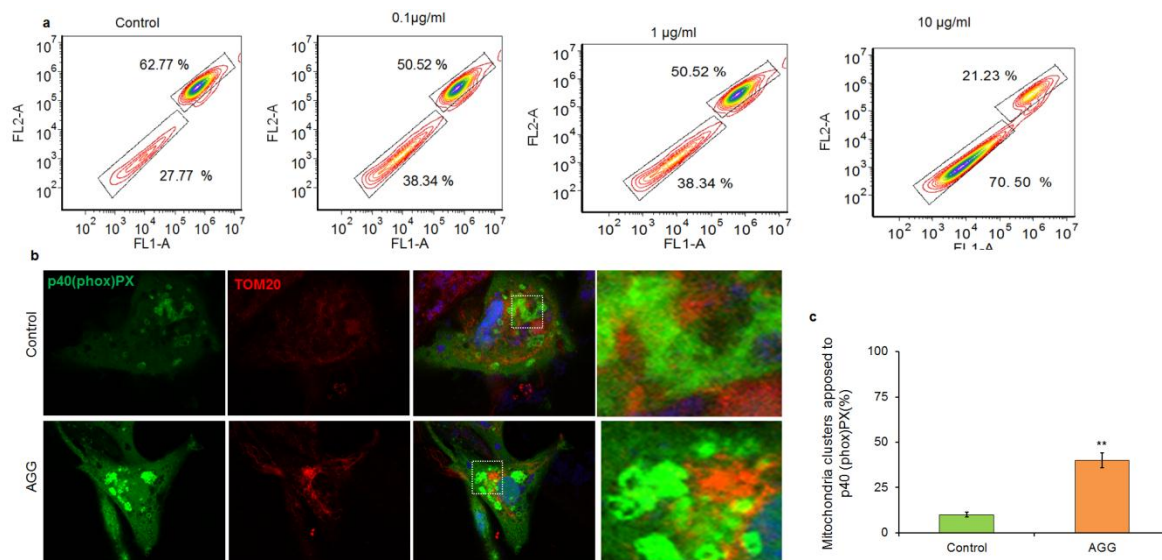


Fig.4.11. AGG induced fragmented mitochondria and activates class III PI3K around depolarized mitochondria U87MG cells were treated with AGG and mitochondria dysfunction was performed through flow cytometry (a). U87MG cells were transfected with p40(phox)PX-EGFP and stained with TOM20 after AGG treatment and analyzed in confocal microscopy (b). Graph represents mitochondrial clusters apposed to p40(phox)PX (c). Data reported as the mean \pm S.D. of three independent experiments and compared to PBS control. ** P value < 0.01 was considered significant.

4.3.6 AGG Induced Mitophagy through Abrogation of Mitochondrial Bioenergetics

After enumerating increase of damaged mitochondria in AGG treated cells, we measured the oxygen consumption rate (OCR), as well as ATP depletion in AGG, treated cells for possible association in mitophagy. Our data showed that there was a sharp decline in the level of OCR as well as ATP in AGG treated U87MG cells (Fig.4.12.a,b). Importantly, we studied OCR in presence of methyl pyruvate (MP), cell permeable form of pyruvate for supplementing ATP and our data showed that AGG abrogated OCR was reappeared to normal in presence of MP as compared to only treated group (Fig.4.12.c). Further, we showed that AGG induced mitophagy and ROS was decreased in presence of MP in U87MG cells (Fig.4.12.d-f) suggesting AGG induced mitochondrial energy crisis regulates ROS and mitophagy. Further, our data showed that pretreatment of ISP-1 elevated OCR in comparison to only AGG treated group in U87MG cells (Fig.4.12.g) confirming involvement of ceramide in regulating mitochondrial energy status for mitophagy.

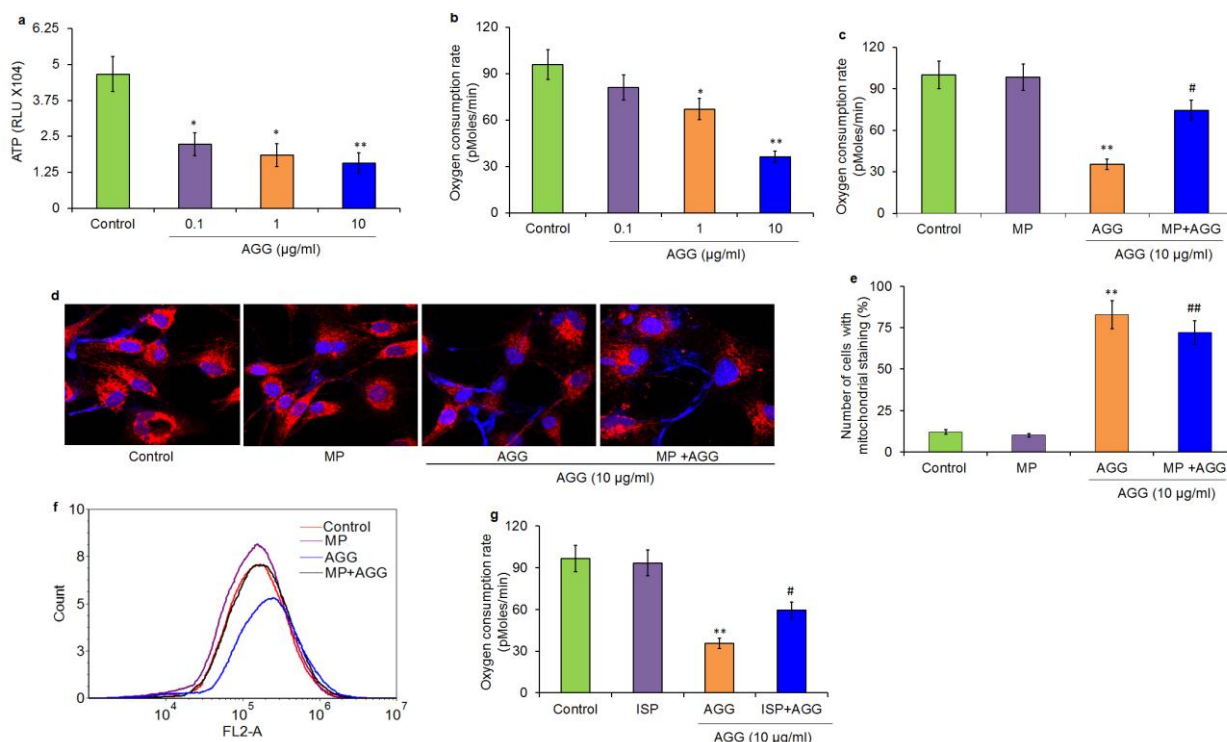


Fig.4.12. AGG induced mitophagy through abrogation of mitochondrial bioenergetics. U87MG cells were treated with AGG for 24 h and, ATP and oxygen consumption rate was quantified (a, b). U87MG cells were treated with AGG in presence of methyl pyruvate (MP, 1 mM, 2 h) and OCR, expression of TOM20, ROS through flow cytometry was quantified (c-f). U87MG cells were treated with AGG in presence of ISP-1 and OCR was quantified (g). Data reported as the mean \pm S.D. of three independent experiments and compared to PBS control. *P value < 0.05, **P value < 0.01 were considered significant. #P value < 0.05, ##P value < 0.01 was considered significant as compared AGG treated group.

4.3.7 PUMA: The Master Regulator of AGG Induces Mitophagy

The Bcl-2 homology-3 (BH3)-only protein PUMA activation is associated with DNA damage mediated apoptosis and our data showed that AGG increased expression of PUMA in dose dependent manner in U87MG cells confirmed by immunofluorescence and Western blot analysis (Fig.4.13.a-c). To investigate whether PUMA could play a role in the degradation of depolarized mitochondria, we transfected U87MG cells with EGFP-PUMA and immunostained with TOM20 and studied the colocalization between PUMA and TOM20 through confocal microscopy in presence of AGG (Fig.4.13.d,e). The data showed that PUMA was colocalized with TOM20 observed as intense yellow color and PUMA containing cells positive for TOM20 significantly increased in AGG treated cells as compared to control indicating PUMA was recruited to the cluster of damaged mitochondria around the nucleus possibly for forming mitophagosome for degradation.

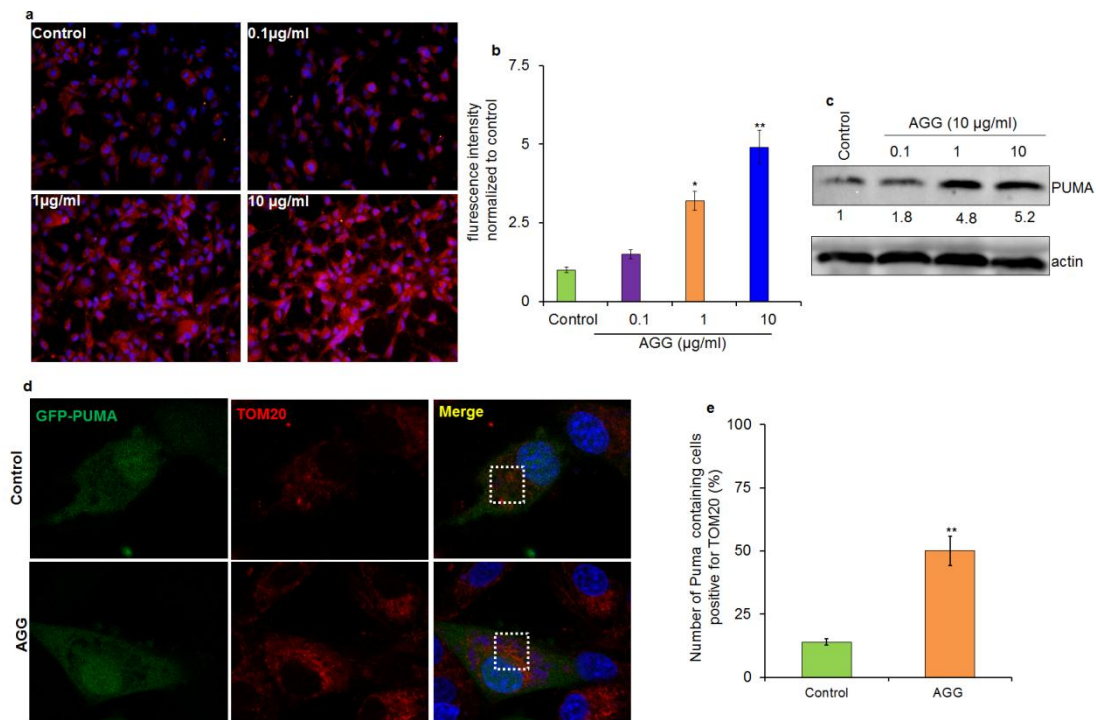


Fig.4.13. AGG induces PUMA and is associated with TOM20 in U87MG cells. U87MG cells were treated with AGG for 24 h and expression of PUMA was measured by fluorescence microscope and Western blot. U87MG cells were transfected with EGFP-PUMA and stained with TOM20 after AGG treatment and recruitment of PUMA in damaged mitochondria was analyzed and graph indicates the percentage of PUMA-containing cells positive for TOM20 (b). Data reported as the mean \pm S.D. of three independent experiments and compared against PBS control. $**P$ value < 0.01 was considered significant. Densitometry was performed on the original blots, considering the ratio of protein to actin in control cells as 1.

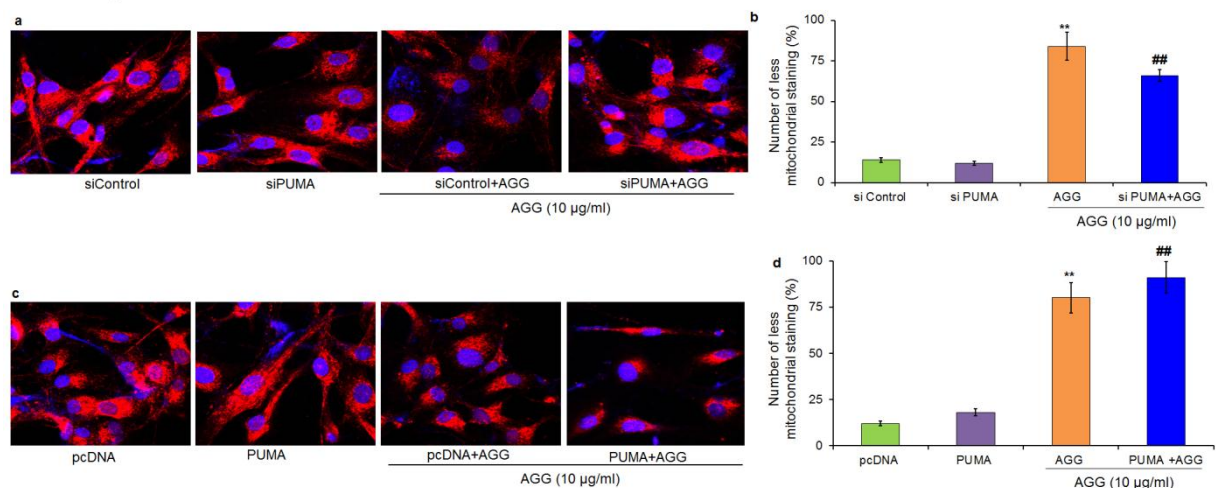


Fig.4.14. Gain and loss of function of PUMA regulates AGG-induced mitophagy. U87MG cells were knocked down with siPUMA and overexpression with PUMA-containing plasmid and expression of TOM20 in AGG-treated cells was quantified by confocal microscopy. Data reported as the mean \pm S.D. of three independent experiments and compared to PBS control. $**P$ value < 0.01 was considered significant. $##P$ value < 0.01 was considered significant as compared to the AGG-treated group.

Further, we analyzed the involvement of PUMA in mitophagy through gain and loss of function of PUMA in the presence of AGG in U87MG cells. The data showed that the knocking down of PUMA inhibited AGG-induced mitophagy, showing a decrease in the percentage of low or no mitochondrial TOM20 staining in U87MG cells (Fig. 4.14.a, b). In addition, transient

overexpression of PUMA in AGG treated cells resulted in a increase in the percentage of cells showing low or no mitochondrial TOM20 staining expression in comparison to mock control groups (Fig.4.14.c, d).

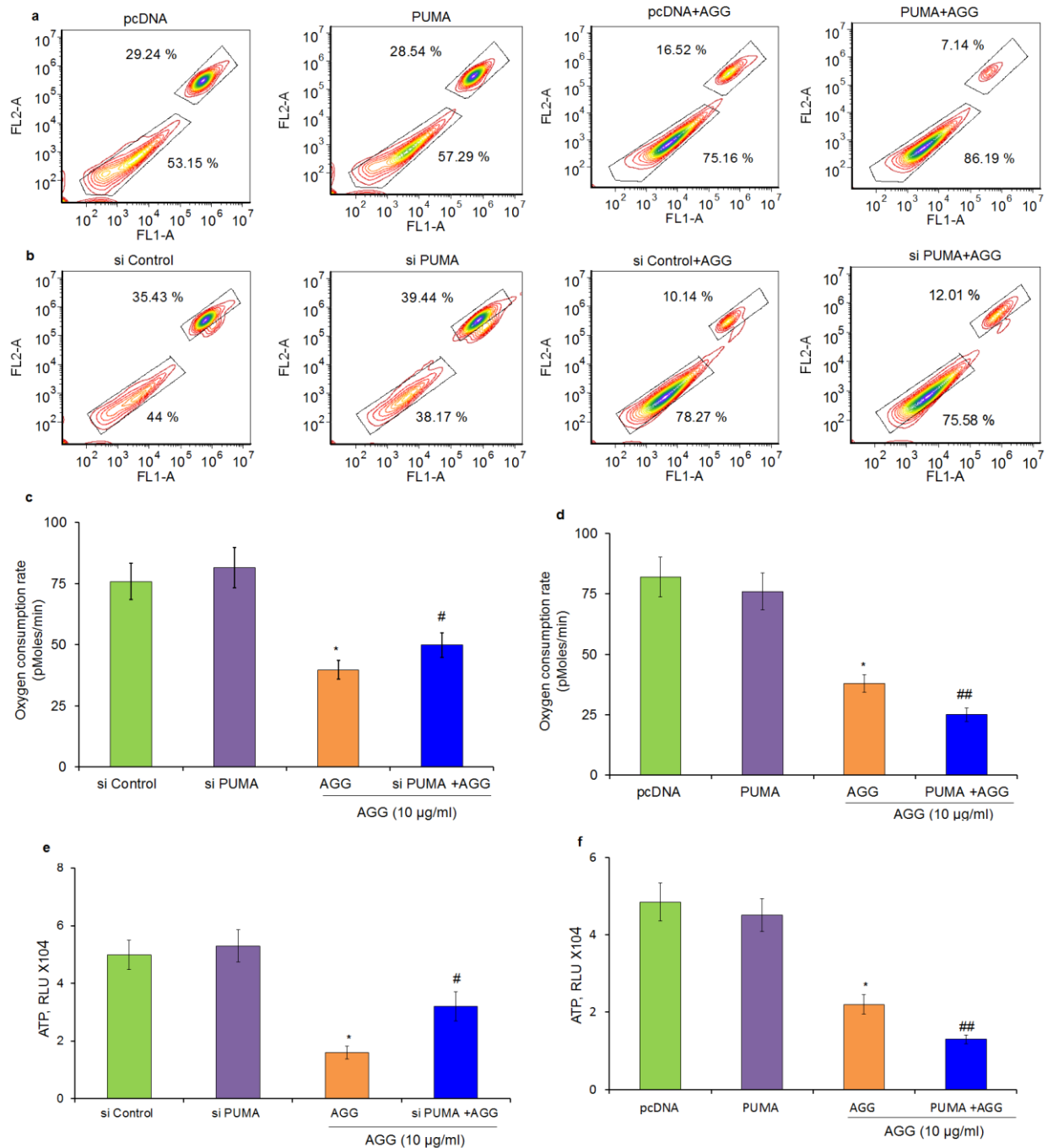


Fig.4.15. Gain and loss of function of PUMA regulate AGG induced mitochondrial bioenergetics. U87MG cells were knockdown with siPUMA and overexpression with PUMA plasmid and treated with AGG. The dysfunctional mitochondria through flow cytometry (a, b) OCR (c, d) and ATP (e, f) were analyzed in U87MG cells. Data reported as the mean \pm S.D. of three independent experiments and compared to PBS control. **P* value < 0.05, ***P* value < 0.01 were considered significant. #*P* value < 0.05, ##*P* value < 0.01 were considered significant as compared AGG treated group.

In agreement with the above findings, we quantified the percentage of healthy and dysfunctional mitochondrial mass in both PUMA overexpressed as well as knock down conditions in AGG treated U87MG cells. Interestingly, percentage of depolarized mitochondria mass was increased and healthy mitochondrial mass decreased with treatment of AGG in PUMA deficient and overexpressed cells respectively as compared to corresponding controls (Fig.4.15.a, b). To strengthen our findings we quantified the OCR and ATP and our data showed that AGG induced abrogation in OCR and ATP was altered in U87MG cells (Fig.4.15.c-f) confirming PUMA triggered mitophagy through disturbing mitochondrial energy demands.

4.3.8 PUMA Interacts with LC3 for Mitophagy Induction

In order to study, the interactions between PUMA and LC3, we performed a 15 ns long molecular dynamics (MD) simulation of the docked PUMA-LC3 complex. At the end of the simulation, the complex looked to be quite stable with root mean square deviations (RMSD) value of 3 to 4.5 Å for the C α backbone atoms. In the current study, 15 ns MD simulation was performed for the LC3-hPUMA complex (Fig.4.16.a, b). The MM-GBSA method was used to calculate the binding free energy and to analyze the binding interactions in detail. Binding free energy decomposition results showed that intermolecular electrostatic and Van der Waals interactions (and to some extent nonpolar solvation) direct the binding of LC3 domain and hPUMA. Through decomposing the binding free energy into the contribution from each residue, it was likely to recognize the binding hotspots for LC3 domain and hPUMA. For LC3 domain, the residues Arg10, Glu14, Glu18, Leu22, Ile23, Phe52, and Ile66 provide significant contributions (>2 kcal/mol). For hPUMA, Ser36, Gln157, Gln161, Arg162, Arg169, Tyr172, Asn173, Met176, Leu181, Pro182 and His185 were recognized as hotspots (Fig.4.16.c-e).

Next, we validated our findings by performing confocal study and coimmunoprecipitation. U87MG Cells were cotransfected with hLC3WT and EGFP-PUMA and colocalization was analyzed with confocal microscopy. The data showed that PUMA was interacted with LC3 as evident with strong yellow color in AGG treated U87MG cells. Importantly, the number of LC3 dots per cell positive for PUMA increased significantly in AGG treated group as compared to control (Fig.4.17.a, b). Moreover, our coimmunoprecipitation data showed that AGG triggered PUMA was shown strongly interacted with LC3 to induce mitophagy in U87MG (Fig.4.16.c). To verify whether lipidated LC3 is necessary for mitophagy induction in AGG treated U87MG cells, we transfected the cells with hLC3 Δ G in which the C-terminal Gly(120) essential for LC3-lipidation is deleted. Intriguingly, we noticed that cotransfection of hLC3 Δ G and

EGFP-PUMA did not show significant colocalization between PUMA and mutant LC3 in AGG treated U87MG cells (Fig.4.16.d) suggesting PUMA specifically binds with LC3 II for induction of degradation of damaged mitochondria.

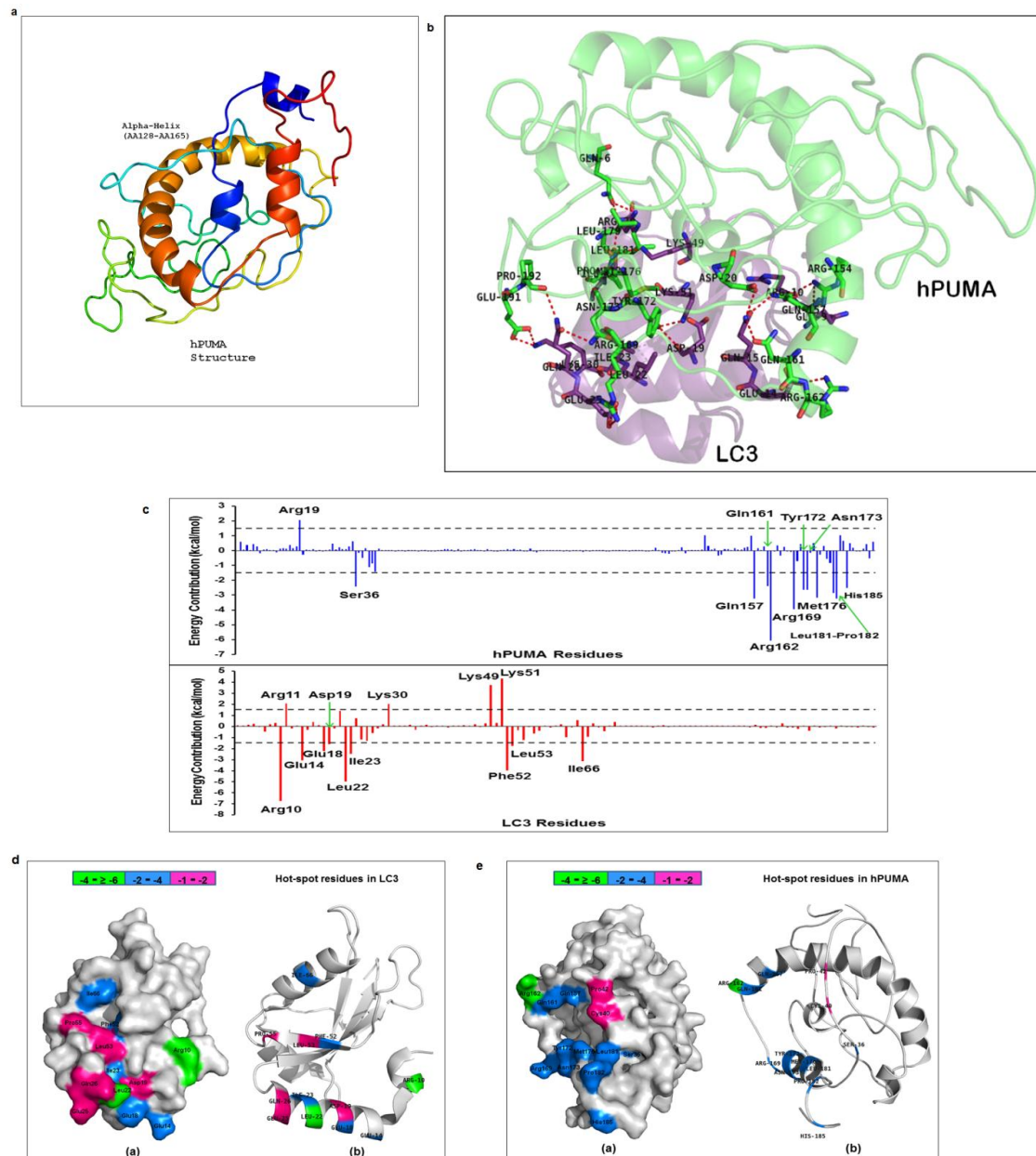


Fig.4.16. PUMA contains LIR to interact with LC3. A schematic ribbon representation of the predicted structure of hPUMA from *ab initio* modeling by PHYRE-2 software (a). A schematic ribbon representation of the LC3 domain-hPUMA complex structure shown in different colors. LC3 domain is shown in violet colour while the hPUMA structure is shown in green colour. Residues showing the interactions are shown in sticks along domain interface for both LC3 and hPUMA (b). Decomposition of ΔG on a per-residue basis or the pair interaction energy between LC3 domain and hPUMA: The contribution of each residue in hPUMA to LC3 domain binding and the contribution of each residue in LC3 domain to hPUMA binding (c). Distributions of the identified hotspot residues on the LC3 (d) and PUMA (e) domain (a) surface representation and (b) cartoon representation. Coloured bars show the range of contributions by residues in the unit kcal/mol.

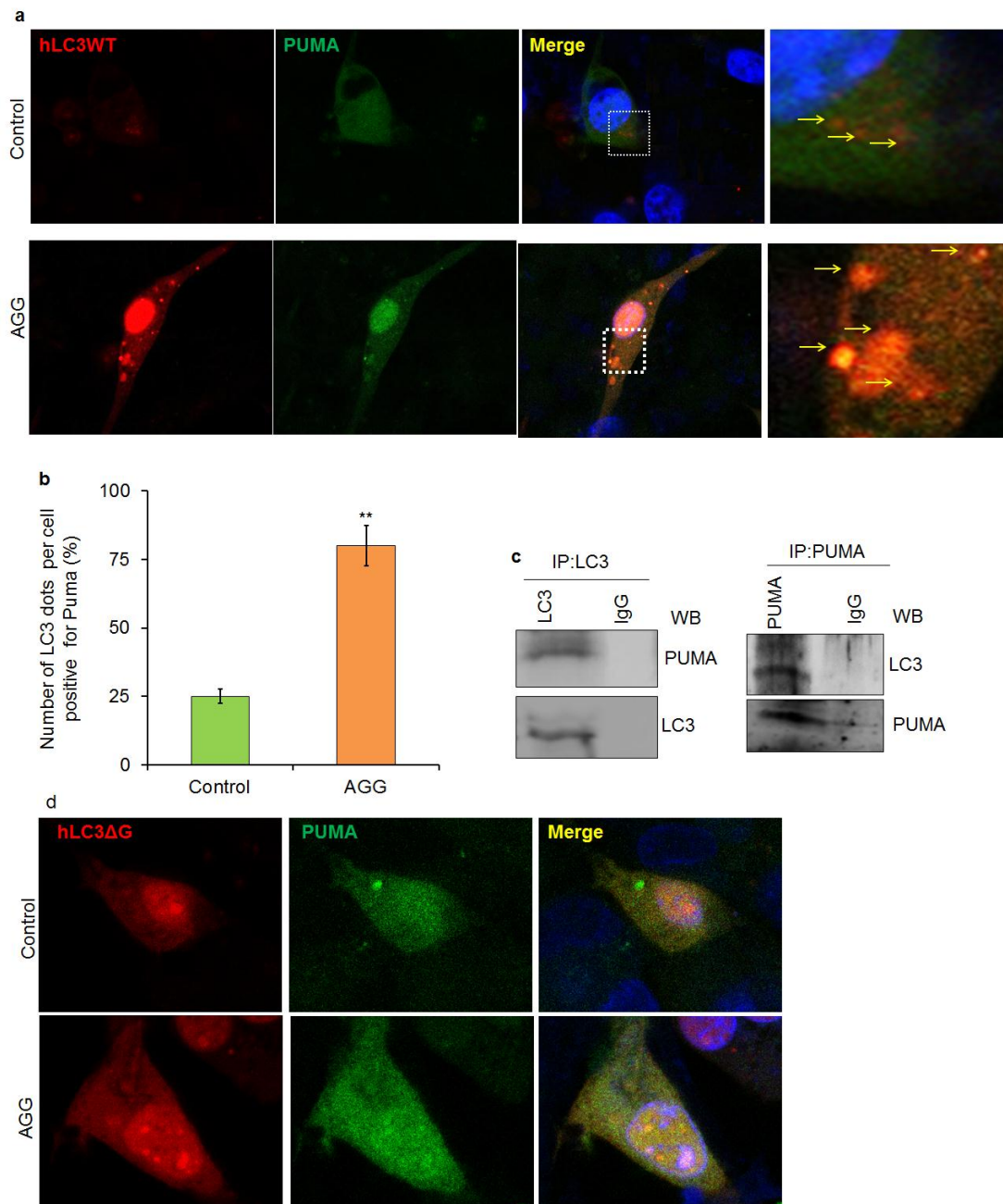


Fig.4.17. PUMA interacts with LC3 for mitophagy induction. U87MG cells were cotransfected with vectors encoding pLAMP1-mCherry and pBI-EGFP-PUMA and treated with AGG for 6 h. cells and analyzed by confocal microscopy (a). The graph depicts the quantification of LC3 and PUMA colocalization and the numbers of colocalized puncta were observed and counted, and the relative percentage of colocalized puncta was counted (b). U87MG cells were treated with AGG for 24 h and immunoprecipitated with anti-PUMA and anti-LC3 followed by immunoblotting with anti-LC3 or anti-PUMA antibodies (c). U87MG cells were cotransfected with HcRed -hLC3 Δ G and GFP-PUMA and treated with AGG and analyzed colocalization between PUMA and LC3 through confocal microscopy (d). Data reported as the mean \pm S.D. of three independent experiments and compared to PBS control. ** P value $<$ 0.01 was considered significant.

4.3.9 Effect of PUMA Ubiquitination on AGG Induced Mitophagy Induction

In the initial observation we have noticed mitochondria recruited to the autophagosome and then we tried to investigate the chronological events executed by PUMA for induction of mitophagy. Whether PUMA translocation to mitochondria leads its ubiquitination for

induction of mitophagy for which we tried to observe the colocalization between ubiquitin and PUMA by staining with both PUMA and ubiquitin. Importantly, significant colocalization between ubiquitin and PUMA were observed in AGG treated cells (Fig.4.18.a, b). The PUMA ubiquitination is further confirmed by performing immunoprecipitation study (Fig.4.18.c). Intriguingly, pretreatment of PYR41, inhibitor ubiquitin activating enzyme reduced the interaction of ubiquitin with PUMA in AGG exposed U87MG cells as shown in immunoprecipitation study (Fig.4.18.d). In this connection, ubiquitination of PUMA might be an important step for priming of mitochondria undergoing mitophagy in AGG treated cells. Further, we investigated whether such interaction has any role for AGG induced mitophagy in U87MG cells. Surprisingly, pretreatment of Pyr41 in AGG treated cells did not decrease significantly in percentage in mitochondrial staining in comparison to AGG treated cells (Fig.4.18.e, f) confirming the existence of a direct association of PUMA-LC3 as an alternative pathway for mitophagy apart from ubiquitination dependent mitophagy.

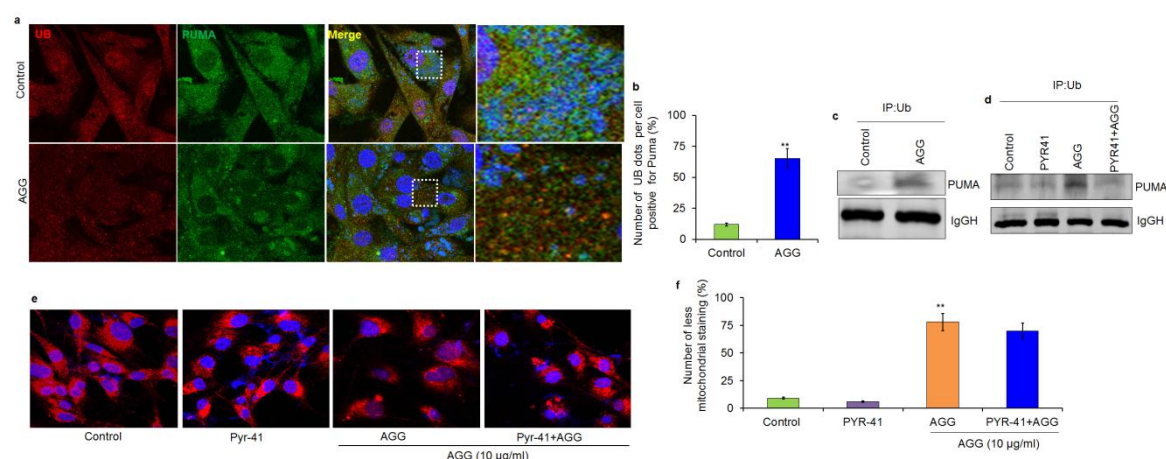


Fig.4.18. Effect of PUMA ubiquitination AGG induced mitophagy induction After AGG treatment U87MG cells was stained with ubiquitin and PUMA and colocalization was studied through confocal microscopy (a, b). After treatment with AGG, PUMA/Ub interaction in U87MG cells was studied in absence and presence of PYR-41 (1 μ M, 2 h) by immunoprecipitation analysis (c, d). U87MG cells were treated with AGG in presence of PYR41 and expression of TOM20 was analyzed through confocal microscopy (e, f). Data reported as the mean \pm S.D. of three independent experiments and compared to PBS control. ***P* value < 0.01 was considered significant.

4.3.10. PUMA Interacts with Adaptor Protein p62/SQSTM1 for Mitophagy Induction

After observing the strong interaction between PUMA and ubiquitin, it is imperative to investigate whether PUMA interacts with p62, selective adapter molecule for autophagy. Our confocal data showed colocalization of p62 and PUMA were observed in AGG treated cells in comparison to control in U87MG cells (Fig.4.19.a, b). Moreover, the interaction of PUMA and p62 was confirmed by our coimmunoprecipitation analysis (Fig.4.18.c).

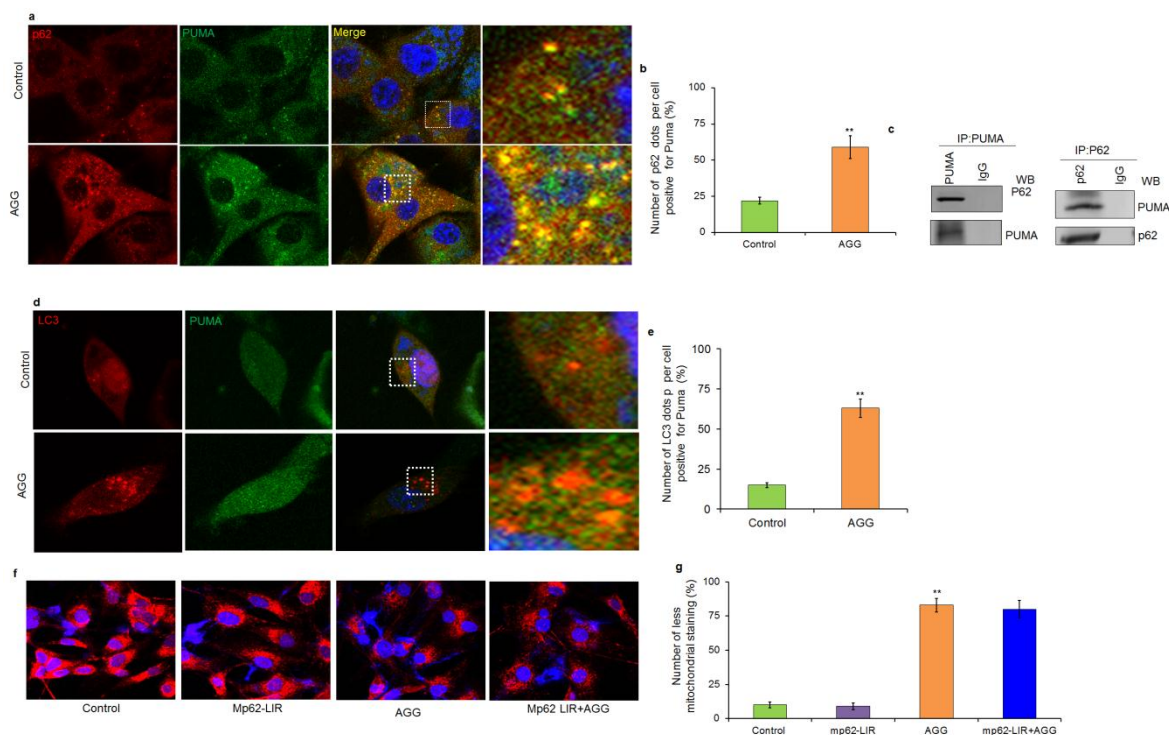


Fig.4.19. PUMA interacts with adaptor protein P62 for mitophagy induction. After AGG treatment U87MG cells were stained p62 and LC3 and colocalization was studied through confocal microscopy (a, b). U87MG cells were treated with AGG for 6 h and immunoprecipitated with anti-p62 and anti-PUMA followed by immunoblotting with anti-PUMA or anti-p62 antibodies (c). U87MG cells were transfected with p62 LIR mutant and stained with PUMA and LC3 after treated AGG and analyzed colocalization between PUMA and LC3 through confocal microscopy (d, f). U87MG cells were transfected with p62 LIR mutant and treated with AGG and expression of TOM20 was analyzed through confocal microscopy (f, g). Data reported as the mean \pm S.D. of three independent experiments and compared to PBS control. ** P value < 0.01 was considered significant.

Next, we tried to analyze the significant contribution of p62 in connection with AGG induced mitophagy. The p62 LIR mutant (W338) was transfected in U87MG cells and colocalization of PUMA and LC3 was examined by confocal microscopy. Our data showed that AGG induced PUMA and LC3 colocalization was did not get affected and percentage of number of LC3 dots per cells positive for PUMA was notably enhanced as compared to control in p62 LIR mutant U87MG cells (Fig.4.19.d, e). Further, AGG induced mitophagy was studied and it was clearly observed that percentage of less mitochondrial staining was did not change in in p62 LIR mutant in U87MG cells as compared to mock control (Fig.4.19.f, g) concluding that AGG induced mitophagy was both p62 dependent and independent way in U87MG cells.

4.3.11 AGG Induced Mitophagy Switches to Apoptosis

Mitophagy may be cytoprotective or lethal deepening on cellular context and in this study, we investigated whether AGG induced mitophagy is associated with cell death. Initially, we studied mitophagy inducing activity of AGG in presence of mitochondrial fission inhibitor Mdivi-1. Our data showed that AGG induced mitophagy was strongly inhibited in presence of Mdivi-1 (Fig.4.20.a, b) conforming AGG prompted mitophagy was DRP1 dependent.

Further, U87MG cells were treated with AGG in presence of Mdivi-1 and cell viability and apoptosis was studied. The data showed that AGG caused decrease in cell viability was enhanced in presence of Mdivi-1 (Fig.4.20.c) indicating inhibition of mitophagy suppressed cell death. Interestingly, the pretreatment of Mdivi-1 reduced the caspase (3/7) activity as compared to control (Fig.4.20.d) confirming mitophagy leads to apoptosis in U87MG cells.

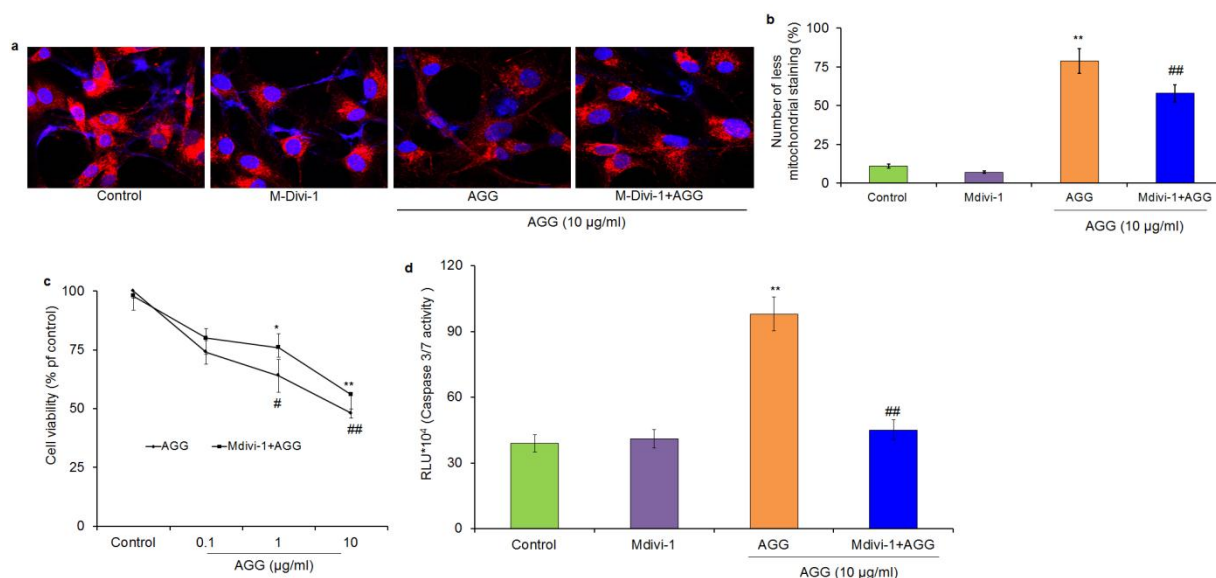


Fig.4.20. AGG induced mitophagy switches to apoptosis. U87MG cells were treated with AGG in presence of Mdivi-1 and expression of TOM20 was analyzed through confocal microscopy (a,b). U87MG cells were treated with AGG in presence of Mdivi-1 and cell viability (c) and caspase (3/7) activity (d) was quantified. Data reported as the mean \pm S.D. of three independent experiments and compared to PBS control. * P value < 0.05 , ** P value < 0.01 were considered significant. # P value < 0.05 , ## P value < 0.01 were considered significant as compared AGG treated group.

4.4 Discussion

The connecting link between autophagy and mitophagy could be joined by the autophagosome biogenesis. Earlier it has been reported autophagosomal double layer vesicles originates from the different sources like ER, Golgi, plasma membrane and currently from the mitochondrial degradation (mitophagy) (Hailey et al., 2010). Interestingly, mitochondria form autophagosome biogenesis for its own degradation. The protective role of mitophagy supported by the clearance of damaged mitochondria and saves from different types of mitochondrial disorder associated diseases. In the other hand, process of mitophagy used as alternative therapeutic mechanism induced by phototherapeutics like plant lectin; particularly here in the present experimental settings, we have taken *Abrus* agglutinin as a mitophagy inducer mediated by PUMA in U87MG cells. Results from the present finding revealed that AGG could generate ceramide in U87MG cells in dose and time dependent manner. AGG induced ceramide synthesis regulates autophagy, apoptosis, ER stress and mitochondrial ROS. For regulation of apoptosis by ceramide, emerging

evidence suggest that ceramide could translocate to the mitochondria from the plasma membrane which led to the accumulation of mitochondrial ceramide and finally apoptosis induction (Babiyuchuk et al., 2011; Babiyuchuk et al., 2008). Beside that ceramide is considered as an important second messenger that participates in the induction of non-apoptotic cell death in glioblastoma by activating mitochondrial BNIP3. Ceramide acts as an upstream signal during mda-7/IL-24-induced ER-stress (Sauane et al., 2010). So, ceramide could be considered as a master regulator for controlling different types of a cellular mechanism including autophagy, mitophagy as well as apoptosis in U87MG.

Accumulating evidence indicate that *Abrus* agglutinin induces apoptosis *in vitro* as well as *in vivo* (Bhutia et al., 2016) but autophagic degradation potential of cancer cells by AGG was not revealed. Therefore in the first objective, we have deciphered autophagy induction capacity of AGG. It inhibits Akt/PH domain to induce endoplasmic reticulum stress mediated autophagy dependent cell death in cervical cancer cells (Panda et al., 2017). However selective autophagy induction, more specifically mitophagy inducing potential of AGG was not found in available literature till the present investigation was documented. AGG induces massive autophagy by decreasing TOM20 and COXIV dose dependently and inhibition of phosphorylation of pDRP1 was noticed in AGG treated cells. Besides that electron microscopic study was performed for physical significance of AGG induced mitophagosome formation in AGG treated cells. Several types of mitochondrial receptors including p62, Nix, BNIP3 are recruited in the damaged mitochondria for execution mitochondrial degradation. As we know BH3 only proteins are involved in death signaling process specifically apoptosis. Very fewer reports are available where BH3 only proteins take part in autophagy and among them, we selected PUMA as our initial report says that AGG induces PUMA upregulation in oral cancer (unpublished data), therefore we choose PUMA a suitable mitochondrial receptor for mitochondrial degradation. Earlier report reveals recruitment of PUMA to the mitochondria (Yee et al., 2009) however detailed molecular mechanisms how PUMA execute mitophagy has not been elucidated.

PUMA interacts with LC3 as we confirmed from the initial docking and simulation study and subsequently validated through confocal and immune precipitation analysis. Moreover AGG activated PUMA contains conserved Tyr 172 earmarked for LIR (LC3 interacting region). The interaction of PUMA containing LIR might be crucial for puma induced mitophagy (Yu et al., 2001; Hamacher-Brady et al., 2016) but the detailed mechanistic approach is needed for exploring PUMA mediated selective autophagy. In agreement with our present findings accumulating evidence indicate that BH3 only protein like Nix and BNIP3 induce mitophagy induction. BH3-only proteins, belongs to Bcl-2-

related proteins activate BAX and BAK by inhibiting Bcl-2 related proteins activation (Willis et al., 2007). Other BH3 only proteins like BNIP3 and NIX (BNIP3L) have been characterized by containing LIR (LC3 interacting region) motif to induce mitophagy. Nix acts as a receptor containing LC3 binding motif for sequestration of mitochondria into autophagosome for mitochondrial clearance (Novak et al., 2011, 2010). Similarly, BNIP3 interacts with LC3 functioning as a receptor for mitophagy induction (Shi et al., 2014). More importantly, our data indicate that PUMA binds only to the lipidated LC3 (LC3-PE) as we failed to find significant colocalization signaling between PUMA and hLC3ΔG (C-terminal Gly 120 of LC3 is deleted). The interaction of PUMA with lipidated LC3 influence for mitophagy induction in AGG treated U87MG cells. In agreement with our study, C18-ceramide also binds with the lipidated form of LC3 for implementing mitophagy (Sentelle et al., 2012).

Initially, we have reported AGG activated PUMA binds directly with LC3, besides that PUMA also binds with ubiquitin as well as p62 for the promotion of mitophagy, which may conclude AGG induced mitophagy is independent of p62 as well as ubiquitin. Interestingly accumulating evidence indicate that p62 is dispensable in case of Parkin mediated mitophagy (Narendra et al., 2010; Okatsu et al., 2010) which supports our present investigation AGG induced mitophagy in PUMA dependent and independent manner. Interestingly, AGG induced massive DRP1 dependent mitophagy ends with apoptosis induction in U87MG cells. Understanding the varied dynamics of damaged mitochondria and molecular machinery associated with PUMA mediated AGG induced mitophagy will ease to unravel the contribution of superfluous mitochondria in the development of glioblastoma. Besides that how does PUMA interacts with the basic autophagy machinery at different stages of mitophagosome formation remain unanswered? More importantly, it may be investigated whether PINK1 is stabilized in PUMA recruited dysfunctional mitochondria. In conclusion, AGG activated PUMA induces mitophagy mediated cell death which may have implication in the treatment of glioblastoma.

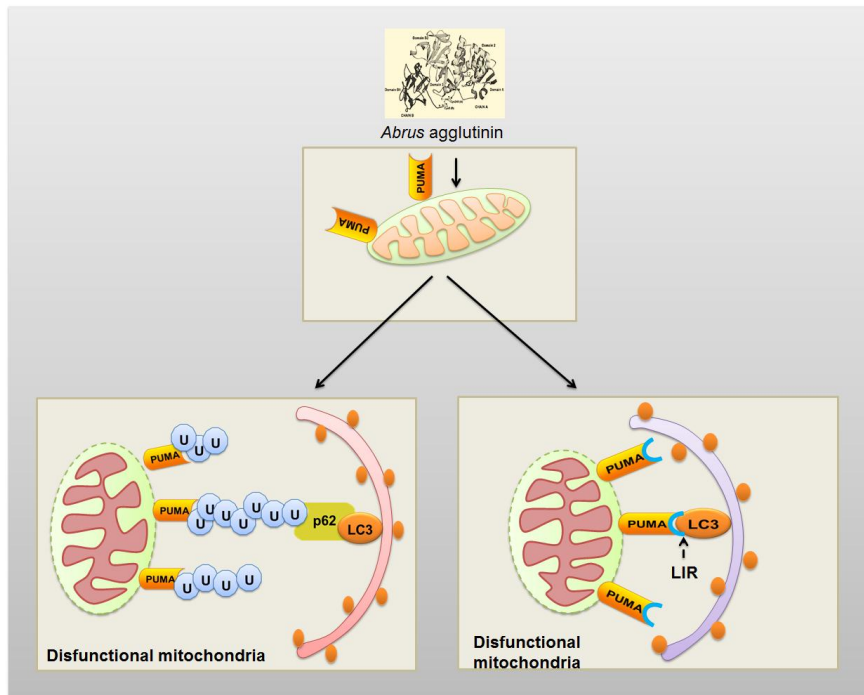


Fig. 4.21. Schematic representation of PUMA and LC3 interaction.

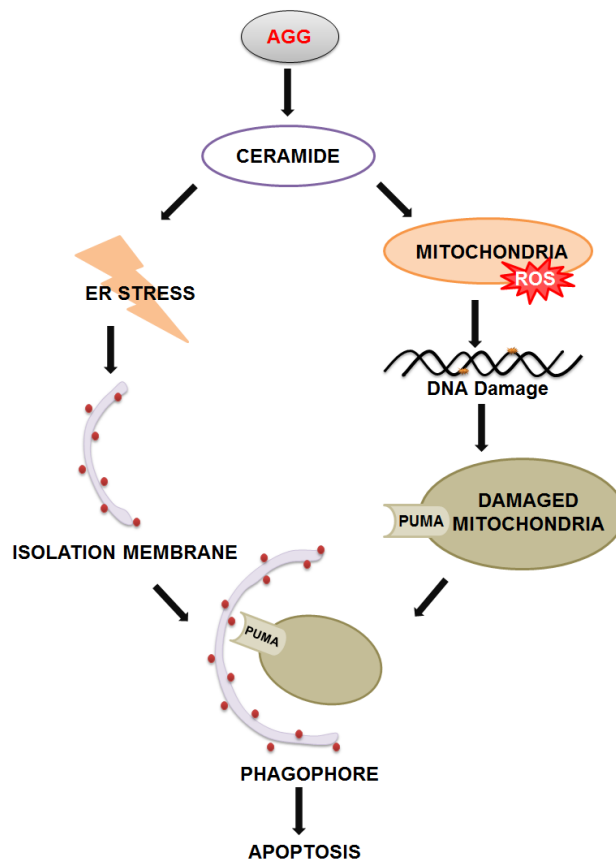


Fig. 4.22. Schematic representation of PUMA induced mitophagy ends with apoptosis.

Chapter 5

SIRT1/LAMP1 signaling activation by *Abrus* agglutinin regulates autophagy-mediated senescence

Abstract

Accumulating evidence indicate that therapy induced senescence is an indicator of loss of self-renewal capacity in the tumor mass. Previously, we have shown that *Abrus* agglutinin (AGG), a type II ribosome inactivating lectin induces apoptotic and autophagy dependent cell death; however senescence induction potential in tumor cell remains obscure. The present study revealed that AGG induced senescence through autophagy as a tumor inhibitory mechanism in prostate carcinoma. We noticed an increase in β -galactosidase activity, upregulation of p16, p21 and degradation of pRb and PCNA in dose dependent manner in AGG treated PC3 cells. Moreover, AGG found to induce autophagy and inhibition of autophagy with 3-Methy adenine (3-MA) reduced β -galactosidase activity in PC3 cells. AGG resulted in the lipophagy-mediated accumulation of free fatty acids (FFA), with a concomitant decrease in the number of lipid droplets and lalistat, a lysosomal acid lipase inhibitor blocked AGG induced lipophagy and senescence in PC3 cells. More importantly for the first time, our group reported AGG prompted SIRT1 facilitate LAMP1 deacetylation in response to AGG insult to trigger autophagy. The present study suggests that SIRT1 mediated deacetylation of LAMP1 may be a breakthrough in autophagy machinery to induce senescence for better cancer therapeutics.

Key words: *Abrus* agglutinin, autophagy, senescence, SIRT1, LAMP1

5.1. Introduction

Senescence, a state in which cells were not proliferated but remain metabolically active, for a prolonged period of time (Kuilman and Peeper, 2009). Senescence have been classified into three different categories: replicative senescence where telomere shortening leads to proliferative arrest (Shay and Roninson, 2004), oncogene-induced senescence where expressed oncogene forced the cells to enter (Lee et al., 1999) and premature (accelerated or stress-induced) senescence when cells are exposed to cytotoxic agent causing DNA damage (Gewirtz et al., 2008). Autophagy is a catabolically driven process whereby stressed cells form cytoplasmic, double-layered, crescent-shaped membranes known as phagophores, which mature into complete autophagosomes. The autophagosomes engulf long-lived proteins and damaged cytoplasmic organelles to provide cellular energy and building blocks for biosynthesis (Panda et al., 2014). In the recent time, few report came showing the existence of a close relationship between the autophagy and senescence in the tumor cells treated with chemotherapeutic drugs. According to Zhu et al when cells undergo excessive cellular damage, it will enter to senescence (Zhu et al., 2014). The presence of various autophagic markers were also detected in the different types of senescent cells like

keratinocytes, endothelial cells and ovarian cells. It reported that during oncogene induced senescence autophagy related genes were highly expressed (Young et al., 2009). As autophagy is often considered to be a cytoprotective response to stress, whereas stress-induced senescence could also reflect efforts by the cell to evade direct cell. Interestingly, a blockade to autophagy using 3-MA in fact, resulted in a collateral interference with senescence, with suppression of senescence in glioma cells (Knizhnik et al., 2013).

Silent mating type information regulation 1 (Sirtuin 1; SIRT1), a nuclear histone deacetylase is associated multifunctional role in cancer and ageing (Houtkooper et al., 2012). In mammals, SIRT1 levels increase upon the nutrient starvation condition and deacetylate non-histone proteins thereby allowing mammalian cell survival under oxidative stress (Chen et al., 2005). Moreover, SIRT1 found to reduce oxidative stress by increasing mitochondrial function and autophagic cell death through interference with BECN1 and the mTOR signaling pathways (Ou et al., 2014). Interestingly, SIRT1 found to regulate autophagy through the deacetylation of autophagy-related genes and mediators of autophagy. It showed that SIRT1 deacetylates nuclear LC3 at Lys49 and Lys51 to initiate autophagy during serum starvation (Huang et al., 2015). The regulation of other autophagic protein by SIRT1 is not revealed. In this study, we proposed to investigate the role of SIRT1 for autophagy modulation through deacetylation of lysosome-associated membrane protein 1 (LAMP-1), a membrane glycoprotein of lysosomes.

Abrus agglutinin (AGG), a plant lectin isolated from the seeds of *Abrus precatorius* having molecular weight 134 kDa. It is a homodimer glycoprotein consisting of two 30 kDa toxic A chain and two 31 kDa B chains linked through disulphide bond having different functions. The B chain of AGG has a high specificity towards β -galactosides which facilitates translocation of the molecule into the cells and the A chain inhibits protein synthesis (Bagaria et al., 2006). The inhibition of protein synthesis induces apoptosis through extrinsic and intrinsic pathway. It has been reported that AGG affects apoptosis by modulating representative signaling pathways involved in Bcl-2 family, caspase family, p53, p38, PI3K/Akt, ERK in different cancers (Bhutia et al., 2008a, Bhutia et al., 2008b.). Moreover, AGG inhibits angiogenesis by reducing the expression of IGFBP-2 (Bhutia et al., 2016). Recently our group draws an attention towards the AGG induced autophagy and autophagy depended cell death through inhibiting Akt/PH domain followed by endoplasmic stress. In the previous objectives, we showed that the highest doses of AGG induce apoptosis and autophagy depended cell death. In this study, we examined the antitumor potential of AGG at its lower doses (25, 50 and 100 ng/ml) in prostate cancer cells. Moreover, AGG found to accelerate therapy induced senescence through autophagy dependent pathway.

AGG induced SIRT1 activation promoted LAMP1 deacetylation to initiate autophagy in PC3 cells. Interestingly, inhibition of autophagy suppressed AGG induced senescence conforming autophagy by AGG leads to therapy-induced senescence as a tumor suppressor mechanism.

5.2. Materials and Methods

5.2.1 Reagents

5-Bromo-4-chloro-3-indolyl β -D-galactopyranoside (X-gal) (B4252), 4,6-Diamidino-2-phenylindole dihydrochloride (DAPI) (D9542), 3-Methyl adenine (3-MA) (M9281), Oil Red O (O0625) and Sirtinol (S7942) were purchased from Sigma–Aldrich (St. Louis, MO, USA). Lalistat was procured from Chemical Synthesis and Drug Discovery Facility, University of Notre Dame, USA. Fetal bovine serum (FBS) (sterile-filtered, South American origin), Dulbecco's Modified Eagle Medium: Nutrient Mixture F-12 (DMEM/F12), antibiotic-antimycotic (100X) solution, and Lipofectamine® 2000 were purchased from Invitrogen (Waltham, MA). AGG was purified as described in chapter 3 of this thesis.

5.2.2 Antibodies

LC3 (NB100-2220) from Novus Biological (Littleton, CO); p21 (556430), p16 (554079), PCNA (610664), pRb (554136) and Cyclin B2 (554179) were purchased from BD Biosciences (Franklin Lakes, NJ); SIRT1 (2493S), BECN1 (3738S), Atg5 (2630S), and acetylated lysine (9681S) were procured from Cell Signalling and Technologies (CST, Danvers, MA). β -actin (A2066) was purchased from were purchased from Sigma–Aldrich (St. Louis, MO, USA).

5.2.3 Cell Culture

Human prostate cancer cell lines PC3 were obtained from the National Centre for Cell Science (NCCS), Pune, India. PC3 cells were cultured in DMEM-F12 and supplemented with antibiotic-antimitotic and 10 % fetal bovine serum (FBS) at 37°C in a humidified 95 % air, 5 % CO₂ incubator.

5.2.4 β -Galactosidase Assay

For detection of Senescence-associated β -galactosidase (SA- β -gal) positive cells, treated cells were washed with PBS and fixed with 2 % formaldehyde/0.2 % glutaraldehyde/PBS for 5 min. Cells were washed and stained with 5-bromo-4-chloro-3-inolyl-D-galactopyranoside in dimethylformamide (20 mg/ml), 40 mM citric acid/sodium phosphate, pH 6.0, 5 mM potassium ferrocyanide, 5 mM potassium ferricyanide, 150 mM NaCl, and 2 mM MgCl₂ and incubated at 37°C for 24 h. After incubation, cells were washed with PBS and imaged by

using an Olympus inverted microscope. All images within a given figure were taken at the same magnification. The percentage of SA- β -gal-positive cells was determined by counting the number of blue cells under bright-field illumination and the total number of cells in the same field under phase contrast. At least eight random fields were counted for each culture dish.

5.2.5 Acridine Orange Staining

Quantification of acidic organelles was done by acridine orange staining. After treatment with various doses of AGG for 72 h cells were stained with acridine orange at 37°C in the dark for 15 min and washed twice with PBS. Images of acridine orange staining were taken immediately using a fluorescence microscope (Olympus IX71, Tokyo, Japan).

5.2.6 Western Blot and Immunoprecipitation Analysis

PC3 cells were treated with AGG followed by extraction of proteins. Cell were lysed with a lysis buffer and about 50 μ g protein was subjected to SDS-PAGE electrophoresis, followed by transfer into a nitrocellulose membrane, which was blocked with 5 % BSA (in PBST) at room temperature for 1 h. Subsequently, the blots were incubated with respective antibodies (LC3, SIRT1, LAMP1, acetylate lysine, p16, p21, Rb, PCNA, and actin) for overnight at 4°C followed by incubation with secondary antibodies for 1h at room temperature. The expression of the protein of interest was detected using a chemiluminescence method and quantified by Image J software. For immunoprecipitation, the cell lysates were incubated overnight at 4°C with the mentioned antibodies followed by coupling with protein A-Sepharose (Invitrogen Corporation, CA, USA) followed by western blotting as described (Mukhopadhyay et al., 2015).

5.2.7 Flow Cytometry Analysis of Cell Cycle Distribution

After treatment with AGG, PC3 cells were harvested and fixed in 70 % ethanol (stored at -20°C). Then, the cells were washed with ice-cold PBS (10 mM, pH 7.4) and resuspended in 200 μ l of PBS followed by incubation with 20 μ l DNase-free RNase (10 mg/ml) and 20 μ l of DNA intercalating dye propidium iodide (PI) (1 mg/ml) at 37°C for 1 h in dark. The distribution of cells in the different cell cycle phases was analyzed from the DNA histogram using BD ACCURI C6 flow cytometer and FCS EXPRESS software.

5.2.8 Immunofluorescence

After treatment, PC3 cells were fixed, permeabilized and incubated with primary antibodies (1:500; Anti-SIRT1 antibody from Cell Signalling and Technologies (CST, Danvers, MA) for overnight. The cells were further incubated with the secondary anti-rabbit and/or anti-mouse antibodies conjugated with Alexa Fluor to study the fluorescence of our desired proteins. Imaging was performed at 40X fluorescence microscope (Olympus IX71).

5.2.9 Total Lipid and Free Fatty Acid Analysis

After 72 h post treatment with AGG cells were washed in PBS and fixed in formalin for 10 min at room temperature. Cells were washed with ddH₂O twice followed by washing in 60 % isopropanol and dried completely. Then the cells were incubated with Oil Red O at room temperature for 10 min. After washing with ddH₂O Oil Red O dye was eluted by adding 1 ml of 100 % isopropanol and incubated for 10 min with gentle shaking. The OD at 500 nm was measured using 100 % isopropanol as blank.

For quantification of free fatty acid, to 100 µl of control and treated sample, 1ml PBS, 6 ml extracting buffer (chloroform: hexane: methanol, 5:5:1) and 2.5 ml copper reagent was added and incubated for 15 min. After incubation organic layer was transferred to another tube containing 500 µL diphenyl carbazide. The absorbance was measured at 550 nm against PBS as blank.

5.2.10 Statistical Analysis

All data are representative of at least five independent experiments which were quantified and plotted as the mean ± standard deviation. Student's t test was used for evaluating statistical differences between experimental groups. Further, a nonparametric test for statistical analysis among groups was also done by a one-way ANOVA Kruskal-Wallis test, with Dunn's multiple group comparison tests as appropriate.

5.3. Results

5.3.1 AGG Induces Senescence and Growth Arrest

To investigate the antitumor activity of AGG at lower doses, we have treated PC3 cells with different concentration of AGG (25, 50 and 100 ng/ml) for 72 h and analyzed for induction of senescence and growth arrest. It is well known that senescent cells express a senescence associated β-galactosidase (SA-β-Gal). We found AGG increase β-Gal in a dose dependent way (Fig. 5.1.a) and AGG induced senescence up to 12.0± 1.5 %, 28.7± 4.3 % and 40.8± 5.5 for AGG dose of 25, 50 and 100 ng /ml respectively in contrast to 6.5± 0.5 % for the control group (Fig. 5.1.b). Further, we found a time dependent increase in the β-Gal staining with AGG treatment (Fig. 5.1.c, d) suggesting that even 100 ng/ml of AGG is able to induce the senescence of PC3 cells. Besides SA-β-gal staining, the flat and hyper sized morphology which is marked as an important hallmark of cellular senescence was observed in presence of AGG.

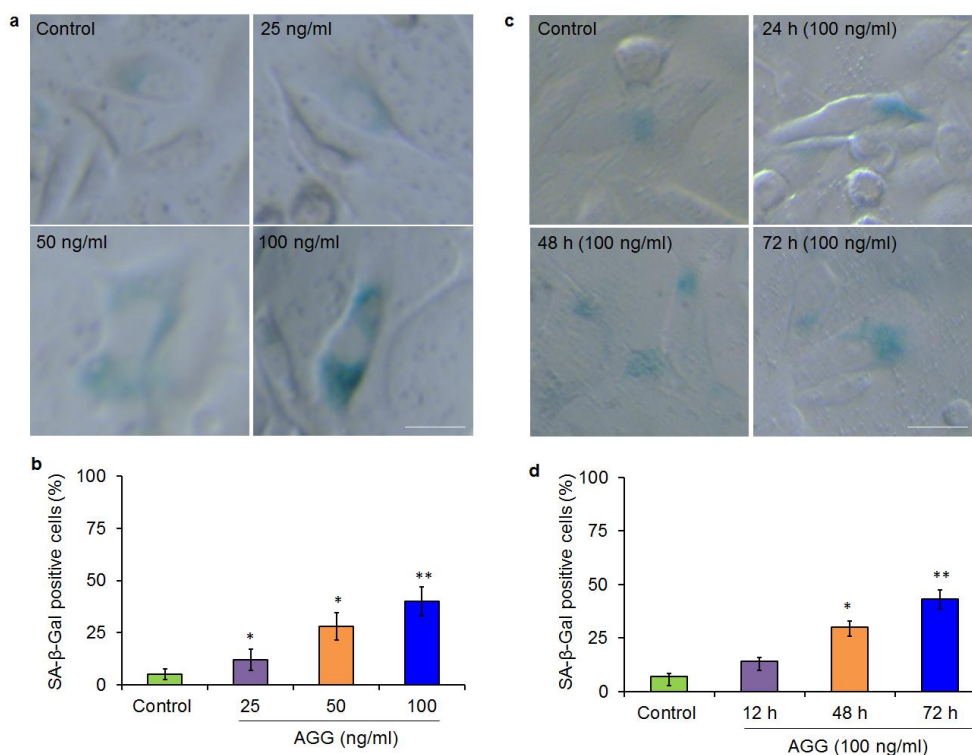


Fig.5.1. AGG induces SA-β-Gal staining in dose and time dependent way in PC3 cells. PC3 cells were treated with different doses of AGG (25, 50 and 100 ng/ml) for 72 h and SA-β-Gal staining performed photographed and quantified (a, b). PC3 cells were treated with AGG concentration of 100 ng/ml for different time intervals (24, 48 and 72 h) and senescent cells were quantified (c, d). Data reported as the mean \pm S.D. of three independent experiments and compared to PBS control. * P value < 0.05 ; ** P value < 0.01 were considered significant.

Next, we examined the role of AGG in cell cycle progression in PC3 cells at different dose by PI staining using flow cytometry. The number of cells in the G0/G1 phase increased in a dose-dependent manner with AGG treatment in PC3 cells. On the contrary, we did not observe any significant alteration in other phase of cell cycle, conforming AGG only arrest G0/G1 phase for senescence induction at lower doses (Fig.5.2.a, b). Further, we evaluated the effect of AGG on a group of proteins that are known to regulate cellular proliferation. Cyclin B is necessary for the progression of the cells into and out of M phase of the cell cycle. Because cyclin B is necessary for cells to enter mitosis and therefore necessary for cell division, cyclin B levels are often deregulated in tumors. When cyclin B levels are elevated, cells can enter M phase prematurely and strict control over cell division is lost, which is a favorable condition for cancer development. Overexpression of cyclin B1, therefore, shortens the G2 phase and occurs in many types of human cancer, whereas inhibition of its expression blocks G2-M transition. Accordingly, our Western blot analysis showed that there was a decrease in the expression of cyclin B1 with increasing dose. Remarkably, the expression of PCNA, an auxiliary protein involved in the control of eukaryotic DNA replication and required for cell cycle progression from G1 to S phase, was

also downregulated in response to AGG. Further, we checked for the expression of the tumor suppressor and cell cycle regulator gene retinoblastoma (Rb). Rb restricts the cell's ability to replicate DNA by preventing its progression from the G1 to S phase of the cell division cycle. When the cell is ready to divide, Rb is phosphorylated, becomes inactive and allows cell cycle progression (Fig.5.2.c).

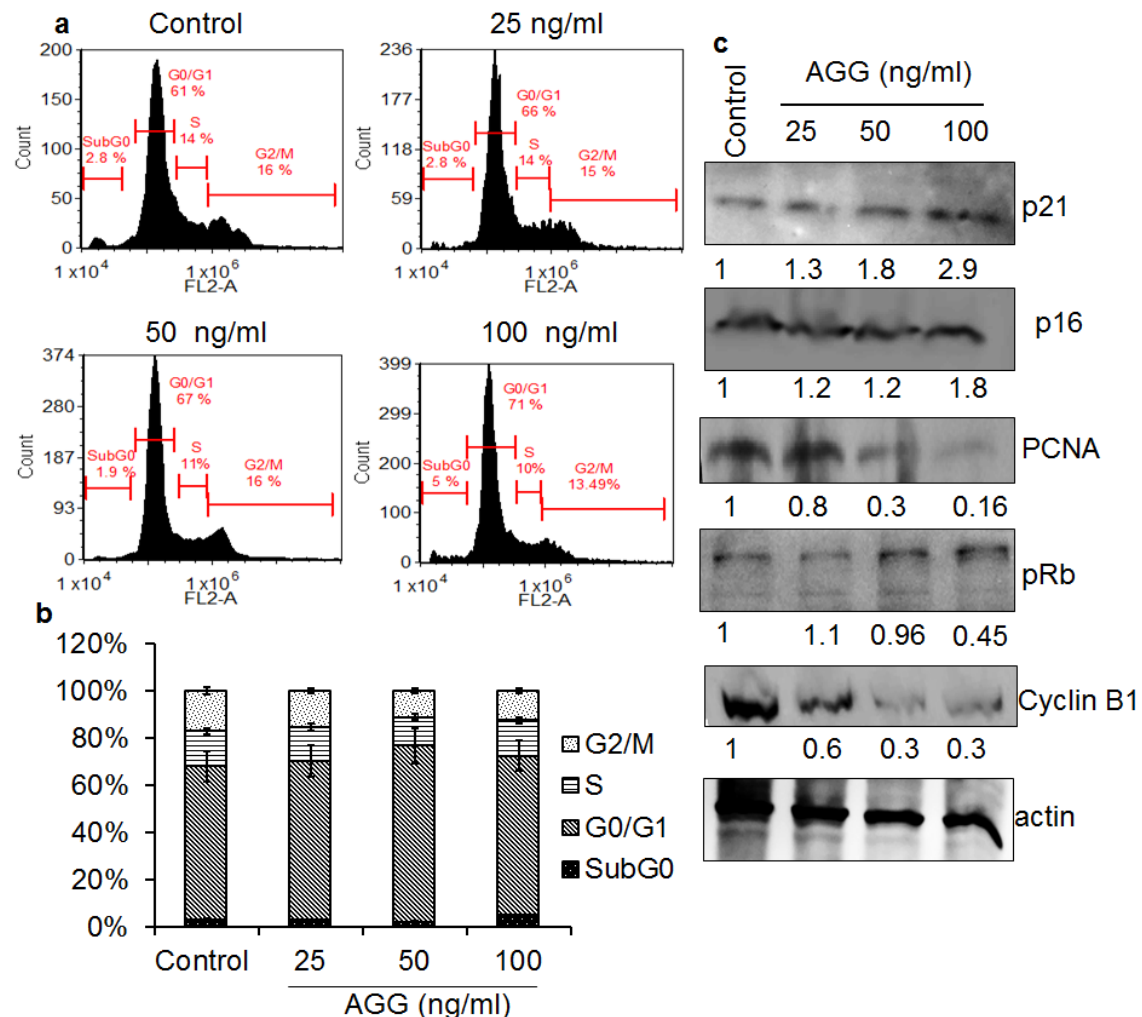


Fig.5.2. Effect of AGG on cell cycle. PC3 cells were treated with different dose of AGG (25, 50, 100 ng/ml) for 72 h and were analyzed for cell cycle distribution by PI staining through Flow cytometry (a, b). After 72 h treatment with AGG, PC3 cells were analyzed for expression of p21, p16, PCNA, pRb, and Cyclin B1 by western blot (c). Data reported as the mean \pm S.D. of three independent experiments and compared to PBS control. Densitometry was performed on the original blots, considering the ratio of protein to actin in control cells was 1.

5.3.2 AGG Induced Autophagy Regulates Senescence

We found that AGG is able to induce senescence in PC3 cells but the mechanism underlying senescence still needs to be established. For which, we analyzed the autophagy induction with AGG. As expected, AGG was also able to effectively induce autophagy at low doses i.e 100 ng/ml. The increase in red intensity of acridine orange standing with different doses of AGG indicates autophagy induction (Fig. 5.3.a, b). We also analyzed the expression of autophagy signature molecules through western blot analysis (Fig 5.3.c). Satisfying our

hypothesis, we again found a dose dependent increase in ATG5, BECN1 with increased LC3-I lipidation to LC3-II suggesting that AGG mediated autophagy induction in PC3 cells.

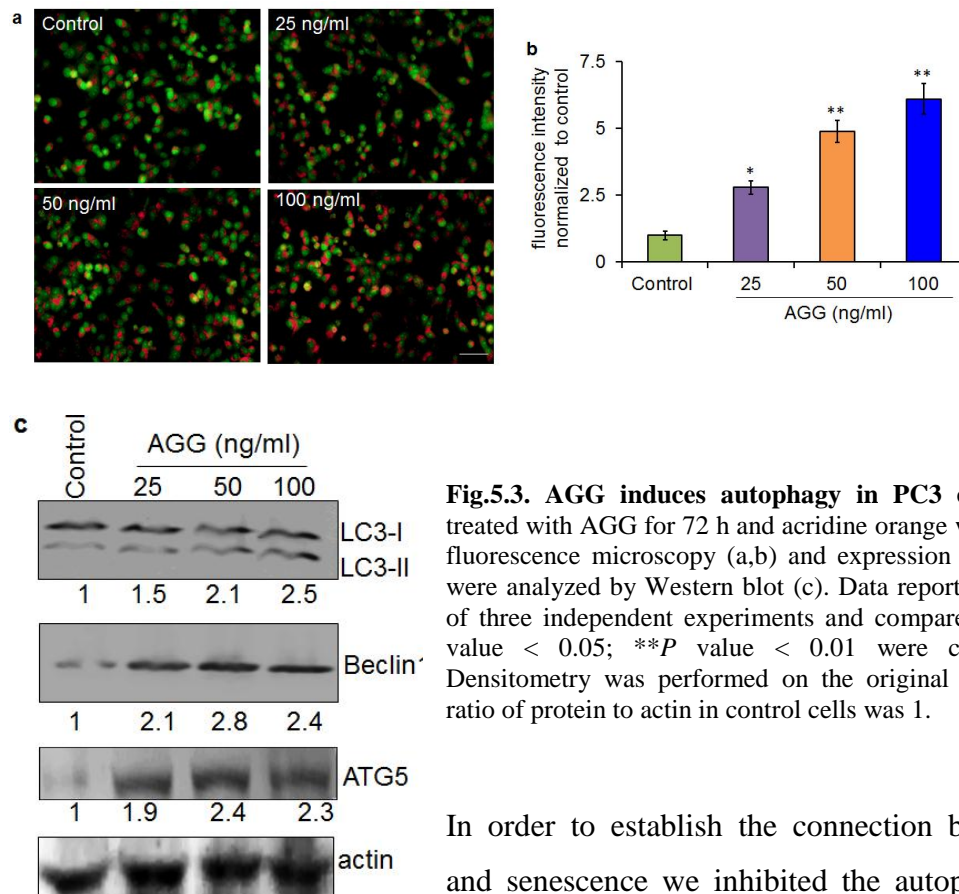


Fig.5.3. AGG induces autophagy in PC3 cells. PC3 cells were treated with AGG for 72 h and acridine orange was performed through fluorescence microscopy (a,b) and expression of autophagy markers were analyzed by Western blot (c). Data reported as the mean \pm S.D. of three independent experiments and compared to PBS control. **P* value < 0.05; ***P* value < 0.01 were considered significant. Densitometry was performed on the original blots, considering the ratio of protein to actin in control cells was 1.

In order to establish the connection between autophagy and senescence we inhibited the autophagy using 3-MA and examined the SA- β -Gal staining. Interestingly, we found that inhibition of autophagy led to reduced SA- β -Gal staining and AGG is not able to increase the SA- β -Gal staining in presence of 3-MA (Fig.5.4.a,b). This suggests that AGG induced senescence in PC3 cells was dependent on autophagy.

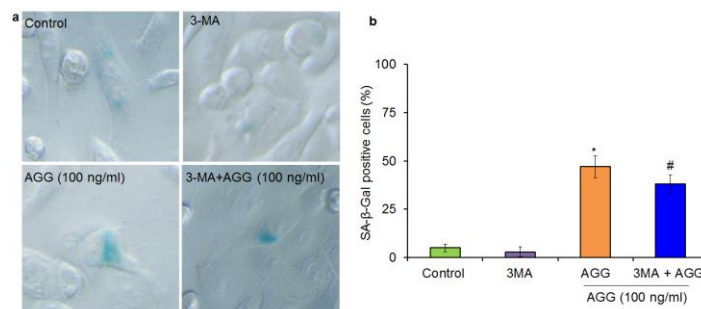


Fig.5.4. AGG induced autophagy regulates senescence in PC3. PC3 cells were treated with AGG (100 ng/ml) in presence of 3-MA (10 mM, 2 h) and SA- β -Gal staining to quantify senescence (a,b). Data reported as the mean \pm S.D. of three independent experiments **P* value < 0.05 was considered significant as compared to control and #*P* value < 0.05 was considered significant as compared AGG treated group.

5.3.3 AGG Induced Lipophagy Modulates Senescence

Autophagy to senescence is well established but specific induction of lipophagy (lipid-specific autophagy) by AGG and its role in senescence has not been yet deciphered. Lipophagy is the selective degradation of lipid droplets (LDs) by the lysosomal acid lipase which converts them into free fatty acids (FFAs).

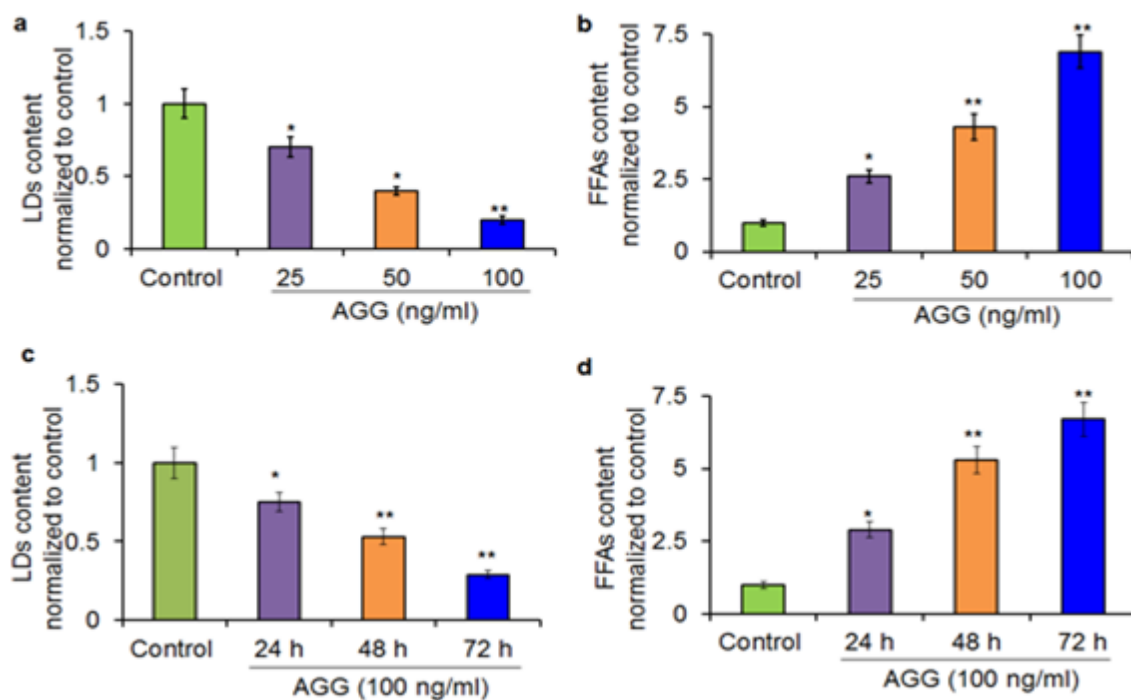


Fig.5.5. AGG abrogates lipid store and escalates free fatty acid content in PC3 cells. PC3 cells were treated with AGG for different doses and time periods and relative content of lipid droplet and free fatty acids were measured. Data reported as the mean \pm S.D. of three independent experiments and compared against PBS control. * P value < 0.05 ; ** P value < 0.01 were considered significant.

In curiosity to establish a connection between lipophagy and senescence, we first investigated the lipid degradation ability of AGG. Intriguingly, we found dose dependent decrease in the LDs with AGG treatment. Correspondingly, we checked the FFAs content and as expected the FFAs content increased with increased AGG concentration suggesting the potential lipophagy inducing ability of AGG (Fig. 5.5). Further we validated our hypothesis by inhibiting the lipophagy by lysosomal lipase inhibitor lalistat and examined the LDs and FFA profile. Corroborating our hypothesis, AGG in presence lalistat is unable to carry out the degradation of LDs into FFAs (Fig. 5.6).

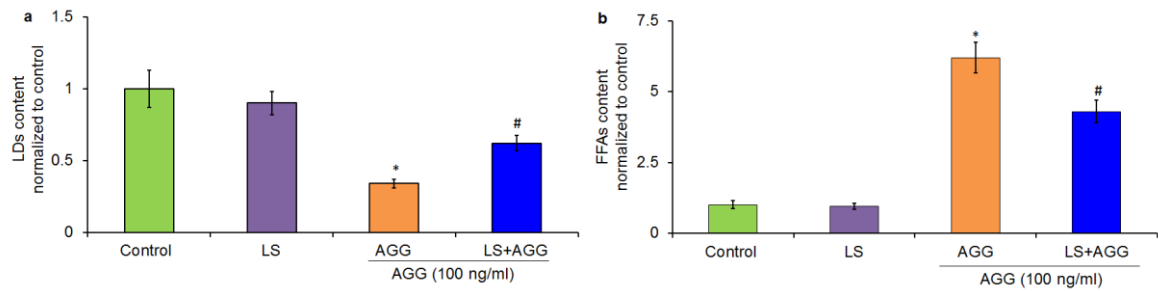


Fig.5.6. Effect of lalistat on AGG induced lipophagy in PC3 cells. PC3 cells were treated with AGG (100 ng/ml) in presence of lalistat (10 μ M, 6 h) and relative content of lipid droplet and free fatty acids were measured. (a,b). Data reported as the mean \pm S.D. of three independent experiments and compared to PBS control. **P* value < 0.05 was considered significant as compared to control and #*P* value < 0.05 was considered significant as compared AGG treated group.

Furthermore, we studied autophagy induction with AGG in presence of lalistat and our data showed that AGG decreased the red intensity of acridine staining in presence of lalistat as compared to only AGG treated PC3 cells (Fig.5.7.a,b). In order to validate that AGG induced lipophagy is associated with senescence, we analysed the β -Gal staining with in presence of lalistat. The data showed that β -Gal staining was significantly reduced in both lalistat and AGG treated cells as compared to only AGG treated cells (Fig.5.7.c,d).

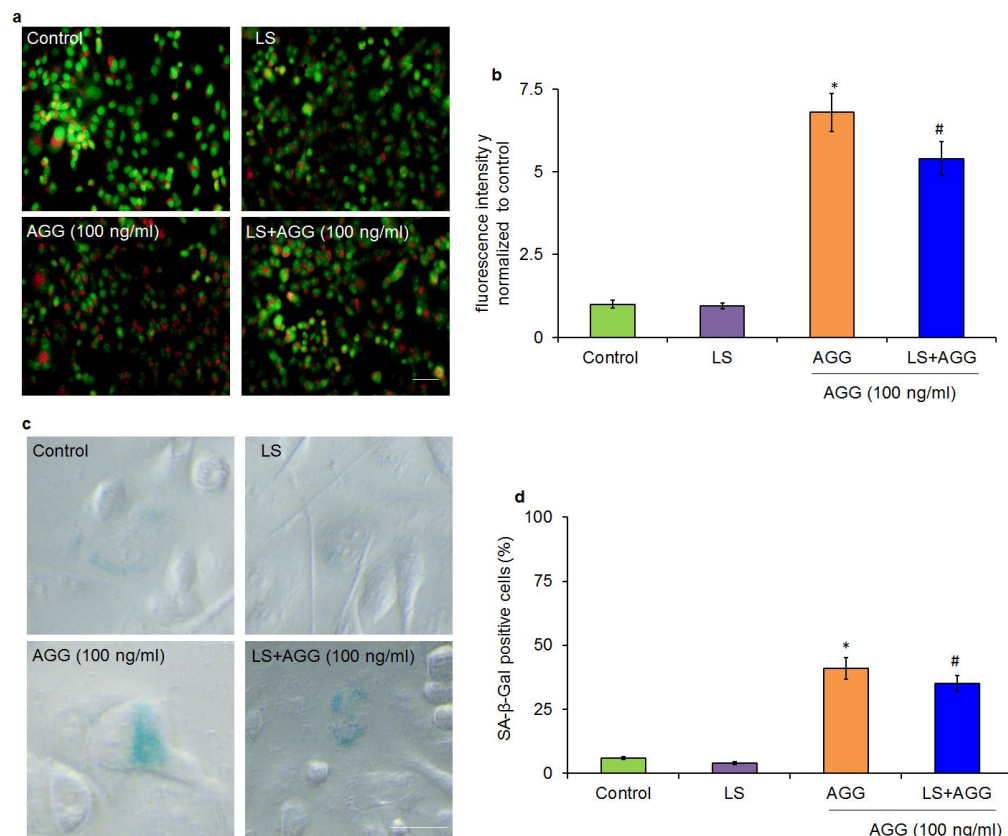


Fig.5.7. AGG induces lipophagy to prompt senescence PC3 cells were treated with AGG (100 ng/ml) in presence of lalistat (10 μ M, 6 h) and acridine orange staining (a, b) and SA- β -Gal staining (c, d) was performed. Data reported as the mean \pm S.D. of three independent experiments and compared to PBS control. **P* value < 0.05 was considered significant as compared to control and #*P* value < 0.05 was considered significant as compared AGG treated group.

5.3.4. SIRT1 Regulates AGG Induced Autophagy

Nuclear histone deacetylase is previously reported to associate with apoptosis under different stress conditions (Houtkooper RH et Al., 2015). In order to examine whether SIRT1 is involved in the AGG induced autophagy, we treated PC3 cells with different doses of AGG (25, 50 and 100 ng/ml) and analyzed the expression of SIRT1 through fluorescence microscopy and Western blot. Our data showed that the SIRT1 expression was found to increase in dose dependent manners in PC3 cells (Fig. 5.8.a-c).

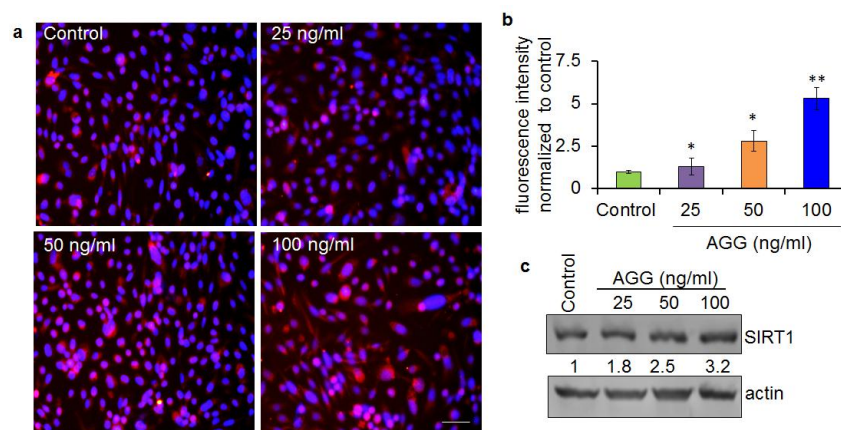


Fig.5.8. Effect of AGG on expression of SIRT1 in PC3 cells. PC3 cells were treated with different doses of AGG (25, 50 and 100 ng/ml) treatment for 72 h and expression of SIRT1 was analyzed through fluorescence microscopy and Western blot. Data reported as the mean \pm S.D. of three independent experiments and compared to PBS control. **P* value < 0.05; ***P* value < 0.01 were considered significant. Densitometry was performed on the original blots, considering the ratio of protein to actin in control cells was 1.

Next, we studied the molecular mechanism of AGG induced autophagy through SIRT1 in PC3 cells. SIRT1 have been shown to deacetylate several different autophagic molecules to initiate autophagy. Here, we examined whether SIRT1 has any role in regulating LAMP1, lysosomal membrane protein, indispensable for autolysosome formation through deacetylation for autophagy induction. Our immunoprecipitation data showed that SIRT1 interacted LAMP-1 upon AGG treatment in PC3 cells (Fig.5.9.a). Further, as SIRT1 is deacetylase, we thought that LAMP1 deacetylation might be the possible outcome of their interaction and it showed that AGG induced strong deacetylase activity in LAMP1 in PC3 cells (Fig.5.9.b). Although detail mechanism of SIRT1 and LAMP1 deacetylation in AGG induced autophagy remains to be identified, it is accepted that SIRT1 activation leads to deacetylation of LAMP1 to initiate AGG induced autophagy.

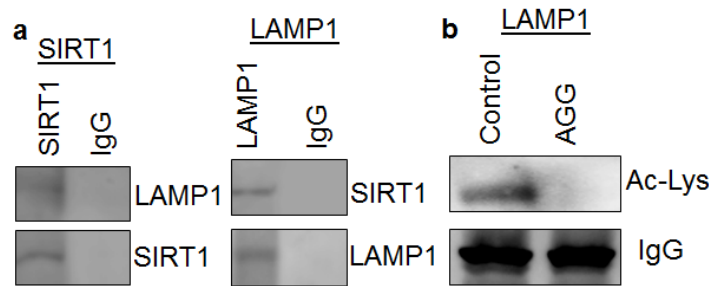


Fig.5.9. SIRT1 interacts and deacetylates LAMP in PC3 cells. PC3 cells were treated with AGG for 72 h and immunoprecipitated with anti-SIRT1 and anti-LAMP1 followed by immunoblotting with anti-LAMP1 or anti-SIRT1 antibodies (a). After treatment with AGG, acetylation of LAMP1 in PC3 cells was studied by immunoprecipitation analysis (b).

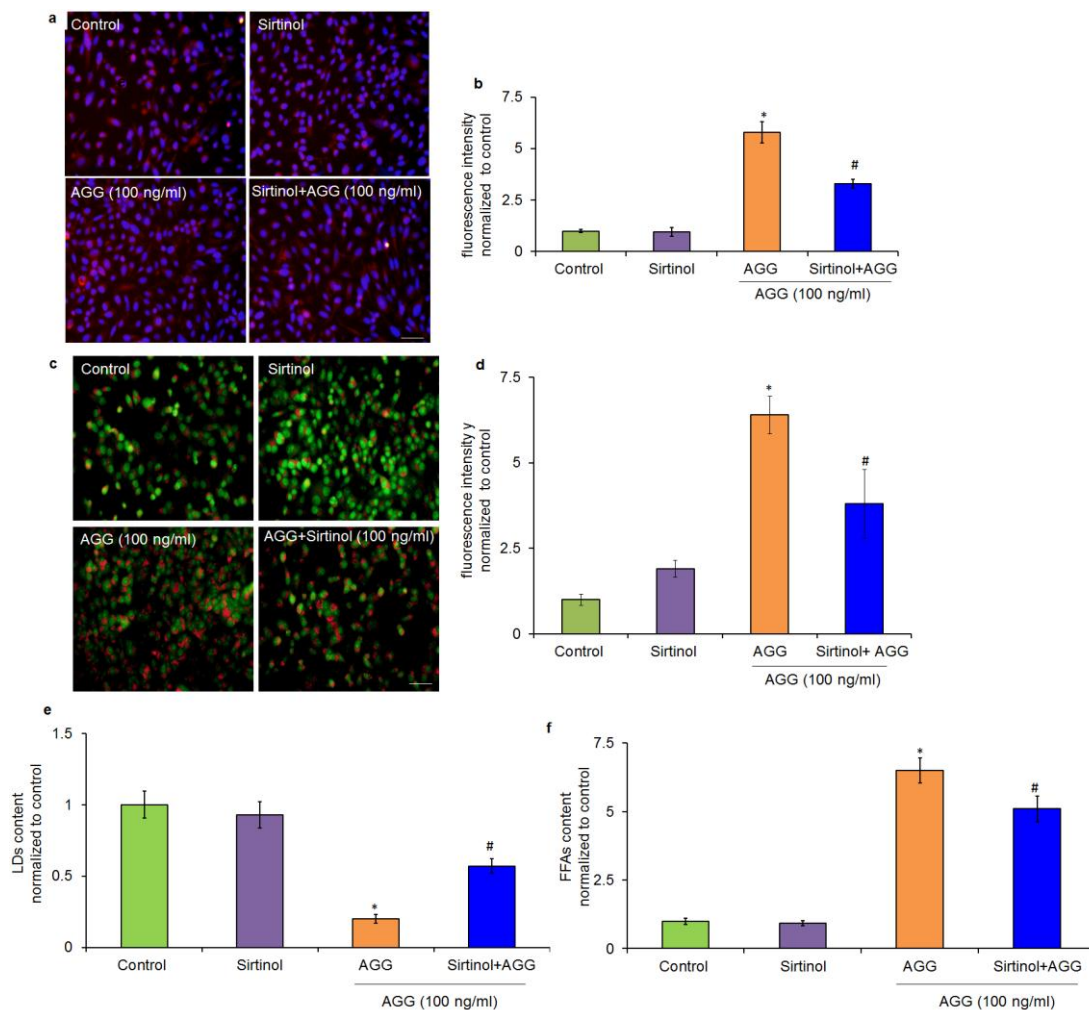


Fig.5.10. Effect of SIRT1 inhibition of AGG induced lipophagy in PC3 cells. PC3 cells were treated with AGG (100 ng/ml) in presence of sirtinol for 72 h and expression of SIRT1 by fluorescence microscopy, autophagy by acridine orange staining and lipophagy by relative content of lipid droplet and free fatty acids were measured. Data reported as the mean \pm S.D. of three independent experiments. * P value < 0.05 was considered significant as compared to control and # P value < 0.05 was considered significant as compared AGG treated group.

Further, we inhibited the SIRT1 activity by a specific inhibitor sirtinol and examined the AGG induced autophagy. Our data showed that SIRT1 expression by AGG was

significantly inhibited in presence of sirtinol as compared to only AGG treated group (Fig.5.10.a,b). Importantly, AGG induced autophagy was significantly reduced with the SIRT1 inhibition confirming that SIRT1 play a pivotal role in AGG induced autophagy (Fig.5.10.c,d). Moreover, we inhibited SIRT1 activity by sirtinol and further analysed the LDs and FFA profile. The data showed that when we inhibited the SIRT1 activity, the LDs content increased in both AGG and sirtinol treated group as compared to only AGG treated group. In accordance with our hypothesis, the FFAs content decreased in both AGG and sirtinol treated group as compared to only AGG treated group (Fig.5.10.e,f). This data suggest that AGG induced autophagy is mediated by SIRT1 dependent lipophagy.

5.4. Discussion

As a mechanism of anticancer therapy, a promising approach to cytostasis induction in cancer cells is therapy induced senescence (TIS) (Ronnison, 2003; Gewirtz, 2008; Ewald et al., 2010). Substantial evidence propose that phytochemicals can effectively promote cancer cell death through autophagy induction (Xhang et al., 2012). Moreover, many reports claim that the process of senescence linked to autophagy (Gewwirtz, 2013). In the present study, we investigated senescence inducing potential of *Abrus* agglutinin on prostate carcinoma. Here we provide experimental data demonstrating that low doses of AGG were able to induce autophagy dependent senescence which is specifically regulated by lipophagy in prostate cancer cells. The results disclose that AGG may exert its anticancer and chemopreventive activities via the induction of autophagy mediated senescence in prostate cancer cells.

TIS were reported to occur in cancer cells both *in vitro* and *in vivo* when exposed to various cytotoxic agents. Growth arrest in senescence is primarily accomplished in either the G1 or G2/M phase of the cell cycle (Ewald et al., 2010). Senescent cells, in particular, are reported to have increased SA- β -Gal activity. Here, we showed that AGG induced senescence associated upregulation expression of SA- β -Gal in both dose and time dependent manner. In fact, we demonstrated that SA- β -Gal expression was robustly increased at a concentration of AGG (100 ng/ml) that induced senescence in PC3cells. Senescence, in contrast to apoptosis, requires much lower concentration of AGG, suggesting that AGG could be useful clinically. Consistent with our observations, it is previously reported that treatment with resveratrol, a phytochemical, has a propensity to generate senescence-like phenotype in cancer cells (Rusin et al., 2009). In contrast to mitotic catastrophe or apoptosis induced by to conventional cytotoxic agents, senescent cells are believed to persist for indefinite time period. Growth arrest at G1 or G2/M stage of the cell cycle occurs in part, by

the increased expression of specific cyclin-dependent kinase inhibitors (CDKIs), including p16Ink4a (CDKN2A), p21Waf1 (CDKN1A, CIP1), and p27Kip1 (CDKN1B). Accordingly, corresponding to the observation by El Hansana et al., (2015) AGG induced cell cycle arrest at G1 phase and promoted the upregulation of p21, cyclin B1, p16, down regulation of proliferation marker PCNA and hypophosphorylation of the tumor suppressor RB. Similarly, Luo et al., (2013) reported that Resveratrol is able to trigger premature senescence in lung carcinoma via ROS-mediated DNA damage. Based on these data, we propose that senescence in AGG would be promising therapeutic agent clinical by virtue of its ability to stimulate the TIS at a low nonlethal dose.

We discovered that AGG induced autophagy was associated with activation of SIRT1. Substantial evidences support the notion that SIRT1 has a Janus-faced role in carcinogenesis. SIRT1 play a pivotal role in genomic stability and cancer cell death and anti-inflammation, suggesting its tumor-suppressor properties. However, SIRT1 may trigger the oncogenic signaling pathways to create a supportive tumor microenvironment as part of its protumorigenic property (Song et al., 2012). On the ground of tumor suppressor role, SIRT1 could be downregulated in many tumors. In this regard, SIRT1 expression was found to be reduced in human skin tumors (Ming et al., 2010). Inconsistently; as an oncoprotein SIRT1 can be overexpressed in cancer (Huffman et al., 2007). Recent reports suggest that as a part of its anticancer activity, natural molecules resveratrol was shown to induce SIRT1 expression (Bora et al., 2005; Singh et al., 2011; Cao et al., 2015; Hou et al., 2016). In accordance, our molecule AGG was shown to induce SIRT1 expression substantially in treated condition. Moreover, the involvement of SIRT1in autophagy regulation is also well established. According to reports, resveratrol is shown to induce autophagy through the activation of SIRT1 (Guo et al., 2013). Likely, Ou et al., (2014) proposed that SIRT1 positively govern autophagic processes in embryonic stem cells under oxidative stress. Moreover, in cellular models of Parkinson's disease, resveratrol was shown to trigger AMPK/SIRT1/Autophagy signaling (Wu et al., 2011). Likewise, in the present investigation, we showed that low doses of AGG in PC-3 cells effectively induce canonical autophagy as evidenced by the marked increase in the expression of BECN1, ATG5 and increased LC3-II lipidation. Moreover, the induction of autophagy was categorically dependent on SIRT1 activation by AGG as pharmacological inhibition of SIRT1 by sirtinol dramatically reduced the acridine orange staining.

Regulation of senescence is controlled by different cellular processes including autophagy. The phytochemical resveratrol was reported to induce autophagy and senescence

in human cancer cells (Patel et al., 2013). In accordance with the prior report, the present investigation proposes that autophagy and its resultant protein turnover induction by AGG facilitates the acquisition of the senescence phenotype whereas inhibition of autophagy by 3-MA substantially reduced the percentage of senescent cells. The lysosomal degradative pathway of lipid metabolism is termed lipophagy where intracellular lipid droplets (LDs) and metabolized by cytoplasmic neutral hydrolases to supply free fatty acid during stress. The free fatty acids generated by lipophagy fuel cellular rates of mitochondrial β -oxidation. Recently, our group reported that lipophagy in cancer induces ER stress mediated apoptosis (Mukhopadhyay et al., 2017). Likely, in the current investigation, the phytolectin AGG was shown to induce lipid degradation by autophagy dependent manner which was further found to regulate the process of senescence in prostate cancer.

Deacetylation lysine by SIRT1 has been recognized as critical events in the regulation of stability, activity and subcellular localization of proteins including autophagic proteins. A recent report demonstrated that galangin, a flavonoid compound induced autophagy through deacetylation of LC3 by SIRT1 in HepG2 Cells (Li et al., 2016). In corresponding to these finding, the current investigation unraveled SIRT1 mediated deacetylation of lysosomal membrane protein LAMP1. LAMP proteins constitute 50 % of lysosomal membrane and deficiency in LAMP1 is reported to impede lysosome biogenesis and autophagy (Eskelinen et al., 2006). Here, we found that AGG induced SIRT1 deacetylates Lys residue of LAMP1, an important molecule in the formation of autolysosome and deciphered involvement of SIRT-1 mediated deacetylation of LAMP1 by AGG to promote lipophagy stimulated senescence. In conclusion, AGG leads to therapy induced senescence through autophagy as a tumor suppressor mechanism.

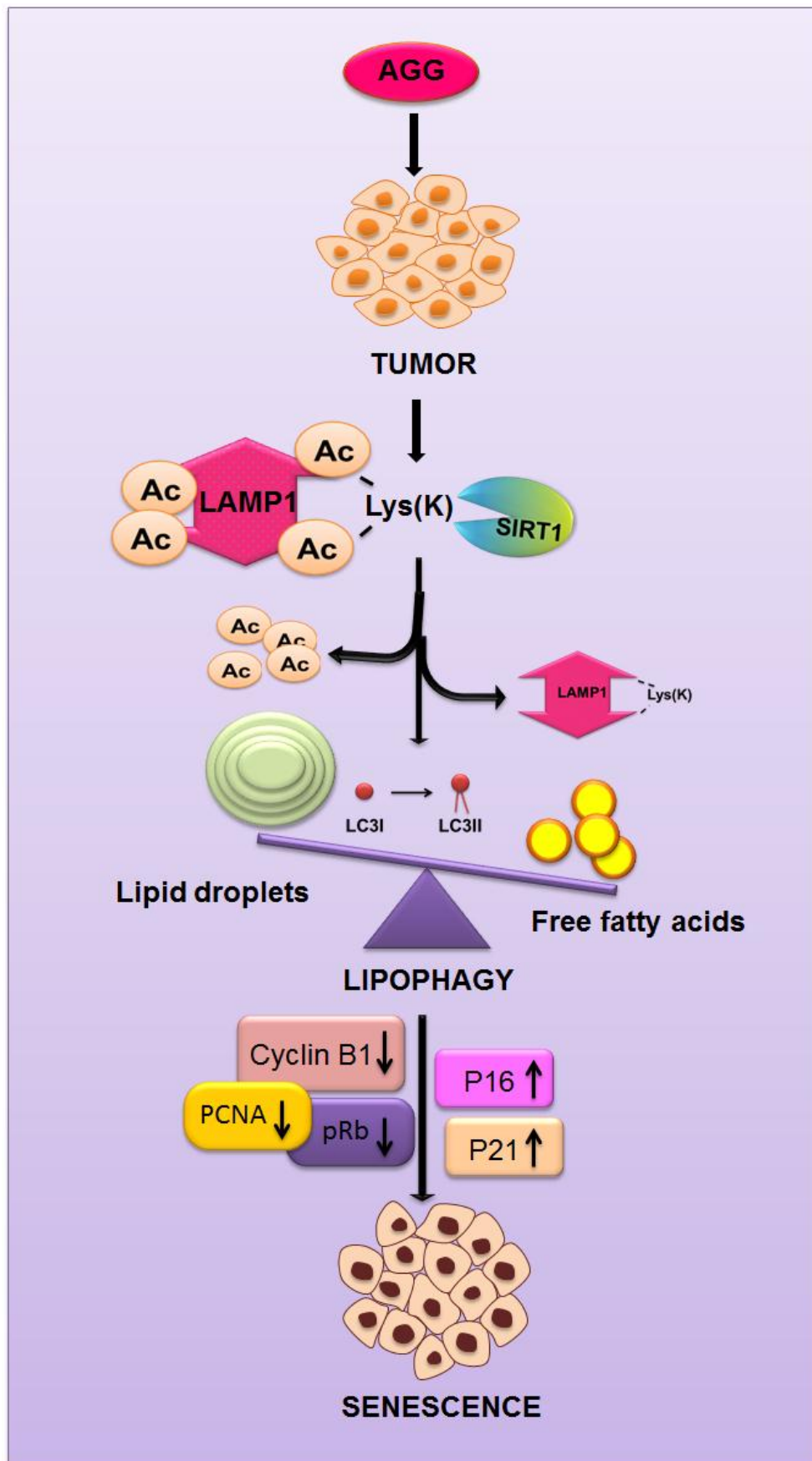


Fig. 5.11. Schematic representation of AGG induced lipophagy mediated senescence

Chapter 6

***Abrus* agglutinin induces cancer stem cell differentiation through BMP2 mediated autophagy**

Abstract

Cancer stem cells (CSCs) in colorectal cancer (CRC) are the prime culprits in the initiation, progression, relapse, and therapy resistance which necessitates the quest for novel therapeutic molecules to target colon bulk tumor population as well as CSC population. In the present study, we showed that *Abrus* agglutinin (AGG), a plant lectin substantially induced colon CSC differentiation by inducing a member of TGF- β superfamily Bone Morphogenetic Protein 2 (BMP2). As per our retrospective tumor specimen analysis, BMP2 expression was downregulated with colon cancer progression indicating its tumor suppressor function. Moreover, β -catenin, a factor responsible for self-renewal potential of CSCs was shown to be upregulated in colon tumor tissue during cancer progression. AGG was shown to induce differentiation and stemness in HT-29 cells derived colonospheres. AGG induced differentiation was shown to be critically dependent on autophagy in colonospheres. Our study showed that AGG increased expression of BMP2 and has interacted with hVps34 suggesting BMP2 was associated in the process of autophagy. Interestingly, inhibition of autophagy by 3-Methyl adenine (3-MA), a known hVps34 inhibitor was shown to prevent AGG induced β -catenin degradation and self-renewing potential in colonospheres. In subcutaneous HT-29 xenograft model, AGG profoundly inhibited the growth of tumors with an increase in LC3 and BMP2 expression conforming antitumor potential of AGG through induction of differentiation in colorectal cancer.

Key words: *Abrus* agglutinin, BMP2, β -catenin, Cancer stem cells (CSCs), Differentiation, hVps34

6.1. Introduction

Autophagy is a ubiquitous and dynamic conserved catabolic process which is essential for survival, differentiation, development and cellular homeostasis. Moreover, autophagy is regarded as a double-edged sword in cancer as experimental evidence substantiates the role of autophagy in both cancer progression and suppression (Bhutia et al., 2013). Recently, many documents portray the autophagic regulation of cellular differentiation in cancer (Panda et al., 2015). Mutation in the autophagy factor UVRAG (Beclin 1/Vps34 complex) leads to abnormal left–right axis formation subsequenting in heterotaxy (Liang et al., 2006). Further, depletion of BECN1 is reported to inhibit both autophagy and differentiation capabilities (Wang et al., 2008).

Colorectal cancer (CRC) is the third most common cancer in men (10.0%) and the second in women (9.4%) worldwide (Ferlay et al., 2008). Despite the availability of early diagnosis techniques and modern treatment choices including surgical resection and adjuvant

chemo/radio-therapy depending on the stage of malignancy, the efficacy of many first line therapeutics are exhausting day by day and 50 % of CRC patients develop recurrent disease, and patients with advanced and metastatic CRC are susceptible to death (Kumar et al., 2014). A growing body of evidence accuses a subset of tumor cells referred as cancer stem cells (CSCs) for such failure of current treatment modules. CSCs refers to a rare subpopulation of tumor cells that have the exclusive ability of self-renewal capacity, aggressive invasive potential, hierarchical differentiation and tumorigenicity (Naik et al., 2016). The CSCs have the important feature of self-renewal, which is a property in common with stem cells. Developmental pathways like Wnt/Notch/Hedgehog have been identified to be essential for the self-renewal behavior of cancer stem cells (Kato et al., 2007; Tang et al., 2007). The Wnt/ β -catenin signaling is one of the key pathways reported to promote self-renewal of cancer stem cells. Activation of Wnt target genes is mediated by β -catenin, which translocates to the nucleus and binds to the transcription factors T-cell factor/lymphoid enhancer factor (TCF/LEF) to activate the downstream signaling (Liu et al., 2002; Fodde et al., 2007).

Colonic epithelium undertakes continual rejuvenation maintained by colon stem cells located at the very base of the crypt of the epithelium. Bone morphogenetic proteins (BMPs), a TGF β superfamily of proteins, are important players in colon stem cell self-renewal and differentiation (Lombardo et al., 2011). Moreover, BMP2 is reported to control a crucial early commitment step in the differentiation of human embryonic stem cell (Pera et al., 2004). Reports also elucidate that BMP pathway is inactivated in the majority of sporadic CRCs (Lombardo et al., 2011). Recent report also indicates the elevated expression of Atg7 and Wnt signaling during BMP2 mediated human osteoblastic differentiation (Ozeki et al., 2016). Moreover, BMP2 was shown to induce chondrogenic differentiation *in vitro* involves by downregulating of membrane bound β -catenin (Zhang et al., 2004).

Identification and development of drugs, especially non-toxic agents, which target this ‘tumor initiating cells’ through differentiation with a loss of self-renewal capacity of CSC might offer prospects to ensure promising results at a late stage in cancer therapy. Differentiation therapy is a relatively less toxic therapeutic modality than classical chemotherapy that centers on reactivating endogenous differentiation program and compels tumor cells to restore terminal maturation. Differentiation agents are basically engaged in the reprogramming of cancer cells that provokes the terminal differentiation of cells, even inducing apoptosis leading to cell death (Pierce et al., 1971). Clinically, all-trans retinoic acid (ATRA) is reported to induce terminal differentiation of acute promyelocytic leukemia

blasts (Warrell et al., 1991; Ge et al., 2014). In this study, our focus was to examine and establish the efficacy of *Abrus* agglutinin (AGG) on colon CSC expansion, self-renewal and differentiation in the context of anti-CRC efficacy. AGG, a plant lectin isolated from the seeds of *Abrus precatorius* is [gal β (1–3) NAc gal] specific and belongs to type II ribosome-inactivating proteins having molecular weight 134 kDa. AGG composed of a toxic enzymatic A subunit of 30 kDa and the galactose-binding B subunit of 31 kDa linked covalently by a single disulfide bond (Panda et al., 2015). AGG were found with a protein synthesis inhibitory activity (IC₅₀) of 3.5 nM and lethal dose (LD₅₀) of 5 mg/kg of body weight (Liu et al., 2000). AGG inhibits growth and proliferation of tumors at sub-lethal doses *in vitro* and *in vivo* (Bhutia et al., 2008 a, b). Further, AGG was found to induce anti-proliferative activity and apoptosis induction in Dalton's lymphoma mice model (Bhutia et al., 2008a, 2009b). It also induced apoptosis in a caspase 3/7, 8 and 9 activities dependent manner *in vitro* and *in vivo* model in human hepatocellular carcinoma (Mukhopadhyay et al., 2014b). Tryptic digestion of *Abrus precatorius* agglutinin protein inhibited Ehrlich's ascites carcinoma (EAC) and B16 melanoma (B16M) bearing mice models and showed increased *ex vivo* proliferation of splenocyte and thymocyte isolated from tumor bearing mice and increase in TNF- α and Interferon- γ in splenocyte culture supernatant (Behera et al., 2014). In human breast cancer, AGG has inhibited tumor growth and angiogenesis as confirmed by the lower expression of Ki-67 and CD-31, respectively in a xenograft model (Bhutia et al., 2016). Based on these finding, the present study is intended to investigate the role of AGG in the differentiation of colon CSC through modulation BMP2 induced autophagy and β -catenin degradation. Furthermore, this study also sheds lights on the interaction of BMP2 with hVPS34, class III phosphatidylinositol 3'-kinase, a key player in the autophagosome biogenesis suggesting the potential involvement of BMP2 in the autophagosome synthesis.

6.2. Materials and Methods

6.2.1 Reagents

4,6-Diamidino-2-phenylindole dihydrochloride (DAPI) (D9542), dimethylsulfoxide (DMSO) (D8418) and 3-Methyl adenine (3-MA) (M9281) were purchased from Sigma-aldrich (St. Louis, Missouri, United States). Dulbecco's minimal essential medium (DMEM), Fetal bovineserum (FBS) (sterile-filtered, South American origin), Fibroblast growth factor (FGF) (Gibco), Epidermal growth factor (EGF) (Gibco), N₂ supplement (Gibco), antibiotic- antimycotic (100X) solution were purchased from Invitrogen. Tissue array with 59 spots of different normal and cancerous colon tissue types from Imgenex,

India; RNeasy kit from Qiagen; IHC kit from BioGenex, Primers from IDT was purchased. *Abrus* agglutinin was purified as described in chapter 3 of this thesis.

6.2.2 Antibodies

LC3 (NB100-2220) was purchased from Novus Biological (Littleton, CO); BMP2 (ab14933-46), CK7 (ab9021), CK20 (ab76126) from abcam; CD44 (21810441) from Immunotools (Germany); β -actin (A2066) from Sigma; ATG5 (2630S), BECN1 (3738S), β -Catenin (#9562), were purchased from Cell Signaling Technology, USA. hVps34 (38-2100) was purchased from Invitrogen (Carlsbad, California, USA).

6.2.3 Cell and Sphere Culture

HT-29, a Human colorectal cancer cell line was purchased from the National Centre for Cell Science, Pune, India. HT-29 cells were maintained in Dulbecco's modified Eagle medium (DMEM) supplemented with 10% heat inactivated fetal bovine serum (FBS) containing 1X antibiotic-antimitotic at 37°C in a humidified 95% air and 5% CO₂.

For sphere formation, HT-29 cells were seeded at 5000 cells per well in ultralow attachment plates in serum-free DMEM media in the presence of fibroblast growth factor (FGF; 20 ng/mL), epidermal growth factor (EGF; 20 ng/mL), and 1% N₂ supplemented with 1% penicillin-streptomycin. It was maintained at 37°C temperature in a humidified 5% CO₂ incubator and media was replaced every 3 days. After 10-12 days of culture, cells were multiplied to form floating single cell cloned spheres, known as colonospheres in colon and/or CRC cells. The colonospheres were treated with AGG for 3 days and analyzed for different assays. For differentiation study, the AGG treated colonospheres were cultured in presence of serum for another 3 days.

6.2.4 Immunofluorescence Staining of Colonospheres Confocal Imaging

Colonosphere were grown on chamber slides fixed in 10% formaldehyde, washed with PBS, permeabilized with 0.2% Triton X-100 for 20 min at RT and incubated overnight with primary antibody CD44, β -Catenin, CK7 and CK20. Then the cells were washed with PBS and incubated with secondary antibody for 6 h followed by DAPI counterstaining. The expression of those marker proteins was analyzed by a confocal laser microscope (Leica TCS SP8).

6.2.5 RNA Extraction and Semiquantitative RT-PCR

Total RNA from spheres of HT-29 cells were harvested by using a RNeasy kit from Qiagen following manufacturer's instruction. The cDNA was synthesized using total RNA with reverse transcriptase enzyme using manufacturers' instruction. RT-PCR was used to study the expression of mRNA for CD44, CK7, CK20 and GAPDH (internal control). The

respective primers (Sigma) and conditions were as follows: for CD44, forward 5'-AGATCAGTCACAGACCTGCC-3' and reverse 5'-GCAAAGTCAAGCCAAGCC-3' (annealing at 56.5°C, 35 cycles); for CK7 forward 5'-TGAATGATGAGATCAACTTCCTCA-3' and reverse 5'-TGTCGGAGATCTGGGACTGC-3' (annealing at 54.5°C, 35 cycles); CK20 forward 5'-CAGACACACGGTGAAGTATGG-3' and reverse 5'-GATCAGCTTCCACTGTTAGAC-3' (annealing at 55.5°C, 35 cycles); for GAPDH, sense 5'-CAC AAT GCC GAA GTG GTC GT-3' and antisense 5'-TCA CCA TCT TCC AGG AGC GA-3' (annealing at 62°C, 35 cycles). Amplified products were separated by electrophoresis on 1.5 % agarose gel and visualized using gel document system (BioRad) after ethidium bromide staining.

6.2.6 Western Blot Analysis

Spheres from HT-29 cells were treated with different concentration of AGG followed by extraction of proteins. Cells were lysed with lysis buffer and an equal amount of proteins were resolved by SDS/PAGE, transferred to nitrocellulose membrane, which was blocked with 5 % BSA (in PBST) at room temperature for 1 h. Subsequently, the blots were incubated with anti-BECN1, ATG5, p62, β -catenin, BMP2, hVps34 and LC3 antibodies for overnight at 4°C followed by corresponding secondary antibodies for 1 h at room temperature. The expression of the protein of interest was analyzed using chemiluminescence Image Quant LAS500 (GE Healthcare, USA).

6.2.7 Alkaline Phosphatase Assay

To detect the differentiation capacity of AGG, HT-29 colonospheres were treated with 3-MA (10 mM) for 2 h prior to AGG treatment. The treated cells were lysed and equal amount of protein mixed with reaction buffer followed by pNPP solution and equilibrated at 37°C. The absorbance was recorded at 450 nm immediately.

6.2.8 Colocalization Study by Immunofluorescence Analysis

HT-29 cells were treated with various 100 ng/ml AGG for 72 h followed by fixation with 10 % formaldehyde. Cell permeabilization was done in 0.1 % Triton X 100 which followed to blocking in 5 % BSA. Following this, cells were incubated with primary antibodies BMP2 (1:500) and hVps34 (1:500). Following washing in PBST, cells were incubated with secondary antibodies conjugated with the Alexa Flour. Imaging was done using high-end fluorescence inverted microscope (Olympus IX71) using Cell Sens Standard software. Colocalization was measured applying JACoP plugin in single Z-stack sections of deconvoluted images.

6.2.9 In Vivo Mice Experiment

To study the therapeutic potential of AGG in human colon carcinoma, athymic balb/c nude mice were implanted with colon carcinoma HT-29 cells (2×10^6 cells) subcutaneously. The tumors were first propagated and subsequently implanted in experimental animals. By this way, tumor induction rate is 90-100 %. When tumors have reached 0.2 cm in diameter the actual therapeutic study was initiated. The mice were administrated intraperitoneally either vehicle control (1X PBS) or AGG 5 μ g/kg body weight and positive control 5-fluorouracil 30 mg/kg b.w. i.p 5 times a week for 4 weeks. The tumor volume and body weight of the mice was measured at the end of every week, for 4 weeks. On completion of the treatment period, tumors diameter was measured. The tumor volume was calculated using the formula $[L \times W^2]/2$, where W and L are the width (short diameter) and the length (long diameter) of the tumor. At the end of treatment period, all the mice were euthanized using carbon-dioxide followed by cervical dislocation to ensure complete immobilization of mice prior to collecting tumor tissues samples for biochemical and histological analysis.

6.2.10 Immunohistochemical Staining and Scoring

For the immunohistochemical study, formalin-fixed and paraffin-embedded specimens of 3–4 mm thickness were sectioned. The tissue sections were stained with anti-BMP2, anti- β -catenin and LC3 as described previously. Immunohistochemical analysis was done by determining the percentage of positive cells by counting the number of positively stained cells (weak, moderate and strong) and the total number of cells from control and treated samples at 40X magnification. IHC score was analyzed for control and treated as 0+ (no staining), 1+ (weak staining), 2+ (moderate staining), 3+ (strong staining), 4+ (very strong staining).

6.2.11 Statistical Analysis

All data are representative of at least five independent experiments which were quantified and plotted as the mean \pm standard deviation. Student's t test was used for evaluating statistical differences between experimental groups. Further, a nonparametric test for statistical analysis among groups was also done by a one-way ANOVA Kruskal-Wallis test, with Dunn's multiple group comparison tests as appropriate.

6.3. Results

6.3.1 Expression of BMP2 and β -Catenin in Colorectal Cancer and Non-Cancer Tissue Samples

Colorectal cancer undergoes continual regeneration which is sustained by cancer stem cells. Bone morphogenetic protein 2 (BMP2) shows its tumor suppressive function by inhibiting

tumor initiating ability of renal cancer stem cells (CSCs). Here, we analyzed the expression of BMP2 and β -catenin in human normal, cancer and metastatic tissue samples through immunohistochemical analysis. The clinicopathological representation of the cohort is given in Table.6.1. We found that there was a decrease in the expression of BMP2 as the tumor progresses suggesting BMP2 as a tumor suppressor (Fig. 6.1.a). Likewise, the stemness and self-renewal protein β -catenin expression increased as the colon cancer progresses from normal to cancerous to metastatic stages (Fig.6.1.b). From the immunoreactive score, it is evident that the expression of BMP2 and β -catenin decreased and increased during the onset of cancer and progression through stage I to metastasis respectively (Fig.6.1c,d).

6.3.2 AGG Inhibits HT-29 Colonospheres Formation

AGG, a type II RIP lectin is previously reported to have many anticancer attributes including the induction of programmed cell death apoptosis and autophagy. However, there is little in-depth in the study its effects on cancer stem cells. In order to investigate the effect of AGG in attenuating growth of colonospheres, we treated the HT-29 derived colonospheres in different doses (10, 50, and 100 ng/ml) for 72 h and for different time intervals (24, 48 and 72 h) with 100 ng/ml and examined the number and size of the sphere produced in respective well. We noticed a significant decrease in the number of colonospheres in a dose as well as time dependent manner. Further, the sphere size reduced remarkably with an increase in dose and time (Fig. 6.2.a-d).

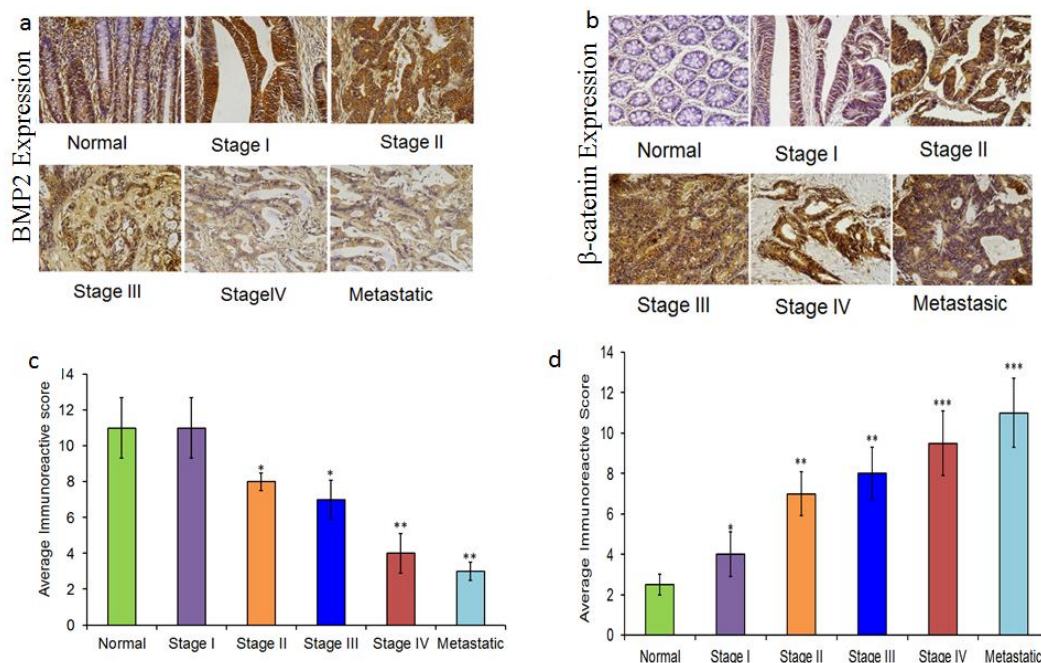


Fig. 6.1. Expression of BMP2 and β -catenin in human colorectal cancer and non-cancer tissue samples. Slide shows representative images of BMP2 (a) and β -catenin (b) staining in normal colon tissue and different grades of colon cancer tissues. The average immunoreactive score was calculated from percentage of positive cells and staining intensity for different tissue samples (c,d). * P value < 0.05; ** P value < 0.01; *** P value < 0.001 were considered significant as compared with control.

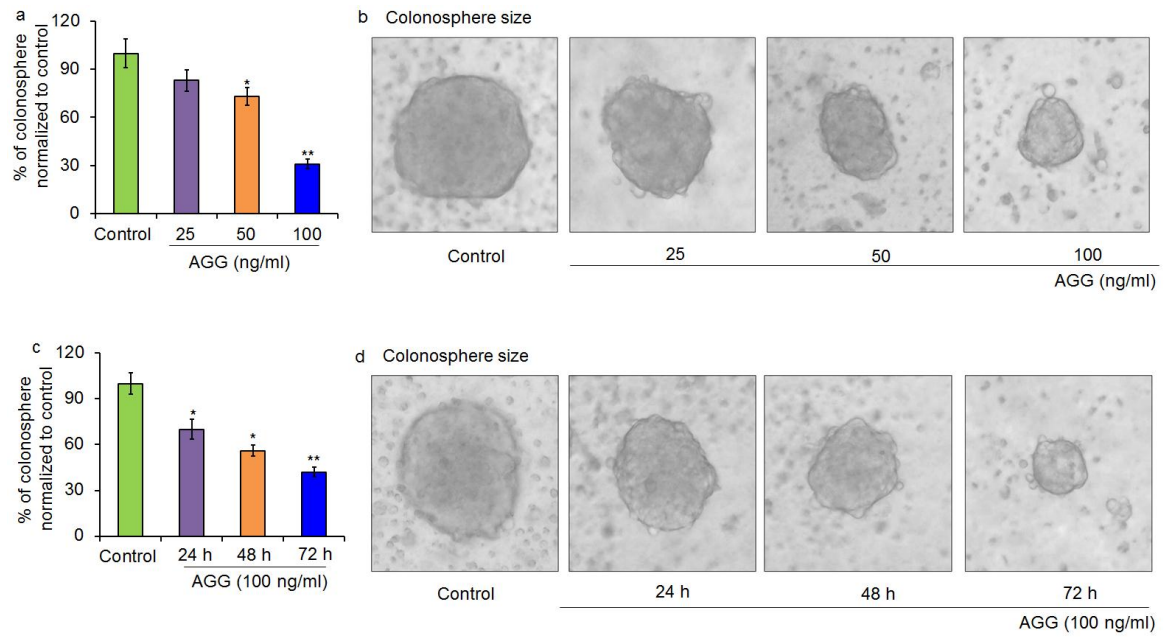


Fig.6.2. AGG inhibited formation of HT-29 colonospheres. The colonosphere were treated with different concentration of AGG (25, 50 and 100 ng) for 72 h and at for different time interval (24, 48 and 72 h) at 100 ng/ml, the colonospheres were photographed and quantified for its number and size (a-d). Data reported as the mean \pm S.D. of three independent experiments and compared to control. * P value < 0.05 ; ** P value < 0.01 were considered significant as compared with control.

Table.1 Clinicopathological representation of the cohort

Variables	Categories	Cases (n=59)	%
Age (Median age 68 year)	≤ 58 years	32	54.23
	>58 years	26	40
	NA	1	0.01
Sex	Male	42	71.1
	Female	17	28.8
Site of cancer	Ascending Colon	6	10
	Transverse colon	3	5
	Descending colon	4	6
	Caecum	2	3
	Sigmoid colon	11	19
	Rectum	14	24
Normal		9	15
Metastatic		10	17
Tumor Differentiation	Well	14	24
	Moderate	23	40
	Poor	3	5
Tumor Stage	Stage I	2	3
	Stage II	12	20
	Stage III	14	23
	Stage IV	12	20
pT	T2	3	5
	T3	3	5
	T4	35	59
pN	N0	15	25
	N1	11	19
	N2	12	20
pM	M0	28	47
	M1	12	20

6.3.3 AGG Inhibits Stemness and Induces Differentiation in Colonospheres

As we saw a sharp decline in the colonosphere formation, we next sought to investigate how AGG is responsible for the inhibition of colonosphere growth for which we analysed the expression of two important molecules responsible for stem properties i.e. CD44, a CSC surface marker and β -catenin, a self-renewal marker. As expected, we found a significant reduction in the expression of CD44 (Fig.6.3.a) and β -catenin (Fig.6.3.b) in HT-29 colonosphere in dose dependent manner.

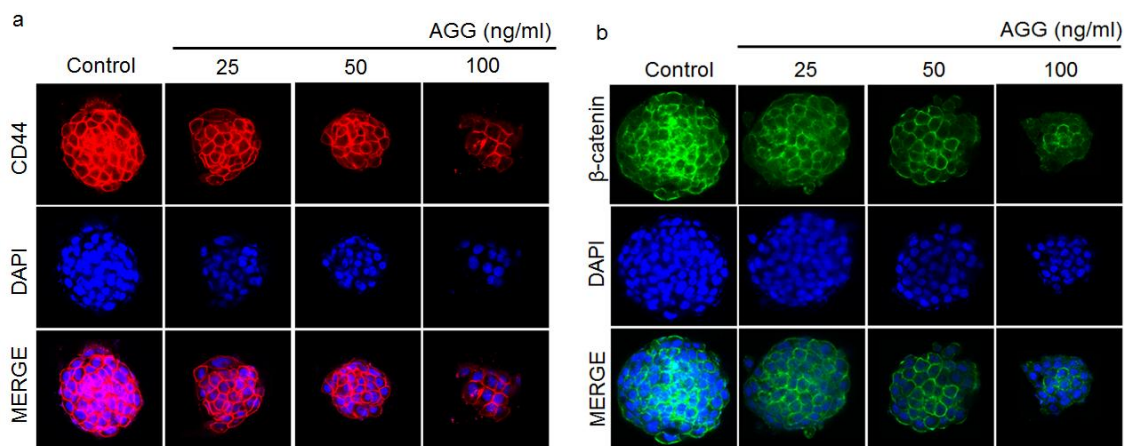


Fig.6.3. AGG inhibits the stemness and preferentially targets self-renewal potential in colonospheres. Colonospheres were treated with different concentration (25, 50 and 100 ng/ml) of AGG for 72 h and expression of stemness surface marker CD44 (a) and self-renewal marker β -catenin (b) was analyzed through confocal microscopy. Data reported as three independent experiments and compared against control.

By virtue of its enhanced resistance to cytotoxic therapies, CSCs are resilient to current therapeutics for which specific targeting of CSCs has become the need of the hour. In view of that, differentiation therapy is being explored for specific killing of CSCs. So, we investigated the differentiation inducing ability of AGG. We checked the expression of differentiation markers CK7 and CK20 in AGG insulted colon spheres. Interestingly, the expression of CK7 and CK20 (Fig.6.4.a) decreased as well as increased respectively in a dose dependent manner. The increase in the ratio of CK20/CK7 expression indicates increased differentiation in AGG treated groups. Likewise, our RT-PCR data showed that AGG treatment could potentially reduce the relative mRNA expression of CK7 and increased the mRNA level of CK20 (Fig.6.5.a). Further, we analyzed the alkaline phosphatase (AP) activity assay as a measure of differentiation ability and got an appreciable dosewise increase in the AP activity in AGG treated groups (Fig.6.5.b).

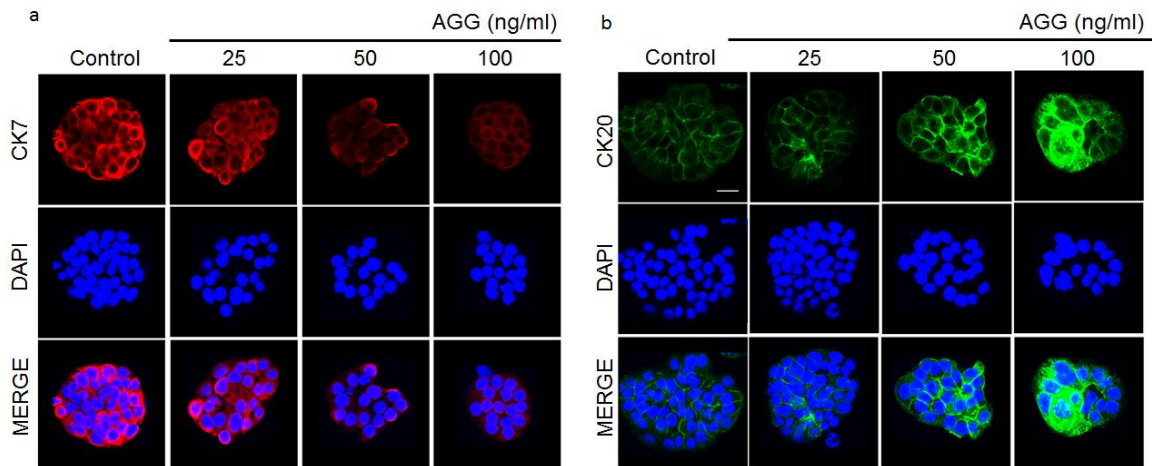


Fig.6.4. AGG induces differentiation in colonosphere. Colonospheres were treated with different concentration (25, 50 and 100 ng/ml) of AGG for 72 h and expression of differentiation marker CK7 (a) and CK20 (b) was analyzed by confocal microscopy. Data reported as three independent experiments and compared against control.

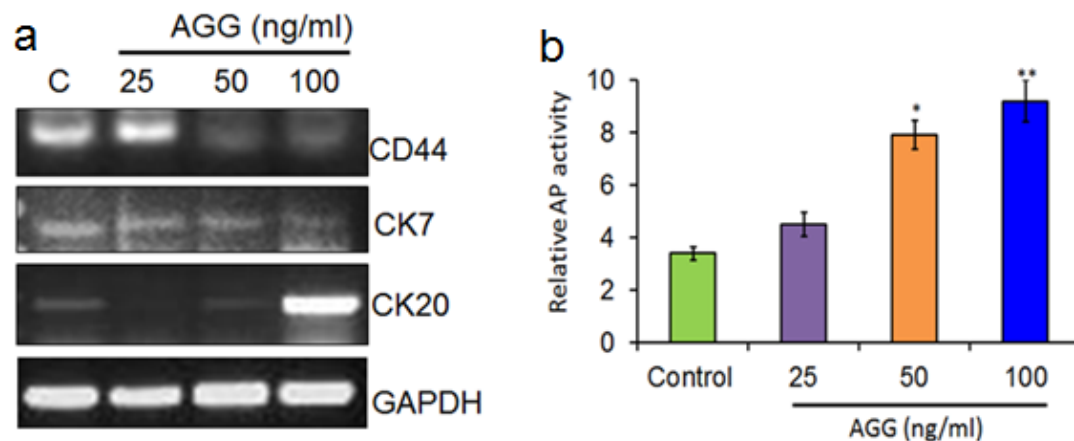


Fig.6.5. Effect of AGG on expression of stemness and differentiation gene and alkaline phosphatase activity in colonospheres. Colonospheres were treated with different concentration (25, 50 and 100 ng/ml) of AGG for 72 h and expression of CD44, CK7 and CK20 was quantified by RT-PCR (a) and alkaline phosphatase activity (b). Data reported as the mean \pm S.D. of three independent experiments and compared to control. * P value < 0.05 ; ** P value < 0.01 were considered significant as compared with control.

6.3.4 AGG Induces Autophagy in HT-29 Colonospheres

Next, we intend to investigate whether AGG induces autophagy in HT-29 derived colonospheres which might regulate AGG elicited differentiation. Colonospheres were treated with different concentration of AGG and analyzed the autophagy induction by western blot. As expected, AGG was also able to effectively induce autophagy at low doses i.e 100 ng/ml. It showed that AGG could increase LC3-II accumulation in dose dependent manner suggesting AGG mediated autophagy induction. Further, the autophagic molecules including BECN1, ATG5, hVps34 were increased in presence of AGG in colonospheres. Likely, we found that the expression of p62, selective adaptor for autophagic clearance was decreased in dose dependent manner conforming AGG induces autophagy in colonospheres.

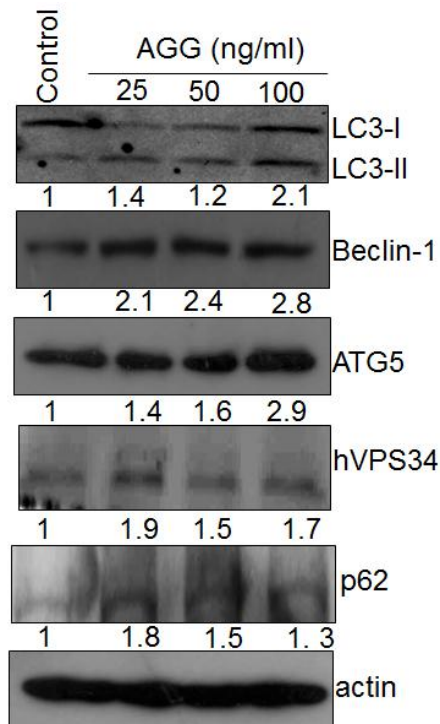


Fig.6.6. AGG induces autophagy in HT-29 colonospheres. Colonospheres were treated with different concentration of AGG for 72 h and expression of autophagic proteins were analyzed by Western blot. Data reported as three independent experiments and compared against control Densitometry was performed on the original blots, considering the ratio of protein to actin in control cells was 1.

6.3.5 AGG Promotes BMP2 Expression in Colonospheres

Bone morphogenetic proteins (BMPs) elicit a plethora of actions and regulate different cellular processes including autophagy and differentiation. Moreover, previous data also showed that BMP2 acts as a tumor suppressor protein in colon cancer. These findings led us to investigate its implications in AGG mediated CSCs inhibition and surprisingly we observed that there was a steep increase in the expression of BMP2 with an increase in AGG doses in colonospheres as demonstrated in western blot and confocal microscopy suggesting the potential role of BMP2 in AGG modulated cellular processes (Fig. 6.. a, b).

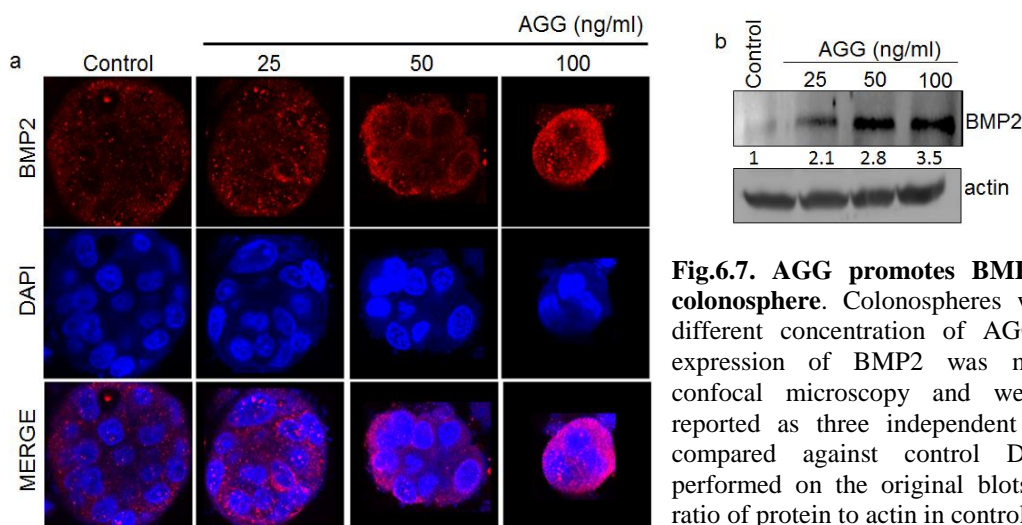


Fig.6.7. AGG promotes BMP2 expression in colonosphere. Colonospheres were treated with different concentration of AGG for 72 h and expression of BMP2 was measured through confocal microscopy and western blot. Data reported as three independent experiments and compared against control Densitometry was performed on the original blots, considering the ratio of protein to actin in control cells was 1.

6.3.6 Role of Autophagy in AGG Induced Differentiation In Colonospheres

Earlier findings suggested the internalization of BMP2 to late endosomal vesicles that might take part in autophagosome biogenesis. Besides, it is documented that hVps34 is essential for the formation of internal vesicles within multivesicular bodies. Based on this reports, we tried to investigate whether and how AGG induced autophagy is related to BMP2. Analyzing the spatial distribution of BMP2 and hVps34 by performing double immunofluorescence analysis using confocal microscopy, we observed that the two concerned proteins visibly overlap to show a dense yellow signal in the merged image (Fig.6.8), which depicted a total overlap coefficient and Pearson's coefficient of 0.87 and 0.83, respectively, in the cytofluorogram scatter plot. Next, we examined the role of autophagy in the inhibition of self-renewal potential with AGG treatment. It is reported that self-renewal protein β -catenin is degraded independent of proteasomal degradation via the lysosomal degradation pathway. In this context, we examined the expression of β -catenin in presence of 3-Methyladenine (3-MA), an inhibitor of hVps34 activity. We found that AGG was not able to inhibit the expression of β -catenin in presence of 3-MA suggesting that AGG mediated inhibition of colonosphere is dependent on autophagic degradation of β -catenin that hinders the self-renewing ability of colonospheres (Fig. 6.9.a). Further, the differentiation activity of AGG was studied in presence of 3-MA. The decrease in the AP activity in 3-MA and AGG treated colonospheres as compared to only AGG treated (Fig.6.9.b) indicates that autophagy is essential for AGG induced differentiation of colonospheres (Fig.6.9.c).

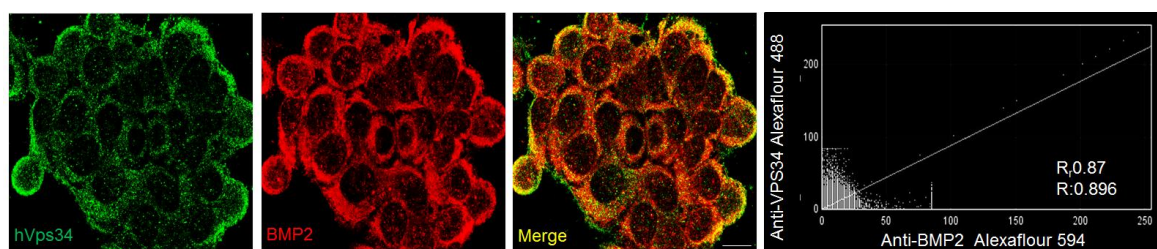


Figure 6.8. Interaction of BMP-2 and hVps34. The interaction of BMP2 (Red) and h Vps34 (Green) was analyzed in confocal microscope after 72 h of AGG (100 ng/ml) treatment. The colocalization parameters were analyzed by using JaCoP plugin in Image J software.

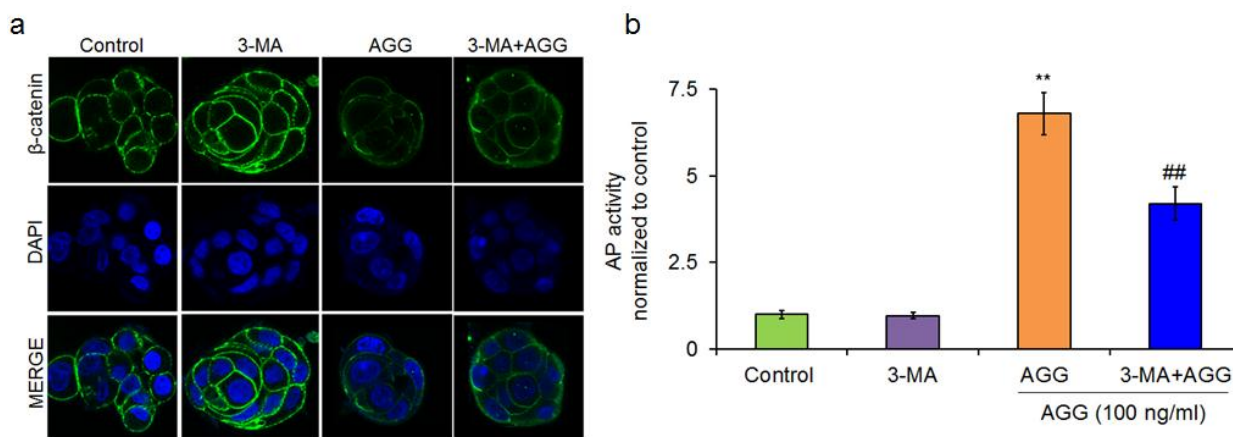


Fig.6.9. Effect of AGG induced autophagy colonosphere differentiation. Colonospheres were treated with AGG (100 ng/ml) in presence of 3-MA (10 mM; 2 h) for 72 h and expression of β -catenin through confocal microscopy (a) and alkaline phosphatase activity was quantified in colonospheres (b). *represents a statistically significant change in comparison to Control (** $P < 0.01$) and # represents a statistically significant change as compared to AGG treated group (## $P < 0.01$).

6.3.7 AGG Induced Differentiation Potential in Mouse Xenograft Model

The *in vivo* study showed that the tumor burden in control and AGG treated animals for 4 weeks significantly reduced the tumor growth by the end of 3rd and 4th week in AGG treated mice. It was also noted that there was no significant loss of body weight in AGG (5 μ g/kg body weight) treated mice compared to control mice (Fig.6.10.a, b). In addition, AGG at the dose level of 5 μ g/kg body weight was found well tolerated by the mice, while in the 5-fluorouracil treated group, three mice died in this group on the 4th week of treatment. Though there was no significant difference between the total body weights, there was a significant reduction of tumor volume from $201 \pm 31.5 \text{ mm}^3$ to $50.4 \pm 23.7 \text{ mm}^3$ at the end of 4th week. Overall, AGG produced significant anti-tumor activity in a colon carcinoma xenograft mouse model. The tumor tissues were subjected to immunohistochemistry for BMP2 and autophagy marker LC3. In the xenograft, the AGG treated group showed a significant increasing in the expression of BMP2 and LC3 staining compared to the control (Fig.6.10.c).

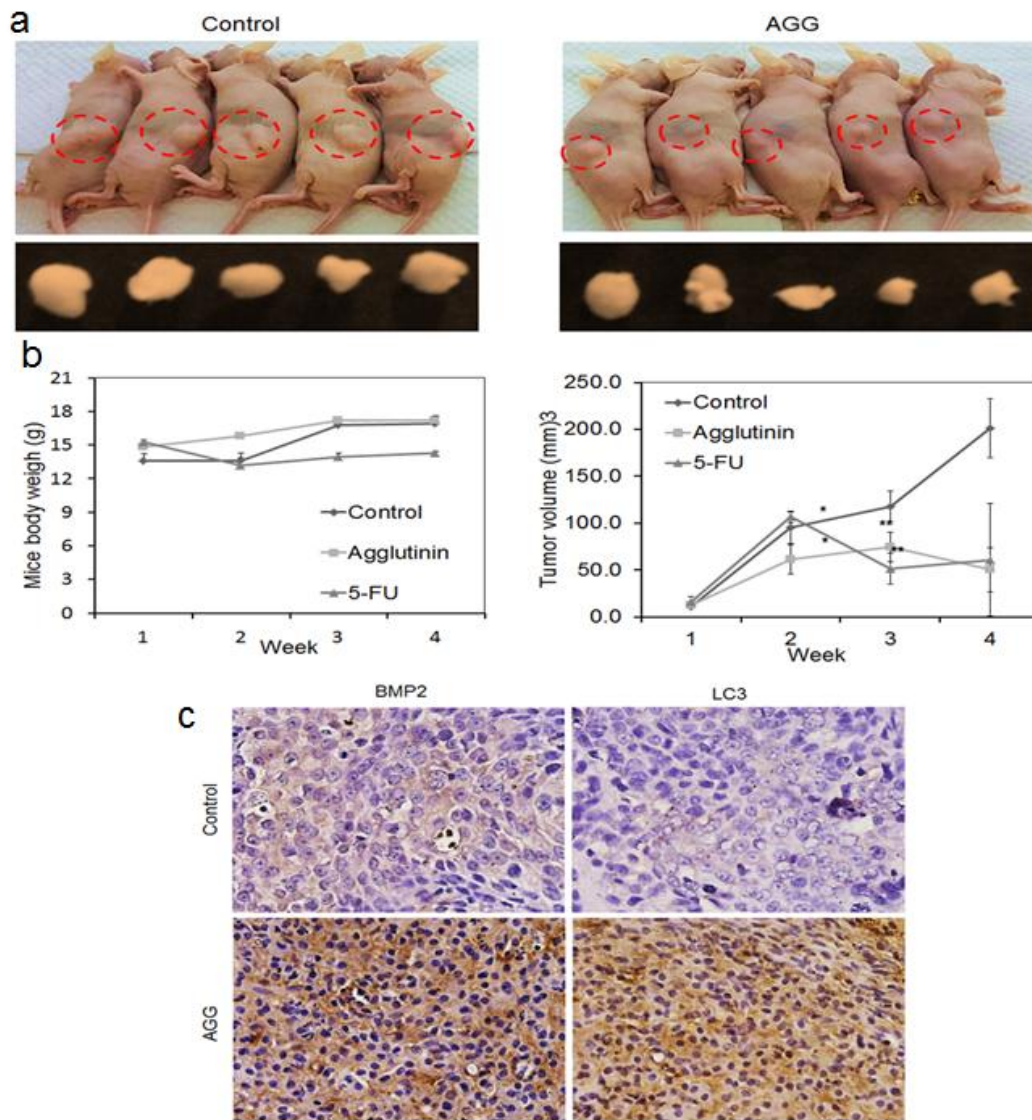


Fig.6.10. AGG elicits the expression of BMP2 and LC3 in HT-29 xenograft tissue. HT-29 cells were subcutaneously injected (5×10^6 cells/mouse) to each mouse. The mice in control group were treated with normal saline (0.9%) and in the treatment group with intraperitoneal AGG at a dose of $5 \mu\text{g}/\text{kg}$ body weight. Tumor weight and tumor volume were plotted in the form of histogram and graph (a,b). Tumor tissues were harvested followed by fixation with formalin and paraffin-embedded sections were immunostained for BMP2 and LC3 in control and treated groups (c).

6.4. Discussion

Despite the development of new targeted therapeutic modalities, none of the treatment options available is satisfactorily successful in patients with advanced colorectal cancer due to the subsistence of colorectal cancer stem cells (Vaiopoulos et al., 2012). Substantial reports reveal that during cancer treatment some of the nonkilled residual tumor cells may acquire stemness property. Moreover, it is hypothesized that drugs that target bulk tumor cells can result in considerable tumor reduction but ultimately leads to CSC enrichment due to the inability to kill therapeutic resistant CSCs (Naik et al., 2016). Based on above perspectives, nonlethal agents with anti-CSC potential would be a coherent attempt for CRC

prevention and treatment. One of the latest hopes in specific targeting of cancer stem cell is the pristine differentiation therapy. Differentiation therapy is focused on restoring the endogenous differentiation programs in leading to the terminal maturation of cancer stem cells making it available to be targeted by routine therapeutic approach (Sell, 2004). Hence, we selected low doses of plant lectin AGG (Max. of 100 ng/ml) as one such investigational drug, because our recent studies have shown that it causes strong anticancer efficacy through acute programmed cell death in cancer cells. The present investigation focusses on the differentiation inducing ability of AGG at a nontoxic dose for its promising candidature a suitable anticancer agent against cancer stem cells. Moreover, we have shown that AGG induced BMP2 activation and autophagy mediated β -catenin degradation is responsible for the differentiation of colonospheres. The autophagy regulatory molecule Class III phosphatidylinositol-3 kinase, hVps34 was found to interact with BMP2 suggesting its potential involvement in autophagy regulation.

According to report, while the typically activated Wnt/ β -catenin pathway exerts a significant influence in the initiating CRC development, abrupt of BMP pathway was shown to induce juvenile polyposis syndrome again suggesting the potential role BMP signaling in CRC progression (Zhang et al., 2014). Similarly, we found that the expression of BMP2 decreased during tumor progression, on the contrary, the expression of β -catenin increased. Using CSC enriched population of CRC cells; we have demonstrated that AGG has an efficient inhibitory effect on both number and size of colonospheres. Since the formation of colonospheres is a measure of stemness, our results provide the evidence portraying AGG as a promising agent to target the self-renewal of CSC as well as bulk tumor cells in CRC. Moreover, the expression of BMP2 increased in colonosphere with AGG treatment. Moreover, corresponding to the report of Kumar et al., 2016, AGG was shown to promote the decrease of self-renewal properties through the downregulation of CD44 and β -catenin and increase in the CK20/CK7 ratio indicating increased differentiation. More importantly, intestinal stem cells are brought to terminally differentiate in the deficiency of Wnt- β -catenin signaling subsequent in a shortfall of basic intestinal function (Fevr et al., 2007). Again, loss of β -catenin was shown to impair the self-renewal of normal and chronic myelogenous leukemia stem cells *in vivo* (Zhao et al., 2007). Interestingly, recent report describes that β -catenin is selectively degraded via autophagy through the formation of a β -catenin-LC3 complex, attenuating the adaptation during metabolic stress (Petherick et al., 2013). Moreover, operational autophagy and low β -Catenin levels are documented to be indispensable during differentiation. Consistent to this, a high β -Catenin level was shown to

inhibit autophagy and stabilize the proliferation ensuing low differentiation ability in acute myeloid leukemia (Kühn et al., 2015). Correspondingly, we have shown that *Abrus* agglutinin was shown to decrease β -catenin content. This decrease in β -catenin content is autophagy mediated degradation of the same as 3-MA treatment reduces the expression of β -catenin as compared to only treated groups.

BMP signaling plays a master role in various stages of development and organ homeostasis. BMP2 in particular, are known to promote differentiation and growth inhibition in glioblastoma cells. For this reason, we investigated whether a AGG based treatment would increase BMP2 response in drug resistant colon cancer cells. Here we show that BMP2 was induced strongly in colon cancer initiating cells and subsequent addition of AGG caused a dramatic increase of BMP2 expression and tumor size reduction. Previously, it is reported that BMP2 induces osteogenic differentiation of rat bone marrow-derived mesenchymal stem cells (Hanada et al., 1997). Recently, it is also reported that BMP2 is induced differentiation involves autophagy protein Atg7 in human stem cell derived osteoblastic cells (Ozeki et al., 2016). Substantial studies have elaborated the participation of autophagy in the cellular differentiation. Genetic knockout studies of ATG genes in lower eukaryotes was reported to play a vital role in the autophagy regulated differentiation and development (Mizushima et al., 2010). Also, it documented that stimulation of autophagy encourages differentiation of glioma-initiating cells and their radiosensitivity (Zhuang et al., 2011). Likely, here we have shown that AGG effectively, induces autophagy at lower doses of AGG (25, 50 and 100 ng/ml) and inhibition of autophagy by autophagy inhibitor 3-MA reduces the differentiation induced by AGG as confirmed by alkaline phosphatase assay. Concomitant with our result, Zhuang et al., 2012 reported that curcumin elevates differentiation of glioma-initiating cells by stimulating autophagy. Earlier findings indicated that internalization of BMP2 to late endosomal vesicles takes place following receptor dependent clathrin mediated endocytosis. However, significantly degradation of BMP2 was not found after its internalization to late endosomal vesicles which may provide a reservoir for BMP2 for participating in other cellular functions (Alborzinia et al., 2013). The report says that inhibition of clathrin mediated endocytosis halted autophagosome biogenesis. Therefore, remnant BMP2 associated with endosomal vesicles may take part in autophagosome biogenesis. Besides that hVps34 is essential for the formation of internal vesicles within multivesicular bodies (Futter et al., 2001; Obara et al., 2008). Interestingly, in the current investigation, we have noticed significant colocalization of BMP2 and hVps34, depicting its combined probable role for phagophore formation. In conclusion, AGG induced BMP2 regulates differentiation of colon cancer stem cells through autophagic

degradation of β -catenin in colorectal carcinoma promising its candidature as a suitable differentiation agent in cancer therapeutics.

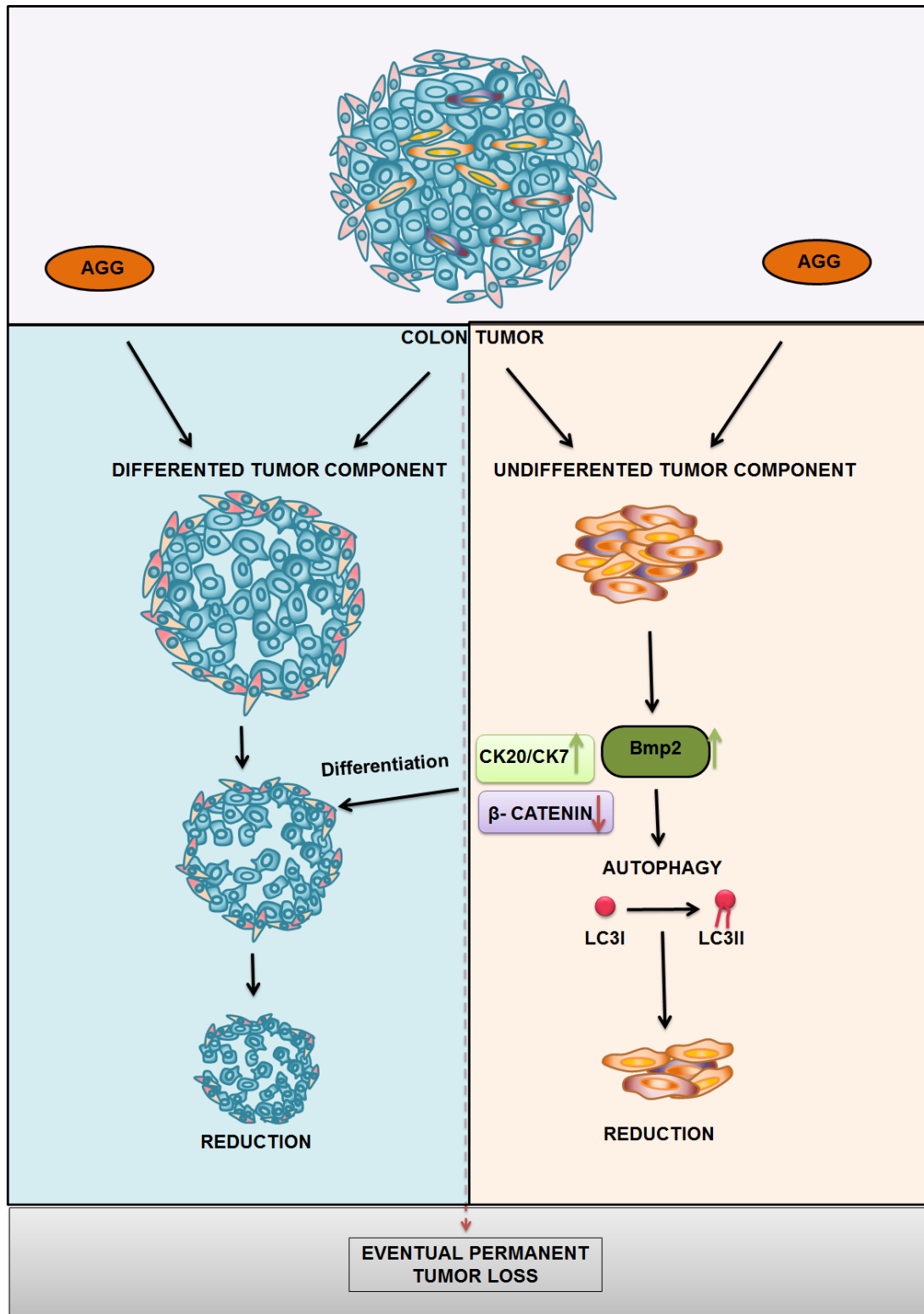


Fig. 6.11. Schematic representation of BMP2 mediated autophagy induces differentiation.

Chapter 7

Summary and Conclusions

7.1. Summary

Autophagy is a conserved catabolic process which plays a very significant role in several patho-physiological conditions including cancer. It is an extremely discussed concept in the field of translational cancer research by virtue of its Janus role. The pro-survival and pro-death autophagy governs the fate of cancer related events like tumorigenesis, invasion, metastasis and necrosis. The pro-death function of autophagy helps in killing cancer cells, either spontaneously or when they are exposed to radiation and chemotherapy. However, Autophagy, as a tumor suppressor, can lead to stress tolerance which allows tumour cells to thrive under adverse conditions like nutrient starvation, hypoxia and chemo-radio-therapeutics. On the other hand, autophagy provides a survival advantage to detached, dormant metastatic cells through nutrient fueling by tumour associated stromal cells. Manipulating autophagy for induction of cell death, inhibition of protective autophagy at tissue-and context-dependent for apoptosis modulation has noteworthy therapeutic implications.

Our group has reported the antitumor and immunomodulatory activity of phytolectin AGG in both *in vitro* and *in vivo* system. AGG induces both intrinsic and extrinsic apoptosis through ROS dependent manner. However, AGG in the field of autophagy is little explored. With this background support, the goals of the present investigation were set up to investigate the (a) Role of *Abrus* agglutinin in inhibiting the Akt/PH domain to induce endoplasmic reticulum stress mediated autophagy dependent cell death (b) Mechanism of PUMA dependent mitophagy by *Abrus* agglutinin in inducing apoptosis through ceramide generation (c) SIRT1/LAMP1 signalling activation by *Abrus* agglutinin in regulation of autophagy mediated senescence and (d) The role of *Abrus* agglutinin in cancer stem cell differentiation through BMP2 mediated autophagy.

In this thesis, we documented that AGG mediated Akt dephosphorylation led to ER stress resulting in the induction of autophagy dependent cell death through the canonical pathway in cervical cancer cells. We found that AGG induced ER stress in PERK dependent pathway. Moreover, the *in silico* study emphasized that AGG interacted with pleckstrin homology (PH) domain of Akt to suppress its phosphorylation and consequent downstream mTOR dephosphorylation in cervical cancer cells. We also established that Akt modulation is the upstream signal during AGG's ER stress mediated autophagic cell death. Next, we monitored the mitophagy inducing potential of AGG via PUMA activation in glioblastoma. Surprisingly, we identified AGG induced ceramide as a chief mediator of mitophagy dependent cell death through activation of mitochondrial ROS and ER stress. At the

molecular level, we identified an LC3 interacting region (LIR) at the C-terminal end of PUMA which interacts with LC3 to induce mitophagy. AGG was also shown to trigger PUMA mediated mitophagy via both in p62 dependent and independent manner. More interestingly, the study reflected that mitophagy induced by AGG finally switched to apoptosis. Further, we monitored senescence inducing potential of AGG in prostate cancer. Notably, for the first time, our group reported accelerated expression of SIRT1 in AGG treated cells is associated with cellular senescence. Besides, we have documented SIRT1 facilitated LAMP1 deacetylation in response to AGG insult to promote autophagy. The present study suggests that SIRT1 mediated deacetylation of LAMP1 may be a breakthrough in autophagy machinery. In the last objective, we showed that AGG was strikingly able to induce colon CSC differentiation *in vitro* by inducing a member of TGF- β superfamily Bone Morphogenetic Protein 2 (BMP2). Further, AGG induced differentiation was discovered to be critically dependent on autophagy. Furthermore, our study established a significant interaction of BMP2 with hVPS34, a class III PI 3-Kinase (involved in phagopore formation and elongation) suggesting a probable involvement of BMP2 in the early events of autophagic process.

7.2. Scope of the Present Investigations

The present investigation depicts AGG induced autophagy as a promising mean for anticancer phytotherapeutics. The study also involves the molecular dynamics that interplay during AGG induced autophagy, mitophagy or lipophagy leading to either autophagic cell death, apoptosis or senescence. Our investigation obviously explains how AGG binding at the Akt PH domain is responsible for its dephosphorylation and lead to ER stress mediated autophagic cell death. However, this study further demands to identify potential Akt inhibitor from peptides A chain of AGG by exploring AGG-Akt-PH domain interaction for the development of novel anticancer peptide for different types of cancer. In the second objective, we confirmed PUMA as a master regulator of mitophagy as we identified an LIR (LC3 interacting region) in its C-terminal domain which is a primary requisite to be an autophagy adaptor. This study further requires investigating whether the inability to undergo mitophagy in diseases such as Molecular dystrophy, Parkinson's disease, Alzheimer's disease and cancer is due to any mutation in LIR domain of PUMA. This study also demands to elucidate the status of PUMA-LIR mutant in human cancer patients. Furthermore, we can investigate PUMA-LIR mutated mice as an *in vivo* disease model that establishes a significant contribution in the field of physiology and medicine. Moreover, we investigated AGG induced autophagy mediated senescence as a promising approach in

inducing cytostasis in cancer cells. Here we identified a novel mechanism in which AGG was shown to promote SIRT1 mediated deacetylation of LAMP1 that promotes autophagy. In the future, it will be of great impact to unravel the intricate mechanism how the deacetylation of LAMP1 contributes to the process of autophagy. Lastly, we vividly discussed how AGG induced BMP2 upregulation is responsible for inducing differentiation in both CSC model and *in vivo* mice model. The key finding that BMP2 significantly interact with hVps34, an enzyme involved in the formation of autophagosome necessitates further detailing of how this interaction is regulating the autophagosome biogenesis. Lastly, it concluded that investigations in the field of autophagy as an alternative approach by phytotherapeutics will broaden the arena of opportunities for the betterment of overall cancer patient survival rates in the coming years. In this context, AGG will serve as a magic bullet.

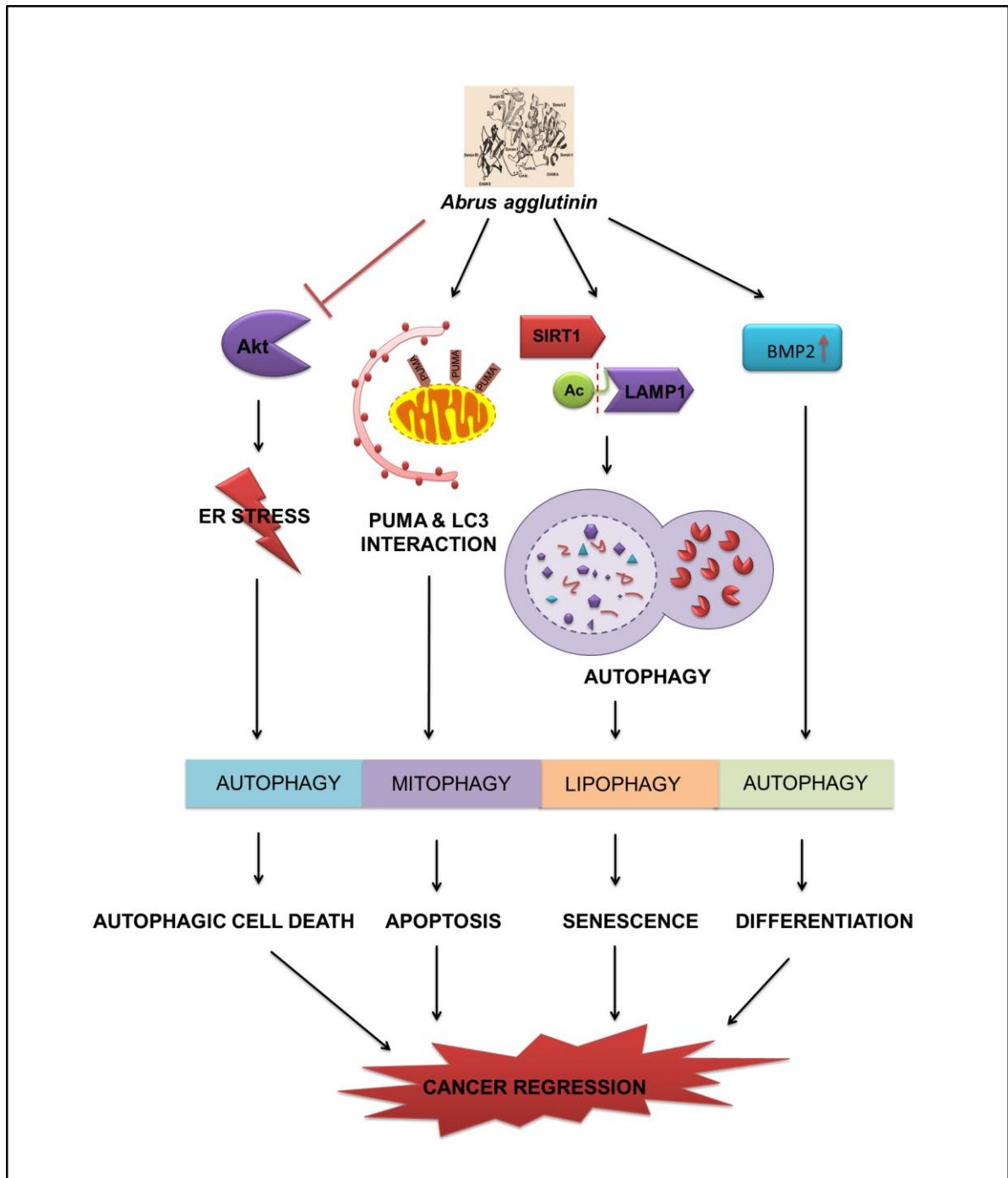


Fig.7.1. Schematic presentation of the present PhD thesis. AGG induces Akt dephosphorylation led to ER stress mediated autophagic cell death. Proapoptotic protein PUMA is the master regulator of AGG prompted mitophagy. AGG induced lipophagy modulates senescence. AGG induced autophagy regulates cancer stem cells differentiation.

References

- Aguirre-Ghiso JA. The problem of cancer dormancy: understanding the basic mechanisms and identifying therapeutic opportunities. *Cell Cycle* 2006; 5:1740–1743.
- Ajabnoor GM, Crook T, Coley HM. Paclitaxel resistance is associated with switch from apoptotic to autophagic cell death in MCF-7 breast cancer cells. *Cell Death Dis* 2012; 3:e260.
- Alborzinia H, Schmidt-Glenewinkel H, Ilkavets I, Breitkopf-Heinlein K, Cheng X, Hortschansky P, Dooley S, Wöfl S. Quantitative kinetics analysis of BMP2 uptake into cells and its modulation by BMP antagonists. *J Cell Sci* 2013; 126: 117–127.
- Ashrafi G, Schwarz TL. The pathways of mitophagy for quality control and clearance of mitochondria. *Cell Death & Differentiation* 2013; 20: 31–42.
- Astle MV, Hannan KM, Ng PY, Lee RS, George AJ, Hsu AK, Haupt Y, Hannan RD, Pearson RB. AKT induces senescence in human cells via mTORC1 and p53 in the absence of DNA damage: implications for targeting mTOR during malignancy. *Oncogene* 2012; 31:1949–1962.
- Babiychuk EB, Atanassoff AP, Monastyrskaya K, Brandenberger C, Studer D, Allemann C, Draeger A. The targeting of plasmalemmal ceramide to mitochondria during apoptosis. *PLoS One* 2011; 6:e23706.
- Babiychuk EB, Monastyrskaya K, Draeger A. Fluorescent annexin A1 reveals dynamics of ceramide platforms in living cells. *Traffic* 2008; 9:1757–1775.
- Bagaria A, Surendranath K, Ramagopal UA, Ramakumar S, Karande AA. Structure-function analysis and insights into the reduced toxicity of *Abrus precatorius* agglutinin I in relation to abrin. *J Biol Chem* 2006; 281: 34465–34474.
- B'chir W1, Maurin AC, Carraro V, Averous J, Jousse C, Muranishi Y, Parry L, Stepien G, Fafournoux P, Bruhat A. The eIF2 α /ATF4 pathway is essential for stress-induced autophagy gene expression. *Nucleic Acids Res* 2013; 41:7683–7699.
- Behera B, Mishra D, Roy B, Devi KS, Narayan R, Das J, Ghosh SK, Maiti TK. *Abrus precatorius* agglutinin-derived peptides induce ROS-dependent mitochondrial apoptosis through JNK and Akt/P38/P53 pathways in HeLa cells. *Chem Biol Interact* 2014; 222:97–105.
- Bhutia SK, Behera B, Nandini Das D, Mukhopadhyay S, Sinha N, Panda PK, Naik PP, Patra SK, Mandal M, Sarkar S, Menezes ME, Talukdar S, Maiti TK, Das SK, Sarkar D, Fisher PB. *Abrus* agglutinin is a potent anti-proliferative and anti-angiogenic agent in human breast cancer. *Int J Cancer* 2016; 139:457–466.
- Bhutia SK, Dash R, Das SK, Azab B, Su ZZ, Lee SG, Grant S, Yacoub A, Dent P, Curiel DT, Sarkar D, Fisher PB. Mechanism of autophagy to apoptosis switch triggered in prostate cancer cells by antitumor cytokine melanoma differentiation-associated gene 7/interleukin-24. *Cancer Res* 2010; 70:3667–3676.
- Bhutia SK, Mallick SK, Maiti S, Maiti TK. Antitumor and proapoptotic effect of *Abrus* agglutinin derived peptide in Dalton's lymphoma tumor model. *Chem Biol Interact* 2008; 174:11–18.

Bhutia SK, Mallick SK, Maiti TK. *In vitro* immunostimulatory properties of Abrus lectins derived peptides in tumor bearing mice. *Phytomedicine* 2009; 16:776–782.

Bhutia SK, Mallick SK, Stevens SM, Prokai L, Vishwanatha JK, Maiti TK. Induction of mitochondria-dependent apoptosis by Abrus agglutinin derived peptides in human cervical cancer cell. *Toxicol In Vitro* 2008; 22:344–351.

Bhutia SK, Mukhopadhyay S, Sinha N, Das DN, Panda PK, Patra SK, Maiti TK, Mandal M, Dent P, Wang XY, Das SK, Sarkar D, Fisher PB. Autophagy: cancer's friend or foe? *Advances in cancer research* 2013; 118: 61–95.

Bjørkøy G, Lamark T, Pankiv S, Øvervatn A, Brech A, Johansen T. Monitoring autophagic degradation of p62/SQSTM1. *Methods Enzymol* 2009; 452:181-197.

Borra MT, Smith BC, Denu JM. Mechanism of human SIRT1 activation by resveratrol. *J Biol Chem* 2005; 280: 17187–17195.

Cao D, Wang M, Qiu X, Liu D, Jiang H, Yang N, Xu RM. Structural basis for allosteric, substrate-dependent stimulation of SIRT1 activity by resveratrol. *Genes Dev* 2015; 29:1316–1325.

Chang CP, Yang MC, Liu HS, Lin YS, Lei HY. Concanavalin A induces autophagy in hepatoma cells and has a therapeutic effect in a murine in situ hepatoma model. *Hepatology* 2007; 45:286–296.

Chang JY, Yi HS, Kim HW, Shong M. Dysregulation of mitophagy in carcinogenesis and tumor progression. *Biochim Biophys Acta* 2016 (In Press).

Chang WT, Cheng HL, Hsieh BS, Chiu CC, Lee KT, Chang KL. Progesterone increases apoptosis and inversely decreases autophagy in human hepatoma HA22T/VGH cells treated with epirubicin. *Sci World J* 2014; 2014: 567148.

Chang Y, Yan W, He X, Zhang L, Li C, Huang H, Nace G, Geller DA, Lin J, Tsung A. miR-375 inhibits autophagy and reduces viability of hepatocellular carcinoma cells under hypoxic conditions. *Gastroenterology* 2012; 143:177–187.

Chen WY, Wang DH, Yen RC, Luo J, Gu W, Baylin SB. Tumor suppressor HIC1 directly regulates SIRT1 to modulate p53-dependent DNA-damage responses. *Cell* 2005; 123:437–448.

Choi JH, Lyu SY, Lee HJ, Jung J, Park WB, Kim GJ. Korean mistletoe lectin regulates self-renewal of placenta-derived mesenchymal stem cells via autophagic mechanisms. *Cell Prolif* 2012; 45:420–429.

Comeau SR, Gatchell DW, Vajda S, Camacho CJ. ClusPro: a fully automated algorithm for protein-protein docking. *Nucleic Acid Res* 2004; 32:96–99.

Coppola D, Khalil F, Eschrich SA, Boulware D, Yeatman T, Wang HG. Downregulation of Bax-interacting factor-1 in colorectal adenocarcinoma. *Cancer* 2008; 113:2665–2670.

Dalby KN, Tekedereli I, Lopez-Berestein G, Ozpolat B. Targeting the prodeath and prosurvival functions of autophagy as novel therapeutic strategies in cancer. *Autophagy* 2010; 6:322–329.

Dang L, Van Damme EJ. Toxic proteins in plants. *Phytochemistry* 2015; 117:51–64.

Degenhardt K, Mathew R, Beaudoin B, Bray K, Anderson D, Chen G, Mukherjee C, Shi Y, Gélinas C, Fan Y, Nelson DA, Jin S, White E. Autophagy promotes tumor cell survival and restricts necrosis, inflammation, and tumorigenesis. *Cancer Cell* 2006; 10:51–64.

Degtyarev M, De Mazière A, Orr C, Lin J, Lee BB, Tien JY, Prior WW, van Dijk S, Wu H, Gray DC, Davis DP, Stern HM, Murray LJ, Hoeflich KP, Klumperman J, Friedman LS, Lin K. Akt inhibition promotes autophagy and sensitizes PTEN-null tumors to lysosomotropic agents. *J Cell Biol* 2008; 183:101–116.

DeNardo DG, Barreto JB, Andreu P, Vasquez L, Tawfik D, Kolhatkar N, Coussens LM. CD4 (+) T cells regulate pulmonary metastasis of mammary carcinomas by enhancing protumor properties of macrophages. *Cancer Cell* 2009; 16:91–102.

El Hasasna H, Athamneh K, Al Samri H, Karuvantevida N, Al Dhaheri Y, Hisaindee S, Ramadan G, Al Tamimi N, AbuQamar S, Eid A, Iratni R. Rhus coriaria induces senescence and autophagic cell death in breast cancer cells through a mechanism involving p38 and ERK1/2 activation. *Sci Rep* 2015; 5:13013.

Ellington AA, Berhow M, Singletary KW. Induction of macroautophagy in human colon cancer cells by soybean B-group triterpenoid saponins. *Carcinogenesis* 2005; 26:159–167.

Eskelinen EL. Roles of LAMP-1 and LAMP-2 in lysosome biogenesis and autophagy. *Mol Aspects Med.* 2006; 27:495–502.

Evan GI and d'Adda di Fagagna F. Cellular senescence: hot or what? *Curr Opin Genet Dev* 2009; 19:25–31

Ewald JA, Desotelle JA, Wilding G, Jarrard DF. Therapy-induced senescence in cancer. *J Natl Cancer Inst* 2010; 102: 1536–1546.

Ferlay J, Shin HR, Bray F, Forman D, Mathers C, Parkin DM. Estimates of worldwide burden of cancer in 2008: GLOBOCAN 2008. *Int J Cancer.* 2010; 127: 2893–2917.

Fevr T, Robine S, Louvard D, Huelsken J. Wnt/ β -catenin is essential for intestinal homeostasis and maintenance of intestinal stem cells. *Molecular and cellular biology* 2007; 27: 7551–7559.

Fimia GM, Kroemer G, Piacentini M. Molecular mechanisms of selective autophagy. *Cell death and differentiation* 2013; 20: 1–2.

Fodde R, Brabletz T. Wnt/beta-catenin signaling in cancer stemness and malignant behavior. *Curr Opin Cell Biol* 2007; 19: 150–158.

Fu LL, Zhou CC, Yao S, Yu JY, Liu B, Bao JK. Plant lectins: Targeting programmed cell death pathways as antitumor agents. *Int J Biochem Cell Biol* 2011; 43:1442–1449.

Fujiwara M, Marusawa H, Wang HQ, Iwai A, Ikeuchi K, Imai Y, Kataoka A, Nukina N, Takahashi R, Chiba T. Parkin as a tumor suppressor gene for hepatocellular carcinoma. *Oncogene* 2008; 27:6002–6011.

Funderburk SF, Wang QJ, Yue Z. The Beclin1–VPS34 complex – at the crossroads of autophagy and beyond. *Trends Cell Biol* 2010; 20:355–362.

Fung C, Lock R, Gao S, Salas E, Debnath J. Induction of autophagy during extracellular matrix detachment promotes cell survival. *Mol Biol Cell* 2008; 19:797–806.

- Futter CE, Collinson LM, Backer JM, Hopkins CR. Human VPS34 is required for internal vesicle formation within multivesicular endosomes. *J Cell Biol* 2001; 155: 1251–1264.
- Ge DZ, Sheng Y, Cai X. Combined staurosporine and retinoic acid induces differentiation in retinoic acid resistant acute promyelocytic leukemia cell lines. *Scientific reports* 2014; 4: 4821.
- Geng J, Klionsky DJ. The Atg8 and Atg12 ubiquitin-like conjugation systems in macroautophagy. *EMBO Rep* 2008; 9:859–864.
- Gewirtz DA, Holt SE, Elmore LW. Accelerated senescence: an emerging role in tumor cell response to chemotherapy and radiation. *Biochem Pharmacol* 2008; 76: 947–957.
- Gewirtz DA. Autophagy and senescence: a partnership in search of definition. *Autophagy* 2013; 9:808–812.
- Ghosh D, Bhutia SK, Mallick SK, Banerjee I, Maiti TK. Stimulation of murine B and T lymphocytes by native and heat-denatured Abrus agglutinin. *Immunobiology* 2009; 214:227–234.
- Ghosh D, Maiti TK. Immunomodulatory and anti-tumor activities of native and heat denatured Abrus agglutinin. *Immunobiology* 2007; 212:589–599.
- Guo H, Chen Y, Liao L, Wu W. Resveratrol protects HUVECs from oxidized-LDL induced oxidative damage by autophagy upregulation via the AMPK/SIRT1 pathway. *Cardiovasc Drugs Ther* 2013; 27:189–98.
- Hailey DW, Rambold AS, Satpute-Krishnan P, Mitra K, Sougrat R, Kim PK, Lippincott-Schwartz J. Mitochondria supply membranes for autophagosome biogenesis during starvation. *Cell* 2010; 141:656–667.
- Hamacher-Brady A, Brady NR. Mitophagy programs: mechanisms and physiological implications of mitochondrial targeting by autophagy. *Cell Mol Life Sci* 2016; 73:775–795.
- Hanada K, Dennis JE, Caplan AI. Stimulatory effects of basic fibroblast growth factor and bone morphogenetic protein-2 on osteogenic differentiation of rat bone marrow-derived mesenchymal stem cells. *Journal of Bone and Mineral Research* 1997; 12: 1606–1614.
- Hanahan D, Weinberg RA. Hallmarks of cancer: the next generation. *Cell* 2011; 144:646–674.
- He C, Bassik MC, Moresi V, Sun K, Wei Y, Zou Z, An Z, Loh J, Fisher J, Sun Q, Korsmeyer S, Packer M, May HI, Hill JA, Virgin HW, Gilpin C, Xiao G, Bassel-Duby R, Scherer PE, Levine B. Exercise-induced BCL2- regulated autophagy is required for muscle glucose homeostasis. *Nature* 2012; 481:511–515.
- Hegde R, Maiti TK, Podder SK. Purification and characterization of three toxins and two agglutinins from *Abrus precatorius* seed by using lactamyl-Sepharose affinity chromatography. *Anal Biochem* 1991; 194:101–109.
- Holla FK, Postma TJ, Blankenstein MA, van Mierlo TJ, Vos MJ, Sizoo EM, de Groot M, Uitdehaag BM, Buter J, Klein M, Reijneveld JC, Heimans JJ. Prognostic value of the S100B protein in newly diagnosed and recurrent glioma patients: a serial analysis. *Journal of Neuro-Oncology* 2016; 129: 525–532.

Hou X, Rooklin D, Fang H, Zhang Y. Resveratrol serves as a protein-substrate interaction stabilizer in human SIRT1 activation. *Sci Rep.* 2016; 6:38186.

Houtkooper RH, Pirinen E, Auwerx J. Sirtuins as regulators of metabolism and healthspan. *Nat Rev Mol Cell Biol* 2012; 13:225-238.

Huang R, Xu Y, Wan W, Shou X, Qian J, You Z, Liu B, Chang C, Zhou T, Lippincott-Schwartz J, Liu W. Deacetylation of nuclear LC3 drives autophagy initiation under starvation. *Mol Cell* 2015; 57:456-466.

Huffman DM, Grizzle WE, Bamman MM, Kim JS, Eltoum IA, Elgavish A, Nagy TR. SIRT1 is significantly elevated in mouse and human prostate cancer. *Cancer Res* 2007; 67: 6612–6618.

Itakura E, Kishi-Itakura C, Koyama-Honda I, Mizushima N. Structures containing Atg9A and the ULK1 complex independently target depolarized mitochondria at initial stages of Parkin-mediated mitophagy. *J Cell Sci* 2012; 125: 1488–1499

Jemal A, Bray F, Center MM, Ferlay J, Ward E, Forman D. Global cancer statistics. *CA Cancer J Clin* 2011; 61:69–90.

Jiang H, Sun J, Xu Q, Liu Y, Wei J, Young CY, Yuan H, Lou H. Marchantin M: A novel inhibitor of proteasome induces autophagic cell death in prostate cancer cells. *Cell Death Dis* 2013; 4:e761.

Jiang Q, Wang Y, Li T, Shi K, Li Z, Ma Y, Li F, Luo H, Yang Y, Xu C. Heat shock protein 90-mediated inactivation of nuclear factor- κ B switches autophagy to apoptosis through becn1 transcriptional inhibition in selenite-induced NB4 cells. *Mol Biol Cell* 2011; 22:1167–1180.

Johansen T, Lamark T. Selective autophagy mediated by autophagic adapter proteins. *Autophagy* 2011; 7: 279–296.

Jung CH, Kim H, Ahn J, Jung SK, Um MY, Son KH, Kim TW, Ha TY. Anthricin isolated from *Anthriscus sylvestris* (L.) Hoffm. Inhibits the growth of breast cancer cells by inhibiting Akt/mTOR signaling, and its apoptotic effects are enhanced by autophagy inhibition. *Evid Based Complement Alternat Med* 2013; 2013:385219.

Kabeya Y, Mizushima N, Ueno T, Yamamoto A, Kirisako T, Noda T, Kominami E, Ohsumi Y, Yoshimori T. LC3, a mammalian homologue of yeast Apg8p, is localized in autophagosome membranes after processing. *EMBO J* 2000; 19:5720–5728.

Kang MR, Kim MS, Oh JE, Kim YR, Song SY, Kim SS, Ahn CH, Yoo NJ, Lee SH. Frame shift mutations of autophagy-related genes ATG2B, ATG5, ATG9B and ATG12 in gastric and colorectal cancers with microsatellite instability. *J Pathol* 2009; 217: 702–706.

Karantza-Wadsworth V, Patel S, Kravchuk O, Chen G, Mathew R, Jin S, White E. Autophagy mitigates metabolic stress and genome damage in mammary tumorigenesis. *Genes Dev* 2007; 21:1621–35.

Katoh M. Networking of WNT, FGF, Notch, BMP, and Hedgehog signaling pathways during carcinogenesis. *Stem Cell Rev* 2007; 3:30–38.

Kelley LA, Mezulis S, Yates CM, Wass MN, Sternberg MJ. The Phyre2 web portal for protein modeling, prediction and analysis. *Nature Protocols*, 2015; 10: 845–858.

Kenific CM, Thorburn A, Debnath J. Autophagy and metastasis: another double-edged sword. *Curr Opin Cell Biol* 2010; 22:241-245.

Kim I, Rodriguez-Enriquez S, Lemasters JJ. Selective degradation of mitochondria by mitophagy. *Archives of biochemistry and biophysics* 2007; 462: 245–253.

Kim J, Kundu M, Viollet B, Guan KL. AMPK and mTOR regulate autophagy through direct phosphorylation of Ulk1. *Nat Cell Biol* 2011; 13:132-141.

Kim MS, Jeong EG, Ahn CH, Kim SS, Lee SH, Yoo NJ. Frameshift mutation of UVRAG, an autophagy-related gene, in gastric carcinomas with microsatellite instability. *Hum Pathol* 2008; 39:1059–1063.

Kimura S, Noda T, Yoshimori T. Dynein-dependent movement of autophagosomes mediates efficient encounters with lysosomes. *Cell Struct Funct* 2008; 33:109–122.

Knizhnik AV, Roos WP, Nikolova T, Quiros S, Tomaszowski KH, Christmann M, Kaina B. Survival and death strategies in glioma cells: autophagy, senescence and apoptosis triggered by a single type of temozolomide-induced DNA damage. *PLoS One* 2013;8:e55665.

Komatsu M, Kurokawa H, Waguri S, Taguchi K, Kobayashi A, Ichimura Y, Sou YS, Ueno I, Sakamoto A, Tong KI, Kim M, Nishito Y, Iemura S, Natsume T, Ueno T, Kominami E, Motohashi H, Tanaka K, Yamamoto M. The selective autophagy substrate p62 activates the stress responsive transcription factor Nrf2 through inactivation of Keap1. *Nat Cell Biol* 2010; 12:213–223.

Komatsu M, Waguri S, Ueno T, Iwata J, Murata S, Tanida I, Ezaki J, Mizushima N, Ohsumi Y, Uchiyama Y, Kominami E, Tanaka K, Chiba T. Impairment of starvation-induced and constitutive autophagy in Atg7-deficient mice. *J Cell Biol* 2005; 169:425–434.

Kraft C, Deplazes A, Sohrmann M, Peter M. Mature ribosomes are selectively degraded upon starvation by an autophagy pathway requiring the Ubp3p/Bre5p ubiquitin protease. *Nat Cell Biol*. 2008; 10:602–610.

Kubli DA, Gustafsson ÅB. Mitochondria and mitophagy: the yin and yang of cell death control. *Circ Res* 2012; 111:1208–1221.

Kühn K, Cott C, Bohler S, Aigal S, Zheng S, Villringer S, Imberty A, Claudinon J, Römer W. The interplay of autophagy and β -Catenin signaling regulates differentiation in acute myeloid leukemia. *Cell death discovery* 2015; 1:15031.

Kuilman T, Peeper DS. Senescence-messaging secretome: SMS-ing cellular stress. *Nat Rev Cancer* 2009; 9:81–94.

Kumar R, Price TJ, Beeke C, Jain K, Patel G, Padbury R, Young GP, Roder D, Townsend A, Bishnoi S, Karapetis CS. Colorectal cancer survival: An analysis of patients with metastatic disease synchronous and metachronous with the primary tumor. *Clin Colorectal Cancer* 2014; 13:87–93.

Kumar S, Raina K, Agarwal C, Agarwal R. Silibinin strongly inhibits the growth kinetics of colon cancer stem cell-enriched spheroids by modulating interleukin 4/6-mediated survival signals. *Oncotarget*. 2014; 5:4972-4989.

- Kuo PL, Hsu YL, Cho CY. Plumbagin induces G2-M arrest and autophagy by inhibiting the AKT/mammalian target of rapamycin pathway in breast cancer cells. *Mol Cancer Ther* 2006; 5:3209–3221.
- Lee CK, Klopp RG, Weindruch R, Prolla TA. Gene expression profile of aging and its retardation by caloric restriction. *Science*. 1999; 285:1390–1393.
- Lemasters JJ. Selective mitochondrial autophagy, or mitophagy, as a targeted defense against oxidative stress, mitochondrial dysfunction, and aging. *Rejuvenation research* 2005; 8: 3–5.
- Li C, Chen J, Lu B, Shi Z, Wang H, Zhang B, Zhao K, Qi W, Bao J, Wang Y. Molecular switch role of Akt in *Polygonatum odoratum* lectin-induced apoptosis and autophagy in human non-small cell lung cancer A549 cells. *PLoS ONE* 2014; 9:e101526.
- Li H, Wang P, Sun Q, Ding WX, Yin XM, Sobol RW, Stolz DB, Yu J, Zhang L. Following cytochrome c release, autophagy is inhibited during chemotherapy-induced apoptosis by caspase 8-mediated cleavage of Beclin 1. *Cancer Res* 2011; 71:3625–3634.
- Li J, Ni M, Lee B, Barron E, Hinton DR, Lee AS. The unfolded protein response regulator GRP78/BiP is required for endoplasmic reticulum integrity and stress-induced autophagy in mammalian cells. *Cell Death Differ* 2008; 15:1460–1471.
- Li X, Wang Y, Xiong Y, Wu J, Ding H, Chen X, Lan L, Zhang H. Galangin induces autophagy via deacetylation of LC3 by SIRT1 in HepG2 cells. *Sci Rep* 2016; 6:30496.
- Liang C, Feng P, Ku B, Dotan I, Canaani D, Oh BH, Jung JU. Autophagic and tumour suppressor activity of a novel Beclin 1-binding protein UVRAG. *Nat Cell Biol* 2006; 8: 688–699.
- Liang XH, Jackson S, Seaman M, Brown K, Kempkes B, Hibshoosh H, Levine B. Induction of autophagy and inhibition of tumorigenesis by beclin 1. *Nature* 1999; 402:672–676.
- Lipatova Z, Shah AH, Kim JJ, Mulholland JW, Segev N. Regulation of ER-phagy by a Ypt/Rab GTPase module. *Mol Biol Cell* 2013; 24:3133– 3144.
- Lisanti MP1, Martinez-Outschoorn UE, Chiavarina B, Pavlides S, Whitaker-Menezes D, Tsiganos A, Witkiewicz A, Lin Z, Balliet R, Howell A, Sotgia F. Understanding the “lethal” drivers of tumor-stroma co-evolution: emerging role(s) for hypoxia, oxidative stress and autophagy/mitophagy in the tumor micro-environment. *Cancer Biol Ther* 2010; 10:537–542.
- Liu B, Cheng Y, Zhang B, Bian HJ, Bao JK. *Polygonatum cyrtoneuma* lectin induces apoptosis and autophagy in human melanoma A375 cells through a mitochondria-mediated ROS-p38-p53 pathway. *Cancer Lett* 2009; 275:54–60.
- Liu B, Wu JM, Li J, Liu JJ, Li WW, Li CY, Xu HL, Bao JK. *Polygonatum cyrtoneuma* lectin induces murine fibrosarcoma L929 cell apoptosis and autophagy via blocking Ras-Raf and PI3K-Akt signaling pathways. *Biochimie* 2010; 92:1934–1938.
- Liu C, Li Y, Semenov M, Han C, Baeg GH, Tan Y, Zhang Z, Lin X, He X. Control of beta-catenin phosphorylation/degradation by a dual-kinase mechanism. *Cell* 2002; 108:837–847.
- Liu CL, Tsai CC, Lin SC, Wang LI, Hsu CI, Hwang MJ, Lin JY. Primary structure and function analysis of the *Abrus precatorius* agglutinin A chain by site-directed mutagenesis.

Pro (199) of amphiphilic alpha-helix H impairs protein synthesis inhibitory activity. *J Biol Chem* 2000; 275:1897-1901.

Liu Z, Luo Y, Zhou TT, Zhang WZ. Could plant lectins become promising anti-tumor drugs for causing autophagic cell death? *Cell Prolif* 2013; 46:509–515.

Lombardo Y, Scopelliti A, Cammareri P, Todaro M, Iovino F, Ricci-Vitiani L, Gulotta G, Dieli F, de Maria R, Stassi G. Bone morphogenetic protein 4 induces differentiation of colorectal cancer stem cells and increases their response to chemotherapy in mice. *Gastroenterology* 2011; 140: 297–309.

Lu Z1, Luo RZ, Lu Y, Zhang X, Yu Q, Khare S, Kondo S, Kondo Y, Yu Y, Mills GB, Liao WS, Bast RC Jr. The tumor suppressor gene ARHI regulates autophagy and tumor dormancy in human ovarian cancer cells. *J Clin Invest* 2008; 118:3917–3929.

Luo C, Li Y, Wang H, Feng Z, Li Y, Long J, Liu J. Mitochondrial accumulation under oxidative stress is due to defects in autophagy. *J Cell Biochem* 2013; 114:212–219.

Mahadevan D, Powis G, Mash EA, George B, Gokhale VM, Zhang S, Shakalya K, Du-Cuny L, Berggren M, Ali MA, Jana U, Ihle N, Moses S, Franklin C, Narayan S, Shirahatti N, Meillet EJ. Discovery of a novel class of AKT pleckstrin homology domain inhibitors. *Mol Cancer Ther* 2008; 7:2621–2632.

Marino G, Salvador-Montoliu N, Fueyo A, Knecht E, Mizushima N, López-Otín C. Tissue-specific autophagy alterations and increased tumorigenesis in mice deficient in Atg4C/autophagin-3. *J Biol Chem* 2007; 282:18573–18583.

Martinez-Outschoorn UE, Trimmer C, Lin Z, Whitaker-Menezes D, Chiavarina B, Zhou J, Wang C, Pavlides S, Martinez-Cantarin MP, Capozza F, Witkiewicz AK, Flomenberg N, Howell A, Pestell RG, Caro J, Lisanti MP, Sotgia F. Autophagy in cancer associated fibroblasts promotes tumor cell survival: role of hypoxia, HIF1 induction and NF κ B activation in the tumor stromal microenvironment. *Cell Cycle* 2010; 9:3515–3533.

Mathew R, Kongara S, Beaudoin B, Karp CM, Bray K, Degenhardt K, Chen G, Jin S, White E. Autophagy suppresses tumor progression by limiting chromosomal instability. *Genes Dev* 2007; 21:1367–1381.

Meher BR, Wang Y. Binding of single walled carbon nanotube to WT and mutant HIV-1 proteases: Analysis of flap dynamics and binding mechanism. *J Mol Graph Model* 2012; 38:430–445.

Meher BR, Wang Y. Exploring the drug resistance of V32I and M46L mutant HIV-1 protease to inhibitor TMC114: Flap dynamics and binding mechanism. *J Mol Graph Model* 2015; 56:60–73.

Meher BR, Wang Y. Interaction of I50V mutant and I50L/ A71V double mutant HIV-1 protease with inhibitor TMC114 (darunavir): Molecular dynamics simulation and binding free energy studies. *J Phys Chem B* 2012; 116:1884–1900.

Milburn CC, Deak M, Kelly SM, Price NC, Alessi DR, Van Aalten DM. Binding of phosphatidylinositol 3, 4, 5-trisphosphate to the pleckstrin homology domain of protein kinase B induces a conformational change. *Biochem J* 2003; 375:531–538.

Ming M, Shea CR, Guo X, Li X, Soltani K, Han W, He YY. Regulation of global genome nucleotide excision repair by SIRT1 through xeroderma pigmentosum C. *Proc Natl Acad Sci USA*. 2010; 107:22623-22628.

Mishra R, Karande AA. Endoplasmic reticulum stress-mediated activation of p38 MAPK, Caspase-2 and Caspase-8 leads to abrin-induced apoptosis. *PLoS ONE* 2014; 9:e92586.

Mizushima N, Levine B. Autophagy in mammalian development and differentiation. *Nature cell biology* 2010; 12: 823–830.

Moreno E, Doughty-Shenton D, Plano D, Font M, Encío I, Palop JA, Sanmartín C. A dihydroselenoquinazoline inhibits S6 ribosomal protein signalling, induces apoptosis and inhibits autophagy in MCF-7 cells. *Eur J Pharm Sci* 2014; 63C:87–95.

Moustapha A, Pérétout PA, Rainey NE, Sureau F, Geze M, Petit JM, Dewailly E, Slomianny C, Petit PX. Curcumin induces crosstalk between autophagy and apoptosis mediated by calcium release from the endoplasmic reticulum, lysosomal destabilization and mitochondrial events. *Cell Death Discovery* 2015; 1:15017.

Mukhopadhyay S, Das DN, Panda PK, Sinha N, Naik PP, Bissoyi A, Pramanik K, Bhutia SK. Autophagy protein Ulk1 promotes mitochondrial apoptosis through reactive oxygen species. *Free Radic Biol Med* 2015; 89:311-321.

Mukhopadhyay S, Panda PK, Behera B, Das CK, Hassan MK, Das DN, Sinha N, Bissoyi A, Pramanik K, Maiti TK, Bhutia SK. *In vitro* and *in vivo* antitumor effects of Peanut agglutinin through induction of apoptotic and autophagic cell death. *Food Chem Toxicol* 2014; 64:369–377.

Mukhopadhyay S, Panda PK, Das DN, Sinha N, Behera B, Maiti TK, Bhutia SK. Abrus agglutinin suppresses human hepatocellular carcinoma *in vitro* and *in vivo* by inducing caspase-mediated cell death. *Acta Pharmacol Sin* 2014; 35:814–824.

Mukhopadhyay S, Panda PK, Sinha N, Das DN, Bhutia SK. Autophagy and apoptosis: where do they meet? *Apoptosis* 2014; 19: 555–566.

Mukhopadhyay S, Schlaepfer IR, Bergman BC, Panda PK, Praharaj PP, Naik PP, Agarwal R, Bhutia SK. ATG14 facilitated lipophagy in cancer cells induce ER stress mediated mitophagy through a ROS dependent pathway. *Free Radic Biol Med* 2017; 104:199–213.

Murakawa T, Yamaguchi O, Hashimoto A, Hikoso S, Takeda T, Oka T, Yasui H, Ueda H, Akazawa Y, Nakayama H, Taneike M, Misaka T, Omiya S, Shah AM, Yamamoto A, Nishida K, Ohsumi Y, Okamoto K, Sakata Y, Otsu K. Bcl-2-like protein 13 is a mammalian Atg32 homologue that mediates mitophagy and mitochondrial fragmentation. *Nat Commun*. 2015; 6:7527.

Naik PP, Das DN, Panda PK, Mukhopadhyay S, Sinha N, Praharaj PP, Agarwal R, Bhutia SK. Implications of cancer stem cells in developing therapeutic resistance in oral cancer. *Oral Oncol* 2016 Nov; 62:122–135.

Nam HY, Han MW, Chang HW, Lee YS, Lee M, Lee HJ, Lee BW, Lee HJ, Lee KE, Jung MK, Jeon H, Choi SH, Park NH, Kim SY, Kim SW. Radio resistant cancer cells can be conditioned to enter senescence by mTOR inhibition. *Cancer Res* 2013; 73:4267–4277.

Narendra D, Kane LA, Hauser DN, Fearnley IM, Youle RJ. P62/SQSTM1 is required for Parkin-induced mitochondrial clustering but not mitophagy; VDAC1 is dispensable for both. *Autophagy* 2010; 6:1090-1106.

Narendra DP, Jin SM, Tanaka A, Suen DF, Gautier CA, Shen J, Cookson MR, Youle RJ. PINK1 is selectively stabilized on impaired mitochondria to activate Parkin. *PLoS Biol* 2010; 8: 1000298.

Narendra N, Tanaka A, Suen DF, Youle RJ. Parkin is recruited selectively to impaired mitochondria and promotes their autophagy. *J Cell Biol* 2008; 183: 795–803.

Nazarko TY. Atg37 regulates the assembly of the pexophagic receptor protein complex. *Autophagy* 2014; 10:1348–1349.

Ng TL, Leprivier G, Robertson MD, Chow C, Martin MJ, Laderoute KR, Davicioni E, Triche TJ, Sorensen PH. The AMPK stress response pathway mediates anoikis resistance through inhibition of mTOR and suppression of protein synthesis. *Cell Death Differ* 2012; 19:501–510.

Novak I, Dikic I. Autophagy receptors in developmental clearance of mitochondria. *Autophagy* 2011; 7: 301–303.

Novak I, Kirkin V, McEwan DG, Zhang J, Wild P, Rozenknop A, Rogov V, Löhr F, Popovic D, Occhipinti A, Reichert AS, Terzic J, Dötsch V, Ney PA, Dikic I. Nix is a selective autophagy receptor for mitochondrial clearance. *EMBO Rep* 2010; 11: 45–51.

Obara K, Noda T, Niimi K, Ohsumi Y. Transport of phosphatidylinositol 3-phosphate into the vacuole via autophagic membranes in *Saccharomyces cerevisiae*. *Genes Cells* 2008; 13:537–547.

Okamoto K, Kondo-Okamoto N, Ohsumi Y. Mitochondria-anchored receptor Atg32 mediates degradation of mitochondria via selective autophagy. *Dev Cell* 2009; 17:87–97.

Okatsu K, Saisho K, Shimanuki M, Nakada K, Shitara H, Sou YS, Kimura M, Sato S, Hattori N, Komatsu M, Tanaka K, Matsuda N. p62/SQSTM1 cooperates with Parkin for perinuclear clustering of depolarized mitochondria. *Genes Cells* 2010; 15:887–900.

Ou X, Lee MR, Huang X, Messina-Graham S, Broxmeyer HE. SIRT1 positively regulates autophagy and mitochondria function in embryonic stem cells under oxidative stress. *Stem Cells* 2014; 32:1183–1194.

Ozeki N, Mogi M, Hase N, Hiyama T, Yamaguchi H, Kawai R, Matsumoto T, Nakata K. Bone morphogenetic protein-induced cell differentiation involves Atg7 and Wnt16 sequentially in human stem cell-derived osteoblastic cells. *Experimental cell research* 2016; 347: 24–41.

Panda PK, Behera B, Meher BR, Das DN, Mukhopadhyay S, Sinha N, Naik PP, Roy B, Das J, Paul S, Maiti TK, Agarwal R, Bhutia SK. Abrus Agglutinin, a type II ribosome inactivating protein inhibits Akt/PH domain to induce endoplasmic reticulum stress mediated autophagy-dependent cell death. *Mol Carcinog* 2017; 56:389–401.

Panda PK, Mukhopadhyay S, Behera B, Bhol CS, Dey S, Das DN, Sinha N, Bissoyi A, Pramanik K, Maiti TK, Bhutia SK. Antitumor effect of soybean lectin mediated through reactive oxygen species dependent pathway. *Life Sci* 2014; 11:27–35.

Panda PK, Mukhopadhyay S, Das DN, Sinha N, Naik PP, Bhutia SK. Mechanism of autophagic regulation in carcinogenesis and cancer therapeutics. *Semin Cell Dev Biol* 2015; 39:43–55.

Panda PK, Mukhopadhyay S, Sinha N, Das DN, Bhutia SK. Autophagy and apoptosis: where do they meet? *Apoptosis* 2014; 19:555–566.

Patel KR, Andreadi C, Britton RG, Horner-Glister E, Karmokar A, Sale S, Brown VA, Brenner DE, Singh R, Steward WP, Gescher AJ, Brown K. Sulfate metabolites provide an intracellular pool for resveratrol generation and induce autophagy with senescence. *Sci Transl Med.* 2013; 5:205.

Pavrides S, Tsigirgos A, Migneco G, Whitaker-Menezes D, Chiavarina B, Flomenberg N, Frank PG, Casimiro MC, Wang C, Pestell RG, Martinez-Outschoorn UE, Howell A, Sotgia F, Lisanti MP. The autophagic tumor stroma model of cancer: Role of oxidative stress and ketone production in fueling tumor cell metabolism. *Cell Cycle* 2010; 9:3485–505.

Pera MF, Andrade J, Houssami S, Reubinoff B, Trounson A, Stanley EG, Ward-van Oostwaard D, Mummery C. Regulation of human embryonic stem cell differentiation by BMP-2 and its antagonist noggin. *J Cell Sci* 2004; 117: 1269–1280.

Peterson TE, Kirkpatrick ND, Huang Y, Farrar CT, Marijt KA, Kloepper J, Datta M, Amoozgar Z, Seano G, Jung K, Kamoun WS, Vardam T, Snuderl M, Goveia J, Chatterjee S, Batista A, Muzikansky A, Leow CC, Xu L, Batchelor TT, Duda DG, Fukumura D, Jain RK. Dual inhibition of Ang-2 and VEGF receptors normalizes tumor vasculature and prolongs survival in glioblastoma by altering macrophages. *Proceedings of the National Academy of Sciences* 2016; 113: 4470–4475.

Petherick KJ, Williams AC, Lane JD, Ordóñez-Morán P, Huelsken J, Collard TJ, Smartt HJ, Batson J, Malik K, Paraskeva C, Greenhough A. Autolysosomal β -catenin degradation regulates Wnt-autophagy-p62 crosstalk. *The EMBO journal* 2013; 32: 1903–1916.

Phillips HS, Kharbanda S, Chen R, Forrest WF, Soriano RH, Wu TD, Misra A, Nigro JM, Colman H, Soroceanu L, Williams PM, Modrusan Z, Feuerstein BG, Aldape K. Molecular subclasses of high-grade glioma predict prognosis, delineate a pattern of disease progression, and resemble stages in neurogenesis. *Cancer cell* 2006; 9: 157–173.

Pierce GB and Wallace C. Differentiation of malignant to benign cells. *Cancer research* 1971; 31:127–134.

Rachel W. Goehe RW, Di X, Sharma K, Bristol ML, Henderson SC, Valerie K, Rodier F, Davalos AR, Gewirtz DA. The autophagy-senescence connection in chemotherapy: must tumor cells (self) eat before they sleep? *J Pharmacol Exp Ther.* 2012; 343:763–778.

Roninson IB. Tumor cell senescence in cancer treatment. *Cancer Res.* 2003; 63: 2705–2715.

Roy B, Pattanaik AK, Das J, Bhutia SK, Behera B, Singh P, Maiti TK. Role of PI3 K/Akt/mTOR and MEK/ERK pathway in Concanavalin A induced autophagy in HeLa cells. *Chem Biol Interact* 2014; 210:96–102.

Rusin M, Zajkiewicz A, Butkiewicz D. Resveratrol induces senescence-like growth inhibition of U-2 OS cells associated with the instability of telomeric DNA and upregulation of BRCA1. *Mech Ageing Dev* 2009; 130: 528–537.

Saito T, J. Molecular mechanisms of mitochondrial autophagy/mitophagy in the heart. *Circ Res* 2015; 116: 1477-1490.

Salazar M, Carracedo A, Salanueva IJ, Hernández-Tiedra S, Lorente M, Egia A, Vázquez P, Blázquez C, Torres S, García S, Nowak J, Fimia GM, Piacentini M, Cecconi F, Pandolfi PP, González-Feria L, Iovanna JL, Guzmán M, Boya P, Velasco G. Cannabinoid action induces autophagy-mediated cell death through stimulation of ER stress in human glioma cells. *J Clin Invest* 2009; 119: 1359–1372.

Salem AF, Whitaker-Menezes D, Lin Z, Martinez-Outschoorn UE, Tanowitz HB, Al-Zoubi MS, Howell A, Pestell RG, Sotgia F, Lisanti MP. Two-compartment tumor metabolism: autophagy in the tumor microenvironment and oxidative mitochondrial metabolism (OXPHOS) in cancer cells. *Cell Cycle* 2012; 11:2545–2556.

Sandoval H, Thiagarajan P, Dasgupta SK, Schumacher A, Prchal JT, Chen M, Wang J. Essential role for Nix in autophagic maturation of erythroid cells. *Nature* 2008; 454:232–235.

Santarpia L, Lippman SM, El-Naggar AK. Targeting the MAPK–RAS–RAF signaling pathway in cancer therapy. *Expert Opin Ther Targets* 2012; 16:103–119.

Sauane M, Su ZZ, Dash R, Liu X, Norris JS, Sarkar D, Lee SG, Allegood JC, Dent P, Spiegel S, Fisher PB. Ceramide plays a prominent role in MDA-7/IL-24-induced cancer-specific apoptosis. *J Cell Physiol* 2010; 222:546-555.

Schuck S, Gallagher CM, Walter P. ER-phagy mediates selective degradation of endoplasmic reticulum independently of the core autophagy machinery. *J Cell Sci* 2014; 127:4078–4088.

Sell S. Stem cell origin of cancer and differentiation therapy. *Critical reviews in oncology/hematology* 2004; 51: 1–28.

Selvaraj S, Sun Y, Sukumaran P, Singh BB. Resveratrol activates autophagic cell death in prostate cancer cells via downregulation of STIM1 and the mTOR pathway. *Mol Carcinog* 2016; 55:818–831.

Sentelle RD, Senkal CE, Jiang W, Ponnusamy S, Gencer S, Selvam SP, Ramshesh VK, Peterson YK, Lemasters JJ, Szulc ZM, Bielawski J, Ogretmen B. Ceramide targets autophagosomes to mitochondria and induces lethal mitophagy. *Nat Chem Biol* 2012; 8:831–838.

Shackelford DB, Shaw RJ. The LKB1–AMPK pathway: metabolism and growth control in tumour suppression. *Nat Rev Cancer* 2009; 9:563–575.

Shay JW, Roninson IB. Hallmarks of senescence in carcinogenesis and cancer therapy. *Oncogene* 2004; 23:2919–2933.

Shi RY, Zhu SH, Li V, Gibson SB, Xu XS, Kong JM. BNIP3 interacting with LC3 triggers excessive mitophagy in delayed neuronal death in stroke. *CNS Neurosci Ther* 2014; 20:1045-1055.

Shinojima N, Yokoyama T, Kondo Y, Kondo S. Roles of the Akt/mTOR/p70S6K and ERK1/2 signaling pathways in curcumin-induced autophagy. *Autophagy* 2007; 3:635–637.

Shrivastava A, Kuzontkoski PM, Groopman JE, Prasad A. Cannabidiol induces programmed cell death in breast cancer cells by coordinating the cross-talk between apoptosis and autophagy. *Mol Cancer Ther* 2011; 10:1161–1172.

Simonsen A, Tooze SA. Coordination of membrane events during autophagy by multiple class III PI3-kinase complexes. *J Cell Biol* 2009; 186:773–782.

Singh NP, Singh UP, Hegde VL, Guan H, Hofseth L, Nagarkatti M, Nagarkatti PS. Resveratrol (trans-3, 5, 4'-trihydroxystilbene) suppresses EL4 tumor growth by induction of apoptosis involving reciprocal regulation of SIRT1 and NF- κ B. *Mol Nutr Food Res* 2011; 55:1207–1218.

Song NY, Surh YJ. Janus-faced role of SIRT1 in tumorigenesis. *Ann N Y Acad Sci* 2012; 1271:10–19.

Sugawara K, Suzuki NN, Fujioka Y, Mizushima N, Ohsumi Y, Inagaki F. The crystal structure of microtubule-associated protein light chain 3, a mammalian homologue of *Saccharomyces cerevisiae* Atg8. *Genes Cells* 2004; 9: 611–618.

Suneja G, Bacon M, Small W Jr, Ryu SY, Kitchener HC, Gaffney DK. The cervix cancer research network: Increasing access to cancer clinical trials in low- and middle-income countries. *Front Oncol* 2015; 5:14.

Tang DG, Patrawala L, Calhoun T, Bhatia B, Choy G, Schneider-Broussard R, Jeter C. Prostate cancer stem/progenitor cells: identification, characterization, and implications. *Mol Carcinog*. 2007; 4:1–14.

Tripathi S, Maiti TK. Efficiency of heat denatured lectins from *Abrus precatorius* as immunoadjuvants. *Food Agric Immunol* 2003; 15:279–287.

Tripathi S, Maiti TK. Immunomodulatory role of native and heat denatured agglutinin from *Abrus precatorius*. *Int J Biochem Cell Biol* 2005; 37:451–462.

Tripathi S, Maiti TK. Stimulation of murine macrophages by native and heat-denatured lectin from *Abrus precatorius*. *Int Immunopharmacol* 2003; 3:375–381.

Ullén A, Farnebo M, Thyrell L, Mahmoudi S, Kharaziha P, Lennartsson L, Grandér D, Panaretakis T, Nilsson S. Sorafenib induces apoptosis and autophagy in prostate cancer cells *in vitro*. *Int J Oncol* 2010; 37:15–20.

Vaiopoulos AG, Kostakis ID, Koutsilieris M, Papavassiliou AG. Colorectal cancer stem cells. *Stem cells* 2012; 30: 363–371.

Van der Vaart A, Mari M, Reggiori F. A picky eater: exploring the mechanisms of selective autophagy in human pathologies. *Traffic* 2008; 9: 281–289.

Van Humbeeck C, Cornelissen T, Hofkens H, Mandemakers W, Gevaert K, De Strooper B, Vandenberghe W. Parkin interacts with Ambra1 to induce mitophagy. *J Neurosci* 2011; 31:10249-19261.

Veeriah S, Taylor BS, Meng S, Fang F, Yilmaz E, Vivanco I, Janakiraman M, Schultz N, Hanrahan AJ, Pao W, Ladanyi M, Sander C, Heguy A, Holland EC, Paty PB, Mischel PS, Liau L, Cloughesy TF, Mellinghoff IK, Solit DB, Chan TA. Somatic mutations of the Parkinson's disease-associated gene PARK2 in glioblastoma and other human malignancies. *Nat Genet* 2010; 42:77–82.

Wang J, Lian H, Zhao Y, Kauss MA, Spindel S. Vitamin D3 induces autophagy of human myeloid leukemia cells. *J Biol Chem* 2008; 283: 25596–25605.

Wang J. Beclin 1 bridges autophagy, apoptosis and differentiation. *Autophagy* 2008; 4: 947–948.

Warrell RP Jr, Frankel SR, Miller WH Jr, Scheinberg DA, Itri LM, Hittelman WN, Vyas R, Andreeff M, Tafuri A, Jakubowski A, Gabrilove J, Gordon MS, Dmitrovsky E. Differentiation therapy for acute promyelocytic leukemia with tretinoin (all-trans retinoic acid). *N Engl J Med* 1991; 324:1385–1393.

Wesche J, Rapak A, Olsnes S. Dependence of ricin toxicity on translocation of the toxin A-chain from the endoplasmic reticulum to the cytosol. *J Biol Chem*. 1999; 274:34443–34449.

White E. De-convoluting the context-dependent role for autophagy in cancer. *Nat Rev Cancer* 2012; 12:401–410.

Wicha MS. Targeting self-renewal, an Achilles' heel of cancer stem cells. *Nat Med* 2014; 20:14–15.

Willis SN1, Fletcher JI, Kaufmann T, van Delft MF, Chen L, Czabotar PE, Ierino H, Lee EF, Fairlie WD, Bouillet P, Strasser A, Kluck RM, Adams JM, Huang DC. Apoptosis initiated when BH3 ligands engage multiple Bcl-2 homologs, not Bax or Bak. *Science* 2007; 315:856–859.

Wu Y, Li X, Zhu JX, Xie W, Le W, Fan Z, Jankovic J, Pan T. Resveratrol-activated AMPK/SIRT1/autophagy in cellular models of Parkinson's disease. *Neurosignals* 2011; 19:163–174.

Xue W, Zender L, Miething C, Dickins RA, Hernando E, Krizhanovsky V, Cordon-Cardo C, Lowe SW. Senescence and tumor clearance is triggered by p53 restoration in murine liver carcinomas. *Nature* 2007; 445:656–660.

Yamaguchi O, Murakawa T, Nishida K, Otsu K. Receptor-mediated mitophagy. *Journal of molecular and cellular cardiology* 2016; 95: 50–56.

Yang F, Chu X, Yin M, Liu X, Yuan H, Niu Y, Fu L. mTOR and autophagy in normal brain aging and caloric restriction ameliorating age-related cognition deficits. *Behav Brain Res* 2014; 264:82–90.

Yee KS, Wilkinson S, James J, Ryan KM, Vousden KH. PUMA-and Bax-induced autophagy contributes to apoptosis. *Cell Death & Differentiation* 2009; 16: 1135–1145.

Youle RJ, Narendra DP. Mechanisms of mitophagy. *Nature reviews Molecular cell biology* 2011; 12: 9–14.

Young AR, Narita M, Ferreira M, Kirschner K, Sadaie M, Darot JF, Tavaré S, Arakawa S, Shimizu S, Watt FM, Narita M. Autophagy mediates the mitotic senescence transition. *Genes Dev* 2009; 23:798–803.

Yu J, Zhang L, Hwang PM, Kinzler KW, Vogelstein B. PUMA induces the rapid apoptosis of colorectal cancer cells. *Mol Cell* 2001; 7:673–682.

Yu KN, Chang SH, Park SJ, Lim J, Lee J, Yoon TJ, Kim JS, Cho MH. Titanium dioxide nanoparticles induce endoplasmic reticulum stress-mediated autophagic cell death via

mitochondria-associated endoplasmic reticulum membrane disruption in normal lung cells. PLoS ONE 2015; 10:e0131208.

Zaffagnini G, Martens S. Mechanisms of selective autophagy. Journal of molecular biology 2016; 428: 1714–1724.

Zhai B, Hu F, Jiang X, Xu J, Zhao D, Liu B, Pan S, Dong X, Tan G, Wei Z, Qiao H, Jiang H, Sun X. Inhibition of Akt reverses the acquired resistance to sorafenib by switching protective autophagy to autophagic cell death in hepatocellular carcinoma. Mol Cancer Ther 2014; 13:1589–1598.

Zhan Y, Gong K, Chen C, Wang H, Li W. P38 MAP kinase functions as a switch in MS-275-induced reactive oxygen species-dependent autophagy and apoptosis in human colon cancer cells. Free Radic Biol Med 2012; 53: 532–543.

Zhang CZ, Fang EF, Zhang HT, Liu LL, Yun JP. Momordica charantia lectin exhibits antitumor activity towards hepatocellular carcinoma. Invest New Drugs 2015; 33:1–11.

Zhang J, Ney PA. Role of BNIP3 and NIX in cell death, autophagy, and mitophagy. Cell Death Differ 2009; 16: 939–946.

Zhang WV, Stott NS. BMP-2-modulated chondrogenic differentiation *in vitro* involves down-regulation of membrane-bound beta-catenin. Cell communication & adhesion 2004; 11: 89–102.

Zhang Y, Chen X, Qiao M, Zhang BQ, Wang N, Zhang Z, Liao Z, Zeng L, Deng Y, Deng F, Zhang J, Yin L, Liu W, Zhang Q, Ya Z, Ye J, Wang Z, Zhou L, Luu HH, Haydon RC, He TC, Zhang H. Bone morphogenetic protein 2 inhibits the proliferation and growth of human colorectal cancer cells. Oncology reports 2014; 32: 1013–1020.

Zhu Y, Armstrong JL, Tchkonina T, Kirkland JL. Cellular senescence and the senescent secretory phenotype in age-related chronic diseases. Curr Opin Clin Nutr Metab Care 2014; 17:324-328.

Zhuang W, Li B, Long L, Chen L, Huang Q, Liang Z. Induction of autophagy promotes differentiation of glioma-initiating cells and their radio sensitivity. International journal of cancer 2011; 129: 2720–2731.

Zhuang W, Long L, Zheng B, Ji W, Yang N, Zhang Q, Liang Z. Curcumin promotes differentiation of glioma-initiating cells by inducing autophagy. Cancer Sci 2012; 103:684–690.

Curriculum Vitae

PRASHANTA KUMAR PANDA

Contact Details:

Room No: MN339,
Cancer and Cell Death Laboratory,
Department of Life Science ,
National Institute of Technology Rourkela,
Sundergarh, Odisha, India- 769008
Email: krishnan_prashanta@yahoo.co.in
prashantanitrkl@gmail.com, 511ls607@nitrkl.ac.in
Mob: +91-9938423959
Lab. 91-661-2464701/4683/2686



Career Objective

To understand the molecular regulation and biological significance of autophagy as well as selective autophagy in cancer and cancer stem cells .Besides that I want to explore how biogenesis of autophagosome is associated with the varying function of previously undeclared molecules.

EDUCATION

- | | |
|--------------------------------|---|
| 2011(September)–2017 (April) : | Doctorate of Philosophy
Cancer Biology(Specialization),
Department of Life Science,
National Institute of Technology Rourkela, Odisha,
India |
| 2010 – 2011: | Master of Philosophy
Developmental Biology (Specialization),
Department of Zoology,
Utkal University, Odisha, India |
| 2005 – 2007: | Master of Science
Zoology (Hons),
Department of Zoology,
Utkal University, Odisha, India |
| 2003 – 2005: | Bachelor of Science
Zoology (Hons), Botany, Chemistry
Department of Zoology,
North Odisha University, Odisha, India |

RESEARCH EXPERIENCE

- Working as a **Senior Research Fellow** in CSIR funded project entitled **“Study on effect of herbal secretagogues on the biochemical, cytochemical and histophysiological activities of the endocrine cells of the gastrointestinal mucosa of broiler chicken with reference to gain in body weight”** at Department of Anatomy, Odisha Veterinary College, Odisha, India, from 2007-2010.

TEACHING EXPERIENCE

- Taught **Biochemistry** at master level during graduate study at National Institute of Technology Rourkela, Odisha, India.
- Taught **“Cell signaling”** at masters level during graduate study at National Institute of Technology Rourkela, Odisha India.
- Guided MSc students in their project work during graduate study at National Institute of Technology Rourkela, Odisha India.

ACADEMIC GRANTS AND HONORS

- Qualified Graduate Aptitude in Engineering (GATE-XL) in 2011, organized by Indian Institute of Technology Madras.
- Availed fellowship from the Department of Biotechnology, Govt. of India and Ministry of Human Resource Development, (MHRD), Govt. of India during graduate study
- Our poster entitled **“Autophagic cell death induction with *Abrus* agglutinin”** was selected for award category at 32nd Annual Convention of Indian Association for Cancer Research (IACR) & International Symposium on "Infection & Cancer", New Delhi, 2013.

DISSERTATIONS/PROJECTS

- 2011– Present: PhD project
“Autophagy dependent cell death, senescence and differentiation by *Abrus* agglutinin in cancer therapeutics”
National Institute of Technology Rourkela, Odisha, India
- 2010 – 2011: MPhil project
“Effects of Vitamin A on tail regeneration in the tadpoles of *Polypedates maculatus*: SDS-PAGE analysis
Department of Zoology,
Utkal University, Vani Vihar, Odisha, India

RESEARCH/SCHOLARLY ARTICLES

Published/Accepted/Communicated (International peer-reviewed, SCI-indexed with Impact factor)

From PhD Thesis

1. **Panda PK**, Behera B, Meher BR, Das DN, Mukhopadhyay S, Sinha N, Naik PP, Roy B, Das J, Paul S, Maiti TK, Agarwal R, Bhutia SK. Abrus agglutinin, a type II ribosome inactivating protein inhibits Akt/PH domain to induce endoplasmic reticulum stress mediated autophagy-dependent cell death. **Mol Carcinog.** 2017; 56:389-401 [PubMed PMID: 27182794]. **IF:4.8**
2. **Panda PK**, Mukhopadhyay S, Das DN, Sinha N, Naik PP, Bhutia SK. Mechanism of autophagic regulation in carcinogenesis and cancer therapeutics. **Semin Cell Dev Biol.** 2015; 39:43-55 [PubMed PMID: 25724561]. **IF:5.85**
3. **Panda PK**, Mukhopadhyay S, Sinha N, Das DN, Bhutia SK. Autophagy and apoptosis: where do they meet? **Apoptosis** 2014; 19:555-566 [PubMed PMID: 4415198]. **IF:3.8**
4. **Panda et al.**, PUMA dependent mitophagy by *Abrus* agglutinin contributes to apoptosis through ceramide generation in human glioblastoma cells (communicated)
5. **Panda et al.**, SIRT1/LAMP1 signaling activation by *Abrus* Agglutinin regulates autophagy mediated senescence. (communicated)
6. **Panda et al.**, *Abrus* Agglutinin induces cancer stem cell differentiation through BMP2 mediated autophagy.(communicated)

Outside PhD Thesis

7. **Panda PK**, Mukhopadhyay S, Behera B, Bhol CS, Dey S, Das DN, Sinha N, Bissoyi A, Pramanik K, Maiti TK, Bhutia SK. Antitumor effect of soybean lectin mediated through reactive oxygen species-dependent pathway. **Life Sci.** 2014; 111:27-35 [PubMed PMID: 25064824]. **IF:2.6**
8. Naik PP, Das DN, **Panda PK**, Mukhopadhyay S, Sinha N, Praharaj PP, Agarwal R, Bhutia SK. Implications of cancer stem cells in developing therapeutic resistance in oral cancer. **Oral Oncol.** 2016; 62:122-135 [PubMed PMID: 27865365]. **IF:3.752**
9. Mukhopadhyay S, Sinha N, Das DN, **Panda PK**, Naik PP, Bhutia SK. Clinical relevance of autophagic therapy in cancer: Investigating the current trends, challenges, and future prospects. **Crit Rev Clin Lab Sci.** 2016; 53:228-252. [PubMed PMID: 26743568]. **IF:4.167**
10. Sinha N , **Panda PK**, Das DN, Mukhopadhyay S, Naik PP, Maiti TK , Shanmugam MK, Chinnathambi A, Zayed ME, Alharbi SA, Sethi G, Bhutia SK" Abrus agglutinin promotes irreparable DNA damage by triggering ROS generation followed by ATM-p73 mediated apoptosis on oral carcinoma. **Molecular Carcinogenesis (Revision MS# MC-16-0176)**
11. Das DN, Naik PP, Nayak A, **Panda PK**, Mukhopadhyay S, Sinha N, Bhutia SK. Bacopa monnieri-Induced Protective Autophagy Inhibits Benzo[a]pyrene-Mediated Apoptosis. **Phytother Res.** 2016; 30:1794-1801. [PubMed PMID: 27432245]. **IF-2.6**

12. Das DN, Sinha N, Naik PP, **Panda PK**, Mukhopadhyay S, Mallick SK, Sarangi I, Bhutia SK. Mutagenic and genotoxic potential of native air borne particulate matter from industrial area of Rourkela city, Odisha, India. **Environ Toxicol Pharmacol**. 2016; 46:131-139. [PubMed PMID:27458701]. **IF-2.1**
13. Bhutia SK, Behera B, Nandini Das D, Mukhopadhyay S, Sinha N, **Panda PK**, Naik PP, Patra SK, Mandal M, Sarkar S, Menezes ME, Talukdar S, Maiti TK, Das SK, Sarkar D, Fisher PB. Abrus agglutinin is a potent anti-proliferative and anti-angiogenic agent in human breast cancer. **Int J Cancer**. 2016; 139:457-466.[PubMed PMID:26914517].**IF:5.5**
14. Mukhopadhyay S, Das DN, **Panda PK**, Sinha N, Naik PP, Bissoyi A, Pramanik K, Bhutia SK. Autophagy protein Ulk1 promotes mitochondrial apoptosis through reactive oxygen species.**Free Radic Biol Med**. 2015;89:311-321.[PubMed PMID: 26409225].**IF: 5.755**
15. Mukhopadhyay S, **Panda PK**, Behera B, Das CK, Hassan MK, Das DN, Sinha N, Bissoyi A, Pramanik K, Maiti TK, Bhutia SK. *In vitro* and *in vivo* antitumor effects of Peanut agglutinin through induction of apoptotic and autophagic cell death. **Food Chem Toxicol**. 2014; 64:369-377. [PubMed PMID: 24333024].**IF:3.2**
16. Mukhopadhyay S, **Panda PK**, Das DN, Sinha N, Behera B, Maiti TK, Bhutia SK. Abrus agglutinin suppresses human hepatocellular carcinoma *in vitro* and *in vivo* by inducing caspased mediated cell death. **Acta Pharmacol Sin**. 2014; 35:814-824. [PubMed PMID: 24793310].**IF:2.4**
17. Das DN, **Panda PK**, Mukhopadhyay S, Sinha N, Mallick B, Behera B, Maiti TK, Bhutia SK. Prediction and validation of apoptosis through cytochrome P450 activation by benzo[a]pyrene. **Chem Biol Interact**. 2014;208:8-217 . [PubMed PMID: 24239969]. **IF:2.9**
18. Bhutia SK, Mukhopadhyay S, Sinha N, Das DN, **Panda PK**, Patra SK, Maiti TK, Mandal M, Dent P, Wang XY, Das SK, Sarkar D, Fisher PB. Autophagy: cancer's friend or foe? **Adv Cancer Res**. 2013; 118:61-95. [PubMed PMID: 23768510]. **IF:6.6**
19. Sinha N, Mukhopadhyay S, Das DN, **Panda PK**, Bhutia SK. Relevance of cancer initiating/stem cells in carcinogenesis and therapy resistance in oral cancer. **Oral Oncol**. 2013; 49:854-862. [PubMed PMID: 23876628]. **IF:3.752**
20. Das DN, **Panda PK**, Naik PP, Mukhopadhyay S, Sinha N, Bhutia SK. Phytotherapeutic approach: a new hope for polycyclic aromatic hydrocarbons induced cellular disorders, autophagic and apoptotic cell death. **Toxicol Mech Methods**. 2016; 1-17. [PubMed PMID: 27919191]. **IF:1.4**
21. Sinha N, **Panda PK**, Naik PP, Maiti TK, Bhutia SK. Abrus agglutinin targets cancer stem-like cells by eliminating self-renewal capacity accompanied with apoptosis in oral squamous cell carcinoma. **Tumor Biology (accepted)**. **IF:2.9**
22. Mukhopadhyay S, Schlaepfer IR, Bergman BC, **Panda PK**, Praharaj PP, Naik PP, Agarwal R, Bhutia SK. ATG14 facilitated lipophagy in cancer cells induce ER stress mediated mitoptosis through a ROS dependent pathway. **Free Radic Biol Med**. 2017; 104:199-213. [PubMed PMID: 28069524]. **IF: 5.755**

SEMINARS/CONFERENCES ATTENDED

- Presented poster entitled "***Abrus agglutinin* induced ceramide as a mediator of apoptosis and autophagic cell death in glioblastoma cells**" at 34th Annual Convention of Indian Association for Cancer Research (IACR) & International Symposium on "Cancer Research: from Bench to the Bedside" from 19th-21st February, Jaipur, 2015.
- Presented poster at 2nd "International Conference on Frontiers In Biological Sciences" (InCoFIBS-2015), at National Institute Of Technology, Rourkela, Odisha, India, from 22nd-24th January, 2015.
- Presented poster entitled "**Autophagic cell death induction with *Abrus agglutinin***" at 32nd Annual Convention of Indian Association for Cancer Research (IACR) "Emerging Trends in cancer research: Road to prevention & cure " & an International symposium on "Infection & Cancer" from 13th-16th February 2013, New Delhi.

WORKSHOPS ATTENDED

- Participated and organized workshop on "**Technologies on molecular analysis of cell and cellular dynamics**" (TMCCD-2015) at National Institute of Technology, Rourkela, Odisha, India, from 19th-21st November 2015.
- Participated workshop on "**Confocal Microscopy basics and applications**" at Institute of Life sciences, Department of Biotechnology. Govt. of India, from December 2nd-4th December 2008.

PERSONAL DETAILS

- Date of Birth: 29th June 1984
- Father's Name: Late Nishakar Panda
- Nationality: Indian
- Gender: Male
- Marital status: Single
- Blood group: A^{+ve}
- Permanent Address: At: Chhatria, Po: Arandua, Via: Basudevpur, Dist: Bhadrakh, State: Odisha, India-756125
- Languages Proficiency: English, Hindi, Oriya

REFERENCES

- I. Dr. Sujit Kumar Bhutia**
Assistant Professor and Head
Department of Life Science
National Institute of Technology Rourkela
Rourkela – 769008
Odisha, India
Phone No.: +91-661-2462686
Email: sujitb@nitrkl.ac.in, bhutiask@gmail.com
- II. Dr. Tapas Kumar Maiti**
Professor
Department of Biotechnology
Indian Institute of Technology Kharagpur
Kharagpur- 721302,
West Bengal, India
Phone No.:+91 - 3222 – 283766
Email: tkmaiti@hijli.iitkgp.ernet.in
- III. Dr. Rama Sankar Verma**
Professor
Department of Biotechnology
Bhupat and Jyoti Mehta School of Biosciences
Indian Institute of Technology Madras
Chennai – 600 036, India
Phone No: +91-44-2257-4109
Email: vermars@iitm.ac.in

I hereby declare that all the details provided in this curriculum vitae is true to the best of my knowledge

Prashanta Kumar Panda
April 19th, 2017
Rourkela